Uncertainty Quantification in Assessment of Damage Ship Survivability

Qi Chen, BEng, MSc

Thesis submitted to the University of Strathclyde in fulfilment
of the requirements for the degree of Doctor of Philosophy

The Ship Stability Research Centre
Department of Naval Architecture and Marine Engineering
Faculty of Engineering
University of Strathclyde

Glasgow, May 2013

ABSTRACT

Ongoing developments in improving ship safety indicate the gradual transition from a compliance-based culture to a sustainable safety-oriented culture. Sophisticated methods, tools and techniques are demanded to address the dynamic behaviour of a ship in a physical environment. This is particularly true for investigating the flooding phenomenon of a damaged ship, a principal hazard endangering modern ships. In this respect, first-principles tools represent a rational and cost-effective approach to address it at both design and operational stages. Acknowledging the criticality of ship survivability and the various maturity levels of state-of-the-art tools, analyses of the underlying uncertainties in relation to relevant predictions become an inevitable component to be addressed.

The research presented in this thesis proposes a formalised Bayesian approach for quantifying uncertainties associated with the assessment of ship survivability. It elaborates a formalised procedure for synthesizing first-principles tools with existing knowledge from various sources. The outcome is a mathematical model for predicting time-domain survivability and quantifying the associated uncertainties.

In view of emerging ship life-cycle safety management issues and the recent initiative of “Safe Return to Port”, emergency management is recognised as the last remedy to address an evolving flooding crisis. For this reason, an emergency decision support framework is proposed to demonstrate the applicability of the presented Bayesian approach. A case study is enclosed to elucidate the devised shipboard decision support framework for flooding-related emergency control.

Various aspects of the presented methodology demonstrate considerable potential for further research, development and application. In an environment where more emphasis is placed on performance and probabilistic-based solutions, it is believed that this research has contributed positively and substantially towards ship safety, with particular reference to uncertainty analysis and ensuing applications.

ACKNOWLEDGEMENTS

This thesis is submitted in fulfilment of the requirement for award of the degree of Doctorate of Philosophy. The research has been carried out at the Ship Stability Research Centre, Department of Naval Architecture & Marine Engineering, University of Strathclyde, during the period of October 2009 to March 2013. The study was jointly supervised by Professor Dracos Vassalos and Doctor Andrzej Jasionowski.

I am deeply indebted to Professor Dracos Vassalos for giving me the opportunity and supervising this work. Especially during the most challenging period of finalising my thesis, without his all-around support and guidance, this work would have never been accomplished.

I would like to express my gratitude to Doctor Andrzej Jasionowski for offering me a position at the SSRC, and encouraging my research continuously. His enthusiasm for research has inspired me a lot.

I am very grateful to Doctor Dimitris Konovessis for his advice and help. The numerous discussions are important to this work.

I am truly thankful to Mrs. Thelma Will for her support with the administrative details of the registration, preparation and submission of my thesis.

The financial support of the European Commission (EC), European Maritime Safety Agency (EMSA), UK Maritime Coastguard Agency (MCA) and the SSRC is greatly acknowledged.

Lastly, I would like to deeply thank my father Yong Chen and my mother Shuzhen Zhang for their love, support and encouragement throughout my life. And I am greatly indebted to my loving, supportive, encouraging, and patient husband Doctor Wenkui Cai whose faithful support during the final stage of this Ph.D. is so appreciated. I never forget the time he spends with me in Glasgow and Singapore. Thank you.

TABLE OF CONTENTS

ABBREVIATIONS

ABS	**:**	American Bureau of Shipping
CFD	**:**	Computational fluid dynamics
DNV	**:**	Det Norske Veritas
DSS	**:**	Decision Support System
EC	**:**	European Commission
EMSA	**:**	European Maritime Safety Agency
FLOODSTAND Project	**:**	Integrated Flooding Control and Standard for Stability and Crises Management http://floodstand.aalto.fi/
GLM	**:**	Generalized Linear Model
GOALDS	**:**	Goal based Damage Stability http://www.goalds.org/
HARDER Project	**:**	Harmonisation of rules and design rationale
IMO	**:**	International Maritime Organisation
ITTC	**:**	International Towing Tank Conference
LHS	**:**	Latin hypercube sampling
LS	**:**	Least Square
LR	**:**	Lloyd's Register
MC	**:**	Monte Carlo
MCA	**:**	Maritime Coastguard Agency UK
MCMC	**:**	Markov Chain Monte Carlo
ML	**:**	Maximum Likelihood
OLS	**:**	Ordinary Least Square
QRA	**:**	Quantitative Risk Assessment
SAFEDOR Project	**:**	Design, operation and regulation for safety, www.safedor.org
SOLAS	**:**	The International Convention for the Safety of Life at Sea, 1974, and the 1988 Protocol
SSRC	**:**	The Ship Stability Research Centre, University of Strathclyde

NOMENCLATURE

p_f	:	Probability of ship capsizing for a specific damage case
Hs_{crit}	:	Critical sea state causing $p_f = 0.5$ within given time
$F_{t_{cap}}$	:	Cumulative probability distribution of time to capsize
t_0	:	A given time period in assessment of ship survivability
t_{cap}	:	Time takes a ship to capsize after flooding
$P(\theta)$	:	Prior probability distribution of an unknown parameter
$P(\boldsymbol{y}\|\theta)$	:	Likelihood function of a response variable
$P(\boldsymbol{y})$	:	Marginal probability of a response variable
$P(\theta\|\boldsymbol{y})$	:	Posterior probability distribution of an unknown parameter
α	:	Input wave steepness
λ	:	Wave length
T_p	:	Peak wave period
T_z	:	Zero crossing period
Φ	:	Cumulative distribution function (CDF) for the standard normal distribution
Λ	:	CDF for the logistic distribution
$\boldsymbol{\beta}$	:	A set of unknown model coefficients
l	:	Log-likelihood function
γ	:	An acceptance ratio by using MCMC sampling
$Q(\boldsymbol{\beta}^*\|\boldsymbol{\beta}^{(i)})$	:	Proposal distribution of unknown parameters
$\boldsymbol{Z}$	:	A set of latent variables describing binary outcomes
$\mathcal{N}$	:	Multivariate normal distribution
$\boldsymbol{\Sigma}$	:	Variance-covariance matrix
$\boldsymbol{\mathcal{H}}$	:	Hessian matrix
L_d	:	Extent of damage
X_d	:	Location of damage
y	:	Penetration of damage
z	:	Height of damage
H	:	Height of car deck

Chapter 1

Introduction

1.1 Preamble

There has been increased interest in applying risk-based approaches in the maritime industry for the technological and regulatory developments to better manage the integrity of ships in service. In view of the facts, numerous first-principles tools have been developed to evaluate the risk levels associated with a series of critical loss scenarios (e.g. collision, grounding, structural failure, fire). However, the risk-based tools and methods that have been put forward to date are subject to several constraints reflecting incomplete knowledge of mankind to comprehend the physics that is governing the universe. In this respect, identification and quantification of the uncertainties pertinent to performance-based risk assessment is a necessity. Nevertheless, little evidence suggests that uncertainty has been considered explicitly in the current process of risk assessment.

Fortunately this situation is gradually changing. Increasing effort (Winkler, 1996) (M.Elisabeth, 1996) (Abrahamsson, 2002) (Cheng, 2009) is being made on how systematic modelling of uncertainties can be an integral part of risk assessment. As far as risk-based approach in the maritime industry is concerned, a formalised procedure for assessing uncertainty needs to be established focusing on the dominant loss scenarios endangering ship safety. In this process, ship survivability (i.e. stability in waves) plays a vital role on ship safety performance. Considering the above, the development of a systematic methodology to quantify the uncertainties of the advanced first-principles tools towards ship survivability assessment has been identified as the core subject of this dissertation.

1.2 Maritime Safety

Today, seaborne trade is playing a critical role in connecting the global economy and driving economic prosperity. Statistics suggest that more than 90% of global trade is carried by sea. In addition, shipping remains a key mode of transport for many private individuals especially for leisure purposes, as shown by the growth of the cruise industry. As a consequence, the 23 million tonnes of cargo and 55,000 cruise passengers those travel by ship every day (AGCS, 2012). This crowning achievement highlights the significance of assuring a satisfactory safety performance of maritime industry.

In the past 100 years since the sinking of the Titanic, maritime safety has improved greatly through advanced technologies, enhancing regulatory standards, carrying out standardized training, etc. It is demonstrated in Figure 1.1 (Konovessis, 2012) that the shipping activities have become a safer and more environmentally benign form of commercial transport than ever before since its hazard rate decreased markedly in the past century. Despite the enhancement of safety record, it is still important to understand that the current accident frequency (as a percentage of the world fleet) leading to serious consequences or total losses still stands at a relatively high level, as indicated in Figure 1.2. Further investigation of the figure from the International Union of Marine Insurance (IUMI) suggests that total losses of ships over 500 gross tonnages (GT) follow a continuing downward trend between 1994 and 2010. Nevertheless, the number of serious incidents (other than total losses) over the last 10 years has increased considerably.

In addition to the existing risk profile of maritime industry, it is also important to appreciate that new hazardous elements continue to emerge and need to be addressed proactively. These include aspects such as the ever increased ship sizes (e.g. the trend towards ultra-large modern cruise ships carrying over 6,000 passengers), ‘human element’ themes such as training, crewing and risk management, and the trend toward arctic shipping with its associated navigational and environmental complications.

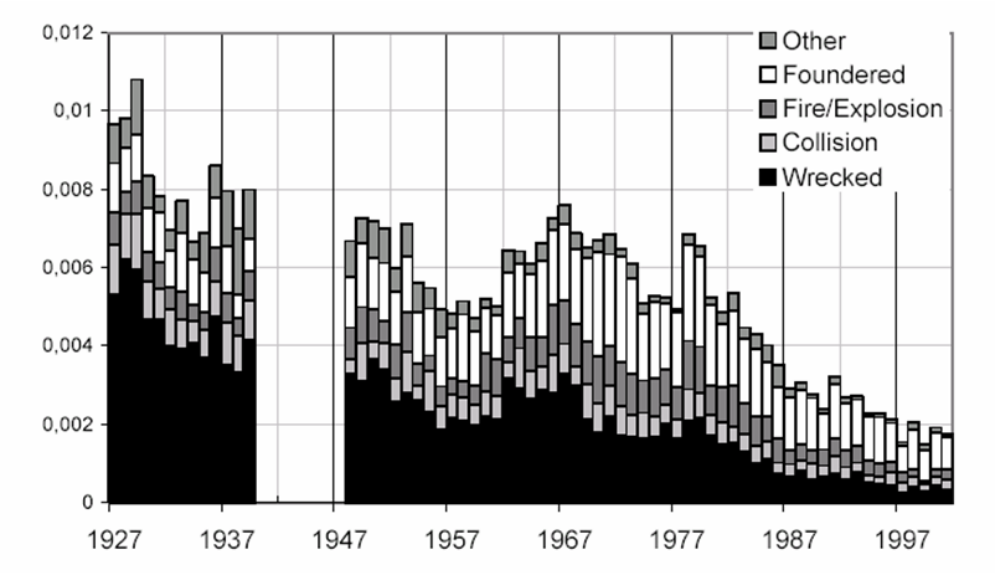

Figure 1.1: Maritime Accident Trend (Frequency of Accident) (Konovessis, 2012)

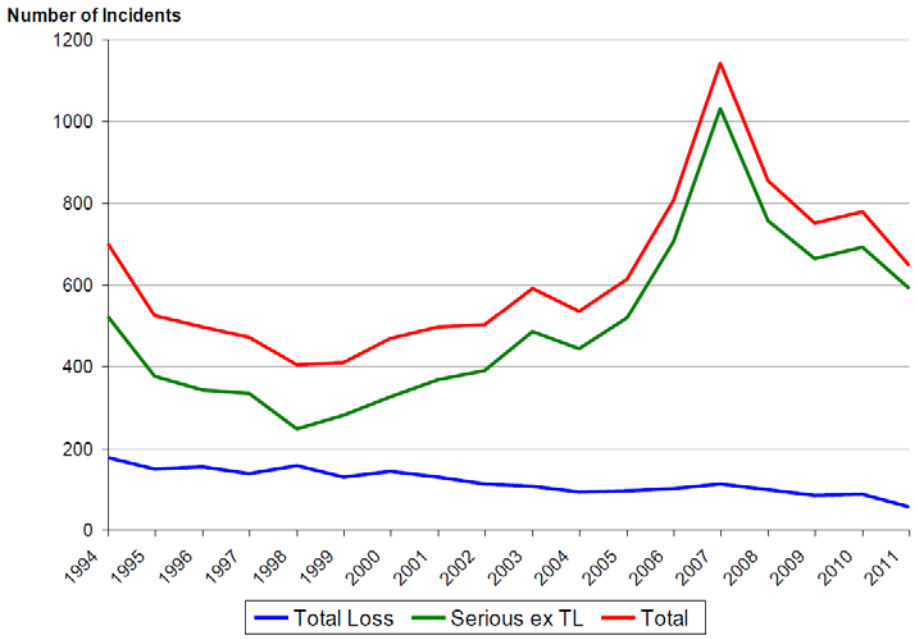

Figure 1.2: Number of Serious and Total Losses Accidents (1994 – 2010, Vessels > 500GT), Source: IUMI, total losses are reported by Lloyds List (Graham, 2011)

1.3 Contemporary Development and Trend on Assessment of Ship Safety

The shipping industry remains alert to new challenges, making preparations for future risks to shipping safety is a prerequisite focus. In this respect, an explicit measure of safety in ship design and operation is essential. This necessitates

employing a consistent and transparent methodology to quantify the life-cycle risk of a ship by considering all design and operational safety measures. Undoubtedly, prevention of the undesirable events giving rise to high consequences at the design phase is the primary cost-effective solution for improving safety performance. In so doing, explicit calculation and use of risk is regarded as a flexible means of evaluating effectiveness of design changes with respect to safety. As the potential risks are identified and estimated, the ship design can be modified to get a satisfactory safety level.

In this vein, ongoing developments in design methodology and regulation are gradually shifting from traditional prescriptive rules-based approach to performance-based (e.g. risk-based) approach. On one hand, contemporary idea in ship design promulgated by the recent researches (e.g., SAFEDOR project (www.safedor.org)) initiates an integration of risk assessment systematically in the design process to treat safety as a design objective rather than through rule compliance (i.e., risk-based ship design). A clear change of the design philosophy is illustrated in Figure 1.3, where the right-hand-side demonstrates that an implementation of a formal procedure of risk assessment is embedded in a high level risked-based framework for design decision-making and design optimisation. On the other hand, the modern regulatory framework established by the International Maritime Organization (IMO) has a tendency of utilising performance-based approaches to manage rules and regulations. For instance, the new harmonised probabilistic rules for damage stability, SOLAS (Safety of Life At Sea) Chapter II-1, which entered into force in 2009, are perceived to be far more realistic than the previous deterministic instruments for passenger ships. Direct reference can be found concerning the statistical evidence of collision damages (accounting for loading conditions, sea states at the time the accident occurred). Contrary to deterministic standards, the probabilistic methodology adopts a set of goal-based regulations (Attained Index of Subdivision, A > Required Index of Subdivision, R) and in principle considers thousands of potential damage cases. It is expected that the new requirements will lead to ship designs accommodating novel sub-division concepts (Papanikolaou, 2007).

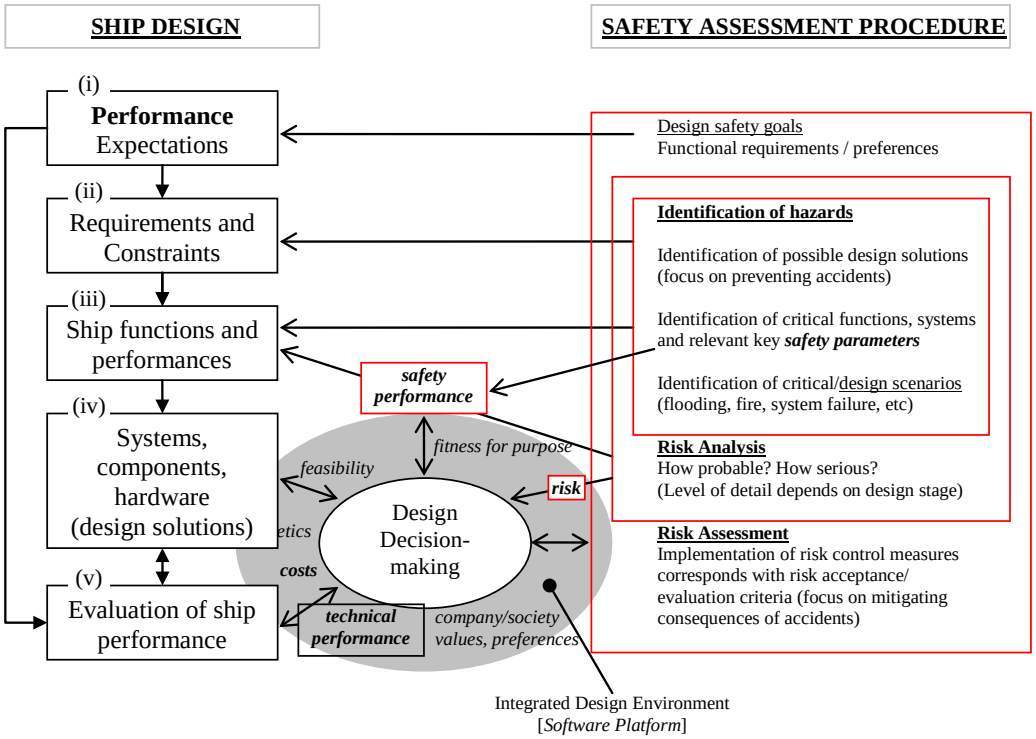

Figure 1.3: Contemporary Trend in Ship Design: from Prescriptive Rules-based to Risk-Based approaches (Vassalos, 2008)

Moreover, for addressing ship safety explicitly, rationally and cost-effectively, advancements in the implementation of performance-based approaches are reflected through employing first-principles tools in a formalised procedure for quantifying risk. As a result, the safety performance of the ship can be measured with respect to specific modes of failure for further decision making in design and operation.

1.4 Uncertainty Analysis in Ship Safety Assessment

In principle, the safety assessment procedure referred in risk-based ship design is a formalised process for risk management. At a fundamental level, risk analysis can be described as a structured process for identifying and analysing the most important contributions to the overall life-cycle risk level of ships at sea. Figure 1.4 elaborates the basic steps of risk analysis and the relationships between risk analysis, risk assessment and risk management. In such a top-down process, risk analysis is an informational tool to determine the major contributions to the overall risk.

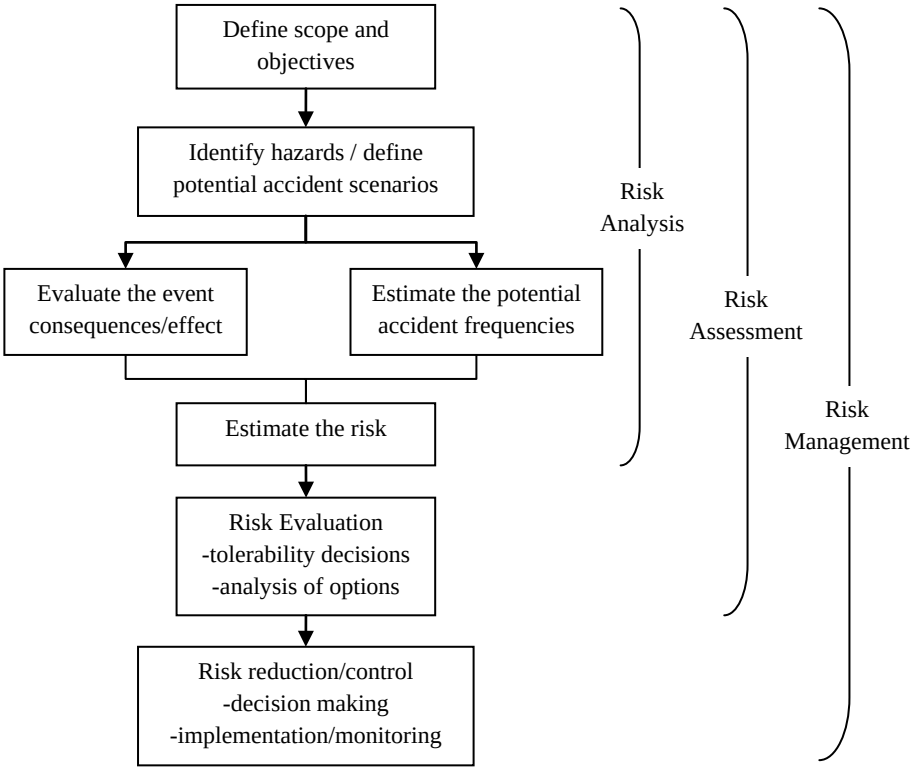

Figure 1.4: Simplified Relationship between Risk Analysis, Risk Assessment and Risk Management (IEC, 1995)

In engineering field, risk is usually measured by combining the probability for an undesirable event to occur and the subsequence consequences given its occurrence (Kaplan and Garrick, 1981). The following four steps need to be followed to perform risk analysis:

1) What can go wrong?
2) How likely is it to go wrong?
3) What are the consequences of going wrong?
4) What is the confidence in the answers to each of the first three questions?

With pre-defined safety goals and objectives, Step 1 systematically identifies major hazards and its related accident scenarios. Step 2 and 3 are designed for determining calculable probabilities of occurrence and consequences of the identified hazards in step 1. In this context, as far as the methodology of risk-based ship design is concerned, it would be desirable to employ performance-based tools for quantifying relevant components in step 2 and 3. For instance, D5.1.5 of the SAFEDOR project

provides a consolidated list of various risk-based simulation tools that currently can be integrated into the risk-based framework (Memeris and Langbecker, 2006). Such as for fire safety e.g. REUME (Guarin et al., 2007) and passenger evacuation e.g. Exodus (http://fseg.gre.ac.uk/exodus/) (Caldeira-Saraiva et al., 2004) (Galea et al., 2004), Evi (http://www.safety-at-sea.co.uk/software-2.html) (Vassalos et al., 2001a) (Vassalos et al., 2001b) (Vassalos et al., 2002) (Vassalos et al., 2003) (Vassalos et al., 2004a). These are derived from various techniques: Bayesian network, artificial neural networks, CFD calculations, non-linear time domain calculations and reliability models, virtual reality models and simulation techniques. Consequently, the quantified risk can be graphically presented (Vassalos and Jasionowski, 2006) using F-N diagram, as demonstrated in Figure 1.5.

During this process, it is important to pay particular attention to the quality of the obtained results from performance-based tools in step 2 and 3. Uncertainty may be introduced at various stages of the process, e.g. statistical evidence, assumptions, simplifications made in risk models. Hence, step 4 aims to estimate the reliability of the quantified risk level.

The underlying uncertainties of performance-based tools represent a key element in risk analysis. They have direct influence on the evaluated risk levels and, ultimately, the subsequent decision-making towards risk reduction and management. Being aware of this, in order to facilitate the safety assessment for high level risk-based framework on ship design and operation, a formalised procedure for the treatment of uncertainties during risk analysis is a crucial subject in pursuit.

Regarding this, a series of studies on uncertainty analysis are observed in nuclear power industry (Helton et al., 1995a) (Helton et al., 1995b) (Helton et al., 1995c) (Helton et al., 1996) (Helton et al., 1997) (Helton, 1998) (Helton et al., 2000a) (Helton et al., 2000b), chemical industry (Lauridsen et al., 2002), offshore sector (Nilsen et al., 1998), and natural disaster studies (Iman et al., 2002) (Bazzurro and Luco, 2005) (Li and Ellingwood, 2006), etc. In comparison, little work is observed in the maritime industry to address uncertainty in the risk-based design and operation framework.

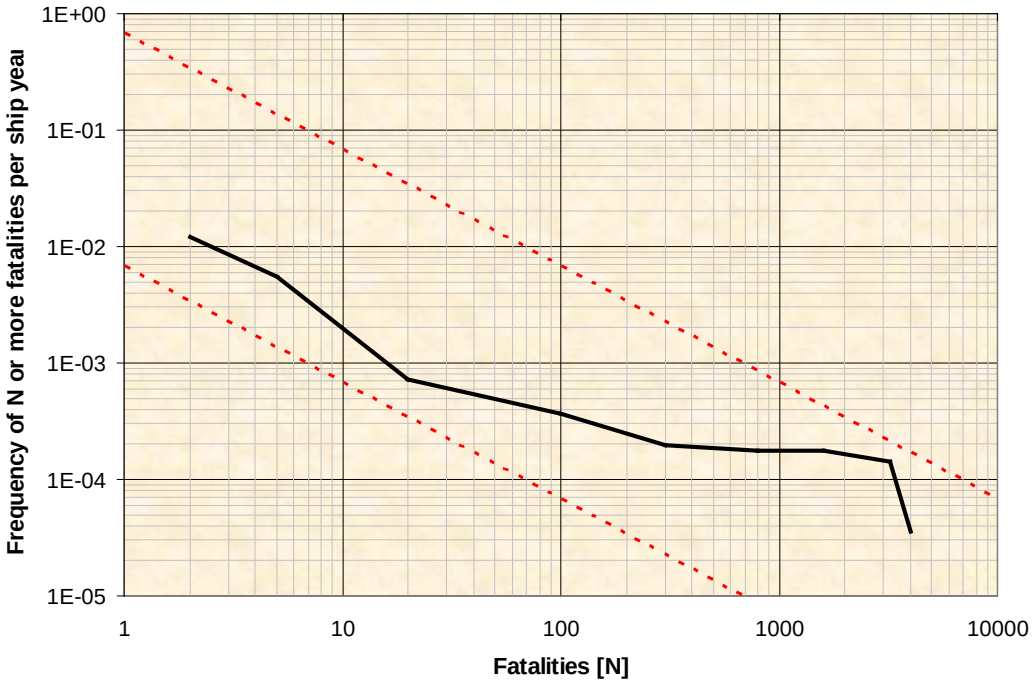

Figure 1.5: Societal Risk Level for Cruise Ships (IMO, 2008)

1.5 Passenger Ship Survivability

Under the risk-based framework for ship safety assessment, applications of advanced tools and techniques aim to have a fast and reliable evaluation of various risk elements associated with ship operations and thus to assess the effectiveness of various risk-control options at both design and operation stages. In this case, understanding the key risk drivers to a ship at sea is a prerequisite so that concerted effort can be put to effectively manage the life-cycle safety performance. Once the critical hazards and their potential accident scenarios governing the overall risk level of a ship are identified, the impact of various types of uncertainty on the risk analysis process could then be addressed.

Looking into the typical sequential shipboard accident scenarios as illustrated in Figure 1.6, ship flooding is considered as a very complex and high-consequence scenario, after which the ship is exposed to the risk of losing its stability and of the subsequent sinking. Within the risk-based framework, flooding-related scenarios are recognized as a principle accident category threatening the overall safety performance of a ship. In particular, with respect to passenger ships, flooding- and

fire-related hazards comprise over 90% of the total risk and almost 100% of all the events leading to decisions to abandon ship (Vassalos, 2008).

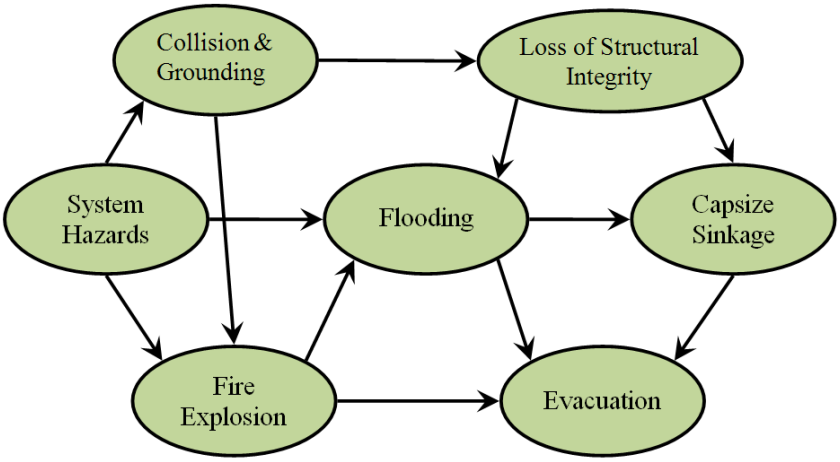

Figure 1.6: Typical Structural Links of Potential Accident Scenarios

The flooding of passenger ships has accounted for the majority of loss of human lives that has been claimed by historical maritime accidents in the times of peace, e.g. the *Titanic* (1912), the *Herald of Free Enterprise* (1987), and the *Estonia* (1994) losses. The ever improved societal expectation for ship safety has been well addressed at the IMO by setting goals of "zero tolerance" towards human life loss through the concept of Safe Return to Port in July 2009 (IMO, 2004a). It demands close scrutiny of all the issues that could upset such expectation, ship survivability after a flooding casualty (damage stability in waves) is a vital subject that necessitates a thorough and systematic analysis.

In this respect, it is worth noting that key regulatory changes concerning damage stability have been driven mainly by individual high-profile accidents, as demonstrated in Table 1.2 and Figure 1.7. It is clear that, emphasis has been placed primarily on mitigating consequences (cure) rather than preventive measures. A review of ship stability standards is outlined in Appendix 1.

Table 1.2: Modern Ferry Accidents in the Western World (Vassalos, 2012)

1953	Princess Victoria capsized and sank when large waves burst open the stern door in rough weather with the car deck and starboard engine room flooded (134 dead).
1974	Straitsman capsized and sank whilst approaching berth with the vehicle door partly open and, as a result of squat, flooding the vehicle deck (2 dead).
1987	Herald of Free Enterprise capsized when the bow wave and bow-trim combined to bring the open bow door underwater, leading to flooding of the vehicle deck (193 dead).
1987	Santa Margarita Dos capsized in port in Venezuela due to heeling while loading vehicles as a result of flooding of the vehicle deck (5 dead).
1994	Estonia capsized and sank due to flooding of the vehicle deck (852 dead).
2006	Al Salam Boccaccio '98 capsized and sank due to flooding of the vehicle deck, following fire (1,002 dead).

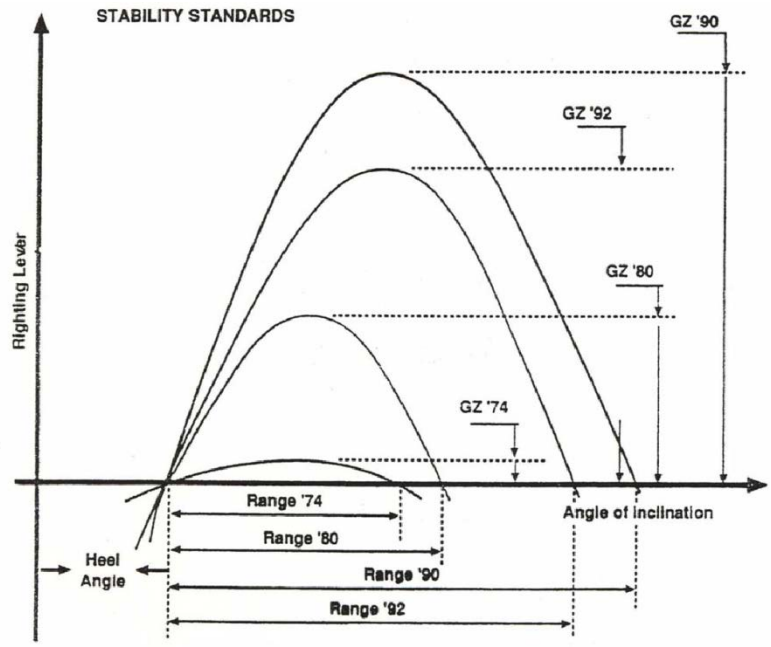

Figure 1.7: Deterministic Damage Stability Standards for Passenger Ships

Apparently, the prevailing regulatory system is often prescriptive. Novel designs could be inhibited due to specific solutions are prescribed, as even designs that would improve ship safety performance may violate existing prescriptive regulations. Under this background, it is widely accepted in the industry that "Probabilistic Concept of Survival" represents a more rational approach to address damage stability and survivability. In turn, probabilistic rules leading to the development of appropriate methods, tools and techniques are capable of addressing the physical phenomena involved. Accordingly, the performance of a vessel in a given environment and loading condition on the basis of first principles can be captured.

Deriving from the above, it is worth emphasising that passenger ships have been selected for this research due to the large societal impact associated with the accidents involving this category of knowledge-intensive and safety-critical ships. In this respect, flooding survivability analysis plays a key role in quantifying the total risk of a passenger ship. In line with the formalised procedure for risk management, a typical "flooding-related safety assessment process" is presented in Figure 1.8.

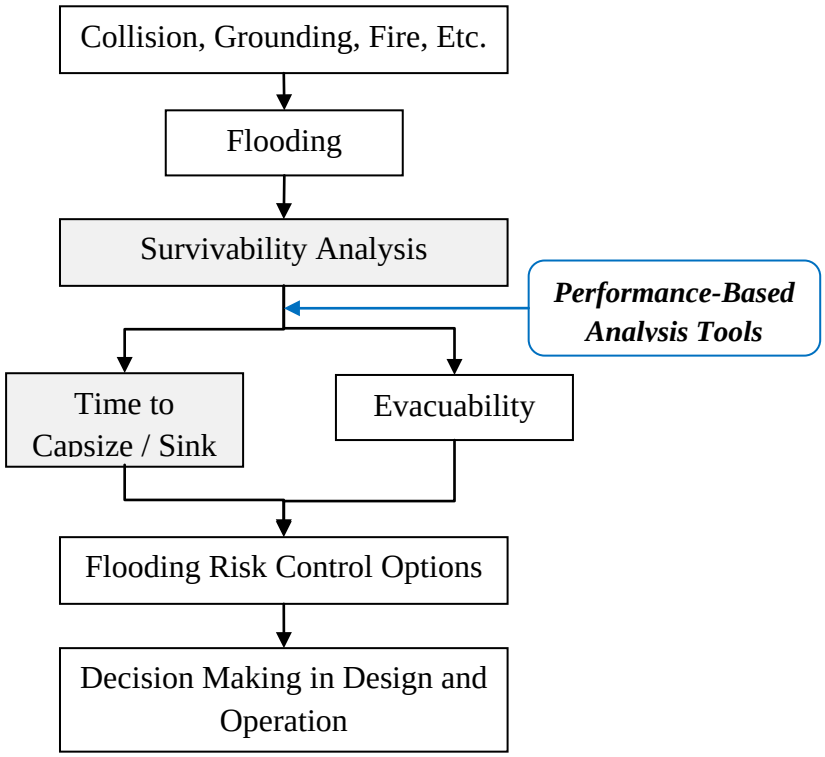

Figure 1.8: Flooding-related Safety Assessment

In this top-down process, collision and grounding are considered to be the most relevant accident scenarios that may cause flooding of passenger ships since the expected annual frequencies of such accidents are comparable with that of fire incidents (Vanem and Skjong, 2004). Existing passenger ships generally carry a large number of people onboard and, especially, modern cruise liners can carry several thousands of passengers. Although the frequency of involving such large passenger ships in a serious accident (e.g. collision, grounding) is relatively low, any single case could lead to catastrophic losses. Under such circumstances, timely and effective evacuation of all passengers and crew will be extremely important, and failure to evacuate in time may lead to catastrophic consequences e.g. the *Costa Concordia* (2012). In this sense, the expected time to capsize / sink should be evaluated in conjunction with the expected time needed for evacuation.

As long as the flooding risk is concerned, dynamic ship survivability analysis and evacuation analysis are the essential steps in determining the actual safety level of a passenger ship. Between them the "time to capsize / sink" is deemed as an appropriate measure towards quantifying survivability (SLF[1] committee of IMO has established "Time dependent survivability of passenger ships in damaged condition" as an important agenda item since SLF48, held in September 2005). Further development is to present such a measure probabilistically: the probability of ship capsizing within a given time for a given initial condition (i.e. damage case). Overall, the "time to capsize / sink" is a key measure in the process of quantifying the risk associated with flooding scenarios. In this respect, the state-of-the-art solutions are realised mainly through the utilisation of sophisticated first-principles tools to carry out explicit, rational and cost-effective investigations. Such as, a time-based numerical tool for dynamic prediction of flooding, e.g. PROTEUS3 (Jasionowski, 2001a).

On the basis of Figure 1.8, ship survivability analysis and eventually the "time to capsize / sink" are the central issues in evaluating the stability residual process in the event of a flooding casualty. The estimated results can be used for further probabilistic risk analysis. However, as it is explained in the previous section,

[1] IMO Sub-Committee on Stability and Load Lines and on Fishing Vessel Safety

Uncertainties are inherent in performance-based simulation tools for dynamic flooding prediction. For more informed decision making to address design and operational issues, uncertainties in the estimated ship survivability based on the available evaluation tools must be estimated through systematic uncertainty analysis.

1.6 Structure of the Thesis

The research to be presented in the thesis is founded on the hypothesis that there is a lack of systematic methodology to quantify the underlying uncertainties in the process of flooding risk analysis. As described in the forgoing, the thesis attempts to establish an uncertainty analysis scheme that is based on an objective and well-integrated principles by proposing relevant procedures/methodologies. The applicability of the proposed approach is demonstrated through a case study and a number of illustrative examples.

The thesis is structured in the following 10 chapters. A brief outline of the content of each chapter is given below:

- Chapter 1 (Introduction), the current chapter, introduces the background and sets the theme to the research described in this thesis.
- Chapter 2 (Aim and Objectives) declares the aim and specific objectives of this particular work.
- Chapter 3 (Critical Review), has reviews of the following subjects:
  - The classes of uncertainty in risk analysis
  - Uncertainties associated with the state-of-the-art performance-based tools and methods used for undertaking the prediction of motions and capsizing of damaged ships in waves. (Uncertainties are introduced according to the constraints on each of them)
  - Probabilistic methods of representing uncertainty
- Chapter 4 (Approach Adopted), discloses a methodology to be followed throughout this thesis and elucidates its implementation procedures.
- Chapter 5 (Preparation of Model Building up for Ship Survivability Assessment), constructs the probabilistic modelling framework for assessment of ship survivability due to flooding after collision (i.e. time-to-capsize), identifies key

aspects/areas (parameters) that influence ship survivability and can be included practically for further decision support.

- Chapter 6 (A Bayesian Approach for Probabilistic Uncertainty Quantification), takes advantage of Bayesian inferential techniques to estimate the predictive regression model and measure uncertainties in modelling.
- Chapter 7 (Implication and Implementation of Uncertainty Modelling), clarifies the proposed uncertainty modelling for flooding emergency management is a potential field of implementation, presents a new philosophy for instantaneous Decision Support System for flooding damage control, and elaborates the configuration of the proposed methodology for decision making during actual crises, in which the working flow and functionalities of the key components are detailed.
- Chapter 8 (A Case Study), demonstrates an application of the proposed uncertainty analysis scheme in a Ro-Ro Passenger (RoPax) ship survivability assessment after flooding and the outcome is employed in shipboard decision support for flooding crisis management.
- Chapter 9 (Discussion), outlines the main contribution to the field, critically discusses the outcome of the thesis on the basis of its objectives, outlines the difficulties encountered and the way in which these were addressed, and provides recommendations for further research.
- Chapter 10 (Conclusion), summarises the main conclusions of the research presented in this thesis.

The logical sequence and interrelationships among the chapters of the thesis are illustrated in Figure 1.9.

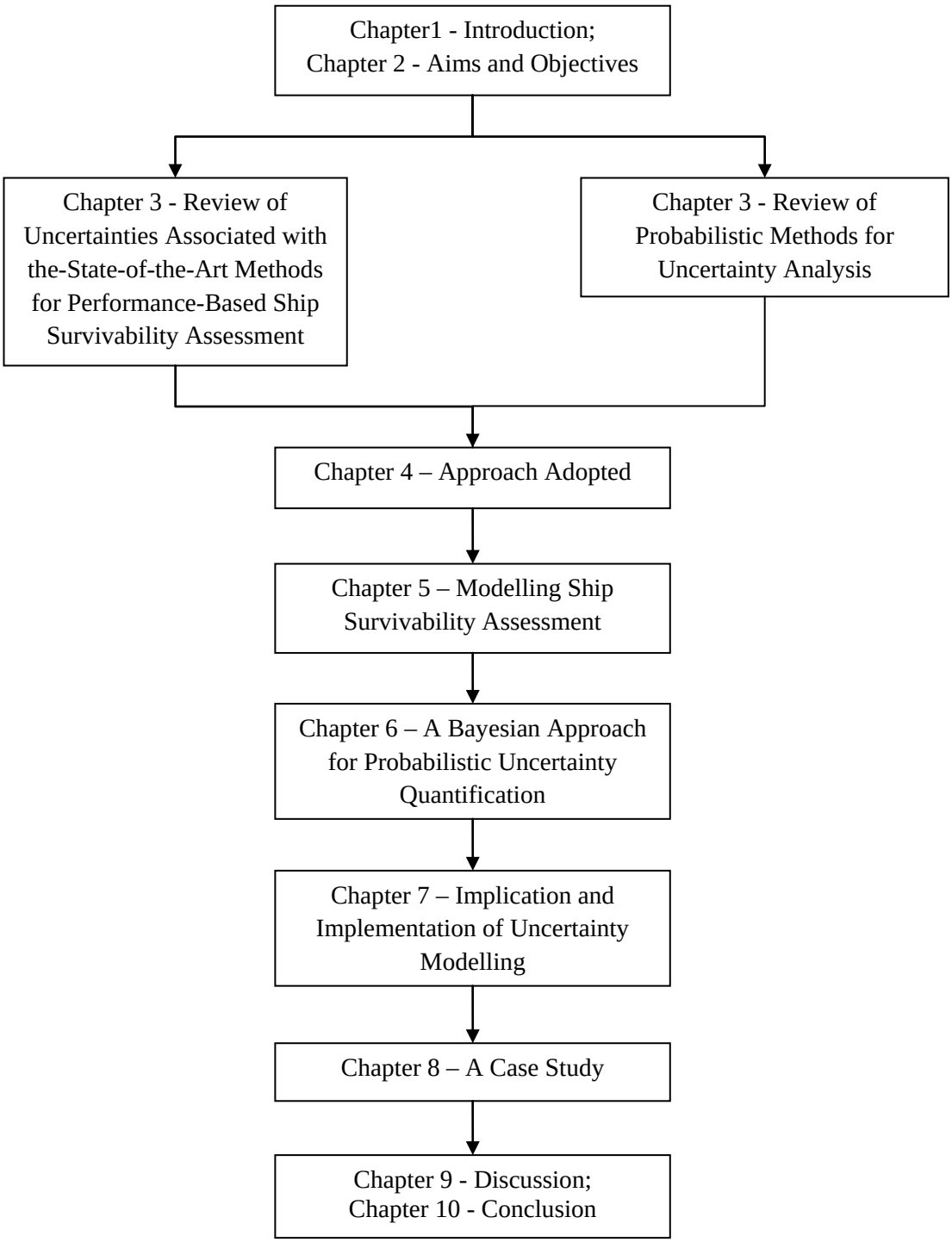

Figure 1.9: Structure of the Thesis

1.7 Closure

The theme of this research can be defined as follows: initially, passenger ships are the type of ships to be investigated in this particular research. Moreover, flooding-related accident scenarios are mainly considered since the hazard of flooding is recognized as a major risk to lives on board according to historical maritime accidents records. Therefore, ships survivability assessment can be considered as a vital subject that necessitates a thorough and systematic investigation. The application of performance-based tools and methods is respected as a more rational approach to assess ship's residual stability since it allows for dynamic flooding predictions. It becomes clearly that, uncertainties are inherent in performance-based analyses and thereby a systematic methodology for quantifying the uncertainties in assessment of damage ship survivability is required.

Chapter 2

Aim and Objectives

This dissertation is devoted to the elicitation of a formalised uncertainty analysis scheme for quantifying the underlying uncertainties of performance-based tools for assessing ship safety against capsizing in case of flooding.

Specific objectives to realise this concept include:

- To comprehend the sources of uncertainty in assessing damage ship stability in waves. It should be based on a critical review of the constraints associated with the state-of-the-art performance-based tools or methods used in the flooding-related risk analysis.

- To propose a formalised procedure for the treatment of uncertainties in performance-based assessment of ship survivability in case of flooding. It should be a generic process, and hence uncertainties in probabilistic risk assessment concerning other critical loss scenarios to ships (e.g. fire, structural failure) can be worked out by the same token.

- To build up the mathematical modelling framework for ship survivability assessment.

- To deploy Bayesian techniques for estimating the predictive model and then to undertake probabilistic uncertainty analysis of model outputs.

- To demonstrate the applicability of the proposed uncertainty analysis scheme in shipboard decision support for flooding damage control through a case study.

Chapter 3

Critical Review

3.1 Preamble

In this chapter, firstly, a brief summary of classes of uncertainty found in literature is presented. Secondly, a comprehensive review is undertaken concerning state-of-the–art performance-based approaches to analyse ship safety against capsizing. Associated uncertainties are discussed based on the limitations revealed by using the existing tools and methods. At last, a range of techniques available for representing uncertainty is identified. In particular, comparisons between them are performed.

3.2 Classes of Uncertainty

At a fundamental level, two major categories of uncertainty in risk analysis are recognised in most of the literature (Hacking, 1975) (Chernoff and Moses, 1959): aleatory uncertainty and epistemic uncertainty. They are also frequently referred to as irreducible and reducible uncertainties or stochastic and subjective uncertainties. The most important distinction between these two is that, in practical terms, the latter can be reduced through possible interventions, which the former cannot. Furthermore, aleatory uncertainty often stems from variability in known populations, and therefore represents randomness in samples. In comparison, epistemic uncertainty comes from basic lack of knowledge about fundamental phenomena.

As far as modelling the dynamic behaviour of a damaged ship in waves is concerned, there are various engineering tools have been developed. This leads to an extremely complex mathematical modelling process, thus the quality of the predictions by different tools needs to be inspected. In this case, the inherent uncertainties can be classified as the epistemic category, which, for a given condition, are presented in a form of inconsistent estimations derived from different performance-based models.

For instance, a number of comparative studies on different methodologies to characterize the time it takes a ship to capsize or sink after damage have been conducted within European Commission funded research projects, e.g. FLOODSTAND (Integrated Flooding Control and Standard for Stability and Crises Management, SCP7-GA-2009-218532) (Rask, 2010), (Jasionowski, 2012a), (Spanos and Papanikolaou, 2011), (Jasionowski, 2012b). The ultimate objective is to explore the underlying uncertainties in the existing approaches so that better quality of ship survivability predictions can be assured.

3.3 Uncertainties in Performance-Based Ship Survivability Assessment

In recent years, particular interest has been placed on the time dependent survivability analysis of ships. There is significant effort (Jasionowski et al., Oct. 1999) (Jasionowski et al., Nov. 2004) (IMO, 2006a) to develop survivability criteria of damaged ships on the basis of survival time, in which the survivability is expressed as a function of predefined time interval. Furthermore, latest regulatory developments on “safe return to port” signify that passenger ships should be designed based on the time-honoured principle. This conveys a concept that a ship is its own best lifeboat in the event of a casualty (IMO, 2004a) (IMO, 2006b). In this way, the damaged ship should either be capable of returning to port or able to survive for three hours to allow for a timely evacuation. Consequently, the time to capsize of a damaged ship plays a central role in the new framework of ship safety.

Performance-based approaches can provide objective means to estimate the damage ship survivability in a given time interval. The relevant research has evolved into two distinct areas: analytical model and numerical simulation. In addition, benchmark model testing can be conducted to validate the quality of the predictions from the aforementioned tools/methods. In this section, different predictive approaches are reviewed primarily. In turn, their associated uncertainties are discussed based on the constraints imposed on each of them.

3.3.1 Analytical Model

In general, the reliability of the acquired prediction addressing ship survivability is proportional to the effort and cost that goes into the adopted methods. Analytical methods may provide rather useful information for the time aspect in case of ship flooding accident. When comparing with first-principles tools (numerical simulations or physical model experiments), the significant advantage of analytical methods is the calculation speed.

The concept of the attained subdivision index is believed to be the most advanced technique that has been regulated for addressing damage stability at design stage, as detailed in (Pawlowski, 2004) (IMO, 2004b). As stated in the latest SOLAS Chapter II-1, the index A denotes the survivability of the ship, which is the summation of the partial indices (A_s, A_p and A_l) calculated for three draughts (fully loaded, partially loaded and lightship conditions). In turn, (1-A) is defined as the marginal probability of ship sinking/capsizing in the flooding scenarios under consideration. For each individual damage case at the final equilibrium floating condition, the probability of survival (survival factor *s*) is a function of hydrostatics (GZ_{max} and range of positive stability) and the equilibrium heel angle after damage, as given by Equation (1):

$$s_{\text{final,i}} = K \cdot \left[\frac{GZ_{max}}{0.12} \cdot \frac{Range}{16}\right]^{\frac{1}{4}} \tag{1}$$

Where:

GZ_{max} is not to be taken as more than 0.12 m;
Range is not to be taken as more than 16 degrees;
K=1 if $\theta_e \leq \theta_{min}$
K=0 if $\theta_e \geq \theta_{max}$
K= $\sqrt{\frac{\theta_{max}-\theta_e}{\theta_{max}-\theta_{min}}}$ otherwise;
"θ_{min}" is 7 degrees for passenger ships and 25 degrees for cargo ships;
"θ_{max}" is 15 degrees for passenger ships and 30 degrees for cargo ships.

Despite the progress, it is important to bear in mind that this probabilistic approach does not relate the probability of survival to time. Some relevant studies have been presented in (Pawlowski, 2008) (Pawlowski, 2009).

In response to this, a time-based analytical model (Univariate Geometric Distribution) for prediction of the time to capsize after flooding, has been proposed in (Jasionowski, 2006) as an alternative in the course of European Commission (EC) funded research project SAFEDOR. It derives from the hypothesis that the process of observing capsizes in number of trails follows closely a Bernoulli trial process (Jasionowski et al., Nov. 2004). The underlying concept for this mathematical model is formulated as follows:

$$F_{cap}(t_{cap}) = 1 - (1 - p_f)^n = 1 - (1 - p_f)^{\frac{t_{cap}}{t_0}} \qquad t_0 = 30min \tag{2}$$

$$p_f(Hs) = \Phi\left(\frac{Hs - Hs_{crit}}{\sigma_r(Hs_{crit})}\right) \qquad for\ Hs \geq 0, Hs_{crit} \geq 0 \tag{3}$$

$$Hs_{crit}(s) = \frac{0.16 - ln(-\ln(s))}{1.2} \tag{4}$$

$$\sigma_r(Hs_{crit}) = 0.039 \cdot Hs_{crit} + 0.049 \tag{5}$$

Considering a specific flooding damage case, the term $F_{cap}(t_{cap})$ represents the cumulative probability distribution of time to capsize in given conditions (e.g. flooding extent, loading, and sea environment). The concept of Bernoulli trials has been employed, under the assumptions that the probability to capsize p_f is constant for the given damage case. In general, the modelled testing period is 30 minutes t_0 per run, the number of trials can be assessed from $n = \frac{t_{cap}}{t_0}$, with t_{cap} is considered as the cumulative amount of time needed for ship capsizing.

As an important input to Equation (2), the rate of capsizing p_f is depicted by a cumulative normal distribution, where the mean value is expressed by the critical sea state Hs_{crit}[1] as shown in Equation (4). The stand deviation is derived from an approximated capsize band width as given in Equation (5). It is noteworthy that Hs_{crit} is established through physical model experiments undertaken in research

[1] A sea state causing the vessel capsizing during about half of the 30 minutes scaled model tests, the damage opening modelled was that known as SOLAS damage

project HARDER (HARDER, 2003) (Tagg and Tuzcu, 2003), and has a direct correlation with the survival factor s in Equation (1).

Concerning the limitations of this analytical model (UGD), the proposed prediction of the rate of capsizing p_f follows a normal distribution. In this situation, inherent uncertainties are directly linked with the mean (defined as the critical sea state) and the standard deviation. More specifically, the prescriptive expressions of both parameters are correlated with the sample size of the acquired experimental results in HARDER. It is identified that the survival factor s has significant influence on these two parameters.

Nevertheless, as the research is still ongoing for reformulation and calibration, it is expected the Equation (1) will be revised further. For instance, recent studies on the survival factor s were conducted in (Tsakalakis et al., 2010) (Pawlowski, 2010). Moreover, a linear equation is used to address the standard deviation $\sigma_r(Hs_{crit})$ as shown in Equation (5), which was derived from a regression of the capsize bandwidth (Jasionowski, 2006) (Jasionowski et al., 2007). In Figure 3.1, it specifies that there is 99% confidence that the variation of the critical sea state where $p_f = 0.5$ spreads within the defined band $(2 \times 2.5758\sigma)$. However, such a linear equation is limited by the size of test matrix (e.g. ship types, duration of simulation, number of test repetitions). Deriving from here, it is appreciated that substantial improvement is needed for the presented analytical model for survivability assessment. An updated work is presented in (Jasionowski, 2012a), which still necessitates the quantification of the associated uncertainties.

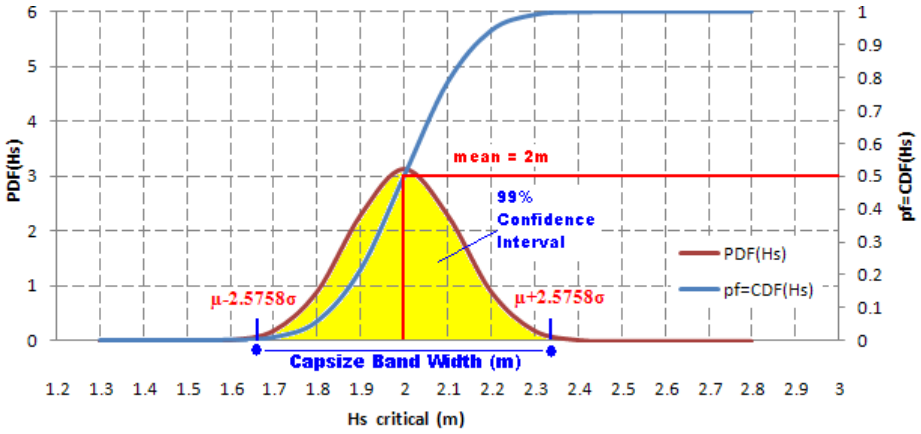

Figure 3.1: The Concept of a Capsize Band

3.3.2 Numerical Simulation

As the maritime industry is progressively moving towards performance-based criteria to address stability safety assessment, considerable effort has been expended to develop numerical simulation tools appropriated for predicting the dynamic behaviour of damaged ships in waves.

In general, dynamic behaviour of damaged ship in random waves is a highly non-linear process and should be studied in time domain simulation. In this case, theoretical-numerical models allow a time-based calculation of the nonlinear motions of the ship and the flooding process. In respect to a list of predefined damage scenarios, the probability of capsizing is measured by inspecting the time series of ship motions and related quantities (e.g., floodwater mass, elevation and attitude in flooded compartments).

Numerical models for simulating the behaviour of damaged ships in waves presented so far comprise four basic components: a model of the ship geometry including subdivision, a model of the sea environment, a model of the flooding process and a model of damaged ship dynamics. As illustrated in Figure 3.2, these models and their interactions are integrated into an overarching model to simulate the damaged ship behaviour (Jensen et al., 2008). It is worth pointing out that the dynamic behaviour of the ship influences the flooding process and conversely floodwater motions affect the

attitude of the ship. Among these models, three main mechanisms affect the behaviour of a damaged ship extensively: i) Ship motions in waves, ii) Flooding process and floodwater dynamics, iii) Interaction between flooding water and ship motions. Accordingly, there are three sub-problems need to be effective tackled in the time-based numerical codes:

- Ship motions in waves: Ship with zero forward speed drifting on the free surface of sea under the excitation of waves.
- Flooding process: The process of water inflow and outflow through damage openings and the progressive flooding through internal spaces.
- Dynamics of Water on Deck: The behaviour of the accumulated floodwater inside the ship's compartments and its interaction with the ship.

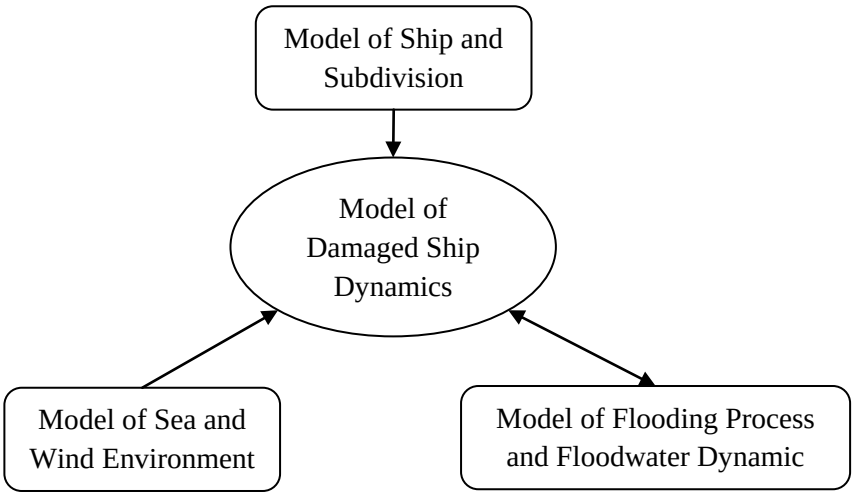

Figure 3.2: Structure of Numerical Models for Modelling Damaged Ship Dynamics

Comparing to physical model experiments, numerical simulations are very attractive due to their flexibility to be employed for assessing the ship behaviour under distinct flooding scenarios with virtually little cost. Nevertheless, the quality of numerical calculations depends very much on the accuracy of the model to approximate the physical phenomena. In fact, several limitations identified in the latest numerical models will contribute to the knowledge-based uncertainties and some crucial aspects need to be elaborated in the following.

3.3.2.1 Modelling Damaged Ship Dynamics

Equations of motion: Most recent numerical models calculate the ship motions in all six degrees of freedom and solve the equations of motion in the time domain. (De Kat and Paulling, 1989) developed the first numerical model in the time domain which is capable of considering all degrees of freedom. Since the nineties, a variety of numerical models have been developed for further addressing the damage stability of ships in waves, (Turan, 1993) (Vassalos and Turan, 1994) (Vassalos and Letizia, 1995) (Letizia, 1997) (Letizia et al., 2003) (Jasionowski, 2001a) (Vermeer et al., 1994) (Journee et al., 1997) (Spanos et al., 1997) (Spanos and Papanikolaou, 2001a) (Spanos, 2002) (Chang and Blume, 1998) (De Kat, 2000) (Santos, 2002) etc. However surge and yaw motions are frequently neglected in practice. A possible reason is that in order to have a standard comparison of the obtained theoretical results with the findings from physical model experiments, the recent numerical codes are in compliance with the testing procedure as specified in the resolution 14/SOLAS'95 (IMO, 1995), to keep the model in beam seas.

Moreover, the ability to calculate ship motions in the time domain using computational fluid dynamics (CFD) methodologies has only been made possible in recent years. The equations of motion of a ship are now routinely included in CFD codes. However, concerning the huge computational requirements for using CFD based seakeeping predictions and the level of uncertainty in the results, CFD methods for full ship motion predictions are a long way from practical application in engineering situations (Gorski, 2002) (Woodburn et al., 2002).

Hydrodynamic forces: Hydrodynamic forces acting on a damaged ship are generally divided into potential forces and viscous forces. The former can be further decomposed into hydrostatic (restoring), Froude-Krylov, radiation and diffraction forces.

On the one hand, as a basis of most numerical methods, potential flow theory is commonly employed to address ship-wave interaction and is adapted to account for large amplitude motions, and also supplemented with empirical models (Himeno, 1981) (Ikeda, 2002) for viscous damping effects. The effect of water inflow on roll

damping remains to be clarified. RANS (Reynolds Averaged Navier Stokes) solvers can be used to estimate roll damping, (Gorski, 2002). The influence of the damage opening on wave forces is generally neglected by all models.

On the other hand, the hydrodynamic properties of a damaged ship are commonly estimated in the frequency domain and transferred to the time domain by means of retardation functions used in the memory effect integrals. Investigations suggest that it is still not clear the appropriateness of making use of the frequency-domain results in time-domain calculations. This is because these results are for the normal seakeeping condition (linear and upright), and they may not be adequate for simulating damaged ship motions. For instance, the non-linear diffraction force has been calculated in time-domain in (Lee et al., 2006). However, the motions in waves were over-estimated. The slow change of hydrodynamic properties as the floodwater is accumulating inside the ship, so changing the mean hull wetted surface (e.g. mean draft and trim), is commonly addressed by updating of ship's hydrodynamic coefficients. This approach has been adopted in (Vassalos and Jasionowski, 2002) (Umeda et al., 2004). The influence of the mean heel angles on hydrodynamic coefficients is generally ignored.

External forces: A range of external forces which are attributable to wind, cargo shift, propulsion, resistance, rudder, automatic pilot, mooring and collisions may have bearings on flooding directly or indirectly.

Firstly, wind has a negative impact on the roll motion of a damaged ship in severe sea states as that may induce a significant inclining moment on the ship. This is particular true for passenger ships owing to large exposed areas. (Isherwood, 1973) demonstrates the earlier studies of the wind effects on ships. Most numerical models applied in damage stability assume a steady wind. In addition, concerning the practical applicability of the Weather Criterion to modern passenger ships, recent work in (Vassalos et al., 2004b) and (Francescutto et al., 2001) attempts to provide pertinent solutions. It should be noted that wind is generally neglected in ship survivability assessment since the wind direction is assumed to be parallel to the incoming waves.

Secondly, cargo shifting due to severe weather conditions is mainly dangerous for Ro-Ro and container ships. However, most numerical models do not take this into account explicitly.

At last, regarding the manoeuvrability of a damaged ship, the forces associated with resistance, propulsion, rudder and automatic pilot are calculated by some numerical models, e.g. (De Kat, 1990), which generally use different methods with empirical information. Forces resulting from mooring and collision may be interested in the initial transient stage of flooding as stated by (Spouge, 1985), but they are generally not considered in the recent practices.

3.3.2.2 Modelling Ship Flooding Process and Floodwater Dynamics

Flow through openings: Modelling of water ingress/egress through damage openings plays an important role in studying damage survivability, as it is highly correlated with the time for a ship to capsize/sink. It is a difficult task because complex hydrodynamics phenomena are involved. In most studies of damaged models, (Vassalos and Turan, 1994) (Hutchinson, 1995) (Vassalos, 1997a) (Zaraphonitis et al., 1997) (Van't Veer and De Kat, 2000), the simple hydraulic model often refers to Bernoull's equation. The general form of the formula of the flow rate is:

$$Q = K \cdot \iint \sqrt{2\mathrm{g}(h_{out} - h_{in})}\, dAdt \tag{6}$$

Where K is an empirical weir flow coefficient (hydraulic coefficient). It is clear that hydraulic coefficients remain an important approach in the prediction of inflow/outflow for damaged ships as they well capture the flow rate and the amount of water in different flooded compartments in the time domain. However, the value of hydraulic coefficient varies in different studies. A valuable study in (Ruponen et al., 2006) presents that the flooding coefficient is between 0.6 and 0.8, 0.7 being a common value. In comparison, other relevant studies report the hydraulic coefficient ranging from 0.5 to 1.2, e.g. (Vassalos et al., 2000). In this situation, a different approach, based on CFD techniques, is developed in (Nabavi et al., 2006) to study the effect of geometrical parameters of damage openings on the discharge rate for water flowing off a deck.

Another effect of the flooding process that needs to be modelled is the trapped air in cases with unventilated or partially ventilated compartments (e.g. flooding of confined spaces like an engine room). Trapped air will affect the water spread and hence has a significant influence on the water accumulation in compartments, especially in the transient flooding phase. This has been considered in a numerical simulation presented in (Palazzi and De Kat, 2002). Nevertheless, in many damage simulation studies, the air is treated as free to flow to external environment. This is because the complexity of the ventilation system, so that it is very difficult to model all possible air ducts in a passenger ship (Van't Veer et al., 2004). Therefore, further investigations are needed regarding the air compression and flow.

Progressive flooding of ship's compartments: In analysing the progressive flooding of multiple compartments through non-watertight openings, the water flow continues until a stage of equilibrium is reached or capsizing takes place. In general, numerical simulations addressing the survivability of damaged ships start from the final static equilibrium in damage condition. The transient flooding is generally not well captured in the current numerical models. Because the strong non-linear effects related to the floodwater dynamics and damage opening geometric properties, the complicated phenomenon has been perceived in the initial stages of flooding as mentioned in (Spanos and Papanikolaou, 2001a).

On the other hand, responding to the complex flooding situations of multiple compartments, the successive flooding across the compartments, door collapse and sometimes structure collapse should be considered. SLF 47/INF.6 (IMO, 2004) suggests a practical assessment of how semi-watertight and non-watertight doors can be treated in the time domain flooding simulation. The most important factor is to determine the leakage and the collapse pressure threshold, but there is a lack of proper data for carrying out a realistic numerical simulation in this respect.

Floodwater dynamics (including CFD): Modelling of the floodwater inside the damaged compartments is a challenge for all numerical methods. There are different approaches addressing floodwater dynamics and its effect on ship motions. Free Surface Plan models are considered as the simplest approach to approximate the water on deck motions with large open decks like Ro-Ro ships. This method is now

widely used for damage stability simulations and it assumes that the floodwater surface is always horizontal, and sloshing is not accounted for. (Papanikolaou et al., 2000) applies the “lump mass” concept to calculate the dynamic effect. The model has been validated that the acceptable loss of accuracy is balanced by the reduction in computing effort (Papanikolaou and Spanos, 2002). Meanwhile, a similar model, FMPS (Free Mass in Potential Surface) is presented in (Jasionowski and Vassalos, 2001b). The major advantage of the commonly used quasi-static approaches is that they are computationally more efficient than those sophisticated methods. However, they may result in unsatisfactory results. For instance, with large deck areas like Ro-Ro ships, dynamic effects of sloshing is significant as reported in (Zaraphonitis et al., 1997) (Molyneux et al., 1997) (Spanos and Papanikolaou, 2001a).

Alternatively, many attempts have been made to use CFD techniques for the simulation of floodwater dynamics in the flooded compartment. With the existence of free surfaces, RANS methods have been employed for floodwater dynamics in (Cho et al., 2005) (Gao et al., 2009) (Strasser et al., 2009) etc. More recently the SPH (Smoothed Particle Hydrodynamics) method was adopted in (Perez-Rojas et al., 2009) (Shen and Vassalos, 2009). These studies suggest sufficiently accuracy level can be achieved, but the computational time is long and which severely affects the productivity of applying CFD methods. The computed results indicate that the numerical accuracy is sensitive to the grid resolution and turbulence model. To increase the grid resolution will improve the numerical accuracy. However, the availability of computer source still restricts the grid size. In addition, the flow problem with vortex demands even finer meshes or flow adaptive grids to resolute delicate flow phenomena, which is still not realistic. Also, the Reynolds-Averaged turbulence model capable to capture the physics of swirling flow is still deficient. Therefore, more studies on turbulence and grid effects are needed. Nevertheless, it is still believed that more and more applications of CFD methods will be found in the industry.

3.3.2.3 Modelling the Sea Environment

Wave theory: Linear deep water theory is commonly adopted in most numerical models. Its application to situations concerning progressive flooding is generally

considered as adequate. Nevertheless, modelling extreme phenomena such as breaking waves is not suitable for linear theory. At this point, the behaviour of small ships in shallow waters would be particularly susceptible to these phenomena when the ships are subject to strong waves and winds. Especially in beam seas, water rotational speeds may have substantial influence on ship capsizing.

Direction and spectrum of waves: Dynamic behaviour of ships is very much influenced by the direction of waves. Numerical models should be able to tackle waves coming from different directions. In assessing damage survivability, at present most of the simulations focus on beam seas conditions, which generally represent the worst case scenarios Furthermore, the numerical models describe the natural sea conditions (irregular waves) by means of wave spectra that indicate the amount of wave energy at different wave frequencies. In general, the JONSWAP (JOint North Sea WAve Project) spectrum is often used to describe the coastal waters where most of the passenger ships ply normally. For deep sea waters, the Pierson-Moskowitz spectrum is found to be more appropriate. Thus it is obvious that spectral characteristics play an important role on the response of ships in the seaway.

Effects of wind, water depth and current: Wind effects are important for passenger ships due to its large exposed areas. Generally they are modelled using constant wind velocity profiles and empirical formulations (Blendermann, 1996). As a part of the external forces, the wind force is generally neglected in numerical assessment of ship survivability. Shallow water effects can also be of importance because it may influence the wave shape. However, most numerical models usually do not consider these types of effects for simulations. In reality, most historical accidents of passenger ships occurred near the coast where the water depth is limited. Besides these parameters, currents are commonly not taken into account in most numerical models, although coastal areas are usually subject to strong currents which also affect the waves and the damaged ship behaviours.

3.3.2.4 Modelling the Damaged Ship

Ship's hull and subdivision: Both the hull geometry and the damaged compartments must be modelled properly in the simulations. Special interest is paid on the openings

involving the internal non-watertight doors and the damaged holes in the hull, due to their influence on the progressive flooding. Considering the calculation of the successive flooding between compartments, there is a lack of proper simulations regarding the collapse and leakage of watertight doors. In the latest studies, the statuses of all doors (i.e. open, closed) are predefined and remain unchanged during the simulations. With respect to the definition of damage openings in terms of the shape, size and location, they are specified according to relevant SOLAS regulations (IMO, 1995). Furthermore, the superstructure of a passenger Ro-Ro ship is normally not modelled in the numerical simulations which may also affect the calculated survival time.

Ship speed: The speed is also importance since it influences the hydrodynamic forces and causes additional wave systems. However, most numerical methods addressing the damage stability problem in accordance with relevant SOLAS regulations, in which the damaged ship is assumed with zero speed and under the excitation of beam waves.

3.3.3 Benchmark Testing of Numerical Modelling

Since 2001, the methodologies of numerical simulations appropriate for the prediction of capsize of damaged ships in waves were monitored and have been benchmarked by the 23rd, 24th and 25th ITTC Specialist Committee on the Prediction of Extreme Motions and Capsizing (now Committee on Stability in Waves). (Papanikolaou, 2001) (Papanikolaou and Spanos, 2004a) (Papanikolaou and Spanos, 2004b).The main objective of the comparative studies is to assess existing mathematical models and software tools developed by qualified research institutions regarding the capability to predict ship survivability.

It is noted that there are only a limited number of independently developed and mature numerical tools/codes available worldwide for assessing damaged ship behaviour in waves. With a detailed summary of three benchmark studies provided in Appendix 2, the following paragraphs attempt to highlight key issues influencing the quality/uncertainty of the analyses.

3.3.3.1 The 23rd ITTC Benchmark Study

A midship damage condition has been selected for this benchmark study (Vassalos and Jasionowski, 2000). Based on the numerical results presented by the five participants, the GZ curves in both intact and damaged cases were depicted in Proceedings of the 23rd ITTC (Greene, 2003), as shown in Figure 3.3.

The observed differences are minor in the intact condition. However, the GZ curve from Participant 3 shows higher initial restoring ability for the flooded ship, whereas the range of stability computed by Participants 2 and 5 is noticeably lower. Only Participants 1 and 4 properly capture the hydrostatic properties of the benchmark ship over the entire stability range.

The accuracy of hydrostatic calculations of the numerical codes depends on the discretisation of the ship's geometry, which explains the differences observed in Figure 3.3. In fact, any inaccuracy in the geometry and ship hydrostatics calculation would affect the estimated restoring ability of the ship and hence her natural frequencies. Therefore, it necessitates estimating underlying uncertainties during this process. In this case, uncertainties can be reduced through a proper modelling of ship hull geometry by using different numerical models and assuring the floodable volume for each of the same damaged compartments are comparable.

The survivability boundaries obtained by using various numerical simulation models and physical experimental results are compared and shown in Figure 3.4. Explicitly, the reliability of the achieved values is not measured. It should be borne in mind that uncertainty analysis represents a key element in this benchmark study and needs to be addressed.

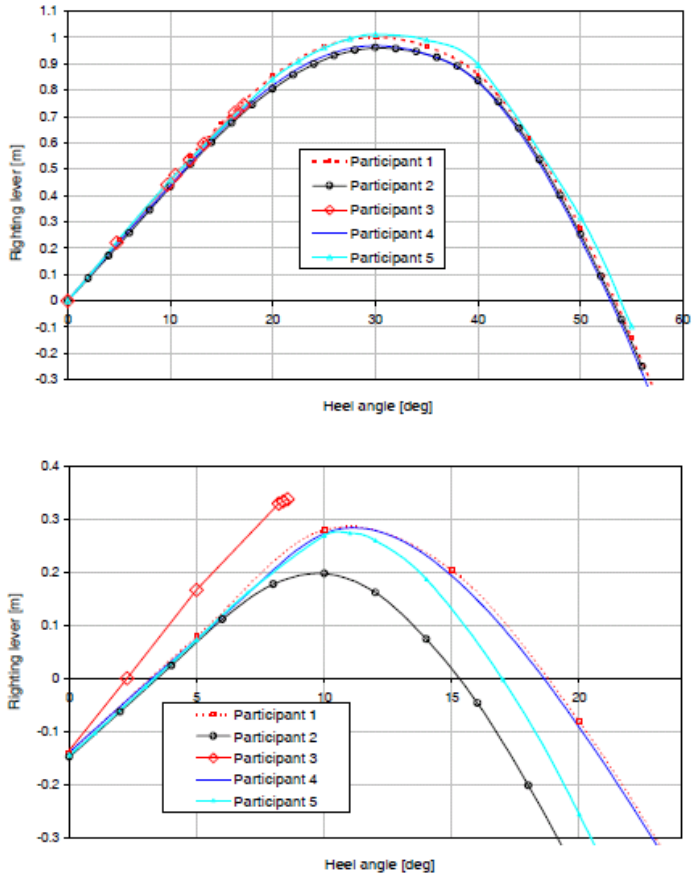

Figure 3.3: Computed GZ curves in intact and damaged condition

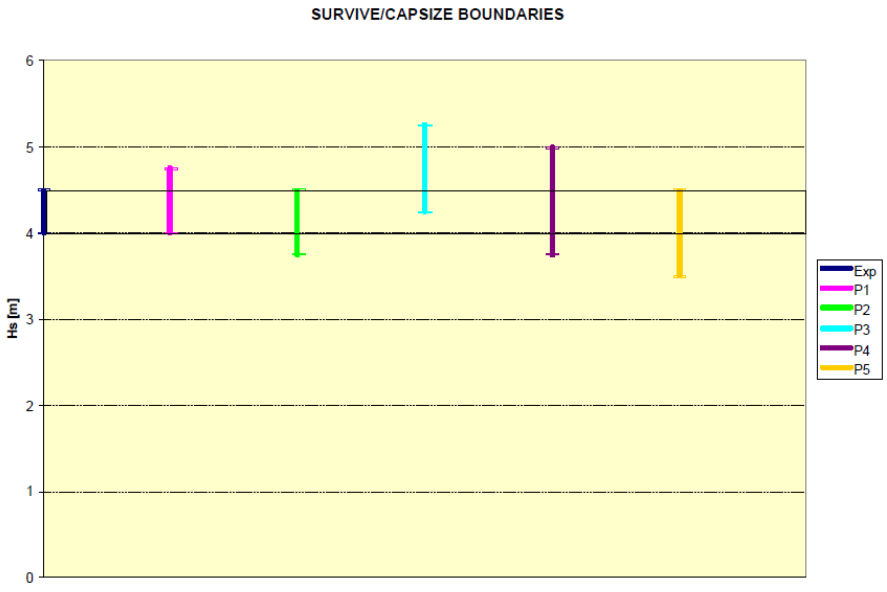

Figure 3.4: Comparison of the Simulated Survive/Capsize Boundaries with Model Experimental Values (Papanikolaou, 2001)

3.3.3.2 The 24th ITTC Benchmark Study

The basic objective of the second benchmark study was to provide insight into the fundamental properties of the numerical methods employed for the prediction of motions and capsizing of damaged ships in waves. Some detailed results can be found in (Papanikolaou and Spanos, 2004a) (Papanikolaou and Spanos, 2004b).

The published results only focused on the 1st phase study, in which the effect of wave induced forces was excluded. There were four test series included. All of them referred to the free roll motion of ship models in calm water. A range of benchmark tests have been performed to study the fundamental physical phenomena taking place in the motion of damaged ships in waves and of the corresponding modelling implemented in numerical methods. The main interests were placed on the flooding process through a damage opening and the floodwater effects on the ship motions.

Based on the comparison of the numerical results with relevant experimental data, some concluding remarks and recommendations were summarised in Proceedings of the 24th ITTC (Hair, 2009).

- Regarding the prediction of the natural roll period, the sensitivity of the various methods with respect to the changes in the hull condition, is less satisfactory in the damage condition, whereas changes in the KG value are satisfactorily captured. Special attention should be given in the evaluation and sensitivity of the roll radius of gyration both as to the inertia and associated hydrodynamic terms.

- Regarding the prediction of the damping rate, observed deviations between the numerical methods in the damage condition were found to be mainly due to different approaches to the effects of floodwater on ship motions. It seems the numerical methods that considered the floodwater having its free surface continuously horizontal could not capture the floodwater dynamics properly. Those methods considering the free surface moving were satisfactory. Therefore, the significance of the floodwater dynamics on ship motion in terms of stability should be assessed.

- The results of the transient flooding tests showed that employed semi-empirical coefficients greatly affect simulated results. Special focus should be given on the semi-empirical weir coefficient as well as the implementation of the flooding model.

3.3.3.3 The 25th ITTC Benchmark Study

The first part of the 25th ITTC benchmark study was carried out in conjunction with the European research project SAFEDOR (2005-2008). As a continuation of the two earlier benchmark studies, this work persisted in reviewing the developments in numerical models of damage stability in waves. Moreover, this benchmark study also assessed the length of time to sink or capsize (time-to-flood) for damaged passenger ships by using existing tools. Results were collected in Proceedings of the 25th ITTC (Kalbfleisch, 1985).

Firstly, as reported in (Papanikolaou and Spanos, 2008), the numerical simulation of the survival boundaries is given in Table 3.1. It appeared that only two codes (P1 and P4) matched well with the experimental results.

Table 3.1: Survival Boundary in (m) for the Basic Test Case

Participant	H_s, surv	Mean	Diff. from mean	Exp.
P1	3.23	3.00	+0.23	≤3.00
P2	1.75		-1.25	
P3	4.00		+1.00	
P4	3.00		+0.00	

Secondly, regarding the benchmark testing on numerical methods for the prediction of time-to-flood of damaged ships in waves, the 2nd sub phase of the study was conducted based on a realistic passenger ship (designed by SSRC) with complex internal geometry. But there was no experimental data available to conduct a true benchmark study. Due to the complexity of the simulation, only two participants (i.e. SSRC, MARIN) completed this study. The results indicated that, for the most severe flooding and sea conditions, there were considerable differences in the predictions from the two numerical codes for the time-to-flood.

It should be borne in mind that the problems identified in the successive benchmark studies are not only caused by the uncertainties associated with the numerical codes (e.g. lacking knowledge on ship dynamics and floodwater dynamics), equal attention should be paid to the uncertainties associated with model testing, as well. Typical restrictions imposed on physical model experiments consist of the limitation of tank dimensions, inaccuracies in model construction and outfit (e.g. construction material, uppermost limit of accurate modelling, model scale, instrumentation and equipment, control of models) and inaccuracies during the test (e.g. initial conditions, start of data acquisition, distance from wave maker, wave spectral shapes, model speed measurement).

3.4 Uncertainty Analysis Methods

As it is stressed in the foregoing, there are constraints associated with performance-based methods for the assessment of damaged stability in waves. There are many sources of uncertainties arising from both natural variability and model imperfections. The uncertainties introduced during the survivability assessment are primarily related to the assumptions and the simplifications made when developing different tools to make the problem manageable or to reduce the complexity. The knowledge-based gaps once again confirm the importance of modelling uncertainty on the prediction of motions and the time-to-flood of damaged ships. A number of research works have been completed since then to explore the encountered technical difficulties (Gao, 2012a) (Gao, 2012b) (Cichowicz, 2012) (Shen, 2011) (Strasser, 2010).

It is known that capsizing is a rarely occurred event creates a significant challenge for verification and validation tasks. In general, uncertainties associated with risk analysis in engineering fields are addressed by employing probabilistic methodologies. There are also some other methods to represent uncertainty, such as interval analysis (Moore, 1966) (Moore and Bierbaum, 1979) (Alefeld and Herzberger, 1983), fuzzy arithmetic (Zadeh, 1965) (Helton et al., 2004) and probability bounds analysis (Ferson and Ginzburg, 1996). Nevertheless, probabilistic approaches still represent the main stream for uncertainty analysis. A literature review of available methods on probabilistic uncertainty analysis is made next.

3.4.1 General Procedure of Probabilistic Uncertainty Analysis

In principle, a general procedure of uncertainty analysis follows the uncertainty propagation process through a model as shown in Figure 3.5 (IAEA, 1989). Within this top-down process, the uncertainties in the model output represented by the probabilistic distribution arise from the propagation of the uncertain input variables through the model with imperfections, as it is unsuspected that any theoretical or simulation model developed to date is inevitably a simplification of the reality.

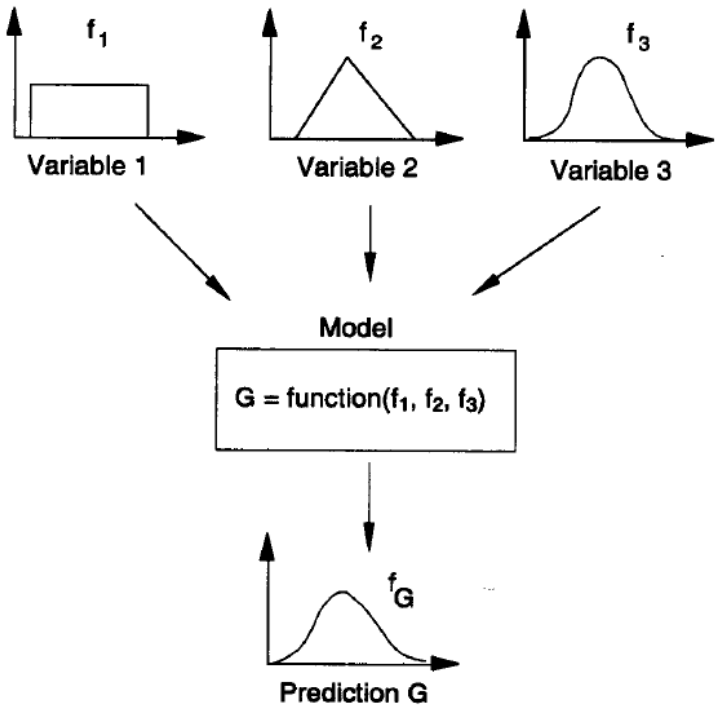

Figure 3.5: Propagation of Uncertainty through a Model. (IAEA, 1989)

There are two sources of uncertainty in modelling that need to be addressed separately. Firstly, the parameter uncertainties displayed at the top level, as shown in Figure 3.5, denotes the uncertainties in the input variables. They can be represented by assigning a proper probability distribution for each of them. Secondly, the model uncertainties, denoted in the mid layer, are mainly stemmed from incomplete knowledge. A common treatment is to make use of several parallel models to enhance the credibility of the final results. The probabilistic methods used to represent the parameter uncertainty are the focus in the following section.

3.4.2 Methods for Probabilistic Uncertainty Analysis

In practice, there are two main and distinct approaches to statistical inference, namely frequentist and Bayesian statistics (Vose, 2008) (Morgan et al., 1990). Thus the nature of probability can be thought differently from two perspectives: i) for the frequentist approach to statistics (also known as the classical approach), the notion of probability is defined as a limiting long-run frequency, and applies only if one can identify a sample of independent, identically-distributed observations of the phenomenon of interest (Von Mises, 1957). It is clear that the considered events should be (at least in principle) repeatable, ii) in contrast, the Bayesian approach defines probability as a degree of belief about the value of an unknown parameter. The supporting information includes not only statistical data and physical models, but also expert (subjective) opinions (Lindley, 1965) (De Finetti, 1974).

3.4.2.1 The Frequentist Statistics

The frequentist approach is the common statistics perceived by most people. The relevant methods for probabilistic uncertainty propagation mainly consist of two aspects: analytical methods and simulation-based methods.

Analytical methods: The exact analytical methods of propagating uncertainty are rarely employed in risk analysis since they are only tractable for simple cases, such as linear models of normal variables. The input variables are assumed to be statistically independent, random, and normally distributed about a mean value. These assumptions simplify the implementation and help quantify the input uncertainties, but they overlook the correlations between the variables and can be easily accounted for the knowledge-based uncertainties in models. The original model is generally approximated based on Taylor series expansion. In this case, the mean, the variance and sometimes higher order moments of the probability distributions are used for uncertainty propagation and analysis. It can be seen that higher order terms in the Taylor expansion must be included when the variance in the input is large. This introduces more complexity in the computations, especially for dealing with the complex models, which is often the case in risk analysis.

Simulation-based methods: Considering the limitations of the analytical methods mentioned above, simulation-based methods become more popular to tackle probabilistic uncertainty analysis due to the rapid development in personal computation power and software technologies.

The core of the simulation-based method is to generate samples of input parameters, which follows the predefined probability distributions. The sampled parameters can then be fed into the model and a sample of model output can be calculated. In turn, the mean, the variance and the empirical distribution of the model output can be estimated. By doing so, the uncertainties in the model itself can be explicitly quantified. In practice, two different sampling procedures for generating the input distributions of a model are considered: random sampling and Latin hyper-cube sampling.

Firstly, the oldest and best known random sampling method that has been extensively employed in uncertainty analysis is the Monte-Carlo simulation (Sobol', 1974). (Vose, 2008) gives an explicit presentation of how the method works. Some basic features are revisited here. Suppose the distribution of an uncertain input variable x satisfies the cumulative distribution function $F(x)$, it provides the probability P that the variable X will be less than or equal to x (i.e. $F(x) = P(X \leq x)$ ranges from 0 to 1). In this situation, the inverse function $G\big(F(x)\big)$ can be used to generate the random input variables x from the given distribution (i.e. $G\big(F(x)\big) = x$). With respect to the reverse function concept, $r = F(x)$ is treated as a random number in order to provide equal opportunity of an x value being generated in any percentile range. Many algorithms have been developed to generate a series of uniformly distributed random numbers r between 0 and 1 (i.e. uniform $(0,1)$). A graphical representation of the relationship between $F(x)$ and $G\big(F(x)\big)$ is depicted in Figure 3.6.

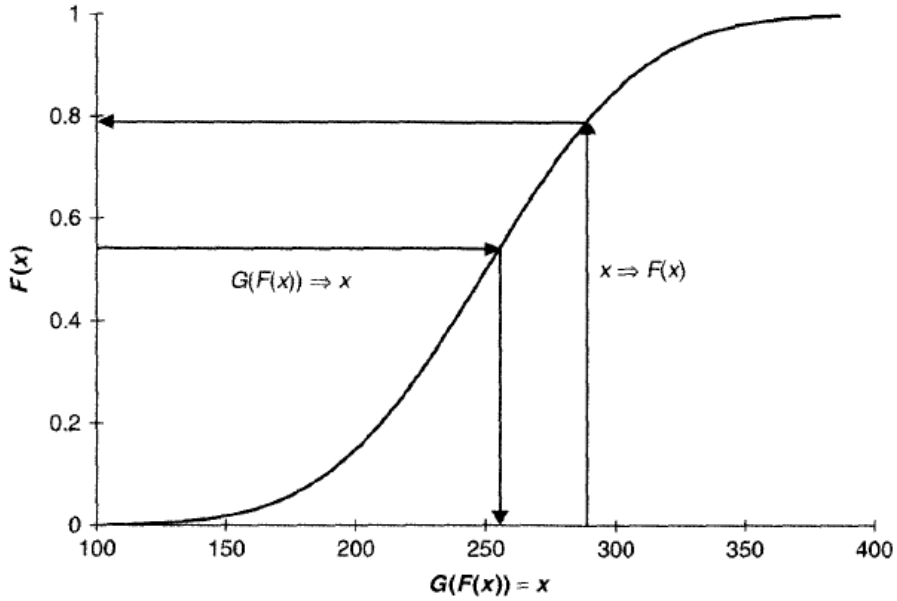

Figure 3.6: The Relationship between x, $F(x)$ and $G\big(F(x)\big)$. (Vose, 2008)

The random sampling method described above is adopted by Monte Carlo simulation. Bearing in mind that the randomness of sampling may lead to over- or under-sampling from various parts of the input distribution of a model, the pre-specified distributions cannot be replicated but the desired shape can be approximated through a large number of iterations. Thus the main concern of this sampling scheme is by which the distributions as determined for the model inputs should be reproducible. In contrast, Latin hypercube sampling addresses this issue by providing a sampling method that appears random but that also guarantees to reproduce the input distribution with much improved efficiency.

Secondly, Latin hypercube sampling (LHS) is an option that is also available for most risk analysis modelling. It uses a technique known as "stratified sampling without replacement" (Iman et al., 1980) and follows a procedure as presented in (Vose, 2008):

- The probability distribution is divided into n intervals of equal probability, where n is the number of iterations that are to be performed. An example of the stratification as illustrated in Figure 3.7, which is produced for 20 iterations of a normal distribution. The bands become progressively wider towards the tails as the probability density drops away.

- In the first iteration, one of these intervals is selected using a random number.
- A second random number is then generated to determine where, within that interval, $F(x)$ should lie.
- $x = G\big(F(x)\big)$ is calculated for that value of $F(x)$.
- The process is repeated for the second iteration, but the interval used in the first iteration is marked as having already been used and therefore will not be selected again.
- This process is repeated for all of the iterations. Because the number of iterations n is also the number of intervals, each interval will only have been sampled once and the distribution will have been reproduced with predictable uniformity over the $F(x)$ range.

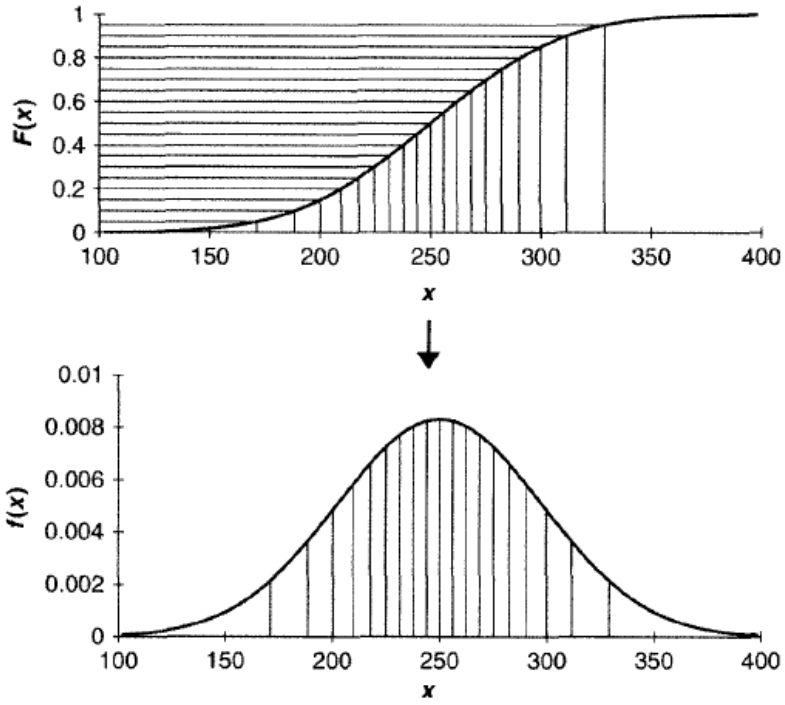

Figure 3.7: The Effect of Stratification in Latin Hypercube Sampling. (Vose, 2008)

Comparing with the random sampling method, the LHS method can reduce the variance of the uncertainty and thus requires much less samples (Stein, 1987).

However, it has poor coverage at both ends of the input parameters and so this is a problem especially when the tails of the distributions are of interest in risk analysis. It is therefore preferable when a large number of samples are infeasible for computationally expensive models. A number of comparisons between random sampling and LHS have been discussed in (McKay et al., 2000) (Helton and Davis, 2002) (Helton and Davis, 2003) (Helton et al., 2005) (Helton et al., 2006). No matter which sampling procedure is adopted, a great deal of empirical information has to be taken into account, for instance, the empirical information on the distribution of all input variables, their correlations and dependencies. In practice, this often forces the analyst to make assumptions (i.e. independence). In short, within the simulation-based methods, it is impossible to separate different sources of uncertainties (i.e. stochastic uncertainty and knowledge-based uncertainty are combined).

3.4.2.2 The Bayesian Statistics

The fundamental feature of the Bayesian approach to statistics is to synthesize two sources of information about the unknown parameters of interest. The first source is the sample data, expressed formally by the likelihood function. The second is the prior distribution, which represents additional (external) information that is available to the analyst. A schematic representation of this process is given in Figure 3.8. The result of combining the prior information and data in this manner is a posterior distribution, from which the inferences about the unknown parameters can be derived.

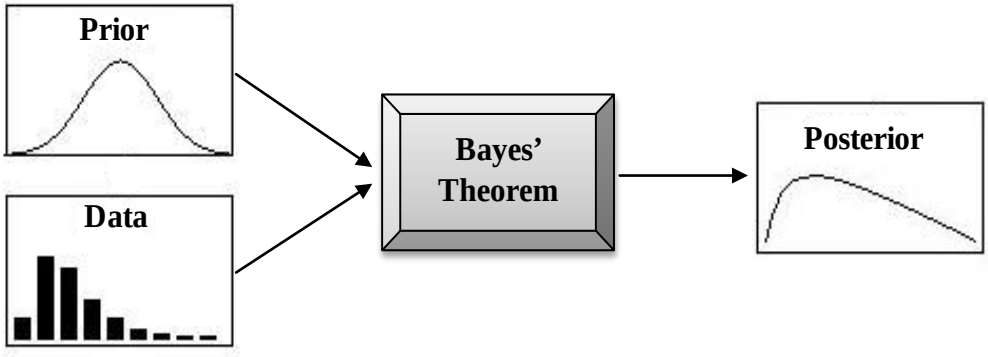

Figure 3.8: The Bayesian Method

With the application of Bayes's Theorem (Lee, 2004), the posterior distributions for the unknown parameters are computed through Bayes' equation:

$$P(\theta|\boldsymbol{y}) = \frac{P(\boldsymbol{y}|\theta)P(\theta)}{P(\boldsymbol{y})} = \frac{P(\boldsymbol{y}|\theta)P(\theta)}{\sum P(\boldsymbol{y}|\theta)P(\theta)} \quad (7)$$

Where θ denotes either a single or a set of unknown parameters, and $\boldsymbol{y}$ is the observed data, then:

- The likelihood function $P(\boldsymbol{y}|\theta)$ is the conditional probability of data $\boldsymbol{y}$ depending on parameter θ, which is also the foundation to frequentist inference.
- The prior distribution $P(\theta)$ is used only in the Bayesian approach. The assignment of distributions should be based on the additional information that is available.
- If the range of possible values of θ is assumed to be discrete, summations can be performed.

In reality, Bayes' equation (7) can be simplified to,

$$P(\theta|\boldsymbol{y}) \propto P(\boldsymbol{y}|\theta)P(\theta) \quad (8)$$

The proportionality symbol $\propto$ denotes that the product of the likelihood function and the prior distribution on the right hand side of Equation (8) must be scaled to integrate to 1 over the range of plausible θ values so that a proper probability distribution can be generated. The scaled product $P(\theta|y)$ is defined as the posterior distribution for θ given the data, and expresses what is now known about θ based on both the sample data and prior information, as shown in Figure 3.9.

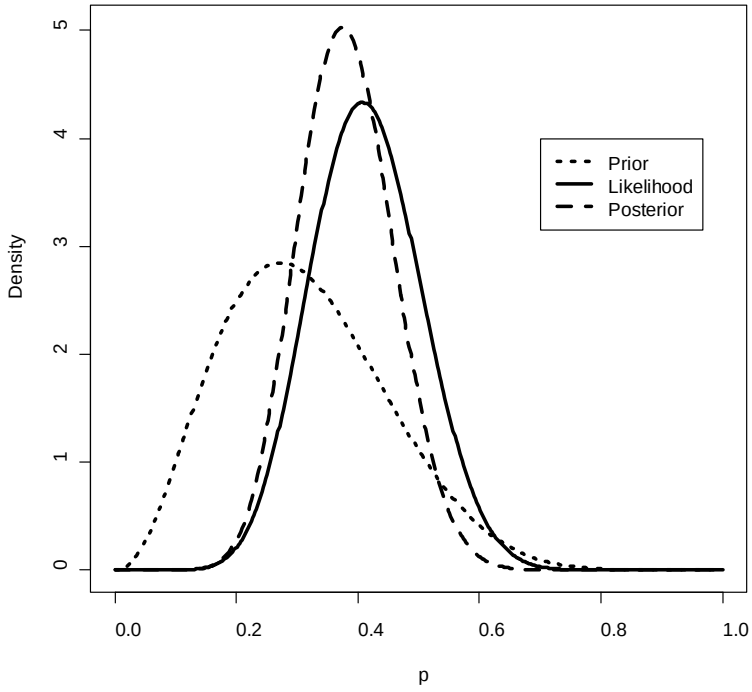

Figure 3.9: Example of a Triplot

As can be seen, the posterior distribution for θ is a weighted compromise between the prior information and the sample data. In general, the posterior probability will be high for some θ only when both information sources suggest so. The simple and intuitive nature of Bayes' theorem as a mechanism for synthesising information and updating personal beliefs about unknown parameters is an attractive feature of the Bayesian method. The mainly concern so far has centred on the reliability of the subjective prior distributions of the unknown parameters.

3.4.3 Comparison between Frequentists and Bayesians

In this section, a brief comparison between frequentist and Bayesian statistics is considered from three fields, comprising the nature of probability, parameters and inferences.

- For the nature of probability, frequentist and Bayesian methods are founded on different notions. In frequentist statistics, probability applies only to the events that are (at least in principle) repeatable. And thus probability is a limiting frequency. In contrast, Bayesian statistics is founded on an interpretation of

probability, which is a measure of the degree of personal belief about the value of unknown parameters. Therefore it is possible to ascribe probability to any event which is uncertain, including those that are not repeatable.

- For the nature of parameter, statistical methods are generally formulated as making inferences about unknown parameters. In frequentist statistics, parameters are recognized as fixed quantities, which cannot be considered as random variables. In contrast, from the Bayesian perspective, the parameters can be thought of as being random variables. It is legitimate to make probability statements about them, simply because they are unknown. A fundamental feature of the Bayesian approach to statistics is the use of prior information represented as all the available knowledge apart from the observed (sample) data, no relevant information is omitted in a Bayesian analysis. In short, under frequentist methods the data is random and the parameter is fixed, while under Bayesian methods the parameter is a random variable and the data is fixed.

- For the nature of inference, the problem is of what values of θ are reasonable given the observed data y. In frequentist statistics, confidence intervals are the major tool to provide an answer. Notice that under this approach the parameter is fixed that cannot be considered to have a distribution of possible values. The true value is not a random variable, but the confidence interval is random as it depends on the random sample. Thus, a confidence interval can be defined as $I \equiv [lb(y), ub(y)]$ with the property of $P(\theta \in I) = 0.95$. It indicates the true value is either in the interval or outside the interval. The confidence interval then is a statement about the likelihood that the interval we have obtained actually has the true parameter value. Thus, the probability statement is about the interval (i.e. the chances that interval has the true value or not) rather than about the location of the true parameter value. In the frequentist term, it is meaningless to speak about the probability that a true value is less than or greater than some values as the true value is a non-random parameter. In contrast, in Bayesian statistics, the true value is assumed as a random variable. Using Bayes's Theorem, the posterior distribution for the parameter vector can be constructed by blending the prior distribution on the true parameter $P(\theta)$ and the observed data $P(\boldsymbol{y}|\theta)$. In

turn interval estimation can be performed using the posterior distribution. A credible interval has the following holds of $P\big(lb(\theta) \leq \theta \leq ub(\theta)\big) = 0.95$. For example, in an experiment that determines the uncertainty distribution of parameter θ, a frequentist 90% confidence interval of 30 – 40 means that with a large number of repeated samples, the calculated intervals (i.e. 30 – 40) contain the true value of the parameter with a probability of 90%. The probability that the parameter is within the given interval is either 0 or 1(the no-random unknown parameter is either there or not). In contrast, from a Bayesian point of view, if the probability that θ lies between 30 and 40 is 90%, and then $30 \leq \theta \leq 40$ is a 90% credible interval. In short, credible intervals capture the current uncertainty in the location of the parameter values and thus can be interpreted as probabilistic statement about the parameter. In comparison, confidence intervals capture the uncertainty about the interval that has been obtained (i.e. whether it contains the true value or not). Therefore, they cannot be interpreted as a probabilistic statement about the true values.

3.5 Closure

The understanding of the diffidence between the frequentist and Bayesian approach signals that choosing an appropriate probabilistic uncertainty analysis method should be based on the problem under consideration. In Section 3.3, it mainly elaborates knowledge-based gaps in the first-principles tools for the assessment of damage ship stability in waves. The epistemic uncertainties on the prediction of motions and the time-to-flood of damaged ships are recognized as a significant challenge and thereby must be quantified.

Through reviewing the classes of uncertainty and probabilistic methods of representing uncertainty, it should be comprehended that randomness or aleatory uncertainties can be treated by classical frequentist methods and propagated through the analysis, for example, by Monte Carlo simulation. Yet, the frequentist definition of probability becomes inapplicable for the knowledge-based uncertainty or when available samples are insufficient to represent the exact phenomenon of interest. However, decisions often have to be made in the absence of such samples. The

Bayesian approach allows the integration of all available evidence in the assessment of probabilities. It enables quantification of both aleatory and epistemic uncertainties, for which the combination of their measures into a single probability distribution is very desirable for representing the consequences of an undesirable event (e.g. time-to-capsized of damaged ships in given condition).

Chapter 4

Approach Adopted

4.1 Preamble

In Chapter 3, a state-of-the-art review of performance-based methods addressing the prediction of motion of damaged ships in waves has been provided. Knowledge-based imperfections in the current numerical tools emphasize that uncertainty analysis in performance-based ship safety assessment is important. This chapter intends to disclose a methodology to be followed throughout this thesis, the constituent components of which are elaborated in turn.

4.2 Outline of the Approach

Concerning the overall objectives of this thesis as stated in Chapter 2, significant emphasis is placed on uncertainty quantification in the assessment of damage ship survivability. Knowing that knowledge-based uncertainties of performance-based tools (e.g. addressing flooding-related risk) are a key element in the procedure for risk assessment and the ensuing decision making, thus uncertainties in the outputs (e.g. ship survivability) should be estimated. By doing so, the quality of risk assessment can be assured.

On the one hand, the prediction of ship survivability in the event of flooding is a critical issue for assessing passenger ship safety. This is because flooding-related scenarios are recognized as a principle accident category. From a ship safety level point of view, uncertainty quantification in risk assessment can be decomposed into more understandable and manageable components in connection with different risk drivers. In this sense, uncertainties associated with the overall ship safety can focus on these individual components rather than on the entire problem. Once this is done, appropriate computations can be performed to piece the components together and produce an overall estimation. This philosophy coincides with the guiding principle

in decision analysis, known as ‘divide and conquer’, for tackling a complex decision-making problem. As a typical application, the elicited methodology for modelling uncertainty in the assessment of ship survivability paves the way for quantifying uncertainties in risk analysis of other dominant loss scenarios.

On the other hand, attempting to treat aleatory uncertainties in parallel with epistemic uncertainties in performance-based safety assessments, Bayesian approach is the method that is believed to be more rational than the classical frequentist approach to undertake more complex problems. This is because the former allows making statistical inferences when sufficient samples are not available to represent the phenomenon of interest (i.e. ship capsizing in the event of flooding), and also it offers more intuitive and meaningful inferences through a posterior probability distribution for quantifying uncertainties directly. In this way, a formalised procedure for addressing uncertainty in survivability assessment of a damaged ship can be established.

4.3 Implementation Process

The approach adopted in this thesis is constituted by a three-stage process as summarised in the following:

Stage 1: Development of a Mathematical Modelling Framework for Ship Survivability Assessment

In the era of performance-based assessments of extreme motions and ship capsizing after flooding, the accuracy of inferences depends on that of the modelling of damaged ship behaviour in waves through various first-principle tools. As indicated in Section 3.4, a general procedure of uncertainty analysis follows the uncertainty propagation process through a model. Probabilistic methods are normally employed to quantify and display uncertainties.

Hence, a mathematical modelling framework must be structured with dual features. Firstly, it should be able to systematically utilise available information (including input and output) from existing performance-based tools and thereby to make predictions on the problem under consideration (e.g. damaged ship survivability).

Secondly, it should be able to provide a platform for uncertainty propagation. In practice, models in the form of analytical expressions are desired. Knowing most of the numerical models commonly used in quantitative risk analysis are computer-based programs, regression analysis may be applied to produce an analytical expression for the expected models, based only on a few dominant input variables, representing the more complex computer model. The regression model can accommodate the propagation of uncertainty afterwards.

In so doing, this stage aims to put forward a mathematical model which is suitable to predict the "time to capsize" (i.e. the time is available for evacuation) for a damaged passenger ship after flooding. The governing parameters having significant influence on the phenomenon of ship capsizing will be identified. Moreover, appropriate multivariate data analysis techniques will be selected for transforming the available information from first-principles tools into interpretable and manageable knowledge.

Stage 2: Probabilistic Uncertainty Analysis through a Bayesian Inferential Procedure

A generic mathematical model is identified in the first stage for making predictions of the interested phenomena. Three elements of the model can be addressed: i) the explanatory variables; ii) the output variable; and iii) the linking function and model coefficients to correlate the explanatory variables and output variable.

The focus of this stage is on estimating the model through assessing the probability distribution for all the model coefficients. It should be borne in mind that each coefficient is affected not just by the relationship between the corresponding explanatory variable with the response variable, but also by the other explanatory variables in the model and the dependent relationships among the explanatory variables.

In order to explore the variability of the unknown model coefficients, available information from a variety of sources (e.g., via numerical models and physical model experiments) should be considered. This can be done through Bayesian inferential procedures (Raiffa and Schlaifer, 1961) (DeGroot, 1970) (Winkler, 1972) (Berger,

1985), since the key feature of Bayesian statistics is it makes use of all available information to infer probability distributions for the unknown parameters. In this manner, uncertainties of unknown model parameters can be quantified, which also implies the model estimation phase is completed. Then uncertainties of the model response can be investigated when the values of model inputs are given.

Based on the predictive model structured in the previous phase, this stage aims to deploy Bayesian inferential techniques for model estimation. At last, probabilistic uncertainty analysis of the model output can be performed.

Stage 3: Implementation of the Proposed Uncertainty Analysis Scheme in Shipboard Decision Support for Flooding Damage Control

In practice, there is no doubt that a fast and reliable assessment of damage ship stability can add value to the real-time decision support for flooding crisis management. Accordingly, a prompt evaluation of ship survivability after flooding and the quantification of uncertainties associated with the whole evaluation process are of vital important in decision making. From this point of view, decision support for flooding-related emergency control characterizes a potential application of the proposed uncertainty modelling.

Deriving from the above, the last stage aims to propose a field of application of the proposed uncertainty analysis scheme, and then to demonstrate its applicability in shipboard decision support for flooding damage control.

4.4 Closure

The key roles of the aforementioned stages can be summarised as follows: i) Model identification; ii) Model sensitivity and uncertainty analysis through model estimation; and iii) Model application.

The relationships among them and their related chapters are depicted in Figure 4.1. Detailed working principles, methodologies, techniques, configurations and illustrative applications for each stage are elucidated in Chapters 5, 6 and 7 respectively.

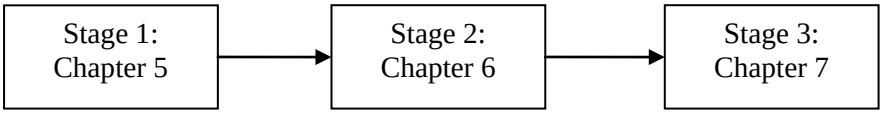

Figure 4.1: Structure of the Implementation Stages

Chapter 5

Modelling Ship Survivability Assessment

5.1 Preamble

This chapter focuses on setting up a mathematical modelling framework for assessment of ship survivability due to flooding after collision, which formalises the assumptions about the relationships between dominant physical parameters and the behaviour of a damaged ship. The expected model should be also appropriate for expressing uncertainty about the predictive phenomenon. In so doing, the model under construction should have two built-in attributes: i) it enables the prediction of ship survivability after flooding to reflect the simulated ship behaviours in waves through various first-principles tools; ii) it allows uncertainty propagation to be observable.

Taking these into consideration, typically there are two parts need to be structured for building up the model:

- Identification of the key influencing parameters that affect and characterise the simulated phenomenon of ship capsizing due to flooding.
- Selection of the relevant methodologies, techniques that facilitate the formulation of particular link functions to explain how input variable(s) and response variable(s) are related with respect to the identified problem.

5.2 Influencing Parameters in Assessment of Ship Survivability

The phenomenon under investigation is the ship behaviour when subject to collision damage. Obviously, a dependent relationship between ship response and input

variables is sought to be established. As depicted in Figure 5.1, propagation of uncertainty can be interpreted as translating uncertainty about model inputs into uncertainty about model outputs by using a particular regression model. Three influencing parameters in modelling (i.e. input variables, first-principles models, and the output variable) are explained individually in the following subsections.

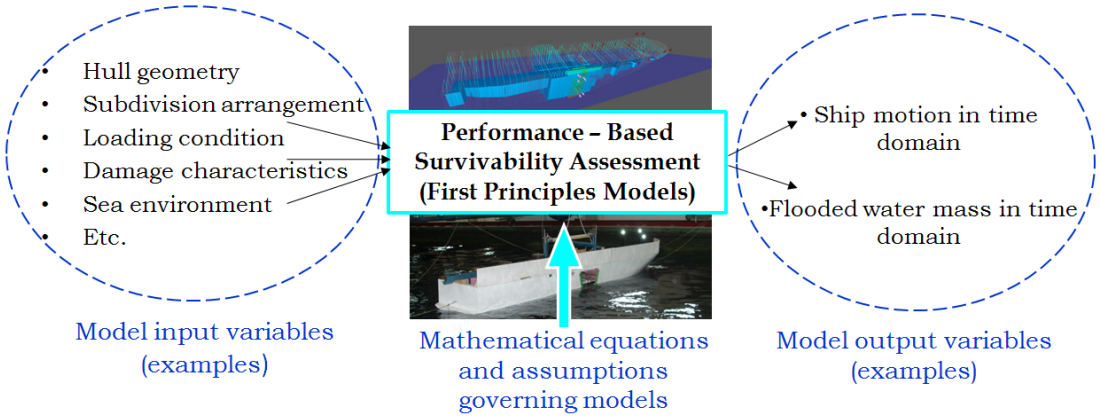

Figure 5.1: Sources of Uncertainty in Modelling

5.2.1 Dominant Explanatory Variables

Ship capsizing presents a complex and dynamic phenomenon, the accuracy of which in numerical prediction depends on the accuracy of the model to capture the nonlinear motions of the ship and the flooding process in time domain. Generally, there are more potentially relevant variables than we can realistically include in a model. It is important to keep the list of explanatory variables compact so as to maintain a well balance between the number of key inputs influencing ship survivability and the quality of the model.

In order to quantify the characteristics of the random process of the time it takes a ship to capsize from the instance of hull breach, the variety of information about the damage condition should be integrated into the model. Bearing in mind ship damage stability is a subject that started to develop as a scientific field in the late 80's and early 90's. The latest development for the assessment of ship survivability, is presented in the current IMO minimum damage stability requirements, detailed in SOLAS Ch II (IMO, 2006c). The probabilistic rules were derived with the help of

the HARDER project and entered into force in 1st of January 2009. Comparing with traditional deterministic methods, this instrument is founded on the basis of detailed studies on the data collected at IMO about historical worldwide collision cases. Hence, it is appropriate to make use of the findings from the work performed to date to summarize the governing explanatory variables in a model. This includes: i) damage characteristics, ii) watertight arrangement provision, iii) ship loading, and iv) sea environment. All of them can be represented through the concept of righting lever (GZ) curves.

5.2.1.1 Damage Characteristics

The extent of damage opening is normally characterised through a set of parameters of its location, length, penetration and height, denoted as $\Omega = \{x, \lambda, b, h\}$. Considering the historical data of possible hull breach characteristics with reference to side collision accidents, the joint probability distribution $f_\Omega = \{x, \lambda, b, h\}$ can be assigned based on the updated damage statistics, as shown in Figure 5.2 (IMO, 2004b). In details, distribution functions for, non-dimensional damage location $f\left(\frac{x}{L_s}\right)$, non-dimensional damage length $f\left(\frac{\lambda}{L_s}\right)$, non-dimensional damage penetration depth $f\left(\frac{b}{B}\right)$, and damage height $f(h)$ are derived from the measure of their complements. It is worth noting that the probability of the vertical extent of damage $f(h)$ is not based on a statistical analysis of actual damages, which is purely a function of draught with the obtained formulae to developing the factor *v* (SOLAS Chapter II-1/7-2).

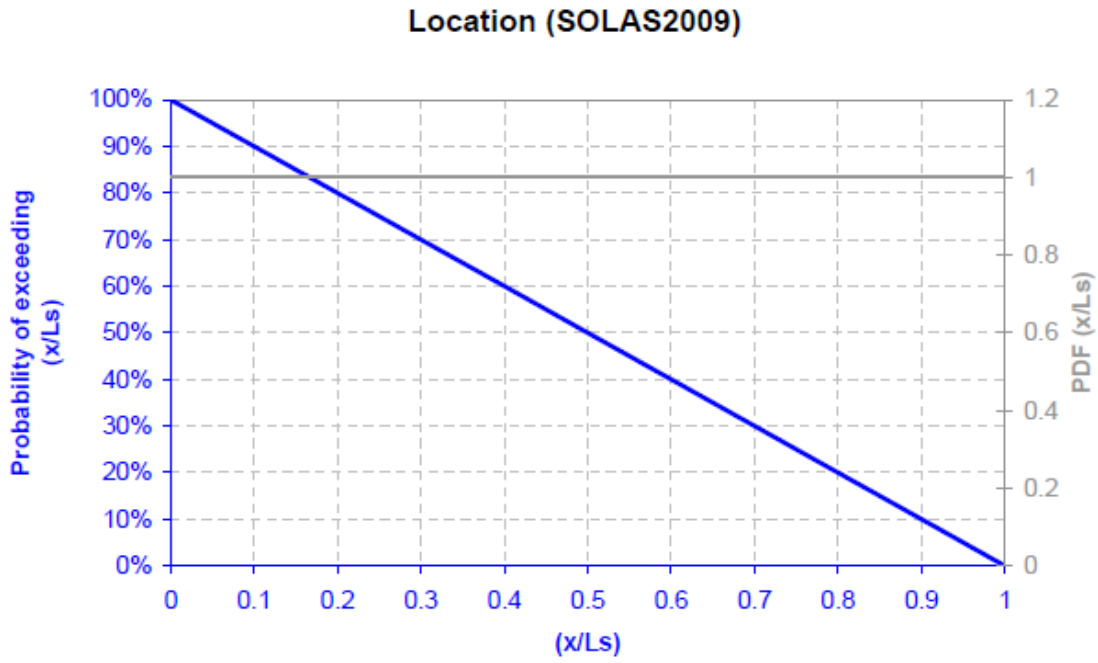
Location (SOLAS2009)
Probability of exceeding (x/Ls)
PDF (x/Ls)
100%
90%
80%
70%
60%
50%
40%
30%
20%
10%
0%
1.2
1
0.8
0.6
0.4
0.2
0
0
0.1
0.2
0.3
0.4
0.5
0.6
0.7
0.8
0.9
1
(x/Ls)

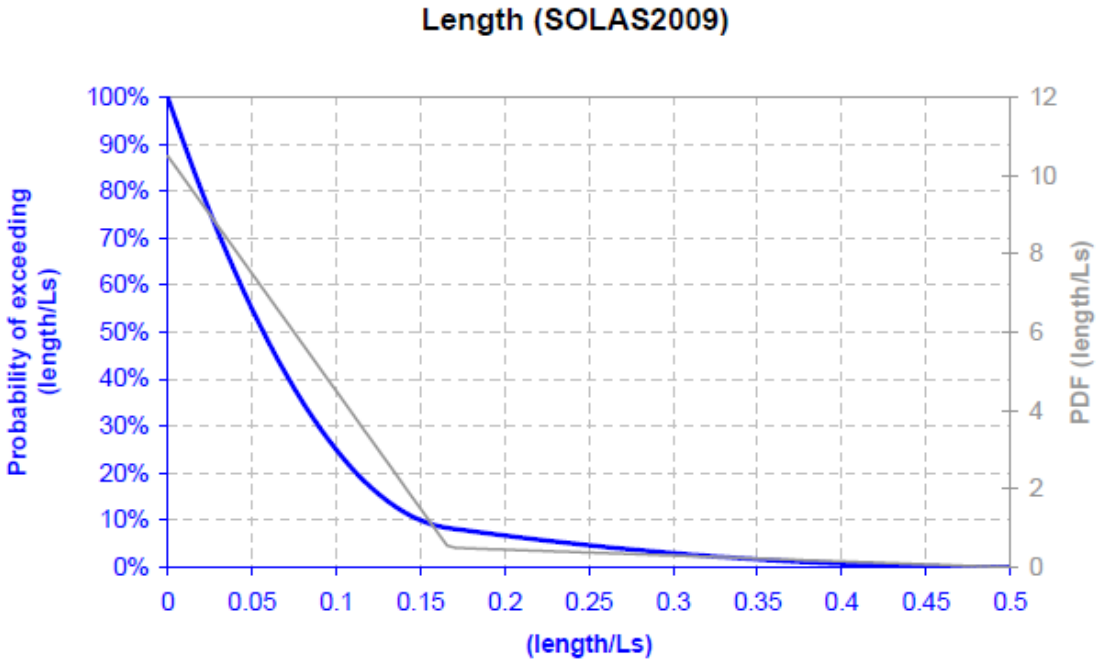
Length (SOLAS2009)
Probability of exceeding (length/Ls)
PDF (length/Ls)
100%
90%
80%
70%
60%
50%
40%
30%
20%
10%
0%
12
10
8
6
4
2
0
0
0.05
0.1
0.15
0.2
0.25
0.3
0.35
0.4
0.45
0.5
(length/Ls)

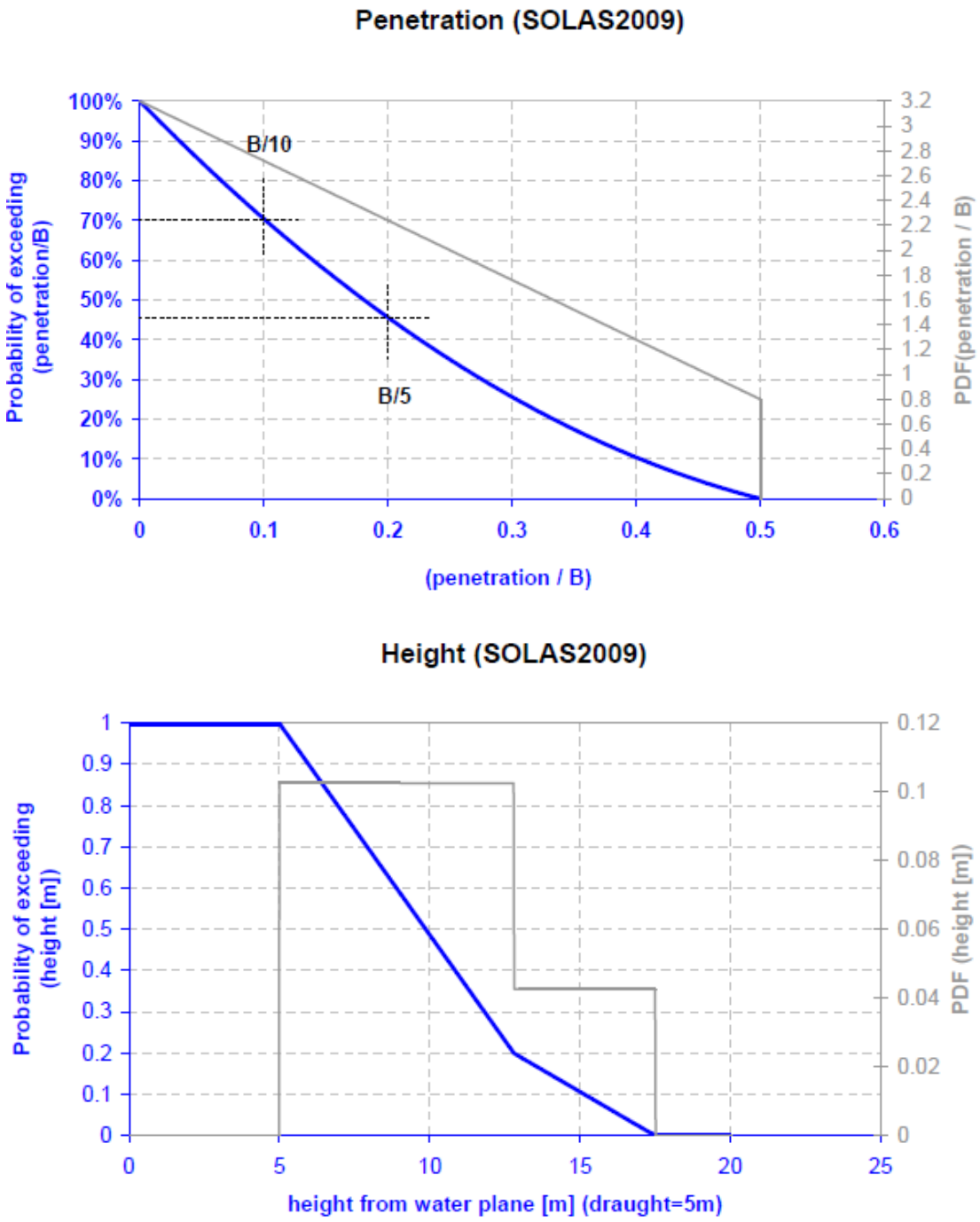

Figure 5.2: Complementary Probability Distributions for Damage Characteristics

5.2.1.2 Ship Subdivision Arrangement

In the design phase, the objective of the "probabilistic" method of determining damage stability is to ensure that ships shall be as efficiently subdivided as possible having regard to the nature of the service for which they are intended. The degree of

subdivision shall vary with the subdivision length of the ship. The common practice is that passenger ships have the highest degree of subdivision.

It is widely known that the internal subdivision restricts the extent of flooding for the damage stability calculation. Modelling both the geometry of the ship's hull and subdivisions has direct effects on the flooding process of a ship, hence the "time to capsize" in numerical predictions.

5.2.1.3 Ship Loading

The ship loading condition is a basic factor affecting ship's survivability. It generally refers to a range of operational parameters, such as draught, Metacentric Height (GM) and trim, etc. In this respect, GM is a crucial indicator of ship stability (Hoste, 1697) (Nowacki, 2007) (Lewis et al., 1988) (Derrett and Barrass, 2006). Additionally, the variation of draughts influences the hydrodynamic forces acting on the hull form. The trim effects may be also important in case of extensive flooding, which can lead to severe trims. Overall, an increment in draught or vertical centre of gravity (i.e. decreasing GM) results in the deterioration of survival wave height limit. Nevertheless, the survivability is less sensitive to the variation of trim conditions (Simopoulos et al., 2008).

5.2.1.4 Sea Environment

Sea environment plays an important role on ship survivability. The effects of wave heights and the direction of waves should be taken into account in the assessment of ship stability after flooding in seaway. Generally the significant wave height H_s is used to specify the sea state. The beam sea condition is the situation predominantly studied in numerical simulations to reflect the worst flooding case scenarios.

Moreover, historical studies on ship survivability suggest that the wave period (i.e. wave height / wave length) can be a notable parameter when short period ($H_s/\lambda = 0.04$) and long period ($H_s/\lambda = 0.018$) are assumed. In most cases ships would sustain side collision damages for a long time in waves of longer period (Spanos and Papanikolaou, 2011). As a result, numerical investigations generally refer to short wave periods so as to consider the worst case situations.

5.2.2 First-Principles Models

For modelling of the stochastic process of ship capsize due to flooding, various first-principles tools have been reviewed in Section 3.3. The following two plays particularly important roles to characterise the damage ship survivability in time-domain: numerical models and physical model experiments.

5.2.2.1 Time-Domain Numerical Simulation

As indicated in the foregoing, there are very few mature numerical models and tools for assessing damaged ship behaviours in waves up to today. In this context, one of the numerical simulation codes proposed at the University of Strathclyde is PROTEUS3. It has been developed and validated on the basis of systematic research work over the past 25 years (Turan, 1993) (Letizia, 1997) (Jasionowski, 2001a). It is elaborated and demonstrated herein mainly for the assessment of flooding and its effects on ship's damage stability. The main elements of the numerical code can be summarised as follows:

- Ship hydrodynamic forces derived from properties of the intact hull, are based either on asymmetrical strip theory formulation with Rankine source distribution or a 3D source code, (Ha, 2000) or (Papanikolaou and Zaraphonitis, 1989).
- Water ingress/egress is based on Bernoulli's equation.
- The effects of floodwater dynamics described by a full set of non-linear equations derived from rigid-body theory.
- Floodwater motions are modelled with a simplified method, as a Free-Mass-on-Potential-Surface (FMPS) de-coupled system in an acceleration field.

The output from PROTEUS3 includes time histories of the ship motions and accelerations, as well as floodwater mass, elevation and attitude in every modelled compartment of the ship. The simulated behaviour to a particular damage case is exposed in Figure 5.3 as the floodwater accumulated on the after of the car deck.

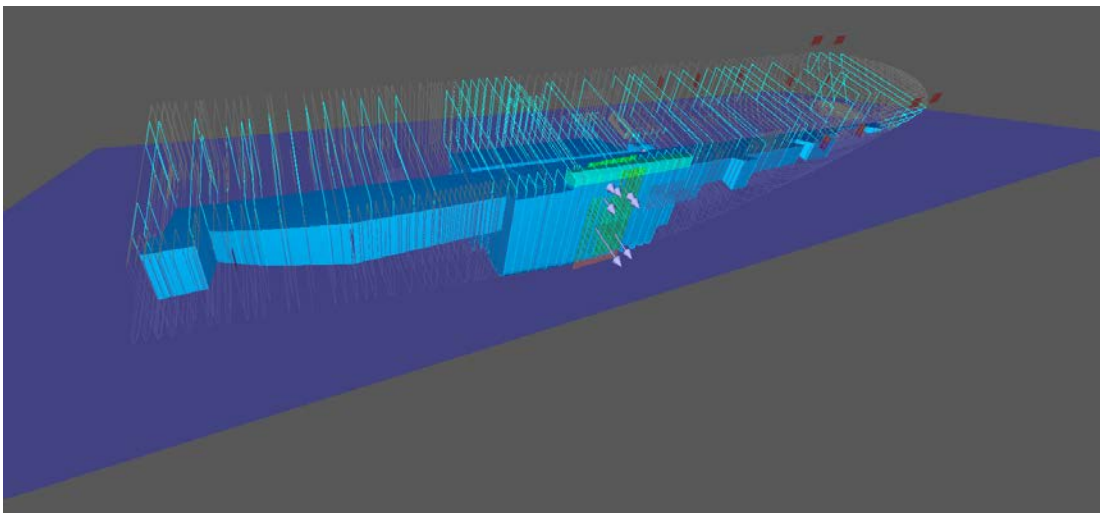

Figure 5.3: Visualization of simulation with PROTEUS3

PROTEUS3 is a ship specific time-domain simulation tool which, when coupled with Monte Carlo (MC) simulation, can estimate the likelihood of capsizing associated with the global range of damages along the ship length. Knowing that both the extents of damage and sea environment are random, a Monte Carlo sampling scheme can be employed to generate damage cases according to the collision damage statistics. Hence, the probability distributions for the damage characteristics used to derive the flooding scenarios are the same as that were employed for the development of the p-factor in SOLAS 2009, drawn from the EU project HARDER. In other words, the considered flooding scenarios reflect the cases which are implicit in the new harmonised rules for damage stability.

As illustrated in Figure 5.4, 500 damage cases of a sample RoPax ship are generated through MC sampling. All of these damages can be sorted out according to the flooding extent at a ship-level and thereby the probability of each feasible extent occurring can be assigned accordingly. Based on up to 30 minutes time domain simulations using PROTEUS3 in this case, as shown in Figure 5.5, it is possible to construct the distribution of probability to survive and capsize within given time against each of the flooding extents in the fully loaded condition. As a result, the "averaged" probability that the ship will survive all the selected flooding scenarios based on MC samplings can be allocated explicitly.

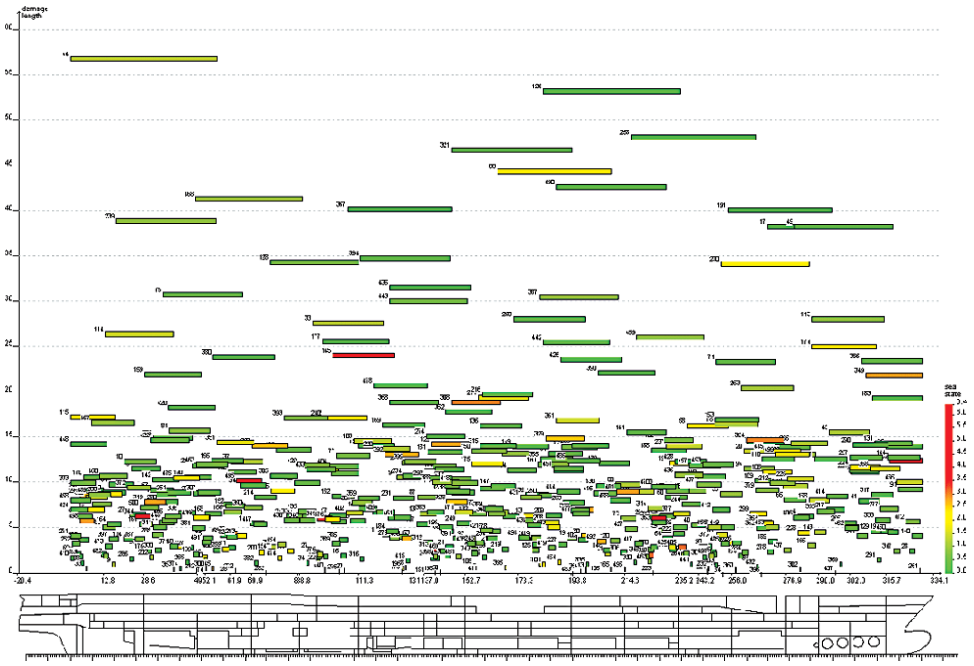

Figure 5.4: Monte Carlo Simulation set up - 500 collision damage cases

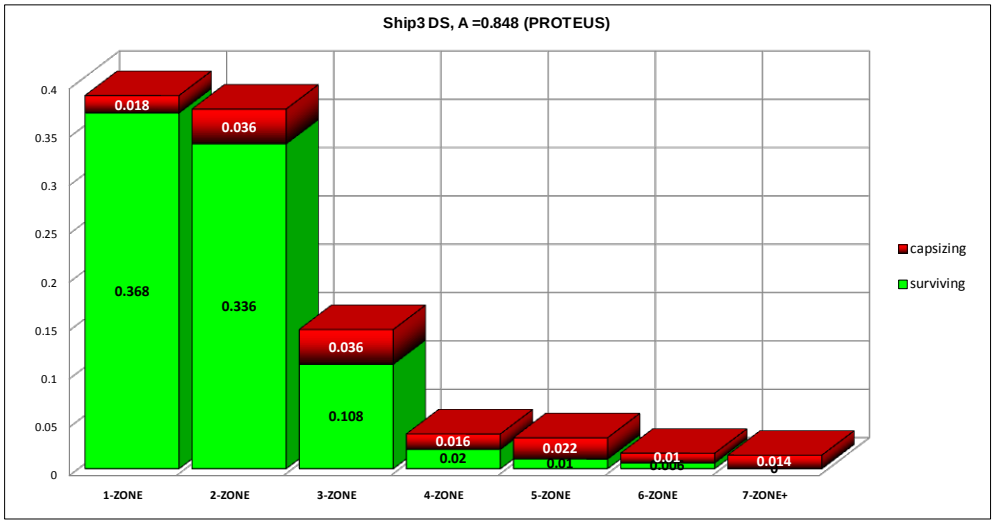

Figure 5.5: Distribution of probability for survival and capsizing at the deepest draught in a given 30 minutes. Cases selected based on MC simulation.

5.2.2.2 Physical Model Experiment

Apart from numerical simulations, the dynamic behaviour of a damaged ship can be also captured through towing tank testing. The model test method in accordance with SOLAS'95 Resolution 14 (IMO, 1995) has been set up to address the key issues in

relation to: water ingress/egress in the damaged compartments, water accumulation, the phenomena of transient, intermediate and progressive flooding. Ultimately, the survivability of a damaged ship can be quantified as a function of related design and operational parameters. The experimental layout is depicted in Figure 5.6 below.

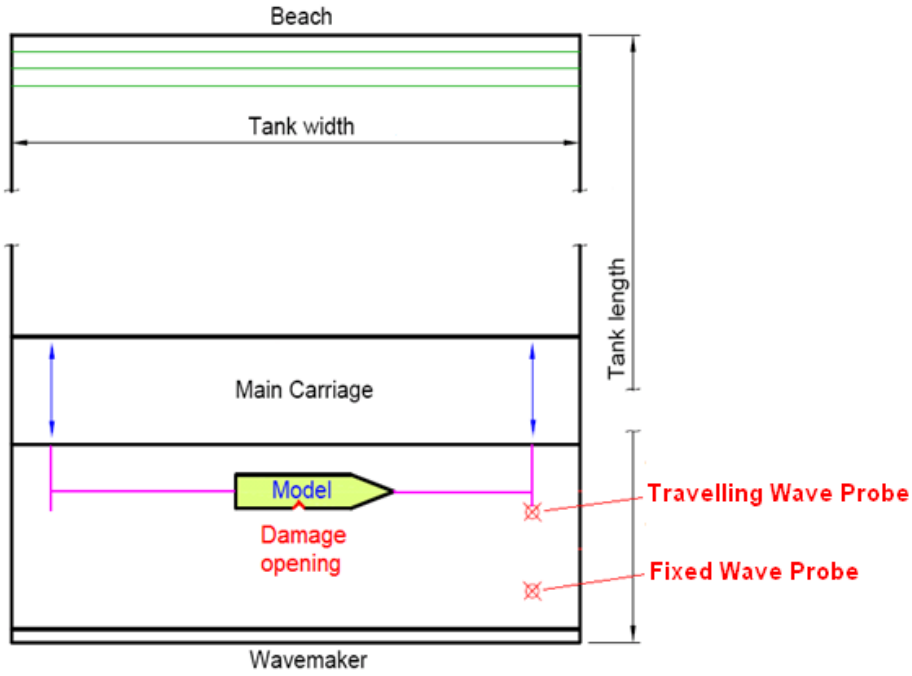

Figure 5.6: The Model Test Method – Experimental Set-up

Regarding the procedure for physical experiments specified in (EC, 2003), the model should be free to drift and placed in beam seas with the damaged hold facing oncoming waves. The sea conditions are modelled based on JOHNSWAP wave energy spectrum, generated through linear theory of random processes. The parameters of the spectrum are determined using the following relations:

$$\alpha = \frac{H_s}{\lambda}, T_p = \sqrt{\frac{2 \cdot \pi \cdot \lambda}{\mathrm{g}}}\,[s], T_p = C \cdot \sqrt{H_s}, C = \sqrt{\frac{2 \cdot \pi}{\mathrm{g} \cdot \alpha}},$$

$$T_z = \frac{T_p}{1.49 - 0.102 \cdot \gamma + 0.0142 \cdot \gamma^2 - 0.00079 \cdot \gamma^3}\,[s]$$

The input wave steepness α is chosen as 0.04 and the spectral peakness parameter γ is fixed at 3.3. The parameter T_p and T_z denotes the peak wave period and zero-

crossing period respectively. A range of successive significant wave heights should be tested (e.g. $H_s = 1.0\text{m} - 4.0\text{m}$), each of which is represented by different wave realizations for simulating irregular waves. The test period for each experiment should not be less than 30 minutes in full-scale. This is consistent with the Stockholm Agreement as the minimum time required for all passengers to abandon the ship orderly before sinking is 30 minutes.

In this way, the outcome of model testing of the damaged ship can be essentially regarded as an event with binary statuses: either survival or capsizing within a given time period. Consequently, from a statistical point of view, the rate of capsizing (capsize probability) can be summarised for a given sea state through the collected experimental results. Moreover, physical model tests are envisioned to provide the necessary benchmark data for validation of other instruments in the assessment of collision survivability of ships, such as the numerical methods. In general, the evidence derived from model experiments has been given greater assent as one of the most reliable sources of information to investigate the flooding phenomenon of damaged ships.

However, testing in tank is an expensive and time consuming method that limits its application to generate a complete set of estimations of the time interval from hull breach to capsize, T_{cap} for a wide range of conditions that a damaged ship may encounter. Being aware of this, the numerical simulation models are believed to be a more cost-effective solution for providing more comprehensive assessment of collision survivability. Therefore, a full picture of the time to capsize for a specific damage case can be generated. The available experimental observations can be regarded as a valuable resource to validate the obtained numerical estimations.

5.2.3 Response Variables

Based on the forgoing, the stochastic nature of ship stability deterioration process after hull breach can be modelled based on numerical simulations and physical model experiments within the performance-based framework. The key aspects characterising the behaviour of damaged ships cover: time-based ship motions, ship hydrodynamic forces, water ingress/egress, floodwater motions inside compartments,

and progressive flooding of internal compartments through openings. In turn, a variety of measuring variables can be calculated explicitly.

As far as the response variable is concerned, IMO has adopted a new philosophy for developing safety standards for passenger ships since 2004, to address the concerns that increasing ship sizes and passenger numbers might increase the risk level to this ship type. As illustrated in Figure 5.7 (IMO, 2004a), passenger ships should be designed based on the time-honoured principle that a ship is its own best lifeboat in the event of a casualty. This essentially necessitate that damaged ships should either be capable of returning to port under its own power or be able to remain stable and afloat for 3 hours to allow safely and orderly evacuation of passengers and crew. Nevertheless, the state-of-the-art stability assessment regulations (the GZ curve and the attained subdivision index A) have been developed only for design purposes and do not disclose vital information such as time to capsize (T_{cap}), although the survival factor "s" has been derived on the basis of 30 minutes model experiments.

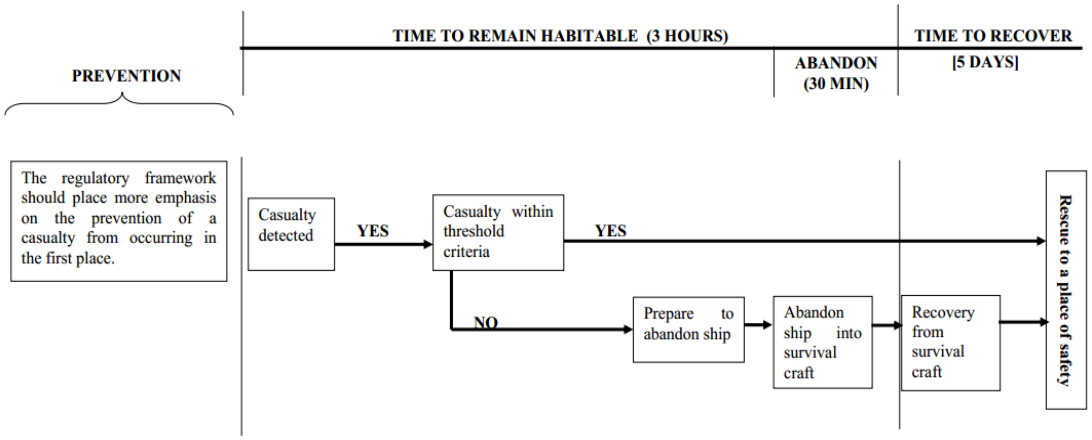

Figure 5.7: The IMO Framework – Passenger Ship Safety (SLF 47/8)

As a result, it can be expected that the measured T_{cap} , time to capsize, is a scientific and intuitive measure towards ship survivability. This can assist the designers for securing the designs with higher safety levels and support the operators for monitoring survivability level at normal operation conditions and making proper decisions in emergencies. Hence, the probability of capsizing for a specific damage

case within a given time $P(t_0, Y = cap \mid damage)$ is sought as the model response variable accordingly.

5.3 Model-Structuring for Ship Survivability Prediction

For the purpose of transforming the available information (i.e. observed inputs and measured outputs through first-principles tools) into interpretable and manageable knowledge (i.e. predictions of ship survivability after flooding in given conditions), a proper mathematical relationship needs to be established so that the impact of input variables on response variables can be appraised.

Regarding the influencing parameters described in Section 5.2, it is important to bear in mind that: i) there are more than a handful of input variables affecting the output of ship survivability to flooding; ii) the focal output variable is binary (i.e. 'capsize' or 'not capsize' within a given time period); iii) the output measure needs to be presented in a probabilistic manner to resonate well with the existing probabilistic safety framework in the maritime industry.

Considering the above, simple statistical approaches (e.g. linear models) are not appropriate to formulate the correlations between the multiple variables. In this case, more sophisticated models are needed. On the other hand, multivariate data analysis (Hair, 2009) provides a promising way out. Selection of appropriate multivariate models in relation to the research problem under investigation should be made based on the research objectives and the characteristics of the available data at hand.

This section attempts to explain a decision procedure of choosing the proper multivariate statistical models for further model estimations and probabilistic uncertainty analysis. This comprises two steps:

- To specify the research problem and put forward a conceptual model for describing the relationship to be examined.
- To select the appropriate multivariate techniques (e.g. link functions) for modelling the impact of input variables on the output one (i.e. probability of ship capsizing).

5.3.1 Identification of Research Problem for Choosing Multivariate Models

In general, the basis for a multivariate analysis is to define the research problem and analysis objectives in conceptual terms before specifying any variable or measure. Currently, the subject under consideration aims to establish a dependent relationship between damaged ship behaviour due to flooding after collision and a list of governing explanatory variables (independent) explained in Section 5.2.1. In other words, the model output (dependent) of whether the ship capsizes after damage within a given time period is to be predicted by other independent variables.

Having the research objective specified above, a conceptual model needs to be established. Due to a dependent relationship is in question, it is important to understand the measurement characteristics (format) of both dependent and independent variables of the model.

In this respect, firstly, regarding the number of dependent variables, this work requires only a single output variable. Secondly, regarding the type of measurement scale employed by the variables, all the independent variables are measured metrically (i.e. quantitative data). In contrast, the dependent variable is nonmetric (i.e. qualitative data) and measured on a binary scale, which is denoted by either 0 (i.e. the damaged ship is survival within a given time period) or 1 (i.e. the outcome is capsizing within a given time period). For selecting the appropriate multivariate dependent method to tackle this research problem, an overview of the multivariate models is illustrated in Figure 5.8.

Meanwhile, various multivariate dependent methods with respect to the nature of variables and the number of dependent and independent variables are defined in Table 5.1 (Hair, 2009). As can be seen, both multiple discriminant analysis and linear probability models are capable of addressing the identified relationship with a nonmetric dependent variable.

Table 5.1: The Relationship between Multivariate Dependence Methods

Canonical Correlation		
$Y_1 + Y_2 + Y_3 + \cdots + Y_n$	=	$X_1 + X_2 + X_3 + \cdots + X_n$
(metric, nonmetric)		(metric, nonmetric)
Multivariate Analysis of Variance		
$Y_1 + Y_2 + Y_3 + \cdots + Y_n$	=	$X_1 + X_2 + X_3 + \cdots + X_n$
(metric)		(nonmetric)
Analysis of Variance		
Y_1	=	$X_1 + X_2 + X_3 + \cdots + X_n$
(metric)		(nonmetric)
Multiple Discriminant Analysis		
Y_1	=	$X_1 + X_2 + X_3 + \cdots + X_n$
(nonmetric)		(metric)
Multiple Regression Analysis		
Y_1	=	$X_1 + X_2 + X_3 + \cdots + X_n$
(metric)		(metric, nonmetric)
Conjoint Analysis		
Y_1	=	$X_1 + X_2 + X_3 + \cdots + X_n$
(metric, nonmetric)		(nonmetric)
Structural Equation Modelling		
Y_1	=	$X_{11} + X_{12} + X_{13} + \cdots + X_{1n}$
Y_2	=	$X_{21} + X_{22} + X_{23} + \cdots + X_{2n}$
Y_m	=	$X_{m1} + X_{m2} + X_{m3} + \cdots + X_{mn}$
(metric)		(metric, nonmetric)

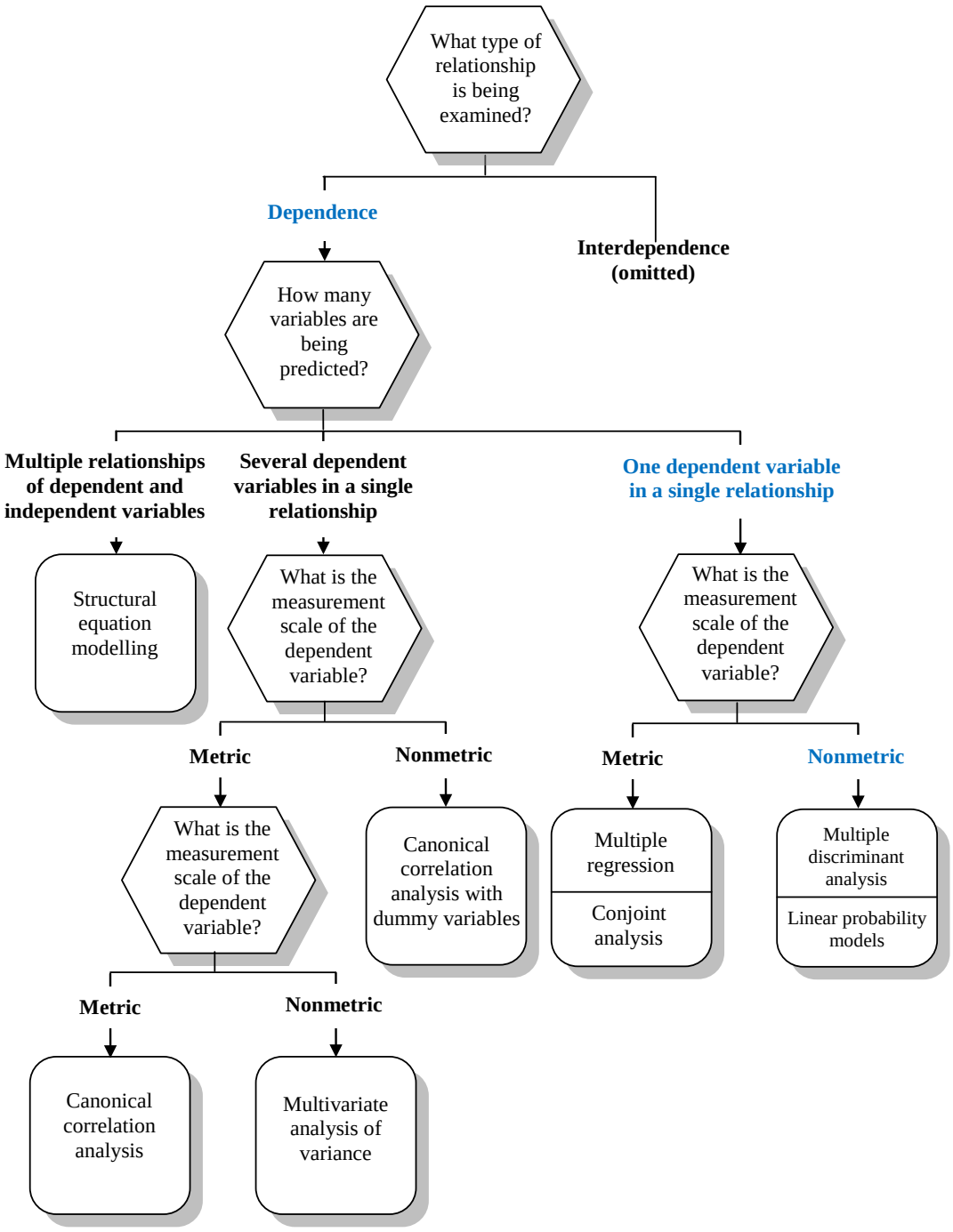

Figure 5.8: Selecting a Multivariate Technique (Hair, 2009)

5.3.2 Model Selection towards the Specified Research Problem

Comparing discriminant analysis and linear probability models, the latter offers a platform where all types of independent variables (either metric or nonmetric) can be accommodated. In this situation, the linear probability model is more appropriate for structuring a relationship between a single dependent variable of ship response and various influential independent variables. The general form is shown as Equation (9):

$$\underset{\text{(binary nonmetric)}}{Y} = \underset{\text{(metric, nonmetric)}}{x_1 + x_2 + x_3 + \cdots + x_n} \tag{9}$$

For the model under construction, the output $\boldsymbol{Y}$ is defined as a binary random variable (i.e. either capsizing or survival denoted by 1 or 0) in performance-based experiments, and such outcomes can be presented from a probabilistic perspective. Thus the distribution of $\boldsymbol{Y}$ can be specified through the probability $P(Y = 1) = \pi$ of capsizing and $P(Y = 0) = 1 - \pi$ of survival. The expected value (mean) is $\mu = E(Y) = \pi$. Hence, a reformulation of Equation (9) is performed by considering the probability π as the output (dependent) variable, which is shown in Equation (10):

$$\pi(x) = P(Y = 1|\boldsymbol{X}) = \alpha + \beta_1 x_1 + \beta_2 x_2 + \cdots + \beta_n x_n = \alpha + \boldsymbol{\beta X} \tag{10}$$

Where: i) the response variable $\boldsymbol{Y}$ has a binomial distribution

ii) Explanatory variables are represented by the design matrix $\boldsymbol{X}$

iii) α is the intercept

iv) $\boldsymbol{\beta}$ represents a set of regression coefficients for all the predictor variables and $\boldsymbol{\beta X}$ is called the linear predictor

As noted, Equation (10) represents a simple linear probability model. The Binomial distribution is usually the first choice for modelling the observations of a process with binary outcomes (Yes/No, True/False, Capsize/Survive, etc.). However, there is a restriction of the estimated probability π as it must be within the interval [0,1]. Accordingly, it is very desirable to have a transformation function to connect the linear predictors on the right hand side with a probability function on the left hand side. Regarding this, the Generalized Linear Models (GLM) (Nelder and

Wedderburn, 1972) is promising for investigating effects of explanatory variables on categorical response variables (Agresti, 2007).

All GLMs have three components: a random component (i.e. the response variable Y and assumes a probability distribution for it), a systematic component (i.e. the explanatory variables) and a link function denoted as $g(.)$ (i.e. a function of the expected value of Y). A typical GLM is defined in Equation (11):

$$g[E(Y|\boldsymbol{X})] = g[\pi(x)] = \alpha + \boldsymbol{\beta X} \tag{11}$$

To ensure that the predicted probabilities π fall within 0-1 interval, it is often modelled with a cumulative probability distribution:

$$\pi = \int_{-\infty}^{t} f(s).ds$$

Where $f(s) \geq 0$ and $\int_{-\infty}^{\infty} f(s).ds = 1$. The selection of a proper probability density function $f(s)$ will have impact on the type of GLMs used. Given the observations on $\boldsymbol{Y}$ by $(Y_1, \cdots, Y_n)$ are binary, two common GLMs, namely Probit model and Logistic (logit) model, satisfy the requirements for providing necessary link functions (Dobson and Barnett, 2009).

The following paragraph focuses on describing both models for binary responses separately.

Firstly, the probit model is based on the assumption that $\pi(x)$ follows a normal (cumulative) distribution, with mean μ and variance σ^2, therefore:

$$\pi(x) = \frac{1}{\sigma\sqrt{2\pi}} \int_{-\infty}^{x} exp\left[-\frac{1}{2}\left(\frac{s-\mu}{\sigma}\right)^2\right].ds = \Phi\left(\frac{\mathrm{x}-\mu}{\sigma}\right) \tag{12}$$

Where $\Phi(\cdot)$ denotes the cumulative probability function for the standard normal distribution $N(0,1)$, thus the probit link function $g[\pi(\mathrm{x})]$ is essentially an inverse function $\Phi^{-1}(\cdot)$. Hence, in GLM form:

$$\Phi^{-1}(\pi) = \alpha + \beta_1 x_1 + \beta_2 x_2 + \cdots + \beta_n x_n = \alpha + \boldsymbol{\beta X} \tag{13}$$

So, the selected linear probit model is depicted in Equation (14):

$$\pi(x) = P(Y = 1|\boldsymbol{\beta}, \boldsymbol{X}) = \Phi(\alpha + \boldsymbol{\beta X}) \tag{14}$$

Overall, the above model offers the following key features and benefits:

- The response curve for $\pi(x)$ [or for $1 - \pi(x)$, when $\beta < 0$] has the appearance of a normal CDF with mean $\mu = -\alpha/\beta$ and standard deviation $\sigma = 1/|\beta|$, which has a sigmoid profile as shown in Figure 5.9. Such flexibility offers a unique platform for presenting the response object, as the ship response that is affected by a set of key random independent variables describing the flooding scenario.

- The model can be easily extended to include more variables simultaneously in the linear predictors (i.e. $\boldsymbol{\beta X}$). This provides a convenient and interpretable means to perform sensitivity study for the subsequent model adjustment and validation.

On the other hand, the logit model assumes that $\pi(x)$ follows a logistic (cumulative) distribution $\Lambda(\cdot)$. It gives numerical results very much like those from the probit model, but which computationally is somewhat easier. The logistic regression or logit model parameterizes $\pi(x)$ as:

$$\pi(x) = \int_{-\infty}^{x} f(s).ds = \frac{exp(x)}{1 + exp(x)} = \Lambda(x) \tag{15}$$

This gives the link function:

$$\Lambda^{-1}(\pi) = \log\frac{\pi(x)}{1 - \pi(x)} = \alpha + \beta_1 x_1 + \beta_2 x_2 + \cdots + \beta_n x_n = \alpha + \boldsymbol{\beta X} \tag{16}$$

The term $\log[\pi/(1-\pi)]$ is called the logit function and it has a natural interpretation as the logarithm of odds. Explicitly, π is restricted within [0, 1], the logit can be any real number. So, the linear logit model is given in Equation (17):

$$\pi(x) = \mathrm{P}(\mathrm{Y} = 1|\beta, \boldsymbol{X}) = \Lambda(\alpha + \boldsymbol{\beta X}) \tag{17}$$

The shapes of the functions $f(s)$ and $\pi(x)$ are similar to those of the probit model (i.e., the PDF and the CDF of normal distribution), except in the tails of the distribution (Cox and Snell, 1989).

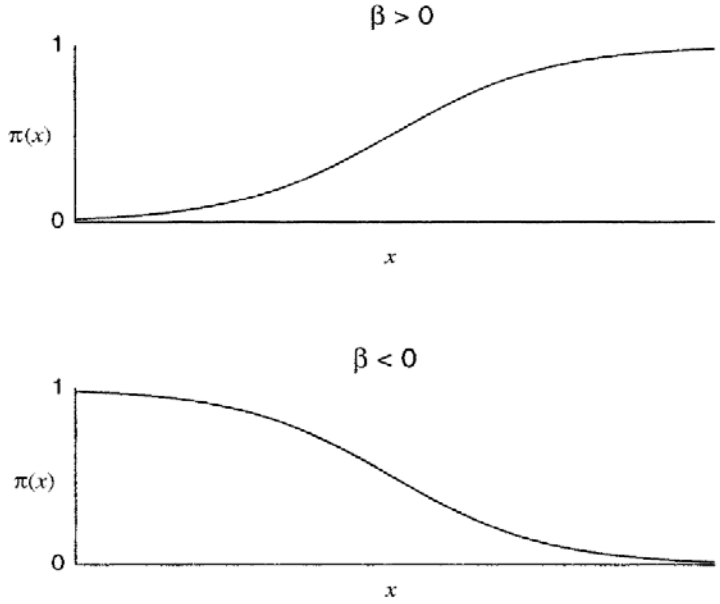

Figure 5.9: Probit and Logistic Regression Functions

5.4 Closure

On the basis of the state-of-the-art development in probabilistic ship damage stability, this chapter starts with identification of the influencing parameters in modelling ship survivability. This involves three elements: i) model input information; ii) mathematical assumptions that have been embedded in performance-based tools; iii) model output which has been exposed as the probability of ship capsizing in a given time interval.

Following this, the research problem has been formulated through a conceptual model. Multivariate data analysis is the technique that has been identified for modelling the dependent relationships towards the identified problem. Accordingly, two common types of GLMs for binary response (i.e., probit and logit regression functions) have been selected to structure the regression models for the following ship survivability assessment as well as uncertainty analysis.

Chapter 6

A Bayesian Approach for Probabilistic Uncertainty Quantification

6.1 Preamble

As mentioned in the preceding chapter, linear regression model is a powerful data analysis tool, useful for a variety of inferential tasks such as prediction, parameter estimation and data description. Accordingly, two common GLMs of the probit model and the logistic model are promising to provide the link functions for the model under construction. This chapter aims to propose a formalised procedure for model estimation and analysing its inherent uncertainty.

Firstly, a discussion of the appropriate model estimation techniques is performed. In this respect, classical techniques (e.g. Maximum likelihood estimation, Least Square estimation) can be easily deployed. However, more sophisticated methodology is needed for uncertainty analysis. Hence, a unique technique, Bayesian inference, is proposed to be adopted for this study (i.e. making inference on ship survivability).

Furthermore, emphasis is placed on applying Markov Chain Monte Carlo (MCMC) algorithms to estimate the regression model. Hence, the posterior probability distributions for each of the model coefficients $\boldsymbol{\beta}$ can be simulated. The model construction is completed once all of these model coefficients are estimated. Accordingly, uncertainty analysis of the model output can be addressed when all the input information is given.

In the end, an example is presented to elucidate the applications of the proposed methodology for probabilistic uncertainty quantification using experimental data.

6.2 A Bayesian Approach for Regression Model Estimation

A Bayesian inferential procedure (i.e. Bayesian inference) is depicted in Figure 6.1. It should be appreciated that probability uncertainty analysis of the model output $P(t_0, Y = 1|\boldsymbol{\beta}, \boldsymbol{X})$ (i.e. ship response within a given time) can be achieved through investigating the posterior probability distribution of model coefficients $\boldsymbol{\beta}$. The unknown parameters $\boldsymbol{\beta}$ can be also regarded as the sensitivity indicator in the model, which indicates the significance of each explanatory variable x on the model output.

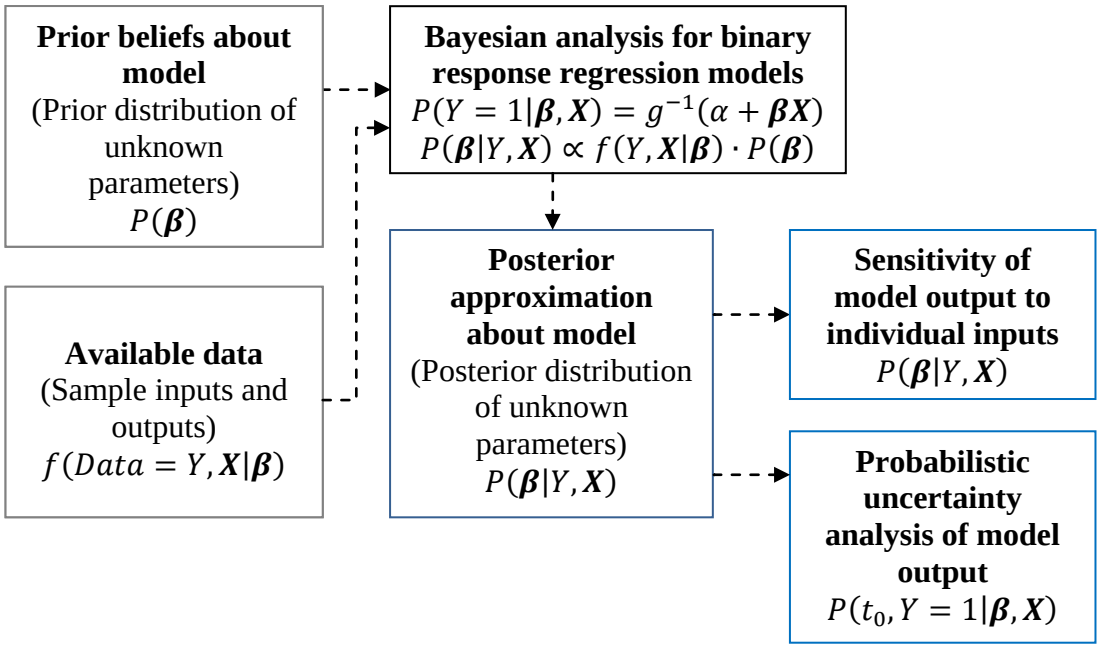

Figure 6.1: A Bayesian Inferential Procedure

According to Figure 6.1, the proposed methodology can be explained by the following four steps:

- This whole process starts from the lower-left corner, generation of data about ship capsizing through first-principles tools is the first step, thereby the input information $\boldsymbol{X}$ and the relevant output Ycan be assembled as evidences for the ensuing model estimation. Meanwhile, based on the available knowledge, the prior probability distribution of model coefficients $P(\boldsymbol{\beta})$ can be assigned.

- On the basis of Bayes' theorem, using the derived data $f(Y, \boldsymbol{X}|\boldsymbol{\beta})$ and the prior information$P(\boldsymbol{\beta})$, a predictive regression model $P(Y = 1|\boldsymbol{\beta}, \boldsymbol{X}) = g^{-1}(\alpha + \boldsymbol{\beta X})$ can be estimated. Thus, the posterior probability distribution of model coefficients can be simulated $P(\boldsymbol{\beta}|Y, \boldsymbol{X})$.

- Probabilistic sensitivity study can be carried out to identify the level of significance of input parameters $\boldsymbol{X}$ in the model based on the sensitivity indicator $P(\boldsymbol{\beta}|Y, \boldsymbol{X})$.

- Once all the input parameters are identified, the probabilistic uncertainty analysis of $P(t_0, Y = 1|\boldsymbol{\beta}, \boldsymbol{X})$ can be addressed.

6.2.1 The Underlying Considerations of Selecting Bayesian Methods

This section intends to stress the underlying considerations for choosing Bayesian inference on binary regression model estimation. A short review concerning the difference between the Bayesian estimates of $\boldsymbol{\beta}$ and the non-Bayesian methods is provided.

In the following sub-sections, two frequentist statistical methods of Maximum-likelihood estimation and Least squares estimation, which are widely used for model estimations, are discussed firstly. Then comments on different estimation methods will be outlined in the end.

6.2.1.1 Maximum-likelihood Estimation

Let $\mathbf{y} = [Y_1, \cdots, Y_n]^T$ be a random vector and drawn from a population with density $h[y_i; f(\boldsymbol{X_i}, \boldsymbol{\beta})]$, where $\boldsymbol{X_i} = \left[x_{i1}, x_{i2}, \cdots, x_{ip}\right]$ $(i = 1, \cdots n)$ is a set of known values of the independent variables, $\boldsymbol{\beta} = \left[\beta_1, \cdots, \beta_p\right]^T$ are unknown parameters, and $f(\boldsymbol{X_i}, \boldsymbol{\beta})$ is a known function of the independent variables and the parameters. The regression function $f(\boldsymbol{X_i}, \boldsymbol{\beta})$ is nonlinear in general and supposes that it is a differentiable function of $\boldsymbol{\beta}$. Given the observed values $Y_1, \cdots, Y_n$, the problem at hand is to estimate parameters $\beta_1, \cdots, \beta_p$.

One approach is to use the maximum likelihood (ML) principle. The maximum likelihood estimator of $\boldsymbol{\beta}$ is the value $\widehat{\boldsymbol{\beta}}$ which maximizes the likelihood function $L(\boldsymbol{\beta}; \mathbf{y})$, that is

$$L\left(\widehat{\boldsymbol{\beta}}; \boldsymbol{y}\right) \geq L(\boldsymbol{\beta}; \mathbf{y}) \quad \text{for all } \boldsymbol{\beta} \text{ in the parameter space } \Omega.$$

Equivalently, $\widehat{\boldsymbol{\beta}}$ is the value which maximizes the log-likelihood function $l(\boldsymbol{\beta}; \mathbf{y}) = \log L(\boldsymbol{\beta}; \mathbf{y})$. Thus

$$l\left(\widehat{\boldsymbol{\beta}}; \boldsymbol{y}\right) \geq l(\boldsymbol{\beta}; \mathbf{y}) \quad \text{for all } \boldsymbol{\beta} \text{ in } \Omega$$

Usually the estimator $\widehat{\boldsymbol{\beta}}$ is obtained by solving the system of equations

$$\frac{\partial l(\boldsymbol{\beta}; \mathbf{y})}{\partial \beta_j} = 0 \quad \text{for } j = 1, \cdots, p. \tag{18}$$

In principle, it is not necessary to be able to solve Equation (18) if $\widehat{\boldsymbol{\beta}}$ can be found numerically. In practice, numerical approximations are very important for GLMs. Other properties of maximum likelihood estimators are discussed in (Cox and Hinkley, 1974) or (Kalbfleisch, 1985).

6.2.1.2 Least Squares Estimation

Another approach to the estimation problem is through adopting the least square (LS) principle. Let $Y_1, \cdots, Y_n$ be independent random variables with expected values $\mu_1, \cdots, \mu_n$ respectively. Suppose that the μ_i 's are functions of the parameter vectors $\boldsymbol{\beta} = \left[\beta_1, \cdots, \beta_p\right]^T, p < n$ which are about to be estimated. Thus

$$E(Y_i) = \mu_i(\boldsymbol{\beta})$$

The most commonly used estimate of a vector of regression coefficient is the ordinary least square (OLS) estimate. The OLS regression estimate is the value $\widehat{\boldsymbol{\beta}}_{\mathbf{ols}}$ of $\boldsymbol{\beta}$ that minimizes the sum of squares of the difference (SSR) between the observed Y_i's and their expected values

$$\text{SSR}(\boldsymbol{\beta}) = \sum_{i=1}^{n} [Y_i - \mu_i(\boldsymbol{\beta})]^2 = \sum_{i=1}^{n} (Y_i - \boldsymbol{\beta}^T \boldsymbol{x_i})^2$$

Usually the estimator $\widehat{\boldsymbol{\beta}}_{\mathbf{ols}}$ is obtained by solving the system of equations

$$\frac{\partial \mathrm{SSR}(\boldsymbol{\beta})}{\partial \beta_j} = 0 \quad \text{for } j = 1, \cdots, p. \tag{19}$$

And then the value $\widehat{\boldsymbol{\beta}}_{\mathrm{ols}} = (\boldsymbol{X}^T\boldsymbol{X})^{-1}\boldsymbol{X}^T\mathbf{y}$ is given as the OLS estimate of $\boldsymbol{\beta}$. It is unique as long as the inverse $(\boldsymbol{X}^T\boldsymbol{X})^{-1}$ exists (i.e. $(\boldsymbol{X}^T\boldsymbol{X})$ is not singular).

Now suppose that the Y_i's are not independent, but temporally correlated. This means the covariance matrix $\sigma^2\mathbf{I}$ in the ordinary regression model must be replaced with a matrix $\boldsymbol{\Sigma}$. Then the weighted least squares estimator is obtained by minimizing

$$\mathrm{SSR}(\boldsymbol{\beta}) = (\mathbf{y} - \boldsymbol{\mu})^{\mathrm{T}}\boldsymbol{\Sigma}^{-1}(\mathbf{y} - \boldsymbol{\mu})$$

6.2.1.3 Comments on Estimation

With a brief review of the two non-Bayesian estimation methods, this part intends to outline some comments together with the Bayesian method in the estimation of $\boldsymbol{\beta}$. Above all, a comparison of the two frequentist methods is given.

1) An important distinction between the methods ML and LS is that the latter can be used without making assumptions about the distributions of the response variable Y_i beyond specifying their expected values and possibly their variance-covariance structure. In contrast, to obtain ML estimator the joint probability distribution of the Y_i's denoted as $f(\mathbf{y}; \boldsymbol{\beta})$, needs to be specified.

2) For many situations ML and LS estimators are identical. For instance, the equivalence of ML and LS estimates when the Y_i's are normally distributed and the regression function is linear in the parameters. (Bradley, 1973) has established that when the density of the Y_i's is in the regular exponential family and the regression model is linear, and then the ML and LS estimates satisfy Equation (19). (Nelder and Wedderburn, 1972) has shown that this result is also true for certain GLMs.

On the other hand, it is very important to appreciate the distinctions between the Bayesian and frequentist methods.

1) In practice, the performance of both non-Bayesian methods dependent heavily on the size of the sampled data. It indicates that the accuracy of the inferences about the regression coefficients is questionable for small sample sizes. In this case, the linear relationship between the values of **y** and $\boldsymbol{X}$ in the dataset (quantified by $\widehat{\boldsymbol{\beta}}$), is often an inaccurate representation of the relationship in the entire population. It should be borne in mind that both the experimental and actual accident data that can be collected are always restricted by the resources allocated (e.g. time and fund). Hence, the objective of predicting ship survivability using only a very limited observed data in the maritime industry can be surely considered as a small sample size problem. Moreover, it is expected that such difficulties will remain to be a challenge in the foreseeable future.

2) In contrast, Bayesian inference approach is less sensitive to the changes of the sample size. This is because that the well-founded Bayes' theorem can naturally combine the evidence from both collected data and prior information. As a result, it offers more intuitive and meaningful inferences. A major barrier for a wider adoption of Bayesian methods in the past is due to the computation complexity (e.g. random sampling). However, this can be easily overcome with today's computation capability. The following section focuses on the simulation techniques for Bayesian computation.

According to the above comparative comments, it can be noted that Bayesian methods suit better to the problem under consideration. However, it is necessary to stress that practical applications of Bayesian analysis sometimes are very complex. For instance, the size of the parameter space is often very large and can become extremely large for problems involving multiple parameters $(\boldsymbol{\beta} = \alpha, \beta_1, \cdots, \beta_p)$. Hence, the subsequent computation is tremendous, which make it infeasible to make the exact inference. Nevertheless, with the profoundly improved computing power in the last 20 years, Markov Chain Monte Carlo (MCMC) methods are generally thought to be promising for solving those previously intractable problems.

6.2.2 Markov Chain Monte Carlo Methods for Bayesian Computation

In recent years statisticians have been increasingly drawn to MCMC methods to simulate complex, nonstandard multivariate distributions. This section attempts to emphasize such advanced mathematical simulation techniques for approximating the posterior probability distribution of the regression coefficients $P(\boldsymbol{\beta} \mid \mathbf{y}, \boldsymbol{X})$.

Referring to the Bayesian's formula given in Equation (7) (Section 3.4.2.2), if θ represents a continuous parameter space, the posterior distribution of the unknown parameter is substituted as

$$P(\theta|\mathbf{y}) = \frac{P(\mathbf{y}|\theta)P(\theta)}{\int P(\mathbf{y}|\theta)P(\theta)d\theta} \tag{20}$$

In fact, this equation is often hard to calculate due to the integral in the denominator. Particularly if there are n unknown parameters, such as $(\boldsymbol{\theta} = \alpha, \beta_1, \dots, \beta_{n-1})$, the denominator involves integration over n-dimensional parameter space which becomes intractable for large values of n. In this case, numerical methods for calculating complex integrals about $\boldsymbol{\theta}$ rather than calculus are needed.

Attempting to have a comprehensive perception of how MCMC methods work towards Bayesian computation, the fundamental features associated with MCMC methods are summarized first. Afterwards, two of the most popular Markov chain sampling algorithms for simulating the posterior distribution are detailed independently. Eventually, the technique to diagnostics of the chain convergence is put forward.

6.2.2.1 Characteristics of MCMC Methods

It is well-known that MCMC techniques combine two methods: Monte Carlo integration and Markov Chain sampling. As suggested by its name, two essential characteristics of MCMC methods are available:

- The feature of Monte Carlo integration: In principle, this method simplifies a continuous distribution by taking discrete samples. It is useful when a continuous

distribution is too complex to integrate explicitly but can be readily sampled (Gelman, 2004). As can be seen in Figure 6.2(a), there is a continuous distribution of $P(\theta)$ which can be approximated by a histogram of the discrete samples in Figure 6.2(b). Clearly, the larger number of samples will lead to a closer approximation of the continuous distribution. Now, as the goal is to evaluate the posterior distribution of model coefficients $P(\boldsymbol{\beta} \mid \mathbf{y}, \mathbf{X})$, if a histogram is a reasonable approximation to the density of each coefficient, any inference about $\boldsymbol{\beta}$ can be made by simply using the sampled values. Moreover, as it is shown in Figure 6.2, it is possible to sample θ from $P(\theta)$ directly and hence numerous independent and identically distributed (i.i.d.) random samples θ can be generated. Hence, it is simple to obtain Monte Carlo approximations of the continuous distribution $P(\theta)$. However, in practice, drawing samples from $P(\theta)$ is not always achievable because it may have a complex, or even unknown form.

- The feature of Markov Chain Sampling: In principle, this method allows drawing samples $\theta^{(i)}$ from the target density $P(\theta)$ to follow a Markov chain. Such process has the Markov property (Bartlett, 1978), which entails the next sample in the chain is dependent on the previous sample. Therefore, a chain of samples $\theta^{(1)}, \ldots, \theta^{(n)}$ can be built up after specifying a starting value $\theta^{(0)}$ as illustrated in Figure 6.3. Two of the widely recognised MCMC algorithms are Gibbs sampler and Metropolis sampler. They adaptively generate Markov chains to approximate the target probability distribution $P(\theta)$. The following two subsections elaborate these sampling algorithms for further applications.

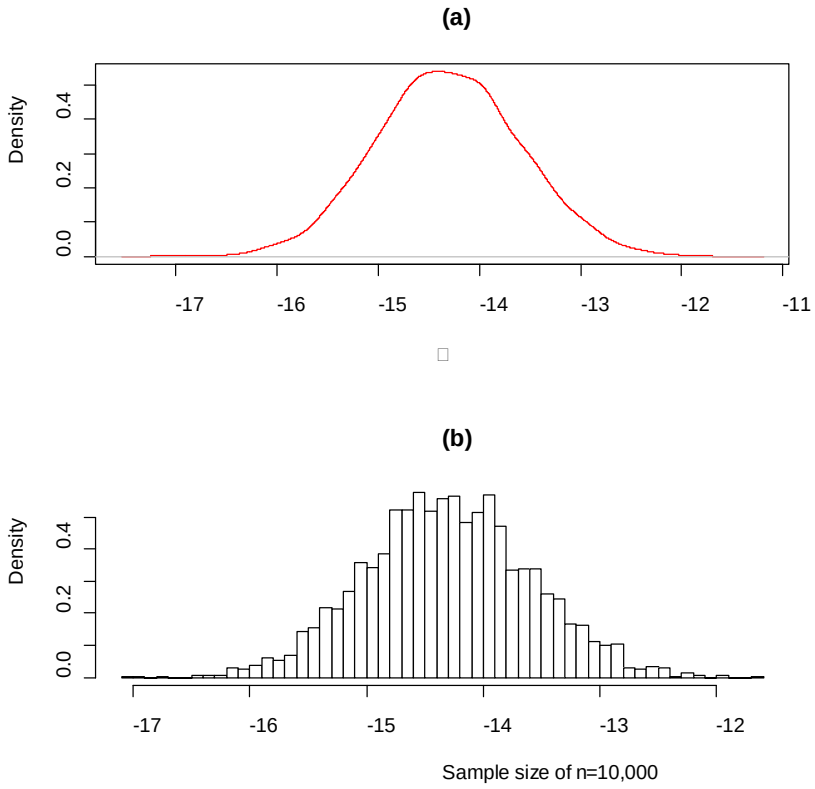

Figure 6.2: (a) a continuous distribution of $P(\theta)$; (b) Approximating $P(\theta)$ using discrete random samples, for sample size of 10,000 and bin width of 0.1.

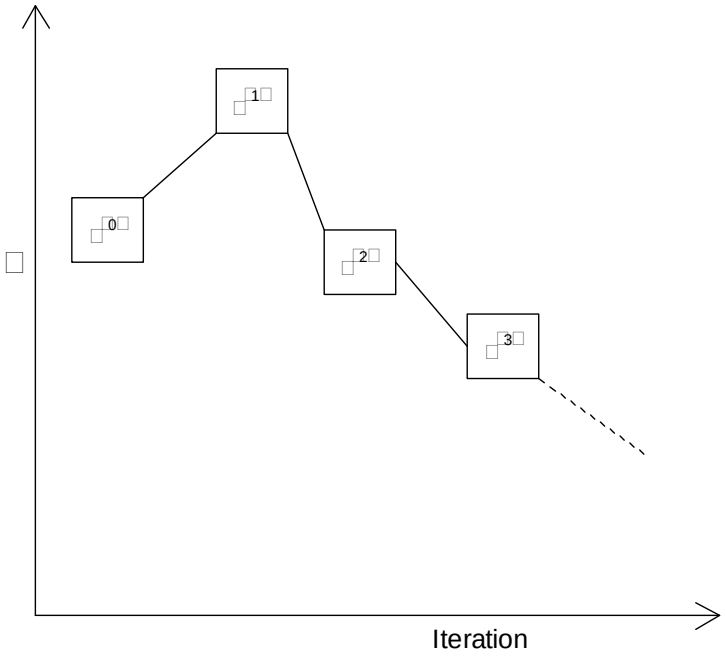

Figure 6.3: A simple example of a Markov chain (Dobson and Barnett, 2009)

Before drawing samples from the posterior distribution of the unknown model parameters, it is necessary to understand a more general Markov chain simulation algorithm, Metropolis-Hastings algorithm (Chib and Greenberg, 1995).. Both the Gibbs and Metropolis algorithms are essentially special cases of the Metropolis-Hastings algorithm.

It is known that $P(\boldsymbol{\beta}|\mathbf{y},\boldsymbol{X})$ is a joint posterior distribution since more than one predictor variable $\boldsymbol{X}$ are considered in a model, thus a set of model coefficients $(\boldsymbol{\beta} = \alpha, \beta_1, \cdots, \beta_n)$ needs to be approximated simultaneously. In so doing, an iteration of the Metropolis-Hastings sampling is a complete cycle through every unknown parameter $\boldsymbol{\beta}^{(i)} = \left\{\alpha^{(i)}, \beta_1^{(i)}, \ldots, \beta_n^{(i)}\right\}$. This sampler works by randomly generating a new value $\boldsymbol{\beta}^*$ from a proposal distribution $Q\left(\boldsymbol{\beta}^*\middle|\boldsymbol{\beta}^{(i)}\right)$. The proposal distributions can be symmetric around of the current values $\boldsymbol{\beta}^{(i)}$, full conditional distributions, or something else entirely. If $P(\boldsymbol{\beta}^*|y) > P\left(\boldsymbol{\beta}^{(i)}\middle|y\right)$ then the next value in the chain becomes the proposed value $\boldsymbol{\beta}^{(i+1)} = \boldsymbol{\beta}^*$. If $P(\boldsymbol{\beta}^*|y) < P\left(\boldsymbol{\beta}^{(i)}\middle|y\right)$ then it seems $\boldsymbol{\beta}^*$ should not necessarily be included, the previous value is retained $\boldsymbol{\beta}^{(i+1)} = \boldsymbol{\beta}^{(i)}$. Fortunately, this comparison can be made using an acceptance ratio γ even if $P(\boldsymbol{\beta}|y)$ is not achievable

$$\gamma = \frac{P(\boldsymbol{\beta}^*|y)}{P(\boldsymbol{\beta}^{(i)}|y)} = \frac{P(y|\boldsymbol{\beta}^*)P(\boldsymbol{\beta}^*)}{P(y|\boldsymbol{\beta}^{(i)})P(\boldsymbol{\beta}^{(i)})} \tag{21}$$

The Metropolis-Hastings algorithm generates a sequence of draws $\boldsymbol{\beta}^{(i+1)}$ from the target probability distribution as follows:

1) Sample $\boldsymbol{\beta}^* \sim Q\left(\boldsymbol{\beta}^*\middle|\boldsymbol{\beta}^{(i)}\right)$;

2) Compute the acceptance ratio

$$\gamma = \frac{P(\boldsymbol{\beta}^*|y)}{P(\boldsymbol{\beta}^{(i)}|y)} = \frac{P(y|\boldsymbol{\beta}^*)P(\boldsymbol{\beta}^*)}{P(y|\boldsymbol{\beta}^{(i)})P(\boldsymbol{\beta}^{(i)})} \times \frac{Q\left(\boldsymbol{\beta}^{(i)}\middle|\boldsymbol{\beta}^*\right)}{Q(\boldsymbol{\beta}^*|\boldsymbol{\beta}^{(i)})} \tag{22}$$

3) Let $U \sim \text{uniform}[0,1]$, and setting

$$\boldsymbol{\beta}^{(i+1)} = \begin{cases} \boldsymbol{\beta}^{*}, & \text{if } U < \gamma \\ \boldsymbol{\beta}^{(i)}, & \text{otherwise} \end{cases}$$

6.2.2.2 The Gibbs Sampler

This section focus on one of the MCMC techniques, the Gibbs sampler (Geman and Geman, 1984) (Gelfand and Smith, 1990), which has emerged as the most widely adopted technique for obtaining marginal distribution $P(\boldsymbol{\theta}|\mathbf{y})$ from a non-normalized joint density $P(\boldsymbol{\theta}, \mathbf{y})$. It is a simulation tool for generating samples from the joint posterior distribution of unknown quantities in a model, conditional on the observed data.

Corresponding to Equation (22), in the Gibbs sampler the proposal distribution $Q(.)$ is the full conditional distribution and the acceptance probability γ is 1. Simulating from the posterior distribution of $\boldsymbol{\theta}$ can be split into a number of components $\boldsymbol{\theta} = (\theta_1, \cdots, \theta_p)$. The idea behind the sampler is that it is far easier to simulate $P(\theta_1)$ from a sequence of the fully conditional distributions $P\left(\theta_1 \middle| \{\boldsymbol{\theta_j}, \boldsymbol{j} \neq 1\}\right)$, than to sample from the joint density $P(\theta_1, \cdots, \theta_p)$. The sampler starts with initial values of the $\boldsymbol{\theta}^{(0)} = \left(\theta_1^{(0)}, \cdots, \theta_p^{(0)}\right)$ and then simulates in turn.

$$\begin{aligned} &\theta_1^{(1)} \text{ from } P\left(\theta_1 \middle| \left\{\boldsymbol{\theta}_{\boldsymbol{j}}^{(0)}, \boldsymbol{j} \neq 1\right\}\right) \\ &\theta_2^{(1)} \text{ from } P\left(\theta_2 \middle| \theta_1^{(1)}, \left\{\boldsymbol{\theta}_{\boldsymbol{j}}^{(0)}, \boldsymbol{j} > 2\right\}\right) \\ &\qquad\qquad \vdots \\ &\theta_p^{(1)} \text{ from } P\left(\theta_p \middle| \left\{\boldsymbol{\theta}_{\boldsymbol{j}}^{(1)}, \boldsymbol{j} < p\right\}\right) \end{aligned} \tag{23}$$

The cycle (23) is iterated $\boldsymbol{t}$ times, generating the sample $\boldsymbol{\theta}^{(t)} = \left(\boldsymbol{\theta}_1^{(t)}, \cdots, \boldsymbol{\theta}_p^{(t)}\right)$. As $\boldsymbol{t}$ approaches infinity, the joint distribution of $\boldsymbol{\theta}^{(t)}$ can be shown to approach the joint distribution $P(\boldsymbol{\theta})$.

Now regarding the implementation of Gibbs Sampler in the binary response models (i.e., probit and logit models), it supposes that the binary regression model can be defined as $P_i = F(\boldsymbol{X}_i'\boldsymbol{\beta}), i = 1, \cdots, n$, where $F(\cdot)$ is a known cumulative link function. The probit model is obtained if F is the standard Gaussian cumulative distribution function (CDF), whereas the logit model is obtained if F is the logistic CDF.

Let $\pi(\boldsymbol{\beta})$, a prior density, summarise the prior information about the vector of unknown parameters $\boldsymbol{\beta}$. Then the posterior density of $\boldsymbol{\beta}$ is given by

$$\pi(\boldsymbol{\beta}|data) = \frac{\pi(\boldsymbol{\beta}) \prod_{i=1}^{n} F(\boldsymbol{X}_i{}'\boldsymbol{\beta})^{y_i} \left(1 - F(\boldsymbol{X}_i{}'\boldsymbol{\beta})\right)^{1-y_i}}{\int \pi(\boldsymbol{\beta}) \prod_{i=1}^{n} F(\boldsymbol{X}_i{}'\boldsymbol{\beta})^{y_i} \left(1 - F(\boldsymbol{X}_i{}'\boldsymbol{\beta})\right)^{1-y_i} d\boldsymbol{\beta}} \tag{24}$$

Equation (24) is largely intractable. Thus a simulation-based tool for computing the exact posterior distribution of $\boldsymbol{\beta}$ is desired. (Albert and Chib, 1993) proposes augmenting the data set in logit and probit models with a set of latent variables $\boldsymbol{Z} = Z_1, \cdots, Z_n$ that are drawn from a truncated normal distribution $N[\boldsymbol{X}_i{}'\boldsymbol{\beta}, \sigma_i^2]$, where $\boldsymbol{X}_i{}'\boldsymbol{\beta}$ denotes the predicted value for the *i*th row of Z_i and σ_i^2 indicate the variance of the prediction.

$$Z_i = \boldsymbol{X}_i{}'\boldsymbol{\beta} + \varepsilon_i,\ \varepsilon_i \sim N(0, \sigma_i^2)\ \forall\ i = 1, \cdots, n$$

and

$$\mathrm{y}_i = \begin{cases} 0 \text{ when } Z_i \leq 0 \\ 1 \text{ when } Z_i > 0 \end{cases}$$

By introducing the Z_i's into the binary regression model, it is clear that the joint posterior density of the unobservable $\boldsymbol{\beta}$ and $\boldsymbol{Z} = (Z_1, \cdots, Z_n)$ given the data $\mathbf{y} = (y_1, \cdots, y_n)$ as $\pi(\boldsymbol{\beta}, \boldsymbol{Z}|\mathbf{y})$ is complicated. This is difficult to normalize and sample from directly. But the computation of the marginal distribution of $\boldsymbol{\beta}$ by using the Gibbs sampler algorithm to estimate probit and logit models requires only the posterior distribution of $\boldsymbol{\beta}$ conditional on $\boldsymbol{Z}$ and the posterior distribution of $\boldsymbol{Z}$ conditional on $\boldsymbol{\beta}$. In usual practice, suppose that a priori distribution of $\boldsymbol{\beta}$ having equal probability for each parameter, it is customary to assign a flat noninformative prior to $\boldsymbol{\beta}$. These fully conditional distributions are of standard forms and given below

$$\boldsymbol{\beta}|\boldsymbol{Z}, \boldsymbol{X}, \mathbf{y} \sim \boldsymbol{N}\left(\widetilde{\boldsymbol{\beta}}, \widetilde{\boldsymbol{\Sigma}}\right) \tag{25}$$

where

$$\widetilde{\boldsymbol{\beta}} = \left(\boldsymbol{\Sigma}_{prior}^{-1} + \boldsymbol{X}'\boldsymbol{X}/\sigma^2\right)^{-1}\left(\boldsymbol{\Sigma}_{prior}^{-1}\boldsymbol{\beta}_{prior} + \boldsymbol{X}'\boldsymbol{Z}/\sigma^2\right)$$
$$\widetilde{\boldsymbol{\Sigma}} = \left(\boldsymbol{\Sigma}_{prior}^{-1} + \boldsymbol{X}'\boldsymbol{X}/\sigma^2\right)^{-1}$$

The random variables $Z_1, \cdots, Z_n$ are independent with

$$Z_i|(\mathbf{y_i} = \mathbf{1}, \boldsymbol{X_i}, \boldsymbol{\beta}) \sim \boldsymbol{N}(\boldsymbol{X_i}'\boldsymbol{\beta}, \sigma_i^2)$$
truncated at the left by 0
$$Z_i|(\mathbf{y_i} = \mathbf{0}, \boldsymbol{X_i}, \boldsymbol{\beta}) \sim \boldsymbol{N}(\boldsymbol{X_i}'\boldsymbol{\beta}, \sigma_i^2)$$
truncated at the right by 0 (26)

Note from Equation (26) that the variance σ^2 is taken to be one in the probit model since the scale of the distribution **y** can be represented by Φ. Accordingly, iterations of $\boldsymbol{t}$ of the Gibbs sampler consist of the following steps:

1) Sample $Z_i^{(t)}$ from respective truncated Normals in (26);

2) Sample $\boldsymbol{\beta}^{(t)}$ from the multivariate Normal in (25)

6.2.2.3 The Metropolis Sampler

The Metropolis sampler is another way of generating a Markov chain. With reference to Equation (22), the Metropolis algorithm (Metropolis et al., 1953) (Hastings, 1970) proceeds by sampling a proposal value $\boldsymbol{\beta}^*$ nearby the current value $\boldsymbol{\beta}^{(i)}$ using a symmetric proposal distribution $Q(\boldsymbol{\beta}^*|\boldsymbol{\beta}^{(i)})$. Symmetric here indicates that $Q(\boldsymbol{\beta}^*|\boldsymbol{\beta}^{(i)}) = Q(\boldsymbol{\beta}^{(i)}|\boldsymbol{\beta}^*)$. Usually the samples from $Q(\boldsymbol{\beta}^*|\boldsymbol{\beta}^{(i)})$ is near $\boldsymbol{\beta}^{(i)}$ with high probability. For instance, $Q(\boldsymbol{\beta}^*|\boldsymbol{\beta}^{(i)}) = \text{normal}(\boldsymbol{\beta}^{(i)}, \delta^2)$, where the parameter δ is generally chosen to make the approximation algorithm run efficiently. In usual practice, given $\boldsymbol{\beta}^{(i)}$, the Metropolis algorithm generates a value $\boldsymbol{\beta}^{(i+1)}$ as follows:

1) Sample $\boldsymbol{\beta}^* \sim Q(\boldsymbol{\beta}^*|\boldsymbol{\beta}^{(i)})$;

2) Compute the acceptance ratio

$$\gamma = \frac{P(\boldsymbol{\beta}^*|y)}{P(\boldsymbol{\beta}^{(i)}|y)} = \frac{P(y|\boldsymbol{\beta}^*)P(\boldsymbol{\beta}^*)}{P(y|\boldsymbol{\beta}^{(i)})P(\boldsymbol{\beta}^{(i)})} \quad (27)$$

3) Let $U \sim \text{uniform}[0,1]$, and setting

$$\boldsymbol{\beta}^{(i+1)} = \begin{cases} \boldsymbol{\beta}^{*}, & \text{if } U < \gamma \\ \boldsymbol{\beta}^{(i)}, & \text{otherwise} \end{cases}$$

The Metropolis algorithm is similar to the Metropolis-Hastings algorithm, except that the acceptance ratio does not contain an extra factor about the proposal distribution $Q(.)$. It is clear that having obtained a proposed value $\boldsymbol{\beta}^{*}$, either which or a copy of $\boldsymbol{\beta}^{(i)}$ is to be added to the sample set, depending on the ratio in Equation (27).

Coming back to the issue of the implementation of the Metropolis Sampler to the probit and logit models, let $F(\boldsymbol{X_i}'\boldsymbol{\beta})$ denote either the standard Gaussian CDF or the logistic CDF. To facilitate the calculation of the acceptance ratio γ given in Equation (27), the likelihood function $P(y|\boldsymbol{\beta})$ of both binary models represents an essential factor for Bayesian computations and is expressed as

$$\boldsymbol{\mathcal{L}}(\boldsymbol{\beta}) = \prod_{i=1}^{n} F(\boldsymbol{X_i}'\boldsymbol{\beta})^{y_i} \left(1 - F(\boldsymbol{X_i}'\boldsymbol{\beta})\right)^{1-y_i}$$

Considering y_i is the observed data generated by performance-based tools and techniques. Then, the log-likelihood function is

$$\ln \boldsymbol{\mathcal{L}}(\boldsymbol{\beta}) = l = \sum_{i=1}^{n} \left[y_i \ln F(\boldsymbol{X_i}'\boldsymbol{\beta}) + (1 - y_i) \ln\left(1 - F(\boldsymbol{X_i}'\boldsymbol{\beta})\right) \right] \tag{28}$$

On the other hand, the prior probability distribution in Equation (27) is supposed to have a multivariate normal distribution $P(\boldsymbol{\beta}) \sim \mathcal{N}(\widehat{\boldsymbol{\beta}}, \boldsymbol{\Sigma}_{\beta})$, where $\widehat{\boldsymbol{\beta}}$ is considered as the starting mean value. This may be taken as the maximum likelihood (ML) estimates, or alternatively the least squares (LS) estimates, as $(\boldsymbol{X}^T\boldsymbol{X})^{-1}\boldsymbol{X}^T\mathbf{y}$. Moreover, $\boldsymbol{\Sigma}_{\beta}$ denotes a variance-covariance matrix for measuring the degree to which two variables change or vary at the same time. Knowing that the covariance of two random variables, β_i and β_{i+1} can be mathematically represented as

$$cov(\beta_i, \beta_{i+1}) = \mathrm{E}[(\beta_i - \mu_i)(\beta_{i+1} - \mu_{i+1})]$$

where $\mu_i = \mathrm{E}(\beta_i)$ is the expected value of the *i*th entry in the vector $\boldsymbol{\beta}$. This relationship can be more explicitly represented as

$$\boldsymbol{\Sigma}_{\beta} = cov(\boldsymbol{\beta}) = \begin{bmatrix} var(\beta_1) & cov(\beta_1, \beta_2) & \dots & cov(\beta_1, \beta_p) \\ cov(\beta_2, \beta_1) & var(\beta_2) & \dots & cov(\beta_2, \beta_p) \\ \dots & \dots & \dots & \dots \\ cov(\beta_p, \beta_1) & cov(\beta_p, \beta_2) & \dots & var(\beta_p) \end{bmatrix}$$

The covariance matrix $\boldsymbol{\Sigma}$ of $\widehat{\boldsymbol{\beta}}^{ML}$ (i.e. Maximum Likelihood Estimation of $\boldsymbol{\beta}$ given $\frac{\partial \boldsymbol{\mathcal{L}}}{\partial \boldsymbol{\beta}}\Big|_{\widehat{\boldsymbol{\beta}}} = 0$) is pointed out to be comparable to the negative of the inverse of the expected value of the Hessian matrix (Yuen, 2010).

$$\boldsymbol{\Sigma}_{\beta} = -\mathrm{E}[\boldsymbol{\mathcal{H}}(\boldsymbol{\beta})]^{-1} \tag{29}$$

where the Hessian $\boldsymbol{\mathcal{H}}$ is the square matrix of second derivatives of the log-likelihood with respect to the parameters $\boldsymbol{\beta} = (\beta_1, \cdots, \beta_p)$. By taking partial differentiations with respect to β_i and β_{i+1}, the component of the Hessian matrix can be obtained

$$\boldsymbol{\mathcal{H}}_{(i,i+1)}(\boldsymbol{\beta}) = \frac{\partial^2 \ln \boldsymbol{\mathcal{L}}(\boldsymbol{\beta})}{\partial\, \beta_i\, \partial\, \beta_{i+1}}\Big|_{\boldsymbol{\beta}=\widehat{\boldsymbol{\beta}}} \tag{30}$$

It is obvious that finding the inverse of the Hessian $\boldsymbol{\mathcal{H}}^{-1}$ in high dimensions can be an expensive operation. In such cases, calculating the Hessian numerically is more reasonable than using an analytic formula. Quasi-Newton methods are normally applied to approximate the Hessian matrix $\boldsymbol{\mathcal{H}}(\boldsymbol{\beta})$. The rationale behind this algorithm is outlined afterwards.

In Newton's method, the second order Taylor series is used to find the minimum value of the function (i.e. defined as $J(\boldsymbol{\beta}) = \ln \boldsymbol{\mathcal{L}}(\boldsymbol{\beta})$) when its derivative is equal to zero.

$$J(\boldsymbol{\beta^k} + \Delta\boldsymbol{\beta}) \approx J(\boldsymbol{\beta^k}) + \nabla J(\boldsymbol{\beta^k})^T \Delta\boldsymbol{\beta} + \frac{1}{2}\Delta\boldsymbol{\beta}^T \boldsymbol{\mathcal{H}}[J(\boldsymbol{\beta^k})]\Delta\boldsymbol{\beta}$$

where $\nabla J(\boldsymbol{\beta})$ is the gradient of a function and $\boldsymbol{\mathcal{H}}[J(\boldsymbol{\beta})]$is an approximation to the Hessian matrix. The gradient $\nabla J(\boldsymbol{\beta^k} + \Delta\boldsymbol{\beta})$ also has a Taylor series approximation

$$\nabla J(\boldsymbol{\beta^k} + \Delta\boldsymbol{\beta}) \approx \nabla J(\boldsymbol{\beta^k}) + \boldsymbol{\mathcal{H}}[J(\boldsymbol{\beta^k})]\Delta\boldsymbol{\beta}$$

And setting the gradient (with respect to $\Delta\boldsymbol{\beta}$) to zero provides the Newton step

$$\Delta\boldsymbol{\beta} = -\boldsymbol{\mathcal{H}}\left[J\left(\boldsymbol{\beta}^{\boldsymbol{k}}\right)\right]^{-1}\nabla J\left(\boldsymbol{\beta}^{\boldsymbol{k}}\right)$$

The Hessian approximation $\boldsymbol{\mathcal{H}}$ is updated iteratively at each stage and chosen to satisfy

$$\boldsymbol{\mathcal{H}}^{\boldsymbol{k+1}} \cdot \left(\boldsymbol{\beta}^{\boldsymbol{k+1}} - \boldsymbol{\beta}^{\boldsymbol{k}}\right) = \nabla J\left(\boldsymbol{\beta}^{\boldsymbol{k+1}}\right) - \nabla J\left(\boldsymbol{\beta}^{\boldsymbol{k}}\right) \tag{31}$$

One of the common quasi-Newton algorithms is named as BFGS method (suggested independently by Broyden, Fletcher, Goldfarb, and Shanno, in 1970). It imposes on this update (given starting point $\boldsymbol{\beta}^0 = 0$ and set $\boldsymbol{\mathcal{H}}^0 = \boldsymbol{I}$) for $k = 1,2,\cdots$, until a stopping criterion as Equation (31) is satisfied.

On the basis of the forgoing, the prior probability distribution $P(\boldsymbol{\beta}) \sim \mathcal{N}(\widehat{\boldsymbol{\beta}}, \boldsymbol{\Sigma}_{\beta})$ in Equation (27) for computing the acceptance ratio γ is accomplished when the covariance matrix $\boldsymbol{\Sigma}_{\beta}$ is worked out depending on the simulated results of the inverse of the Hessian $\boldsymbol{\mathcal{H}}^{-\boldsymbol{1}}$. In other words, the Metropolis sampler can progress effectively if the prior to $\boldsymbol{\beta}$ is linked with the likelihood function given in Equation (28).

From the consistent introductions to the above two sampling algorithms, it can be appreciated that there are two important differences between the Gibbs sampler and the Metropolis sampler: 1) the Gibbs sampler always takes a step e.g. $\boldsymbol{\beta}$ is always updated until t times of iteration approached, whereas the Metropolis may remain in the same position; and 2) the Gibbs sampler uses the full conditional distribution $P(\boldsymbol{\beta}|\boldsymbol{Z}, \boldsymbol{X}, \mathbf{y}, \sigma^2, \rho)$, not the marginal for the parameter being considered.

6.2.2.4 Diagnostics of Chain Convergence

In practice, probit and logistic regression models provide similar fits. For example, Figure 6.4 graphs the sample data and the estimated probabilities. Some literatures also indicate that the inferences from either probit or logistic models are often the same (Greene, 2003) (Agresti, 2007). A key focus in this chapter is on introducing MCMC sampling methods for computing the exact posterior distribution of $\boldsymbol{\beta}$. Therefore, Only probit model, for which the link function F is the standard Gaussian CDF Φ, will be put forward due to tight schedule.

For example, the Markov chain samples of β_1 generated through the sampling algorithms as described in the previous two sections are illustrated in Figure 6.5 and Figure 6.6. The first 1000 Markov chain samples are traced. Evidently the starting value $\beta_1^{(0)} = 0$ shown on each top plot is far from a reasonable estimate, the lack of knowledge about $\beta_1^{(0)}$ leads to such poor estimates at initial stages. The early estimates are not allowed for any inference of β_1 and usually to be defined as burn-in period. As a result, both bottom plots discard the first 500 iterations and show an immediate convergence of the simulation to the correct value for β_1.

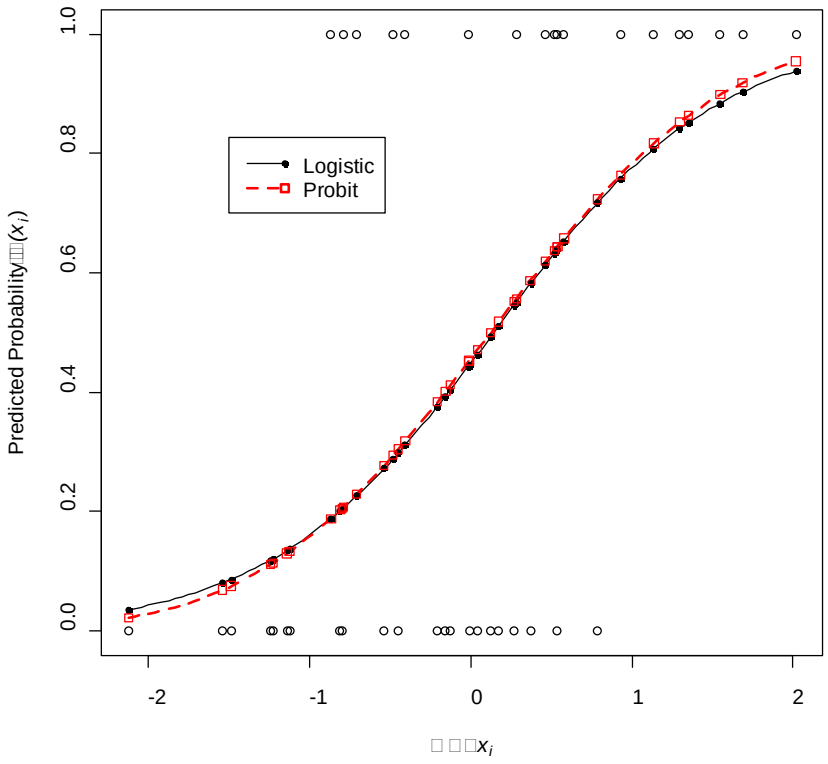

Figure 6.4: The Logistic and Normal Cumulative Distribution Functions

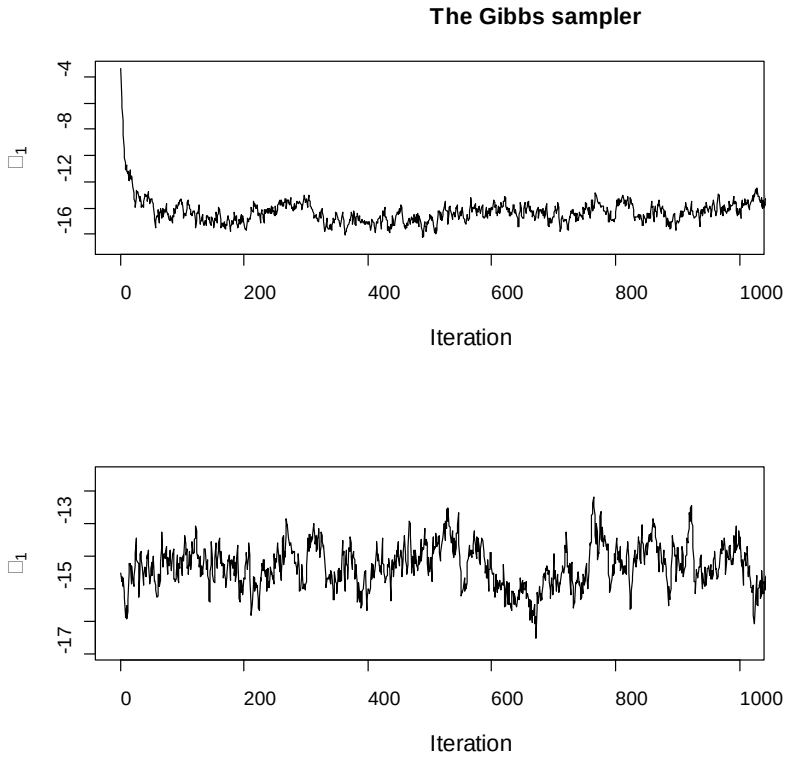

Figure 6.5: Markov Chain Samples Using Gibbs Sampling for β_1

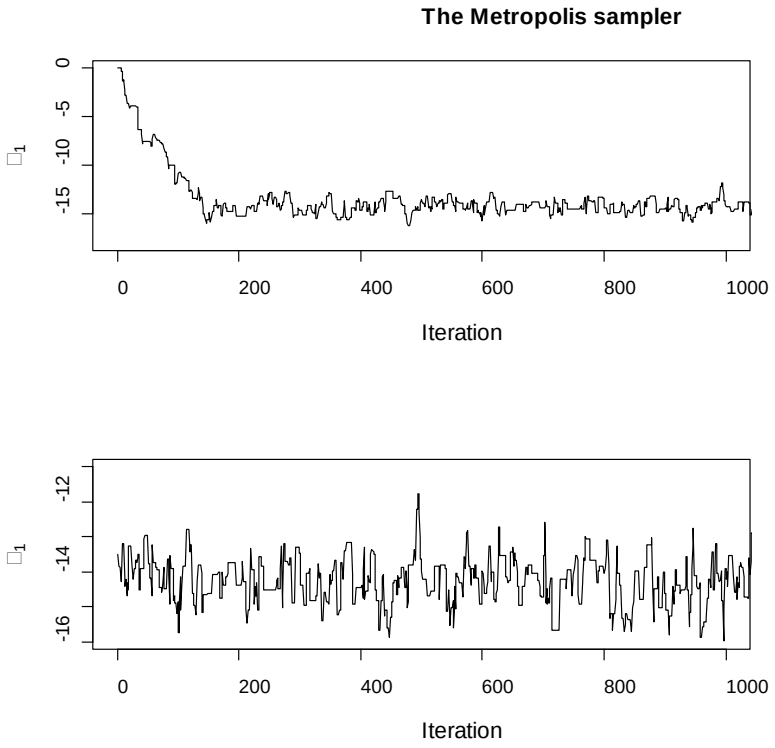

Figure 6.6: Markov Chain Samples Using Metropolis Sampling for β_1

It should be noted that the inferences of $\boldsymbol{\beta}$ made in Figure 6.5 and Figure 6.6 by using the Markov chain samples are based on the assumption that the sample densities for the unknown parameters are good estimates of the target densities (the marginal posterior density). With this in mind, valid inferences can only be made when a chain has converged to the target density. Assessing chain convergence is a key component of any analysis about the sampling with Markov chains. This section mainly presents the method for diagnosing chain convergence.

There are several methods that have been proposed on testing the convergence of MCMC samplers (Cowles and Carlin, 1996). Looking at the history of iterations using a time series plot (e.g., Figure 6.6) is commonly believed as a simple method of assessing chain convergence. It can provide a useful checking and identify problems with the chain. Furthermore, it is more acceptable to use more formal testing procedures. A plot of the serial autocorrelations as a function of the time lag is a more informative approach, as it summarizes the dependence between neighbouring samples. Ideally consecutive samples should be completely independent, leading to an efficient chain. This indicates the higher autocorrelation in the chain, the larger the MCMC variance and the worse the approximation is, thus the more MCMC samples are needed to attain a precise approximation. In practice, large values of the autocorrelation (greater than 0.4) normally show that the chain is problematic. For instance, concerning an observed chain $\beta = \left[\beta^{(1)}, \cdots, \beta^{(n)}\right]$, the autocorrelation function (ACF) at lag *k* is

$$\mathrm{acf}_k(\beta) = \rho(k) = \frac{\frac{1}{n-k}\sum_{t=1}^{n-k}\left(\beta^{(t)} - \bar{\beta}\right)\left(\beta^{(t+k)} - \bar{\beta}\right)}{\frac{1}{n-1}\sum_{t=1}^{n}\left(\beta^{(t)} - \bar{\beta}\right)^2}$$

where $\bar{\beta}$ is the sample mean. If there is a high autocorrelation between the β_i's, this indicates that more iterations of the sampling are required to obtain a decent approximation to the posterior distribution. Actually the autocorrelation can be reduced by systematically using every *j*th sample and discarding the others (this process is known as thinning).

An example of the reduction in the autocorrelation due to thinning is shown in Figure 6.7. The plot shows the chain histories and autocorrelation from lag 0 to 30 ($k = 0, \cdots, 30$) for a chain with no thinning and the same chain thinned by 10 ($j = 10$). The chains are the estimates of β_1 using Metropolis sampling. The first 500 iterations were discarded as a burn-in. For the chain with no thinning the autocorrelation at lag 1 is large $\rho(1) = 0.866$. Thinning by 10 reduces the autocorrelation at lag 1 to $\rho(1) = 0.281$. The cost of this reduction is an extra 9000 samples to give 1000 thinned samples.

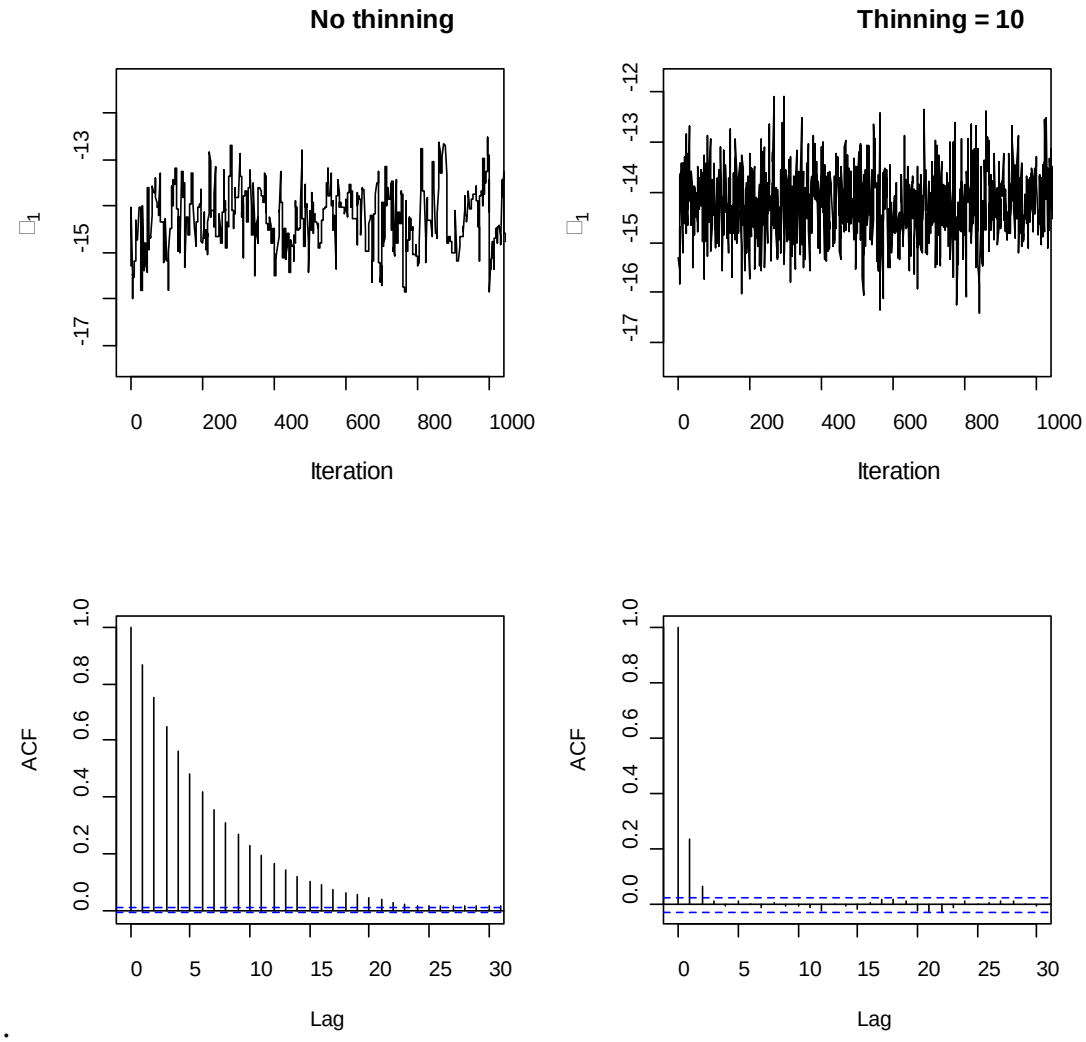

Figure 6.7: Reduction in Autocorrelation of Metropolis Samples after Thinning. Chain History (top row) and ACF (bottom row) for the Estimate of β_1

6.2.3 Uncertainty Bounds Estimation

The previous section shows that the Markov chain samples can provide a complete posterior distribution when the chains have correctly converged. This enables further inferences of unknown parameters. As it is demonstrated in Figure 6.8, a histogram of β_1 is generated by using Metropolis sampling. The first 1000 samples are shown in Figure 6.6. The following histogram is based on discarding the first 500 samples (burn-in) and using a sample size of 10,000. A bell-shaped distribution is displayed and it is possible that the posterior distribution about β_1 is approximately Normal. Hence, a range of analysis to β_1 can be formulated, for instance, the mean of $\beta_1$is computed using the mean of the sampled value, as given in equation (32).

$$\overline{\beta} = \frac{1}{N}\sum_{i=1}^{N} \beta^{(i)} \tag{32}$$

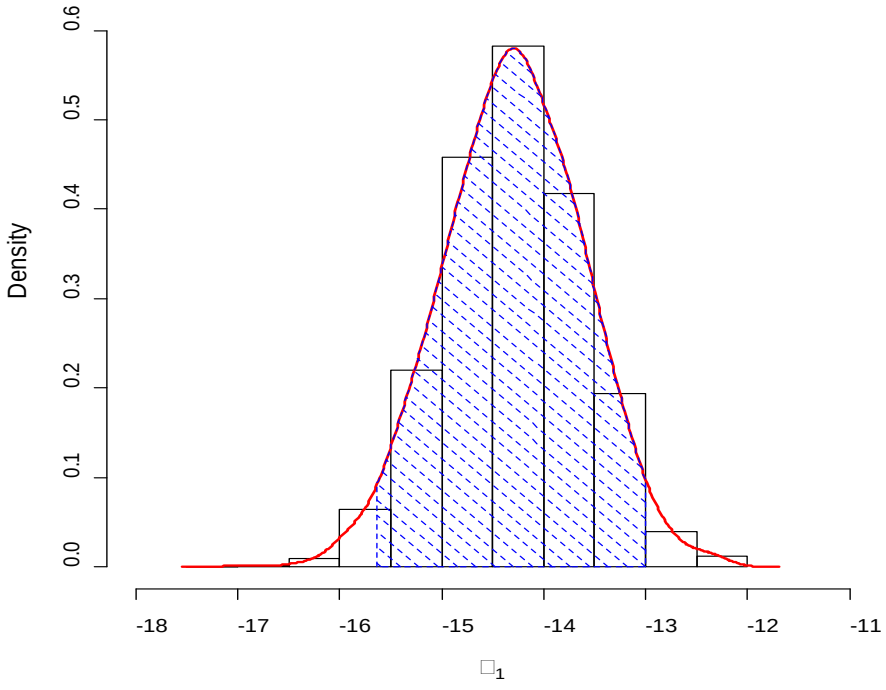

Figure 6.8: Histograms of Markov Chain Samples Using Metropolis Sampling for β_1

By doing so, a likely range for β_1 can be estimated using a posterior interval. The α% posterior interval contains the central α% of the sampled values, and so the

interval contains the true estimate with probability α. The lower limit of the interval is the $(50 - \alpha/2)$th percentile of the Markov chain samples, and the upper limit is the $(50 + \alpha/2)$th percentile. So a 95% posterior interval goes from the 2.5th to 97.5th percentile. As shown in Figure 6.8, using our sampled β_1 the empirical mean $\overline{\beta_1} = -14.3$ and standard deviation $\sigma_{\beta_1} = 0.68$ for the sample size N=10,000. Meanwhile, a 95% posterior interval for β_1 is from -15.64 to -12.99. It means that the posterior probability $P(\beta_1 | \boldsymbol{Z}, \boldsymbol{X}, \mathbf{y})$ lies in such an interval is 0.95. In the case of the probit model shown in Equation (14) (see Section 5.3.2), the model coefficients $(\boldsymbol{\beta} = \alpha, \beta_1, \cdots, \beta_n)$ are random variables. So once the empirical distribution of each model coefficient is appropriately simulated by Markov chain samples, the corresponding posterior probability $P(Y = 1|\boldsymbol{\beta}, \boldsymbol{X})$ will be attained, so it will be straightforward to quantify the uncertainty boundary through quantile estimations.

6.2.4 Bayesian Analysis for Binary Response Regression Models in Ship Survivability Prediction

With the detailed algorithms of MCMC methods for Bayesian computation, this section focuses on how Bayesian inference can be deployed to address ship survivability assessment after damage. A simplified example presents Bayesian analysis for estimating generalized linear model with a probit link function.

6.2.4.1 An example of Ship Survivability Prediction

As Bayesian methods enable plausible inferences based on the assembled data deriving from first-principles tools (e.g. numerical simulations and physical model experiments), it is a good practice to use Bayesian analysis to predict the stochastic ship behaviour follow flooding with relevant data. Knowing that the interested phenomenon is physically influenced by a list of variables as identified in Section 5.2.1 (e.g. damage characteristics, ship subdivision arrangement, loading condition, and sea environment), the following example focuses on training a predictive model towards the probability of capsizing within given time $P(t_0 = 30min, Y = 1 \,|\, \boldsymbol{\beta}, \boldsymbol{X})$. Here only a single influential variable (i.e. sea environment measured by Significant

Wave H_s) is used to illustrate the applicability of the proposed Bayesian approach. Concerning the probit regression model for binary outcomes, the question at hand can be easily formulated as shown in Equation (33), in which a series of predictor variables ($\boldsymbol{X} = x_1, \ldots x_n$) can be included at once. For the time being, only a single variable H_s is considered for the model training, where $\boldsymbol{X} = x = H_s$.

$$P(t_0 = 30min, Y = capsize|\boldsymbol{\beta}, \boldsymbol{X}) = \Phi(\alpha + \boldsymbol{\beta X}) \quad (33)$$

Following this, an immediate task is to assemble evidence so that Bayesian methods can be managed to solve the proposed model. The data is collected from physical model tests on survivability of RoPax vessels. The experiment has been undertaken in European Commission research project FLOODSTAND (http://floodstand.aalto.fi/) under Task 4.1(Rask, 2010). In total, there are 83 measured records, as tabulated in Table 6.1. Having the data, the target densities $P(\boldsymbol{\beta}|\boldsymbol{Z}, \boldsymbol{X}, \mathbf{y})$ are approximated by using 10,000 iterations with a burn-in sample size of 500.

Regarding the Metropolis algorithm, in order to avoid having a highly correlated Markov chain, generally an acceptance rate (i.e. the ratio of No. of acceptance of a proposal value $\boldsymbol{\beta}^*$to the total No. of samples) is an indicator to check the chain convergence. In normal practice, the chain is considered to have a low correlation if the acceptance rate stands between 20 and 50%. This example illustrates that $\boldsymbol{\beta}^*$ is accepted as $\boldsymbol{\beta}^{(i+1)}$ for 28.5% of all iterations (i.e. 2996 times out of total 10500 iterations).

Table 6.1: M/V Estonia, Experimental Test Matrix, $t_0 = 30$ minutes

Theoretical H_s	No. of Capsize	No. of tests	Rate of Capsize
2	0	3	0
2.5	2	20	0.10
2.6	13	20	0.65
2.75	16	20	0.80
3	20	20	1

The estimated model coefficients are summarized in Table 6.2. The value of β pertinent to H_s is positive that indicates a positive correlation between the probability of capsizing and the significant wave height. Figure 6.9 plots the MCMC approximations to the marginal posterior densities of the two coefficients α and β.

The 99% confidence interval of each parameter is measured based on 0.5% and 99.5% posterior quantiles of $P(\boldsymbol{\beta}|\boldsymbol{Z},\boldsymbol{X},\mathbf{y})$.

Table 6.2: Fitting a Ship Response Model (after Flooding) to the Experimental Data

Parameter	Mean	SD	99% posterior interval
α	-21.63	4.631	-34.833, -11.228
β for H_s	8.295	1.769	4.334, 13.368

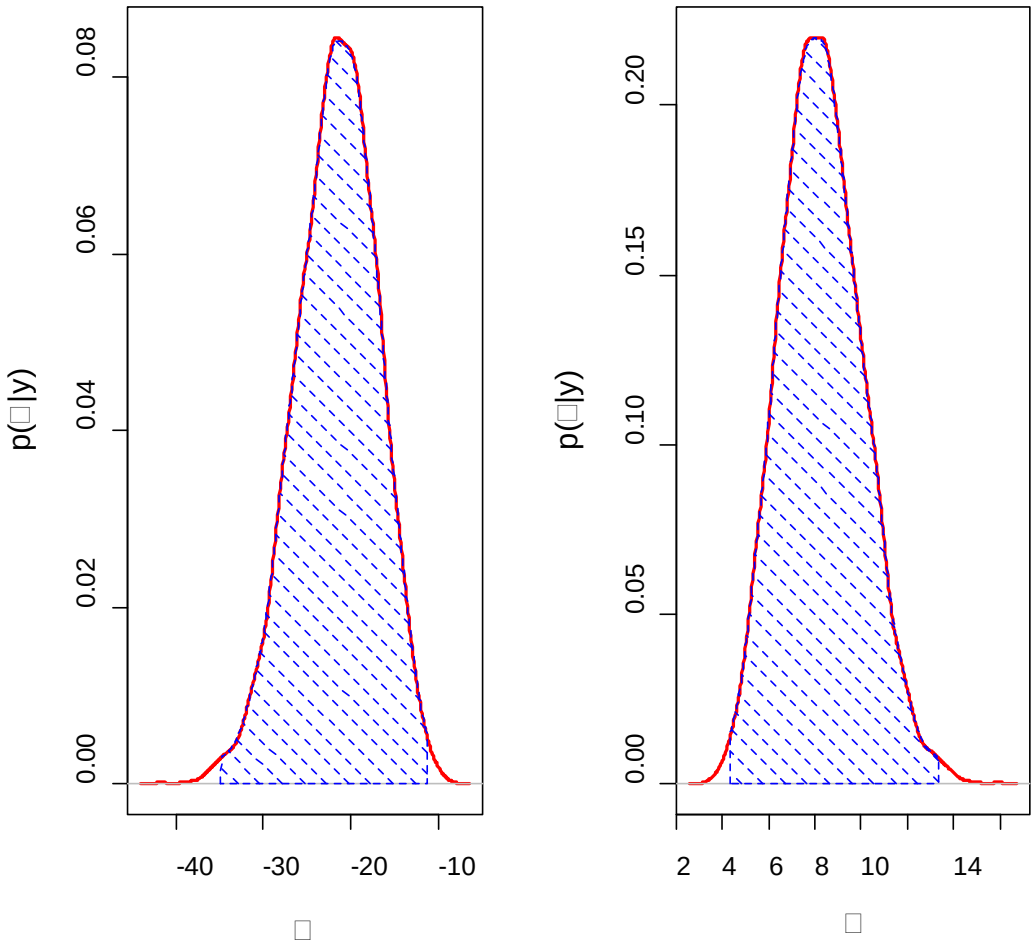

Figure 6.9: MCMC approximations to the posterior distributions of α and β

With the simulated distribution of the model coefficients $P(\boldsymbol{\beta}|\boldsymbol{Z},\boldsymbol{X},\mathbf{y})$, the corresponding posterior density of the response variable, probability of capsizing $P(Y = cap|\boldsymbol{\beta},\boldsymbol{X} = H_s)$ within 30 minutes can be estimated easily at a given sea state. In so doing, a continuous distribution of the rate of capsizing is accomplished as shown in Figure 6.10, if a range of sea states are considered. It is noted that the

depicted Bayesian distribution, cooperated with 99% confidence interval, have a good agreement with the experimental results.

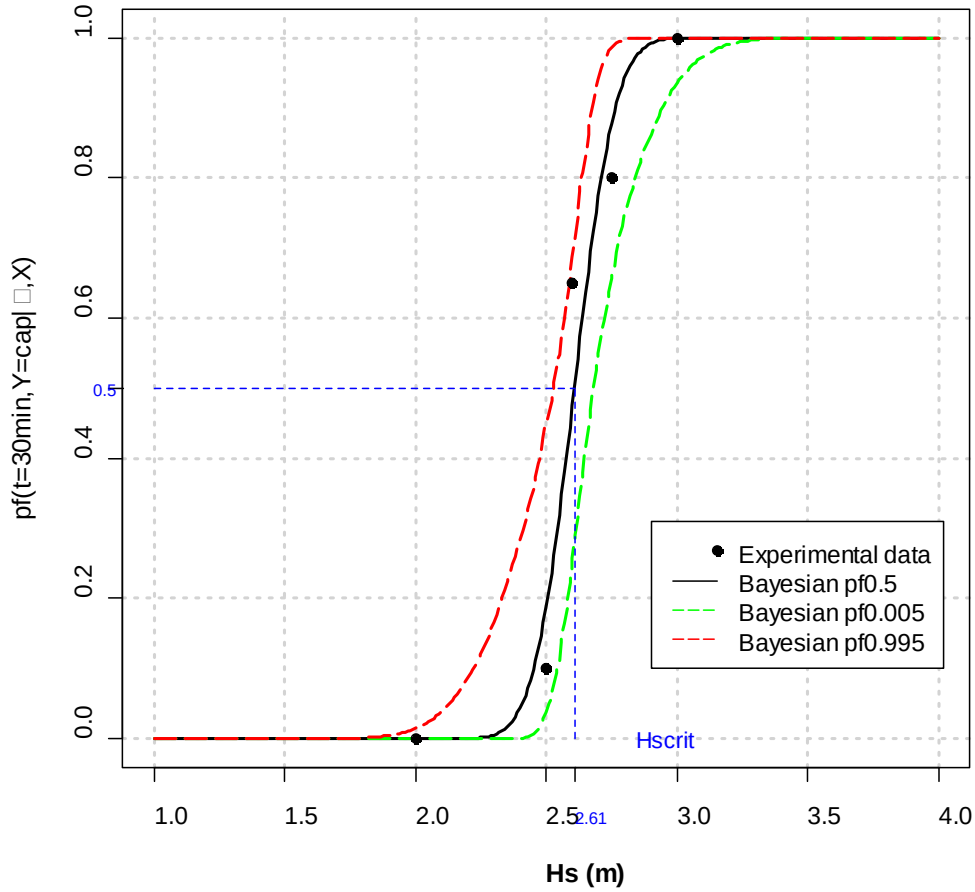

Figure 6.10: M/V Estonia, Posterior distribution of the Rate of Capsizing Simulated by Bayesian inference (Applying Tailored Testing Data for Model Training)

6.2.4.2 Ship Survival Time Assessment

In Figure 6.10, the rate of changes has a sigmoid shape that varies with the encountered sea states. Obviously the estimated probit model is able to predict the rate of capsizing for a specific flooding case. Nevertheless, it is important to understand that such survivability predictions are performed based on data collected from tank tests which last for 30 minutes for each round in this case. Hence, it is necessary to set up a relationship between the time and the ensuing survivability for given damage conditions.

Under such circumstance, the theory of the Bernoulli trial process can be adopted (Jasionowski, 2006). Suppose that the probability of capsizing $p_f = P(Y = 1|\boldsymbol{\beta}, \boldsymbol{X})$ is constant for a given damage j, consequently, the probability that the nth test is a case of "capsizing" can be measured by Equation (34). The number of trials can be determined from $n = \frac{t_{cap}}{t_0 = 30min}$, where t_{cap} (in minutes) is the cumulative time leading to the capsizing of a damaged ship. Thus the probability of capsizing against the encountered sea states within t_{cap} can be determined.

$$F\left(t_{cap}\middle|H_s, j\right) = 1 - \left(1 - p_f\right)^n = 1 - \left(1 - p_f\right)^{\frac{t_{cap}}{t_0}} \tag{34}$$

As a result, the matching probability density function PDF of "time to capsize" can be formulated as shown in Equation (35).

$$g\left(t_{cap}\middle|H_s, j\right) = \frac{\partial F_{t_{cap}}}{\partial t_{cap}} = -\ln\left(1 - p_f\right) \cdot \left(1 - p_f\right)^{\frac{t_{cap}}{t_0}} \cdot {t_0}^{-1} \tag{35}$$

Concerning the experimental results as tabulated in Table 6.1, the case of $H_s = 2.6$m where $p_f = 0.65$ measured within 30 minutes has been select to demonstrate how the ship survivability assessment can be extended to any time interval. After 20 independent survivability tests, the histogram of time to capsize is plotted in Figure 6.11. In contrast to the rate of capsizing observed from tank test, a predicted value of $p_{f\_Bayes} = 0.477$, which is obtained through Bayesian inference as depicted in Figure 6.10, is substituted into Equation (35) to compute the resultant PDF at the same wave height $H_s = 2.6$m.

Keeping in mind that no initial transient flooding has been modelled during the tank testing. The wave tests start from an equilibrium stage when the damaged compartments have been flooded. Thus a reasonable divergence exists between the experimental histogram and the Bayesian computed PDF in the first 600s of Figure 6.11. Afterwards, the corresponding cumulative distributions $F\left(t_{cap}\middle|H_s\right)$ are also graphed for both methods of assessment, where the CDF curve provides the probability of the cumulative amount of time that it takes the ship to capsize/sink. Meanwhile, Bayesian confidence statements as a 99% confidence interval of

$F(t_{cap}|H_s)$ represent a good way to quantify the uncertainties associated with the measurements.

In the same way, Figure 6.12 and Figure 6.13 show cases when the experiments are performed at $H_s = 2.75$m with $p_f = 0.8$ and $H_s = 3.0$m with $p_f = 1$. The related Bayesian results $p_{f\_Bayes} = 0.878$ and 0.999 are also illustrated. It can be seen that all of the measured probabilities (rates) of capsizing within 30 minutes from tank tests lie within the assigned 99% uncertainty bounds.

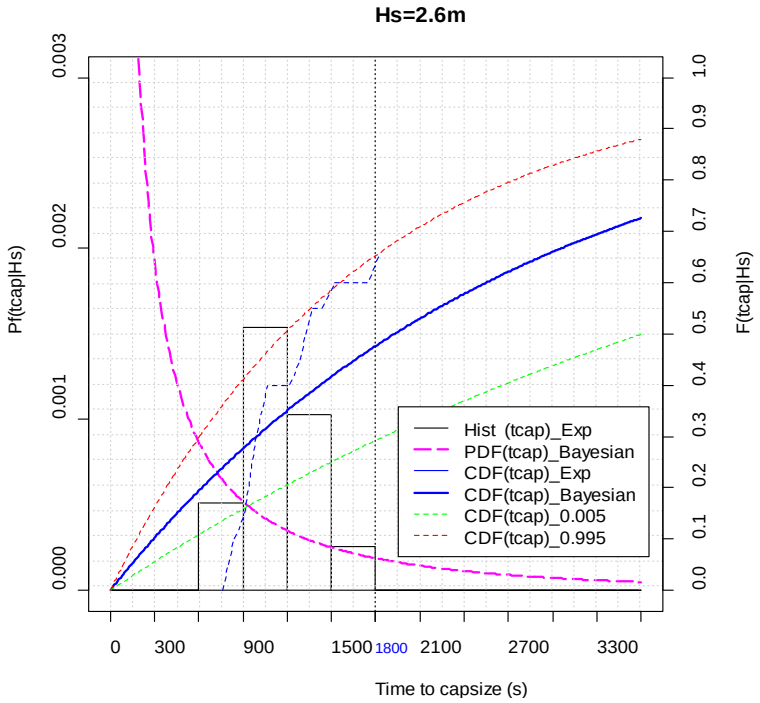

Figure 6.11: M/V Estonia, 1) Histogram of Probability Density Function of Time to Capsize Given the Damage Case Tested at *Hs* =2.6m with $p_f = 0.65$; 2) Bayesian Estimate of the PDF of Time to Capsize; 3) Cumulative Probability of Time to Capsize $F(t_{cap}|H_s)$ from Experimental Measurements; 4) Bayesian Estimate of the CDF with the quantified 99% uncertainty bounds. The Evaluation Time of Tank Testing = 30 minutes.

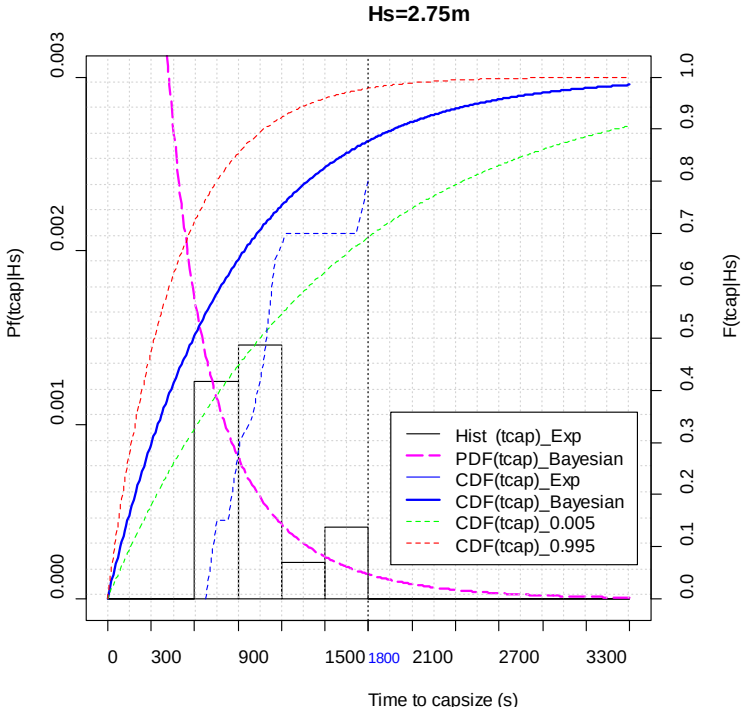

Figure 6.12: M/V Estonia, the PDFs and CDFs of Time to Capsize Given the Damage Case Tested at *Hs* =2.75m with $p_f = 0.8$

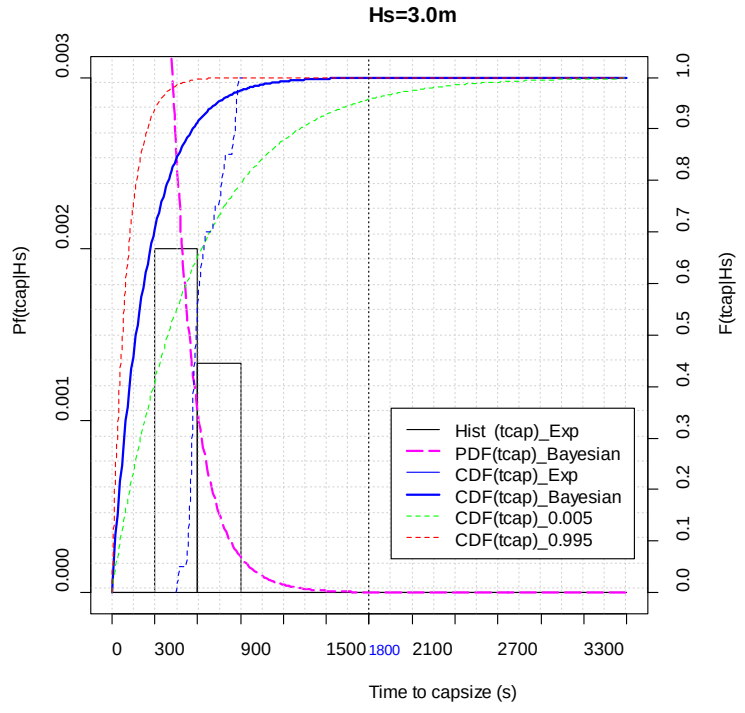

Figure 6.13: M/V Estonia, the PDFs and CDFs of Time to Capsize Given the Damage Case Tested at *Hs* =3.0m with $p_f = 0.999$

6.3 Procedures for Probabilistic Uncertainty Quantification in Ship Survivability Prediction

After the demonstration of using Bayesian inference to make an assessment of ship survivability following flooding, this section aims to illustrate a more comprehensive procedure which details the proposed Bayesian approach for undertaking the probabilistic uncertainty quantification in ship survivability prediction. The whole procedure consists of five consecutive steps:

i) It starts with data collection to extract information of both inputs and outputs.

ii) It performs a complete model estimation to simulate the marginal posterior densities of unknown model parameters.

iii) It carries out a probabilistic sensitivity study to investigate how each element of the model inputs contributes to the uncertainty in the output.

iv) An uncertainty analysis of the model output can be achieved once all the inputs have been identified.

v) Model validation is needed to express the discrepancy between Bayesian estimates and the tangible measurements.

6.3.1 Experimental Data Collection

Referring to Section 5.2.2, it is mentioned that both the numerical models and the model experiments are the first-principles tools which are commonly employed for better characterizing the physical phenomenon of ship capsizing in time-domain. In this section, the data collected from the benchmark model testing has been given greater assent as one of the reliable sources of information for the proposed model estimation. A series of experiments (consistent with 2003/25/EC (EC, 2003)) on survivability assessment of RoPax vessels have been undertaken in the related projects funded by the European Commission (e.g. HARDER (Tuzcu and Tagg, 2001), SAFEDOR (Chen et al., 2009), FLOODSTAND). In total, the measurements

from 756 runs of the repetitive test over three diverse ship models are available for the subsequent uncertainty analysis.

Having a perception of the source of data, the key input variables in a model need to be distinguished in accordance with the governing variables described in Section 5.2.1. A set of relevant variables affecting ship survivability after flooding could be divided into three categories: i) sea environment represented by the significant wave height H_s, ii) ship intact loading conditions are addressed by draught, *KG*, and trim, iii) damage attributes is only characterized by the damage length L_d in this case study and additionally the angle of heel of a ship at the damaged equilibrium stage is also considered.

As the size of experimental data is always restricted by both allocated time and budget, it is necessary to maximize the utility of the limited data for statistical inference. Therefore, non-dimensional measurements of the aforementioned variables, that will be favorable for processing the data analysis regardless of the size of the ship. In this way, the ratios between draught and depth (T/D), the centre of gravity and the transverse Metacentric (KG/KMT), the damage length and the subdivision length of a ship (L_d/L_s) are adopted together. As it is discussed in Section 5.2.1.1, the hull breach is generally described by a set of parameters concerning location, penetration, height besides length. However, the principle assumption underlying the model test method complying with Stockholm Agreement (IMO, 1996) is that the "assumed" damage is resulting from a hull breach of $0.03 \times L + 3m$ and penetrating the hull up to B/5. So a non-dimensional parameter about the damage penetration is a constant factor here as 0.2 and thus cannot be selected as an input variable when estimating a model.

Apart from this, the angle of heel (degree) is denoted by its absolute value despite its direction. The applicable experimental data is tabulated in Table 6.3. It can be seen that three RoPax ships PRR01 (HARDER), Pentalina (SAFEDOR), and M/V Estonia (FLOODSTAND) are modelled in tank testing to provide the necessary benchmark data for a validation of the ensuing Bayesian estimates.

Table 6.3: Experimental Data Assembled for Model Training

Damage case	No. of Tests	Measured Hs	Intact Condition			Damage Condition	
			KG/KMT	T/D	Trim [m][1]	Heel at EQ	Ld/Ls
PRR01_case 2			0.8306	0.6944	0	3.17	0.0466
PRR01_case 3			0.8669	0.6944	0	4.07	0.0466
PRR01_case 5			0.7962	0.6944	+3.12	2.54	0.0466
PRR01_case 6			0.8413	0.6944	+3.12	3.23	0.0466
PRR01_case 7			0.8782	0.6944	+3.12	4.14	0.0466
PRR01_case 9			0.7747	0.6944	-3.12	2.36	0.0466
PRR01_case15			0.8483	0.6389	0	3.72	0.0466
PRR01_case16			0.8898	0.6389	0	5.32	0.0466
PRR01_case17	425	1.5 - 6.25	0.7990	0.7500	0	2.59	0.0466
PRR01_case18			0.8443	0.7500	0	3.34	0.0466
PRR01_case21			0.7860	0.6944	0	1.76	0.0466
PRR01_case23			0.8306	0.6944	0	2.25	0.0466
PRR01_case24			0.8669	0.6944	0	2.89	0.0466
PRR01_case25			0.9093	0.6944	0	4.33	0.0466
PRR01_case26			0.7962	0.6944	+3.12	1.65	0.0466
PRR01_case27			0.8413	0.6944	+3.12	2.08	0.0466
Pentalina	248	1.5 - 2.5	0.8533	0.7860	0	1.00	0.0717
M/V Estonia	83	2.0 - 3.0	0.8949	0.7046	+0.435	4.25	0.0518

6.3.2 Model Estimation based on Experimental Observations

For a particular damage case, six governing variables ($\boldsymbol{X} = x_1, \cdots, x_6$) including ($H_s, T/D, KG/KMT,$ trim, heel at EQ, L_d/L_s) are taken into account as the relevant parameters for model estimation. In such case, seven model coefficients must be evaluated and each target distribution $P(\boldsymbol{\beta}|\boldsymbol{Z}, \boldsymbol{X}, \mathbf{y})$ is to be approximated by using both the Gibbs and the Metropolis samplers. All of the collected data (756 tests) are employed for model training. The MCMC methods simulate 10,000 times with a burn-in size of the first 500 samples. Diagnosing chain convergence is to be acted next.

Firstly concerning the convergence of the Gibbs sampler, the chain autocorrelation functions (ACF) for the estimates of $\boldsymbol{\beta}$ at lag 20 are shown in Figure 6.14. After sampling every 50th observation, the autocorrelation to each model coefficient at lag

[1] Trim by the stern is defined as positive, vice versa.

one is clearly under 0.4. Then again, as to the Metropolis sampler, $\boldsymbol{\beta}^*$is accepted as $\boldsymbol{\beta}^{(i+1)}$ for 22.2% of the iterations, which satisfies the requirement that the chain of Metropolis samples is considered as convergence if the acceptance rate roughly stands between 20% and 50%.

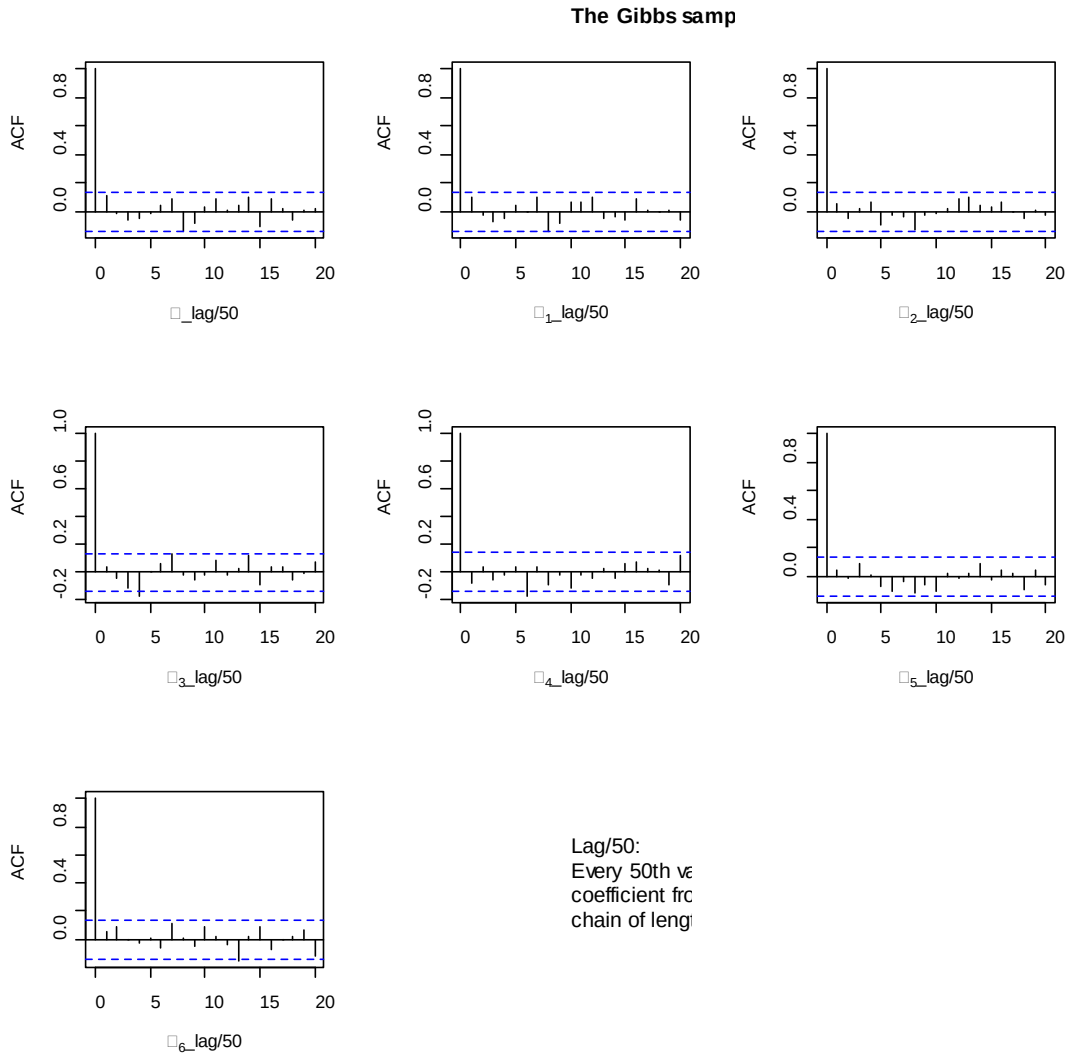

Figure 6.14: Plots of Autocorrelation Functions for Model Coefficients

Now it can be assumed that the sample densities for the unknown parameters $\boldsymbol{\beta}$ are good estimates of the target densities since the convergence of both samplers have been verified. Accordingly, the simulated model coefficients $(\alpha, \beta_1, \cdots, \beta_6)$ are summarized in Table 6.4. Meanwhile the MCMC approximations to the posterior densities $P(\boldsymbol{\beta}|\boldsymbol{Z}, \boldsymbol{X}, \mathbf{y})$ for all the coefficients are depicted graphically in Figure 6.15. These distributions seem to interpret that all these variables (except β_6 for the intact

trim) have much influence on ship survivability following flooding since the 99% quantile-based posterior intervals don't contain zero. The estimated magnitude of β_6 is negative represents that the initial trim is inversely proportional to the rate of ship capsizing. In usual practice, slightly trimming by the stern increases stability of the vessel and thus the estimation agrees well with the phenomenon observed.

Table 6.4: Summary of Markov Chain Samples of Model Coefficients

	Mean		SD		0.5% quantile		99.5% quantile	
Var.	Gibbs	Metro.	Gibbs	Metro.	Gibbs	Metro.	Gibbs	Metro.
α	-57.2522	-57.1509	2.8695	2.8261	-66.3607	-66.196	-48.6214	-49.8532
β_1	1.6057	1.6028	0.0704	0.0687	1.4023	1.4197	1.8029	1.8354
β_2	23.0359	23.019	1.7884	1.8303	17.1343	17.4692	28.1511	28.8479
β_3	41.6928	41.5953	2.6553	2.5748	33.5185	34.3353	50.3424	50.0041
β_4	0.2717	0.2698	0.0651	0.0662	0.0781	0.0805	0.4858	0.4619
β_5	42.1021	42.0337	11.1821	11.614	8.4102	9.8745	81.3684	77.4899
β_6	-0.0451	-0.0485	0.0292	0.0284	-0.1363	-0.1276	0.0477	0.0341

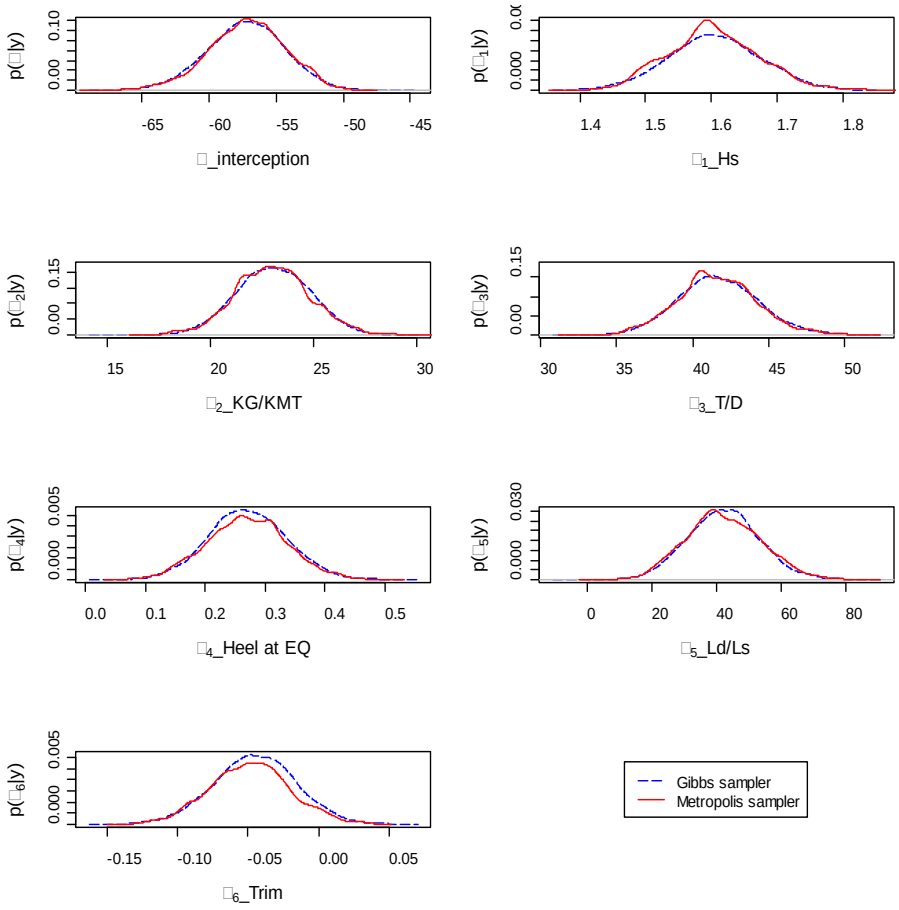

Figure 6.15: Comparison of MCMC Approximations to Posterior Distributions of Model Coefficients

Depending on the estimated results shown in Table 6.4, it seems both Markov chain samplers give similar approximations. For instance, the estimated predictive model by using the Metropolis sampler is defined as

$$P(t_0, Y = cap \,|\, \boldsymbol{\beta}, \boldsymbol{X}) = \Phi(-57.15 + 1.6H_s + 23.02\frac{KG}{KMT} + 41.60\frac{T}{D} + 0.27Heel + 42.03\frac{L_d}{L_s} - 0.049Trim) \quad (36)$$

6.3.3 Probabilistic Sensitivity Study of Model Inputs

The model shown in Equation (36) is derived from Bayesian inference for a probit regression model. It is visible that the model has an analytic expression by using such regression analysis. A difficult aspect of regression modelling is deciding which explanatory variables should be included in a model, so it is imperative to ensure that the variables addressed in the model are the critical ones for uncertainty analysis. In addition, it is also important to ensure that the model is not used outside the parameter range as defined during regression analysis. Keeping this in mind, a systematic sensitivity study is desired for exploring the significance of individual inputs to the estimated model.

The variation of the significant wave height H_s, the initial loading at a specific operational draught (KG/KMT, trim) and the damage attributes (Heel, L_d/L_s) are examined to identify how changes in each of them affect the rate of ship stability loss in a specific flooding case. In this section, the tested damage case to a RoPax model of M/V Estonia (in scale 1:40) is selected for sensitivity analysis. The initial draught $T = 5.39m$ refers to the fully loaded condition and the depth is considered as 7.65m.

A wide spread of model parameters is used to rank the impact of each model input on the output. In this case, a study at a ship level is encouraging. All the experimental data, as tabulated in Table 6.3, plays a part in the following investigation. Given the derived model in Equation (36), all the model coefficients are considered to be constant. The next step is to define the range of variations for all the model inputs.

- Significant wave height: In accordance with the wave heights performed in Task 4.1 of the research project FLOODSTAND (Table 6.1), the variation of sea environment H_s is assumed to follow a uniform distribution on the interval from 2m to 3m.

- Centre of gravity: The initial loading condition at a specific operation draught ($D_s = 5.39m$) is represented by a ratio of the centre of gravity over the transverse metacentre(KG/KMT) and the initial trim. Focusing on the variation of the non-dimensional input, it is assumed to have a normal distribution. The relevant mean and standard deviation are sampled from the experimental data as outlined in Table 6.3.

- Initial Trim: Suppose the vessel is slightly trimmed in the intact condition, the variation of trim is defined to follow a uniform distribution on the interval from -2m to 2m, which corresponds to the conditions of trimming by the bow, even keel and trimming by the stern.

- Angle of heel at EQ: as a wide spread of the angle of heel at the damaged equilibrium stage is expected, therefore all feasible damage situations should be considered. The principal assumption underlying the probabilistic damage stability standard of SOLAS 2009 (IMO, 2006b) is that the assumed damage could be any collision hull breach that has historically taken place. These damages generally follow agreed probability density functions (Wendel, 1968) (Lutzen, 2002) (Pawlowski, 2004) (Pawlowski, 2005). Therefore regarding the ship model of M/V Estonia, there are 1200 flooding cases (in accordance with SOLAS 2009), which extend up to 5-zone damages along the ship length generated in NAPA[2]. Hence the floating position of the ship for each damage case can be examined through a damage hydrostatics calculation. In this way, a range of heel angles related to flooding cases up to 4-zone damages is selected and the deviation of such variable is based on a truncated normal distribution.

[2] NAPA is a ship design and operation software supplying solutions related to the ship's Hydrostatics, Intact stability, Damage stability, Longitudinal strength and Cargo planning.

- Extent of flooding: Now suppose that the damage length L_d is the single parameter used for characterising the extent of flooding. In order to avoid the variation of damage length to be limited by the evidence collected through model testing, resembling the selection of heel angles, the variation of the flooding extend is assumed to have a truncated normal distribution. All feasible sizes of flooding up to 4-zone damages are selected.

In line with the above assumptions, the values of all the model coefficients are simulated randomly with a sample size of 10,000. The range of variation for each of them is depicted in Figure 6.16. After that, substituting the Equation (36) with the sampled five inputs separately, meanwhile, the rest variables keep using sample means as a fixed value of input. In consequence, the variation of the rate of ship capsizing $P(t_0, Y = cap|\boldsymbol{\beta}, \boldsymbol{X})$ against the input variable x_i under evaluation can be estimated in turn. Table 6.5 gives a summary of the sampled input values coming from Figure 6.15. The largest observations of the heel angle and the extent of flooding L_d/L_s are 12.658 deg and 0.258 respectively.

Table 6.5: Summary of the Sampled Values of Five Model Inputs

	Mean	SD	0.50%	50%	99.50%
H_s	2.4982	-	2.0051	2.5008	2.9944
KG/KMT	0.8424	0.0382	0.7466	0.8423	0.9410
Heel at EQ	3.2631	2.0531	0.0448	2.9994	9.2796
L_d/L_s	0.0899	0.0426	0.0032	0.0882	0.2079
Trim	-0.0101	-	-1.9808	-0.0188	1.9794

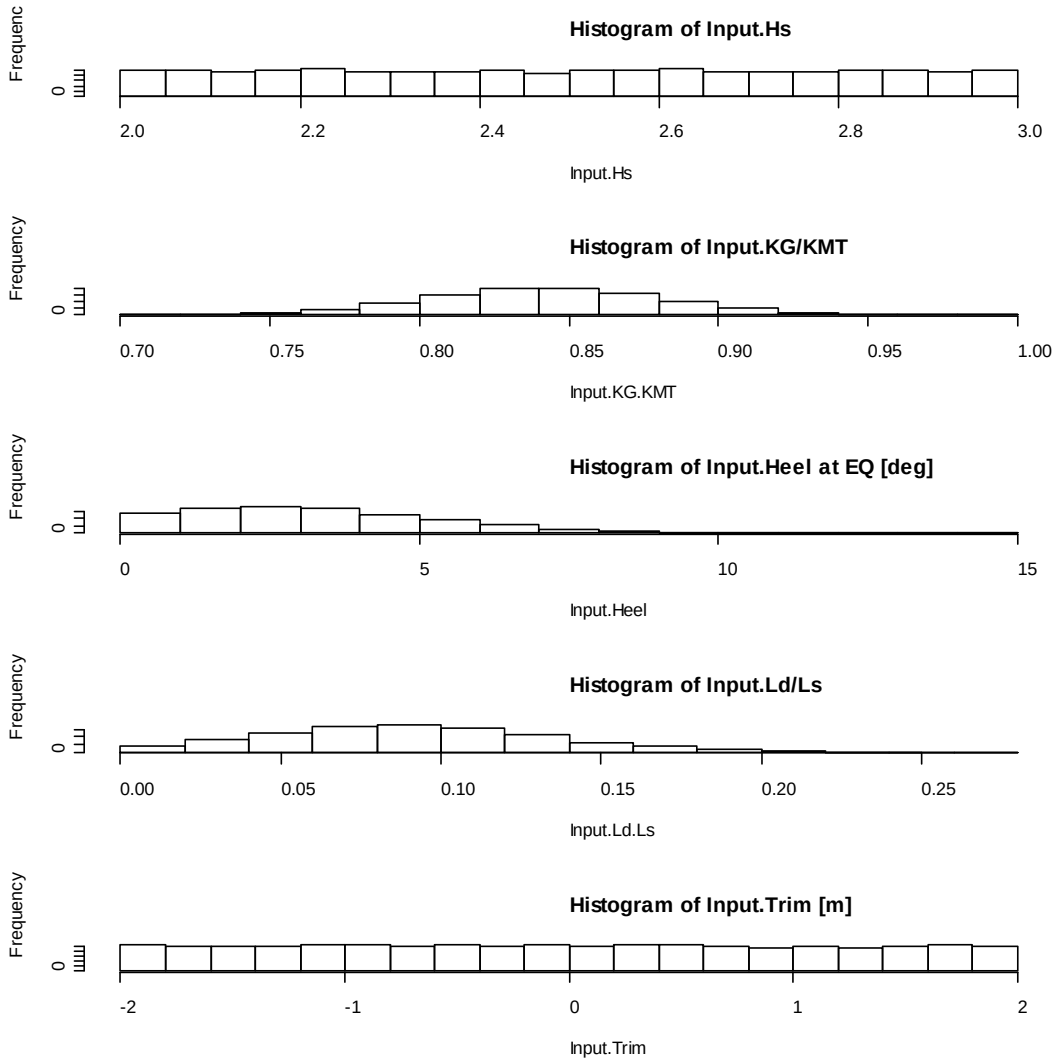

Figure 6.16: Histograms of Model Input Values, Using a Sample Size of 10,000

After solving the model given in Equation (36), 10,000 outputs of $P(t_0, Y = cap|\boldsymbol{\beta}, \boldsymbol{X})$ are obtained for describing the rate of capsizing within given time period varies with the changes of the interested model input x_i. The measured effects of each input ($\boldsymbol{X} = H_s, KG/KMT, Heel, L_d/L_s, Trim$) over the model output are illustrated by a boxplot as given in Figure 6.17.

The bottom and top of the "box" indicate the 25% and 75% quantile of the model output $P(t_0, Y = cap|\boldsymbol{\beta}, \boldsymbol{X})$, and the band near the middle of the box is always the 50% quantile (the median). The whiskers (i.e. T-shaped lines) represent the highest and lowest datum within $1.5 \times IQR$ of the upper and lower quantile defined for the "box"

(IQR=75% - 25% quantile). A wider box and whisker denotes a greater uncertainty in the model output given the variation in a particular input.

According to such features, with respect to Figure 6.17, it is noted that change of the extent of flooding is ranked to have the greatest influence on ship survivability. In reality, the lack of knowledge in determining the extent of flooding experienced during crises may lead to the greatest uncertainty in the survivability prediction. In contrast, the variation of the output is less sensitive to the changes of the initial trim. This finding is consistent with the conclusion drawn from Figure 6.15. A summary of the key values represented in the boxplot is given in Table 6.6.

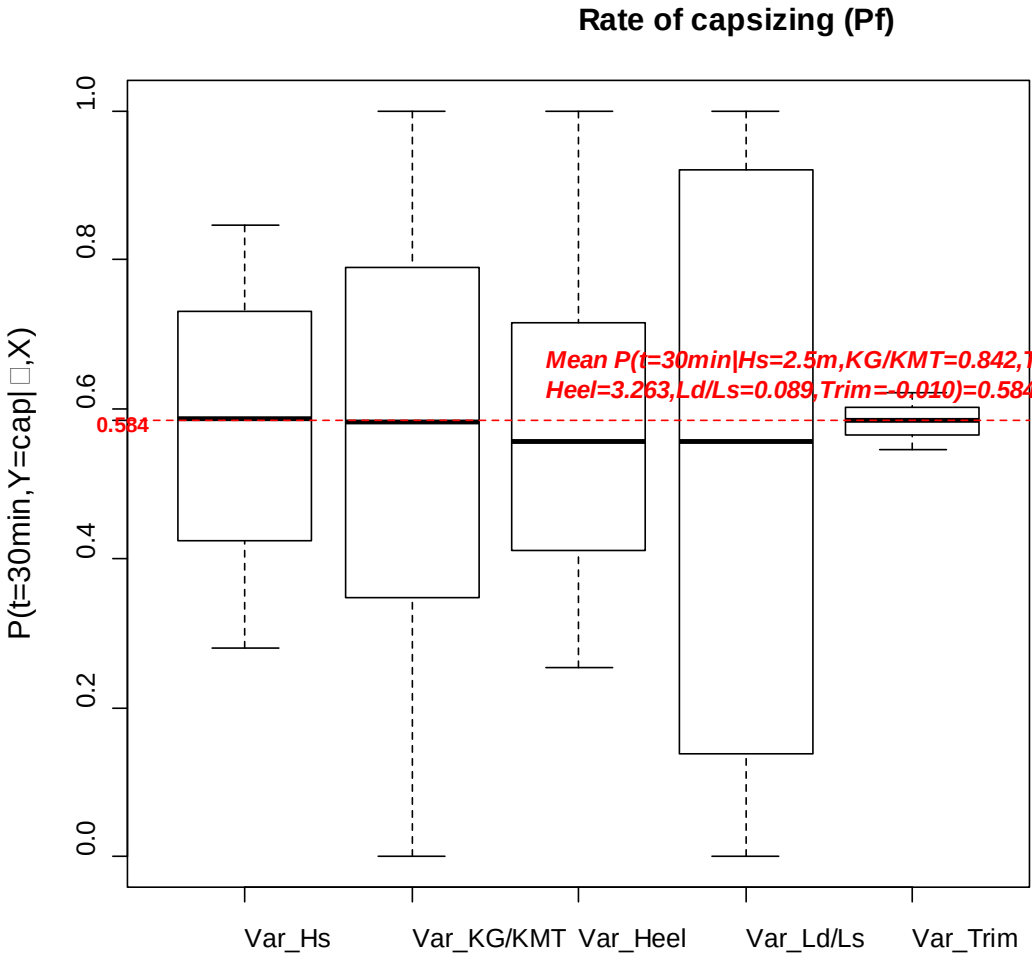

Figure 6.17: Boxplot of the Model Outputs $P(t_0, Y = cap|\boldsymbol{\beta}, \boldsymbol{X})$ vary with Changes in Each Model Input ($\boldsymbol{X} = H_s, KG/KMT, Heel, L_d/L_s, Trim$)

Table 6.6: Summary of the Variation (Uncertainty) in the Model Output

Var. $P(t_0,Y=cap\|\boldsymbol{\beta},\boldsymbol{X})$		*Var. Hs*	*Var. KG/KMT*	*Var. Heel*	*Var. Ld/Ls*	*Var. Trim*
p_f	Min.	0.2792	0.001166	0.2527	0.000182	0.5461
	25% Qu.	0.4237	0.347648	0.4109	0.138712	0.5656
	Median	0.5861	0.583294	0.5565	0.556442	0.5846
	Mean	0.5763	0.562755	0.5692	0.530031	0.5843
	75% Qu.	0.7306	0.789886	0.7162	0.920882	0.6030
	Max.	0.8454	0.999758	0.9994	1.000000	0.6217

The mean value of the rate of capsizing $P(t_0, Y = cap|\boldsymbol{\beta}, \boldsymbol{X}) = 0.584$ depicted in Figure 6.17 is measured given the condition of using sample means of all input variables. Based on Figure 6.17, the percentage change of the rate of capsizing(ΔP) , as shown in Figure 6.18, is a more intuitive way to express the change in the model output compared to its measured mean value ($P = 0.584$). At this time, the 0.5th and the 99.5th percentiles are adopted to demonstrate the range of 99% uncertainty in the ΔP contributed by the variations in each model input. The corresponding key values are summarized in Table 6.7. By doing so, this boxplot can be regarded as a quantitative means of measuring the significance of several input variables to the model output.

Table 6.7: Summary of the Variation (Uncertainty) in the Percentage Change of the Model Output (ΔP)

ΔP	*Var. Hs*	*Var. KG/KMT*	*Var. Heel*	*Var. Ld/Ls*	*Var. Trim*
Mean	-0.01396	-0.03712	-0.02611	-0.09311	-0.00022
SD	0.29131	0.45411	0.32189	0.63939	0.03719
99.50%	0.44308	0.69986	0.65433	0.71101	0.06309
50%	0.0028	-0.00198	-0.04781	-0.04792	0.00028
0.5%	-0.51759	-0.96043	-0.56163	-0.99949	-0.06501

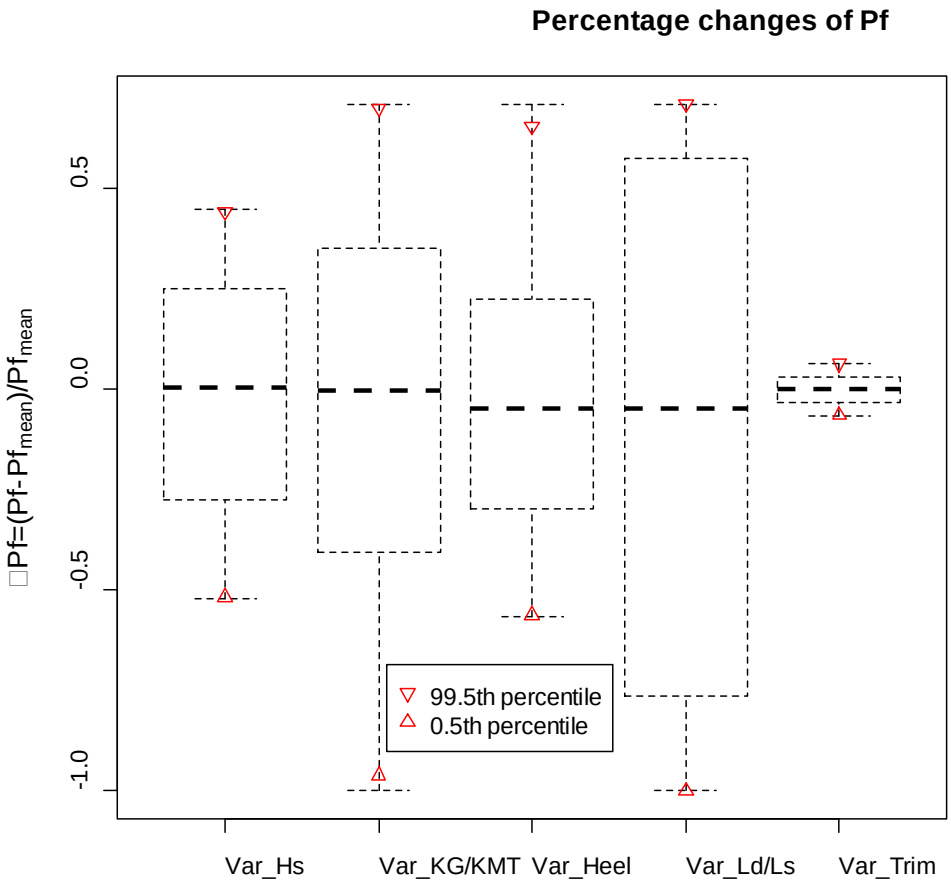

Figure 6.18: Sensitivity Analyses of Input Variables on Percentage Changes in Output $P(t_0, Y = cap|\boldsymbol{\beta}, \boldsymbol{X})$

From Figure 6.15 and Figure 6.18, it can be verified that a probabilistic sensitivity study is helpful to determine which parameters are the key drivers of a model's result. It is also good to assess the impact that changes in a certain input parameter on the model output. The simulated model coefficients can be deemed as the sensitivity indicator. Apparently the uncertainty (within 99% quantile-based posterior interval) in the coefficient β_6 contains zero, which expresses an idea that the parameter of initial trim has minor effect on the model output. Derived from this finding, the model of Equation (36) should be simplified through eliminating such an irrelevant input parameter to strive for model parsimony.

Consequently, a new relationship can be established without the parameter of initial trim. The range of variations in the residual model coefficients $\boldsymbol{\beta}$ will be revised, but

it can be anticipated that the impact of excluding the initial trim on the model output $P(t_0, Y = cap|\boldsymbol{\beta}, \boldsymbol{X})$ is negligible, and the changes in the remaining $\boldsymbol{\beta}$ are not obvious. Nevertheless, this section demonstrates the key steps of how uncertainty quantification in the assessment of ship survivability can be achieved. The next part put main effort on the interpretation of model output.

6.3.4 Uncertainty Analysis of Model Output

As described in Section 6.2.4, there are two phases concerning an analysis of time-based ship survivability to a certain damage case: i) a prediction of the rate of capsizing within given time $P(t_0, Y = cap|\boldsymbol{\beta}, \boldsymbol{X})$, ii) an assessment of the cumulative probability of time to capsize in any time period $F(t_{cap}|P)$.

Due to the values of model coefficients obtained by using two different Markov chain samplers are comparable respecting a summary outlined in Table 6.4, as a demonstration, the following elucidation is only dependent on the results derived from the Metropolis sampler. In so doing, the rate of capsizing can be computed directly when the values of input parameters $\boldsymbol{X}$ are provided. Regarding the flooding case tested for M/V Estonia model, the survivability prediction coupled with the 99% uncertainty bounds (within 30 minutes) are depicted in Figure 6.19, where the inputs are $\boldsymbol{X}$ = (H_s, 0.9008, 0.7046, 4.25deg, 0.0518, 0.435m).

Comparing with the experimental data, it can be seen from Figure 6.19 that the model as presented in Equation (36) underestimates the ship survivability when $H_s < 2.6m$, and vice verse. The discrepancy can be interpreted in a way that the data set used for model training involves data from other sources of benchmarking tests. Hence, current Bayesian estimates for this particular damage case can be best understood as a compromise among all the observations on the survivability of RoPax vessels given in Table 6.3. In this context, it is important to mention that further expansion of the training database is essential, so as to ensure that the developed model could make a plausible inference of ship behaviour in any flooding situation.

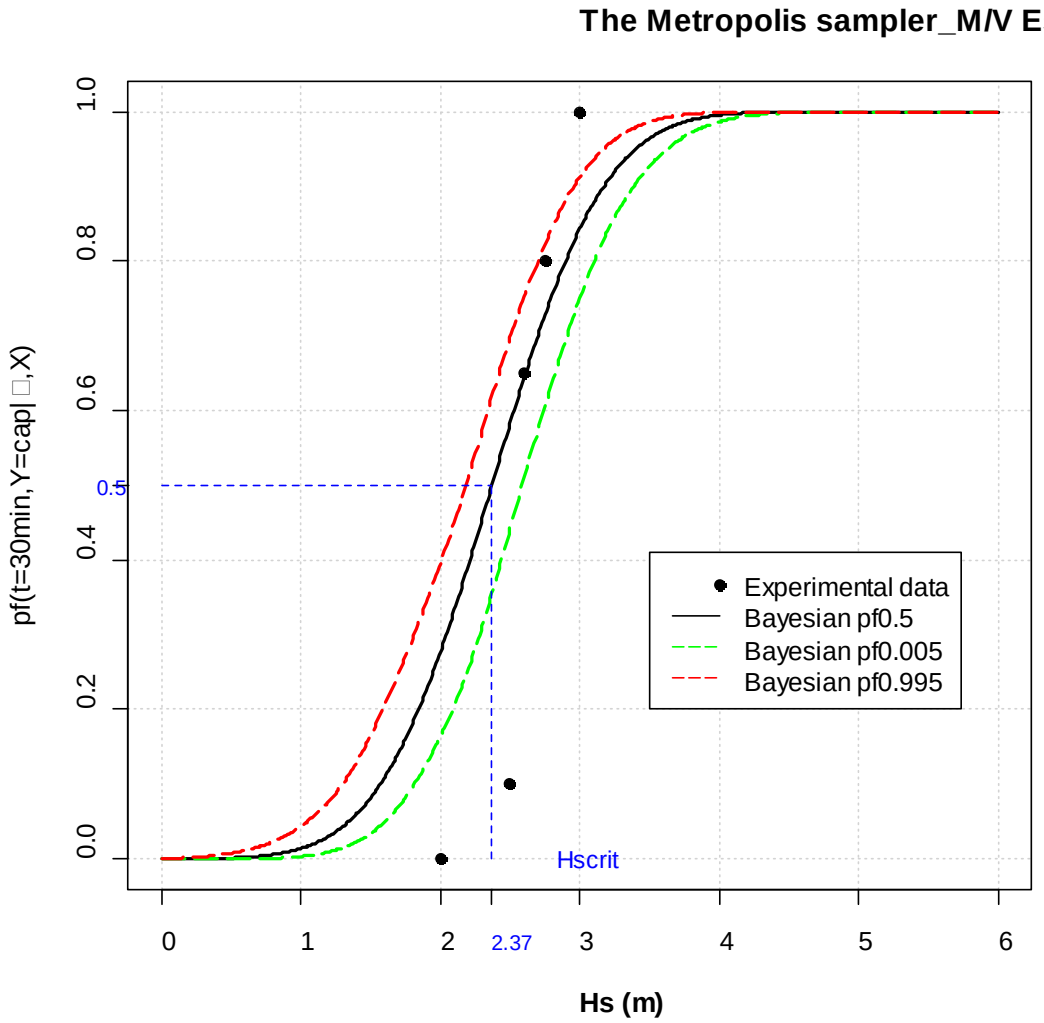

Figure 6.19: M/V Estonia, Posterior Distribution of the Rate of Capsizing

$$P(t = 30min, Y = cap|\boldsymbol{\beta}, \boldsymbol{X} = H_s, KG/KMT, T/D, Heel, L_d/L_s, Trim)$$

As far as the survival time assessment is concerned, a principle assumption underlying the estimation of a cumulative probability distribution of "time to capsize" $F(t_{cap})$ is that the stochastic nature of the time which takes the vessel to capsize after flooding can be modelled by a Bernoulli trial process (Section 6.2.4.2). As the computed rates of capsizing $P(t = 30min, Y = cap|\boldsymbol{\beta}, \boldsymbol{X})$ are less than the experimental records at $H_s > 2.6m$, it can be expected that the predicted probability that the ship may capsize within 30 minutes $F(t_{cap}|H_s, P)$ is to be smaller than the measured values during the scaled model tests. Figure 20 proves such phenomenon.

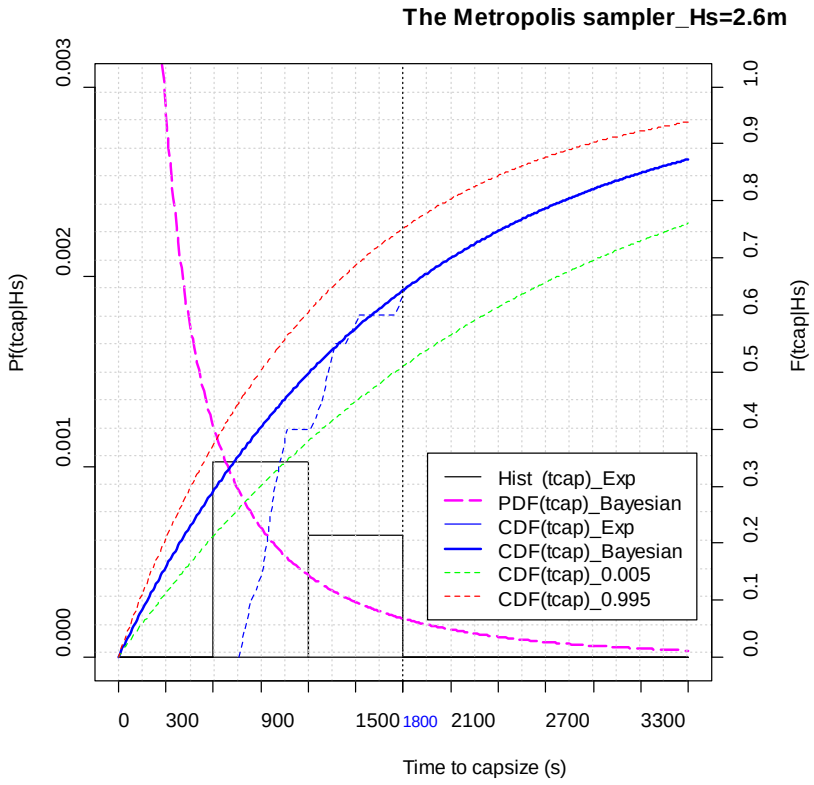
The Metropolis sampler_Hs=2.6m
Pf(tcap|Hs)
F(tcap|Hs)
Time to capsize (s)
Hist (tcap)_Exp
PDF(tcap)_Bayesian
CDF(tcap)_Exp
CDF(tcap)_Bayesian
CDF(tcap)_0.005
CDF(tcap)_0.995

(a)

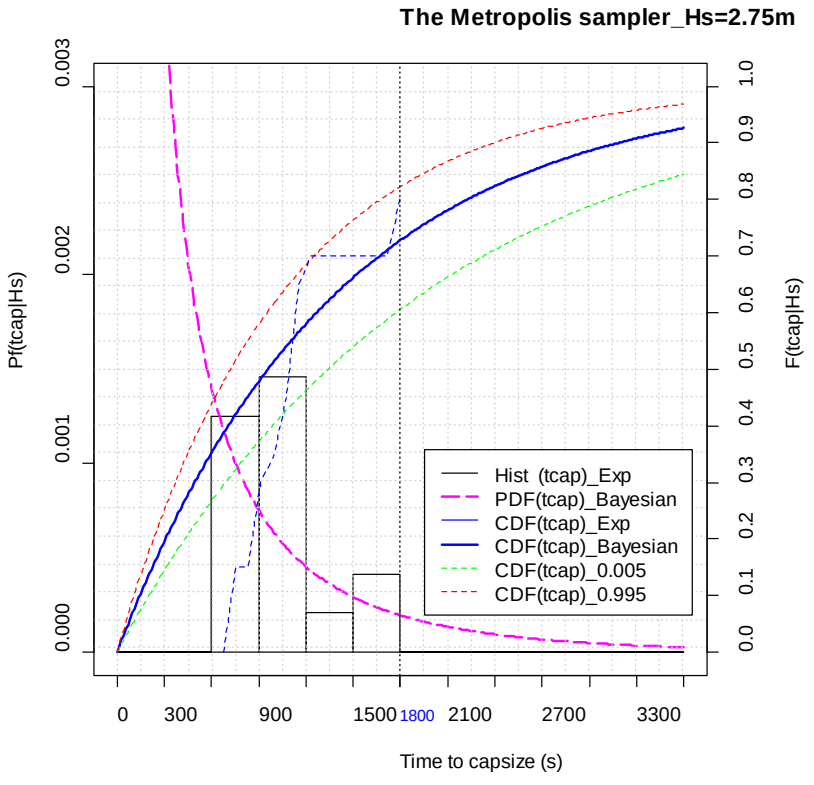
The Metropolis sampler_Hs=2.75m
Pf(tcap|Hs)
F(tcap|Hs)
Time to capsize (s)
Hist (tcap)_Exp
PDF(tcap)_Bayesian
CDF(tcap)_Exp
CDF(tcap)_Bayesian
CDF(tcap)_0.005
CDF(tcap)_0.995

(b)

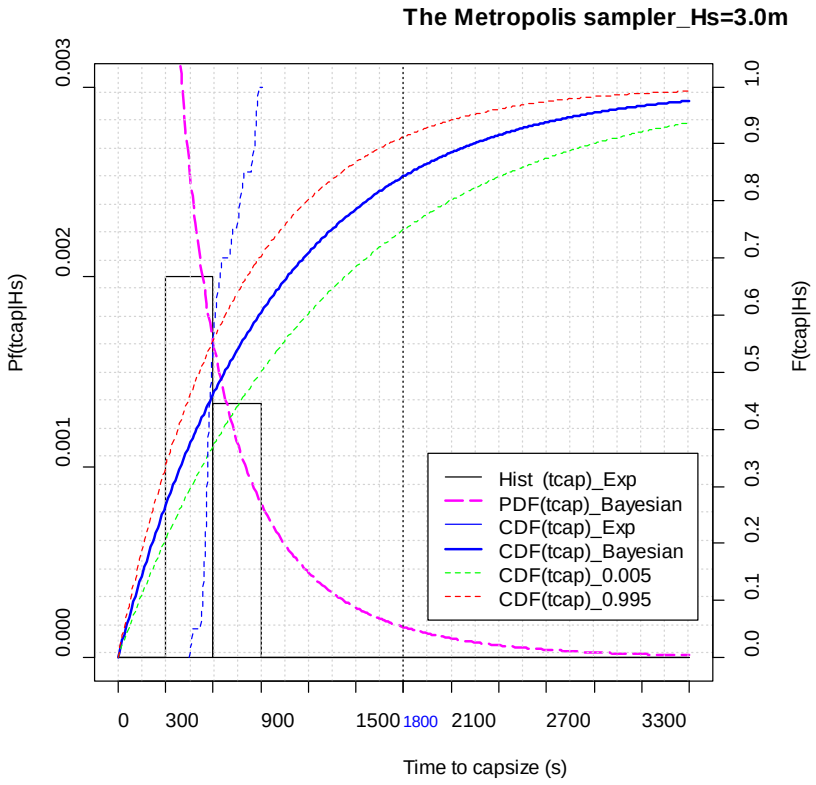

(c)

Figure 6.20: M/V Estonia, Cumulative Probability of Time to Capsize.

The evaluation time of experiment = 30 minutes

(a) H_s =2.6 m with $p_f = 0.65$ and $p_{f\_Bayes} = 0.644$

(b) H_s =2.75 m with $p_f = 0.8$ and $p_{f\_Bayes} = 0.728$

(c) H_s =3.0 m with $p_f = 1.0$ and $p_{f\_Bayes} = 0.843$

6.3.5 Model Validation

Other than the investigated damage case on the model of M/V Estonia, a series of parallel estimations on the remaining observations (see Table 6.3) related to the models of PRR01 and Pentalina can be performed as well. At present, a mean critical sea state Hs_{crit} (where the rate of capsizing is 0.5) is deployed as an indicator to compare the survivability between the real measurements and Bayesian estimates.

As shown in Figure 6.19, the critical sea state $Hs_{crit} = 2.37m$ is not hard to measure when a plot of the rate of capsizing against the encountered sea states is available. A comparison is displayed in Figure 6.21, it can be found that the predicted Hs_{crit} are comparable with that measured results during the experiments. Over half of the total

18 damage cases (11 cases) are below the diagonal line. In the meantime, the upper confidence bound (e.g. a 99% confidence interval) of each estimated mean Hs_{crit} is also allocated (i.e. denoted by red dots). Clearly, considering the critical survival sea where $p_f = 0.5$, the tested M/V Estonia case has a conservative prediction comparing with the actual measurements.

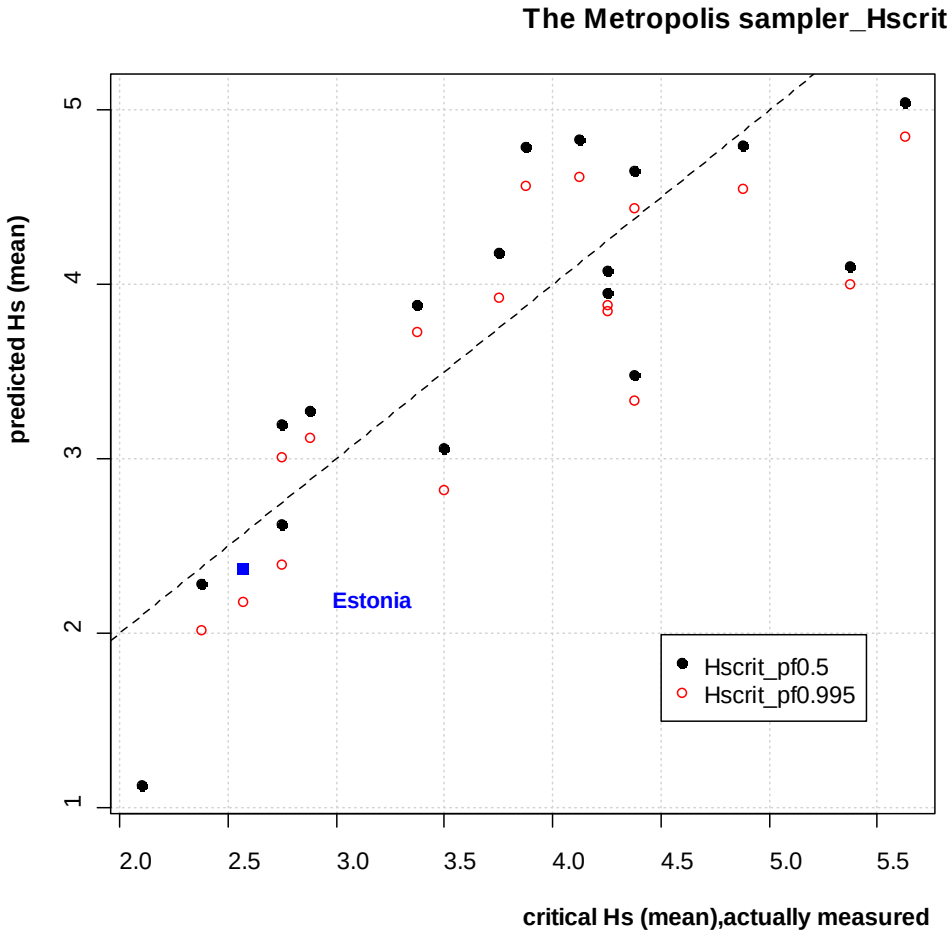

Figure 6.21: Comparison of the Mean Critical Sea States $(p_f = 0.5)$ between Bayesian Estimates and Experimental Measurements

6.4 Closure

In connection with the finding from Section 5.3, either probit or logistic function allows one to specify a model linking the binary response (ship capsize/survival) and a set of explanatory variables (damage attributes, loading condition, sea environment, etc). As a result, this chapter put more effort into estimating unknown parameters used in the model.

The key task is to elaborate on the MCMC sampling algorithms to approximate the target posterior distributions of model coefficients $P(\boldsymbol{\beta} \mid \mathbf{y}, \boldsymbol{X})$. Taking the probit regression model as an example, both the Gibb's sampler and the Metropolis sampler are employed to accomplish model estimation. Accordingly, an exact Bayesian method for modelling binary response data can be developed.

The establishment of uncertainty bounds of the model output is satisfied after having the range of variations for each of the model coefficients. The values of model inputs need to be provided to characterise a certain damage condition. Then, a simplified example of using Bayesian inference to make an assessment of ship survivability following flooding is demonstrated.

In the end, Section 6.3 put forward an extensive procedure which is feasible to address the probabilistic uncertainty analysis in the assessment of damage ship survivability.

Chapter 7

Implication and Implementation of Uncertainty Modelling

7.1 Preamble

In the light of unprecedented scientific and technological developments on handling damage ship stability (through performance-based assessment), as well as the progress of Bayesian approach to deal with probabilistic uncertainty analysis in projection of ship survivability after damage, presently the emphasis is placed on the implication and implementation of the proposed methodology for managing ship safety.

This chapter starts with an elucidation of the implementation of the aforementioned uncertainty modelling techniques in a context of ship life-cycle safety management. After that, integration of such uncertainty analysis scheme into a devised framework of decision support system for flooding damage control is discussed.

7.2 Application of Uncertainty Modelling for Crisis Management

It has been brought to light in Chapter 1 that uncertainty analysis is one of the key components in the procedures of estimating risk level of ships. Flooding-related hazards stand for a key risk driver influencing the overall level of ship safety at sea, thus ship survivability after flooding is a vital subject that necessitates a thorough and systematic analysis in the life-cycle of a ship. For this reason, sophisticated methods, tools and techniques are demanded to address the performance of a ship after flooding. In principle, first-principles tools (e.g., numerical simulations, model tests, etc) represent a rational and cost-effective approach to deal with some design and operational issues for minimising the potential risks. Being aware of this, it is

worth to indicate that a systematic methodology for quantifying the uncertainties associated with the performance-based assessment of ship survivability is needed.

In view of a life-cycle safety (risk) management framework as presented in (Vassalos, 2012b), it starts at the concept design stage and continue throughout the life of a ship. In such a process, safety must be monitored and reviewed to ensure developments / changes in the design and operation are reflected in the way safety is managed. The safety management process must be formal to facilitate the measurement of safety performance, which constitutes the basis for continuous safety improvement, as shown by the virtuous cycle in Figure 7.1.

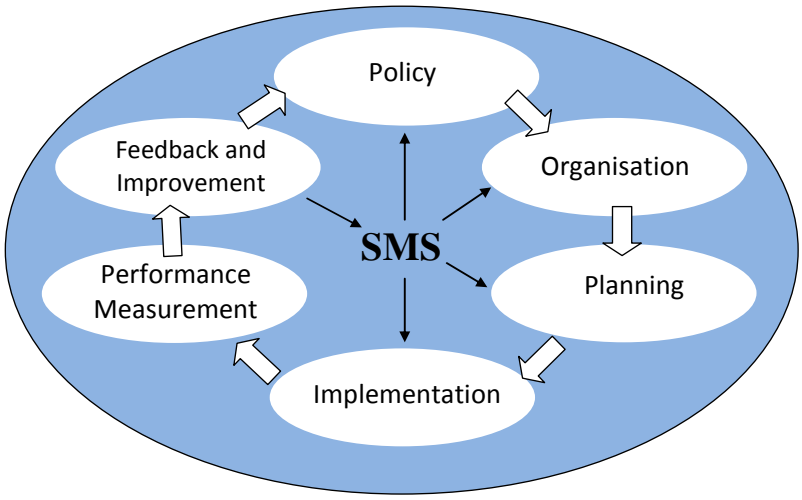

Figure 7.1: A Virtuous Life-Cycle Safety Management (Vassalos, 2012b)

The above 'close loop' process points to the fact that risk should be addressed from three phases in the life-cycle of the ship:

- Design phase: It focuses on design safety verification activities (e.g., engineering analysis, model test, etc.) to reduce / mitigate risk cost-effectively. Substantial effort has been devoted to assess the risk level and verify that adequate measures are taken into account to ensure that the operational risks are acceptable.

- Operational phase: It necessitates monitoring / measuring of ship safety performance and provides review / feedback to verify and manage residual risks. This stage should be linked to SMS (Safety Management System), outlining the

organization and procedures required to maintain an acceptable level of safety throughout the life of the ship. This has to be aligned with the ISM (International Safety Management) Code implemented onboard.

- Emergencies: Either onboard decision support system DSS (the pre-prepared emergency plan / plans, computer-based decision support) or shore-based emergency response service should be provided for crisis management, intends to present a list of recommended remedial actions and thereby aid decision making in the event of an incident / accident.

It can be concluded that this safety management process could ensure an acceptable level of risk (safety assurance) in all phases.

Additionally, in 2000 the IMO agreed that future large passenger ships should be designed based on the principle that a ship is its own best lifeboat. It led to a concept of "Safe Return to Port" in July 2009 (new SOLAS Regulations II-1/8-1 & II-2/21). According to the latest regulatory changes and the on-going research work it is promoting "zero tolerance" explicitly for loss of life following accidents (i.e. flooding, fire). Human life loss is counted as the most critical indicator for measuring the safety performance of ships.

Deriving from the foregoing, onboard decision making (crisis management) is deemed as the last option to effectively mitigate high consequences during an evolving flooding crisis. Therefore, it can be specified that the proposed uncertainty modelling adhering to performance-based assessment of ship survivability for decision support in emergencies is a potential application (demonstrated in this thesis) to manage the operational risk.

7.3 Decision Support System for Crisis Management

Considering the emergency situations with severe time constraints, such as accidents involving flooding, the decision made will have a direct bearing on the outcome of the incident. It is important therefore that the officers on the navigation bridge should be provided with accurate and relevant information with which to make their

decision. In this respect, a DSS for emergency management has been required to be provided on board passenger ships (SOLAS Regulation III/29).

7.3.1 The Legislation Roadmap of "Decision Support"

The special focus on passenger ships, advocating a DSS for emergency management in rule-making is at an all time high. The following is a summary of legislation that slowly but steadily targets and supports the development of computerised decision support to aid decision making.

- ISM performance monitoring system, MSC 81/17/1 (2005): Assessment of the impact and effectiveness of implementation of the ISM Code made the following conclusions:

  1) There is a need to "motivate seafarers to use the reporting and monitoring systems in the improvement of safety management systems".

  2) Need to "improve ISM compliance monitoring and developing performance indicators".

- SOLAS - Guidelines for Damage Control Plans and Information to the Master, MSC.1/Circ. 1245, MSC 82/24/Add.1 – Resolution MSC. 216 (28), entry into force on 1 January 2009:

  These Guidelines are intended as advice on the preparation of damage control plans and to set minimum level for the presentation of damage stability information for use on board passenger and cargo ships to which SOLAS regulation II-1/19, as amended by resolution MSC. 216 (82), applies.

- SOLAS 2009. Chapter II-1/8-1: System capabilities and operational information after a flooding casualty on passenger ships:

  The Sub-Committee SLF53 agreed[1] in November 2010 to propose amendments to SOLAS regulation II-1/8-1, to introduce a mandatory requirement for

[1] "STABILITY AND SEA-KEEPING CHARECTERISTICS OF DAMAGED PASSENGER SHIPS IN A SEAWAY WHEN RETURINING TO PORT BY OWN POWER OR UNDER TOW –

passenger ships for either onboard stability computers or shore-based support, for the purpose of providing operational information to the Master for safe return to port after a flooding casualty. The amendments were adopted in May 2012 by MSC 90th session, and it will be applied to ships constructed on or after 1 January 2014.

- SOLAS 2009, Chapter III: Life-saving appliances and arrangements, part B, Regulation 29 - Decision support system for masters of passenger ships, (1 July 1999):

  1) In all passenger ships, a decision support system for emergency management shall be provided on the navigation bridge.

  2) In addition to the printed emergency plan and plants, the Administration may also accept the use of a computer-based decision support system on the Navigation Bridge, which is able to present a list of recommended actions to be carried out in foreseeable emergencies.

7.3.2 A New Philosophy for Instantaneous Decision Support System

The value of instantaneous DSS for flooding crisis management is attributed to a scientific and transparent platform to promptly provide vital information concerning ship survivability and the corresponding actions to be taken so that safety of life at sea can be assured. Through systematically extracting information from remote sensors, monitoring and assessing the ship's systems and condition after damage, making informed decisions, thereby the most appropriate remedial actions could be made to minimise the consequences, in particular loss of lives.

For this purpose, it is crucial to adhere to a properly developed framework for the realisation of a DSS platform. This entails two issues to be addressed concurrently: prompt evaluation of ship survivability and the quantification of uncertainties associated with the whole evaluation process.

Operational information for masters of passenger ships for safe return to port by own power or under tow", Report of the SDS Correspondence Group, 53rd session, Agenda item 7, SLF 53/7/1, 5 November 2010, Submitted by the United Kingdom

The state-of-the-art approaches towards DSSs for flooding crisis management is briefly reviewed and summarized in Appendix 3 (i.e. damage stability booklet, loading computer, emergency response service, and shipboard DSS). It can be argued that an anticipated automated or semi-automated DSS should have several superior advantages:

1) It is capable of instantly accessing the actual ship loading at the time of the incident, rather than the pre-documented damage stability booklet in which all the information is generated based on a set of theoretical initial conditions.

2) It is possible to incorporate first-principles tools into this system to make fast and accurate predictions of the dynamic behaviours of a damaged ship with little expenses.

3) It has the flexibility to deploy more sensible, time-related, and case-specific measures on damage stability, comparing with the classic residual GZ curve and the recent survival factor from a hydrostatic stability point of view. The performance-based measures at run time will facilitate the ensuing evaluation of various damage control options.

4) With the computation system onboard, the officers on the bridge could make decisions on the basis of both the recommendations from DSSs and personnel experience without delay, miscommunication may be caused by ERS services (shore-based support).

Nevertheless, it is also important to realise the key challenges remain in the state-of-the-art technologies for shipboard DSSs:

1) Although first-principle tools offer a unique platform to carry out time-domain simulations of damage scenarios and thereby to make corresponding predictions, it is still a time-consuming exercise. As a result, advance prognoses have only had limited success in proliferating the field of instantaneous decision support (Jasionowski, 2011).

2) Due to the presence of potentially significant uncertainties associated with the prognosis process (i.e. input information, model development), the importance of addressing the uncertainties has been pointed out in (Tellkamp et al., 2008). Evidence can be found from the latest development of the onboard DSS from NAPA (Penttila and Ruponen, 2010), in which dedicated effort has been spent on estimating of damage opening using level sensors rather than using personnel judgement. Hence, an instantaneous DSS can be hardly considered as mature if a holistic treatment of the underlying uncertainties is missing.

Along with the existing difficulties, it requires to have a perception of the current philosophy on instantaneous decision support. Despite it is acceptable that the best crises management is through "preparedness", the "reactive" mentality has deeply implanted in the existing systems. That is, all the work (computation) is only performed when it is urgently needed. Similar phenomenon can be observed from the passive development of safety standard at the IMO (Vassalos, 1999).

Considering the life-cycle of a ship from its design to operation, a DSS for flooding-related damage control is only necessary when such a casualty is encountered. Since "time" is a critical aspect for concern during the decision making process, computing the residual GZ curve is a standard mechanism to quickly measure the damage stability. However, such theoretical estimations use a very simplified static simulation to replace an essentially very complex dynamic process.

In contrast, a performance-based method for demonstrating the ship's dynamic behaviour in the worst damage condition was developed in Stockholm agreement for the first time. It has no doubt that the first-principle tools can provide higher predictive accuracy than the analytical inference model due to the physical phenomenon of ship capsizing has been considered. However, such dynamic simulations are time-consuming. Thereby its potential can be restrained in an emergency situation.

Figure 7.2 reveals the philosophy underpinning the contemporary instantaneous decision support platforms. It leaves the intensive computation to the very last moment in the context of a ship's life-cycle. As a result, the current DSS is

practically difficult to make use of advanced first-principle tools for the relevant predictions. Even with the rapid development on computing power, it is still a challenge to shorten the computation time in a single run of simulation to the magnitude of "seconds".

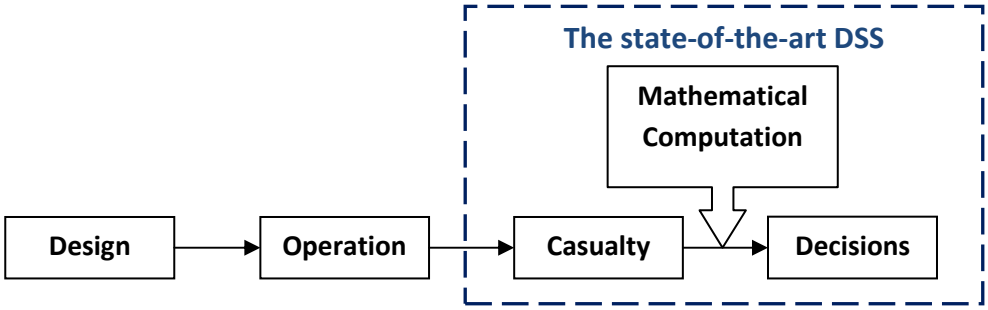

Figure 7.2: The existing philosophy towards instantaneous DSS

In this case, a new philosophy towards instantaneous DSS is proposed in this chapter as shown in Figure 7.3. In comparison to the conventional "last-minute" principle, the new viewpoint is to shift the intense computation to the pre-casualty phase (i.e. design, operation) so that instant computations can be performed once the detailed information of the encountered damage case is certain. Accordingly, transparent and informed decisions can be made promptly.

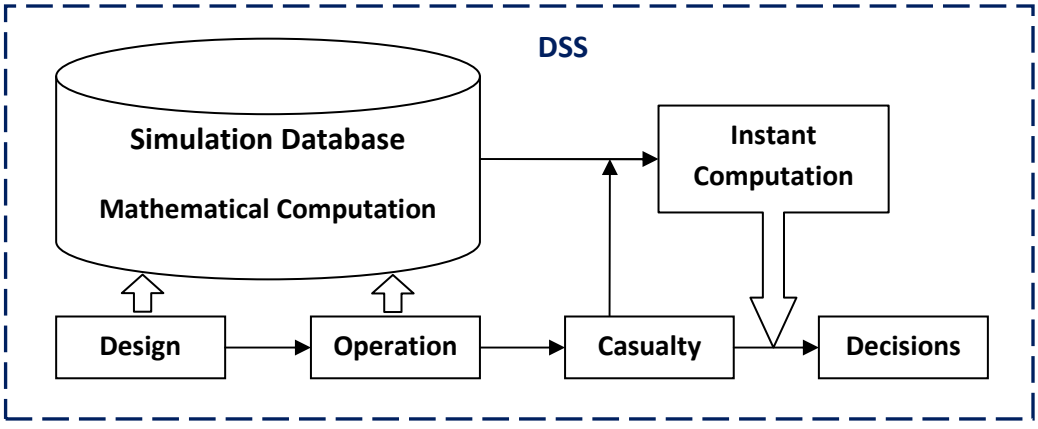

Figure 7.3: A new philosophy towards instantaneous DSS

Deriving from the high-level framework illustrated above, the following fundamental principles need to be adhered to:

1) The framework advocates "one ship, one database", which necessitates an exhaustive flooding-related simulation database to be carried on-board for the whole life-cycle. Such an exclusive database can be updated all the time in order to expand the coverage of damage and improve the precision of the case-specific projection.

2) The first-principle tools play a central role in the new DSS to accomplish performance-based assessment of ship damage stability. Detailed simulations take place at both detailed design and operational stages.

3) The probabilistic method is adopted to generate damages on a specific ship at a ship level based on ship collision statistics. Each assumed damage scenario (i.e. the extent of damage) is considered as the input for the subsequent time-domain numerical simulation to determine the likelihood of loss. The outputs (capsize / survive) pertinent to simulated cases, in company with the input information, are stored as the new evidences of the database.

4) Realising the information of damage after a flooding casualty, the proposed uncertainty modelling (elucidated in Chapter 6) which is a coupling of the binary regression model (probit function) and Bayesian inference will be deployed to train a specific predictive model aligned with the damage, addressing ship vulnerability to flooding[2]. The most relevant cases stored in the simulation database will be retrieved for model estimation. Such instant computation method involves three attributes: i) the processing time could be greatly shortened, ii) the prediction quality could be assured, and iii) underlying uncertainties of the model output could be quantified.

7.4 Major Steps in Decision Making

In practice, three main steps are involved in the decision making process: i) damage situation ascertainment (gather relevant data), ii) ship status evaluation and prediction (process data), iii) informed decision making (act upon data). It is worth

[2] "Vulnerability" has been used by the Ship Stability Research Centre relates to "the probability that a ship may capsize within a certain time when subjected to any feasible flooding case."

noting that the speed at which the decision is made can have a significant impact on the outcome of the incident.

In line with the aforementioned major steps after a flooding casualty, it is essential for the proposed instantaneous DSS to be equipped with three key modules: i) monitoring module, ii) prediction module, and iii) advice module. The interrelationship among them is illustrated in Figure 7.4.

The information assembled in monitoring module has direct impact on not only the prediction module but also the advice module to provide a fast and transparent decision support. In addition, the prediction module must interact with the advice module to evaluate the performance of various damage control options through "What-if" analysis.

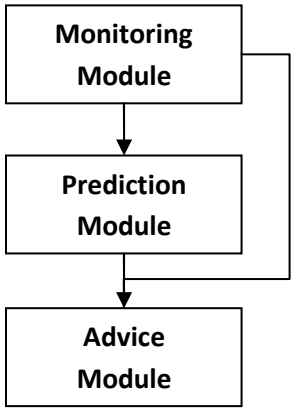

Figure 7.4: Information Flowchart of the Instantaneous Decision Support Platform

7.5 Decision Support System Configuration

The obvious discrepancy between two philosophies of instantaneous DSS is that the intensive mathematical computation with first-principles tools in the proposed DSS is to be shifted from the post-casualty phase to the pre-casualty phase. By doing so, a fast approximation of ship behaviour following a flooding casualty can be expected. In consistent with Figure 7.4, passing information on the correlation among three modules for decision-making, a new framework of shipboard decision support for flooding damage control is laid out in Figure 7.5. The new framework is composed

of three elements: monitoring module, prediction module, and advice module. A brief discussion of the key tasks in each module is enclosed in order.

7.5.1 An Overview of A New Framework of Shipboard DSS for Flooding Damage Control

In principle, the monitoring module deals with real-time information collection, whilst the prediction module is the central module for the case-specific ship survivability prediction. The last advice module is responsible for recommending appropriate remedial actions to mitigate the loss.

As illustrated in Figure 7.5, the general working principle behind the intended framework is that:

1) The remote shipboard sensors and devices are activated in the monitoring module once a casualty has been reported or detected, for the purpose of gathering relevant information to have a quick knowledge of the current situation.

2) The assembled instantaneous information is passed to the prediction module for the subsequent model estimation to assess the case-specific ship survivability. On the one hand, the actual damage details are utilised as a filter to extract the most relevant flooding scenarios stored as the evidences in the pre-prepared simulation database. On the other hand, such damage information is applied as the direct input once the model estimation has been done, thus whether the ship could survive the current situation is obvious.

3) Alternatively, the estimated predictive model can be applied in the advice module as one of the optimisation criteria for damage control options prioritisation.

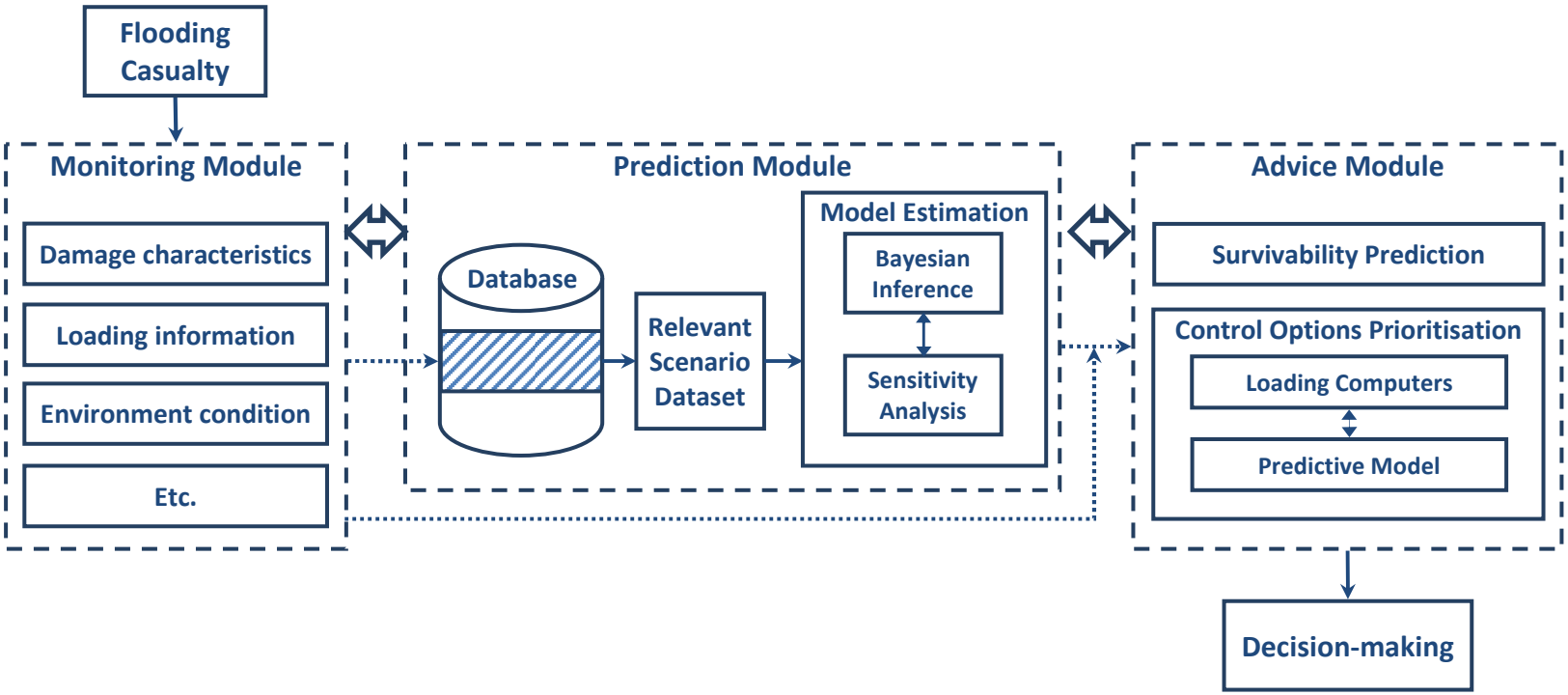

Figure 7.5: A New Framework of Shipboard DSS for Flooding Damage Control

It should be borne in mind that technological advancements have enabled rapid deployment of new equipments/systems for real time information collection. Moreover, various optimisation techniques have been adopted for the identification of the most appropriate damage control operations. Hence, the focus of the proposed framework is placed on the prediction module, which can be readily integrated into any of the available optimisation algorithm for control options evaluation. The following sections endeavour to clarify the key elements in each of the essential modules of the proposed framework.

7.5.2 Monitoring Module

The current status with shipboard monitoring is that there is still a lack of rigorous research into the issue of ship stability, especially concerning the monitor of the instantaneous ship state during crises (exact loading, exact flooding extent, and realistic sea state). This will be a long road to resolve. As indicated in Section 5.2.1, the explanatory variables are both statistically significant and practically accessible. They have been classified into three categories for quickly ascertaining the ship status following flooding: i) damage characteristics, ii) loading information, and iii) environmental conditions. A discussion about how to acquire such information reflecting the real situation is the focus in this section. Corresponding instruments to achieve this are outlined as below.

7.5.2.1 Damage Characteristics

Recalling the results from the sensitivity study in Chapter 6, it is disclosed that the predictor variables (i.e. damage length L_d, heel angle at static equilibrium position EQ) addressing damage attributes have significant influence on the ship survivability following flooding. In this respect, these two variables deserve further elaboration. The damage length L_d is still an instance cited here for ascertaining the extent of flooding rather than a set of parameters (location, penetration, height).

7.5.2.1.1 Damage Length

The damage length represents the maximum longitudinal extent of damage as shown in Figure 7.6. Nowadays most new large passenger ships have been equipped with flooding sensors in cabin areas, machinery spaces and void spaces. Meanwhile, a recent IMO report SLF-51/11 (IMO, 2008d), recognizes that all information used in the operational decisions should be as accurate as possible and be based upon the actual damage, flooding extent and the rate of flooding.

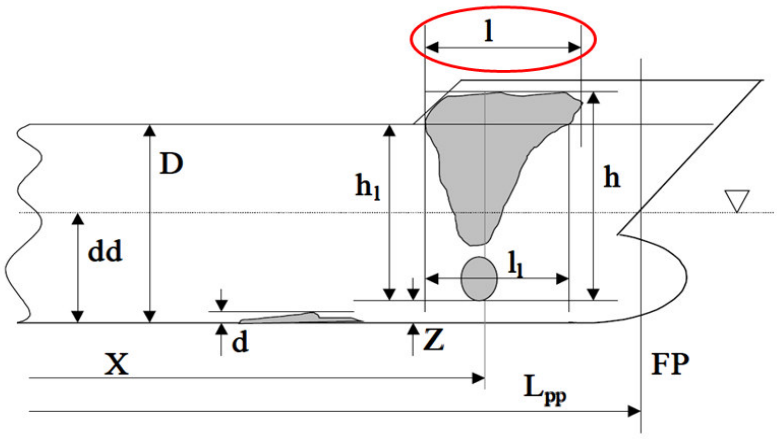

Figure 7.6: The Definition of Damage Length for Measurement

In this respect, if the initial location and size or area of the breach can be calculated automatically according to the flooding sensor output without human intervention, it is possible to determine how the flood water will progress and then enabling the DSS to produce accurate predictions. Some recent research is focusing on the question as to whether a breach can be calculated purely from the flooding sensor measurements.

In particular, an inverse method based on the iteration algorithm is introduced by NAPA (Penttila and Ruponen, 2010) for detecting a breach in a real situation onboard a damaged ship from level sensor signals. This study is an attempt to find the right set of breaches that result in the progressive flooding simulation results matching with the measured outcome in a real situation. In this process, the estimated breach is represented by a set of properties as the number of damaged rooms and the corresponding areas of all flood water entry points. In addition, the outcome indicates the actual measured flood water level that is compared with the predicted

result through flooding simulations, so that the “best-fit” breach origin can be selected inversely. The results of this study strongly point out this approach is applicable in determining the breach from the water level data only if the sensor arrangement is dense enough. Consequently, there is still much room for further development in the breach detection analysis.

Another proposed approach as presented in (Mermiris, 2010) (Mermiris and Vassalos, 2010) is founded on the idea that the total available energy in the system (struck ship – water – striking ship) remains constant. The available kinetic energy is quasi-statically conveyed via contact to the side panels and transforms into strain energy and heat. The breach size and the magnitude of penetration either in a probabilistic or deterministic mode are to be estimated eventually. Similar first-principles approaches are also presented in (Lützen, 2001) and (Zhang, 1999).

The above analytical models generally are capable of improving the approximation of the breach origin. Nevertheless the proposed approaches have yet to be widely used in practice due to a time-consuming calculation procedure. As a result, the overall time in the decision making would be notably prolonged.

7.5.2.1.2 Angle of Heel at EQ

The most recent, the angle of heel is not hard measured from inclinometer on the bridge. One can use the conventional mechanical or electronic inclinometers for measurement. Nevertheless, it should be noted that ship rolling in the damaged condition has dynamic behaviours. Hence, an averaged value can be taken from the records over a limited time period. In this respect, more sophisticated electronic platforms can be deployed for collecting the pertinent information (WYLER, 2012).

For instance, an environmental monitoring system SMCems from Ship Motion Control (SMC) provides a centralised platform for various environmental and meteorological instruments monitoring and recording (SMC, 2012). It enables the crew and shore based staff to monitor environmental information before, during and after sea going operations. More importantly, all measured data from the connected instruments can be integrated into one graphical system. As given in Figure 7.7, the

information of ship motions is presented both in graphical charts and as numerical data in real time. Thereby the current angle of heel (roll motion) in the event of flooding can be extracted easily.

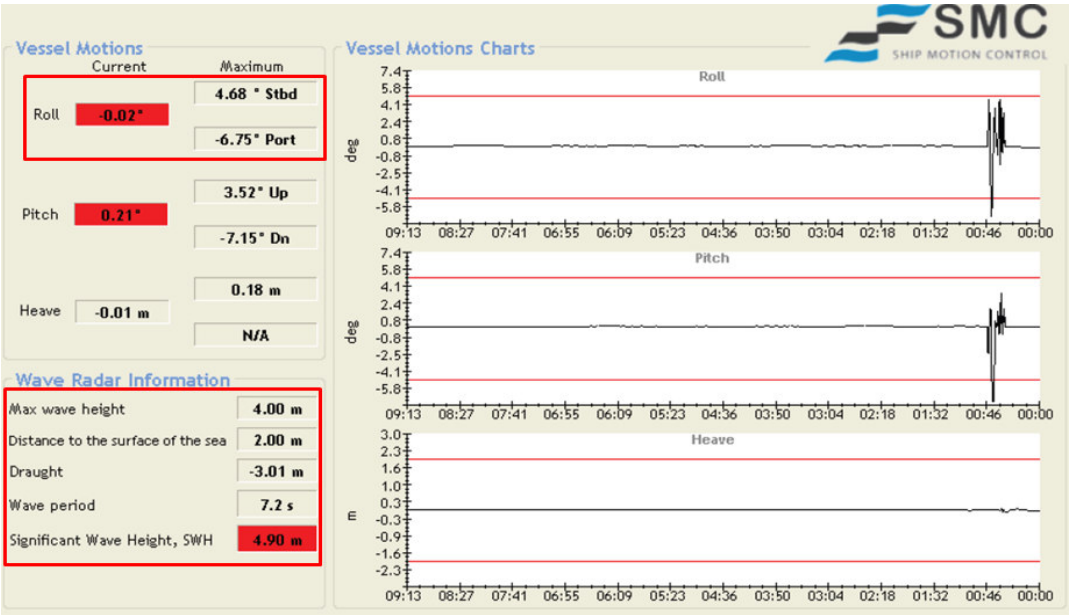

Figure 7.7: A Snapshot of Graphical Information Displayed in the SMCems Interface (SMC, 2012)

7.5.2.2 Loading Information

In respect to the loading condition of a passenger ship prior to its departure, the determination of the ship's trim and stability is mandatory in order to ascertain the ship is in compliance with stability criteria in relevant regulations. Thus the intact loading information could be obtained at that time. As reviewed in Appendix 3, currently a few on board ship loading computer systems have been approved by the major Classification Societies as they are able to promptly and accurately provide real-time information on the ship's floating position (draught, trim, heel), displacement, intact stability (*GM, KG, KMT*), and the ship's longitudinal strength (Bending moment, shear force). In this case the ship's loading condition can be accessed from a visible window directly. Other than the information concerning the intact condition, the ship's actual loading based on the real situation is recognized as a more accurate input to enhance the reliability in assessment of ship survivability.

Therefore, it is desirable to acquire the actual information from the onboard loading computer if it is feasible.

7.5.2.3 Environment Conditions

Wind and wave data constitute a significant part of environmental information that will have a direct bearing on the outcome of the incident. As identified in Section 5.2.1.4, the wave height value reported by ships is the significant wave height (H_s) and which characterising the operational sea state is the only indicator to represent the real sea environment. Following a flooding casualty, it is necessary to acknowledge the consistent wave information of the time. On the strength of the advanced environmental instruments, all measured data from the wave radar in real-time can be processed and displayed on an environmental monitoring interface. As shown in Figure 7.7 as well, the numerical information of H_s is achieved instantly and normally the captured wave data is presented through the pertinent wave radar charts against timeline concurrently for further analysis.

7.5.3 Prediction Module

The principal concept of the proposed approach is to shift the computational effort to pre-casualty phase, so that a fast and reliable survivability assessment can be carried out for instant decision support. From this point of view, development of an all-embracing database concerning potential flooding damage scenarios plays an important role.

Having in mind of the cost-effective, but time-consuming features associated with first-principles tools, the proposed approach attempts to utilise them to perform assessment in advance so that one can avoid the long time required for model preparation, processing, and post-processing in the event of a flooding accident.

In the prediction module, it advocates "*one ship, one dedicated life-cycle database*". As far as flooding-related safety is concerned, the database should include all the data derived from systematically simulations of various flooding scenarios. Figure 7.8 illustrates the data process at both pre-casualty and post-casualty phases.

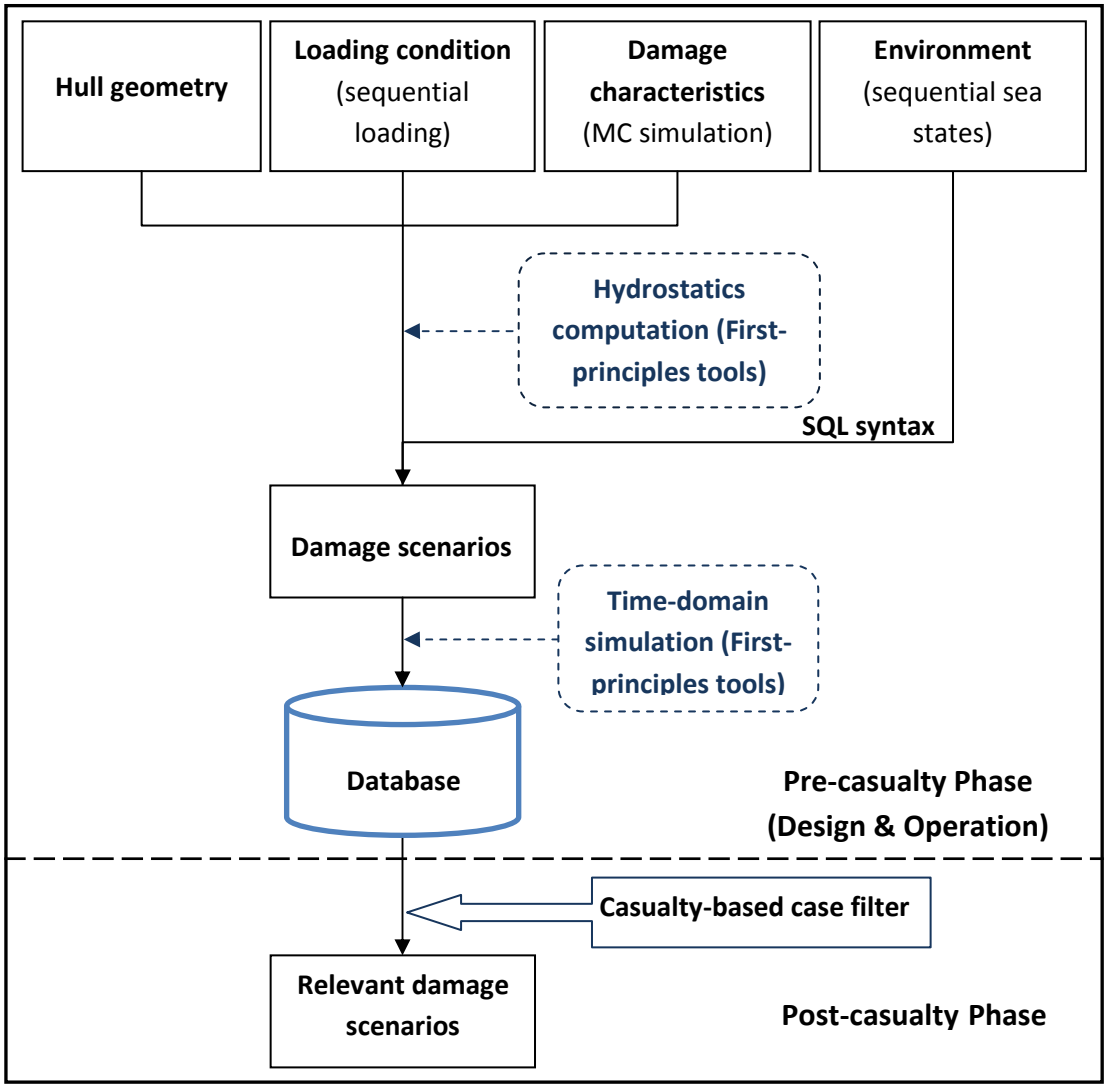

Figure 7.8: A Flowchart of Data Processing

7.5.3.1 Simulation Database Preparation

As indicated in Section 5.2.2.1, an in-house time-domain simulation tool PROTEUS3 is deployed for the numerical assessment of ship survivability. There are six analysis procedures that PROTEUS3 can execute as given in Table 7.1.

Table 7.1: Analysis Type of PROTEUS3

Analysis Number	Analysis Procedure
0	Frequency domain analysis for the production of intact vessel RAO's
1	Time domain simulation
2	Static equilibrium position in intact / damage condition
3	Development of righting arm curves (GZ) in intact / damage condition
4	Creation of hydrodynamic database for use in a time domain simulation
5	Creation of an (.IV) file for viewing in Open Inventor software

7.5.3.1.1 Underlying Considerations

Regarding the simulation run length, it should coincide with the required duration of model tests which lasts for 30 minutes (1800 seconds) in full-scale. To assess the probability of capsizing for a given damage case and conditions during 30 minutes $P(t_0 = 30min, Y = cap \mid \boldsymbol{\beta}, \boldsymbol{X})$, each run of simulation can be considered as a Bernoulli trial with either of two possible outcomes, "capsize" or "survive". Moreover, the opening of the damage in the case of a time-domain simulation should be delayed to 20 - 30 seconds before the flooding starts, whereby the inherent transient effects of the motion can be allowed for. Under such circumstances, the simulation run length is set to 2000 seconds in total which includes the first 20 seconds of intact ship conditions. In the current form of simulation, with a computer having 4 × Intel Core 2 Quad CPU with 3.00 GHz (needs to update), a fully simulated case (no capsize within 1800 seconds from the moment of hull breach) takes approximated 3 minutes.

In the knowledge that the flooding-related damage can occur at any moment in ship operation, hence it is necessary to ensure a minimum amount of cases have been simulated in order for the system to be readily functioning when the ship is delivered. Such as, a minimum of 100,000 cases is recommended. This can be achieved by

using one aforementioned computer to work 24/7, which will take roughly 6 months to finish. Such duration can be greatly shortened if more computers with improved computational power are considered. For instance, 2 similar computers require only 3 months and 4 of such can reduce the whole computation time to only 1.5 months.

In view of the time needed, it is recommended that such a process should be initiated at the later detailed design and construction stage. This can be justified as the ship major subdivisions and her internal configurations becomes almost certain, which is more than enough to facilitate the initiation of the detailed simulations. With the mentioned roughly 100,000 simulated cases stored in the database, it provides a solid foundation embracing possible variations of the considered factors in damage characteristics, loading conditions, and environmental conditions. With its current resolutions, it can ensure a significant number of relevant damage cases can be selected out of the database.

Upon ship delivery, it is recommended that such a system should be continuously running so that a higher resolution can be gained by considering more damage scenarios. By doing so, the quality of the subsequently obtained mathematical model addressing ship survivability can be improved.

7.5.3.1.2 Variations of Decision-Critical Situation Parameters

In order to make sure there is always enough relevant damage scenarios that are selected in the post-casualty phase (Figure 7.8), the method adopted for the generation of damage scenarios at a ship level plays a central role. In this respect, considering the random nature of the phenomenon of flooding scenarios, it is necessary to make use of the experience gained from historical accidents. A probabilistic approach is proposed. This is achieved by drawing the probability distributions of the status of the concerned variables from historical data as shown in Figure 5.2. Afterwards, Monte Carlo (MC) simulation is executed to randomly generate each damage case in turn. The information collected about damage is still concluded from three aspects: damage characteristics, loading conditions, and environmental conditions.

- Damage characteristics: Although only damage length L_d is included for predictive model estimation, it still requires generating damage case with detailed attributes of damage location, length, penetration and height so that the simulations can be initiated. For this purpose, the damage statistics reported from HARDER and the latest research project GOALDS (GOALDS, 2009) can be used openly. Having the probability distribution of each parameter characterising the damage cases, MC simulation can facilitate the generation of damage scenarios through a combination of all information in respect to damage attributes.

- Loading conditions: Another set of influencing input variables on the ensuing numerical simulations is the information of loading conditions for a ship in operation. Especially in terms of the ship's draughts, sequential variations of which should be allowed for in line with the definitions given in SOLAS Regulation II-1/2 (i.e., the deepest subdivision draught d_s, the partial subdivision draught d_p and the light service draught d_l). For each of the three loading conditions, the related variations of *KG* should never exceed the maximum allowable *KG* versus draught for assuring compliance with the relevant intact and damage stability requirements.

  With each loading condition properly defined (i.e., the initial information of draught, *KG*, trim and heel), hydrostatics computations is needed for both intact and damage conditions to determine the ship's stability. As described in Table 7.1, PROTEUS3 is available to execute such analysis (Number 2). An example of hydrostatic and damage stability calculation of a Ro-Pax vessel is illustrated in Figure 7.9.

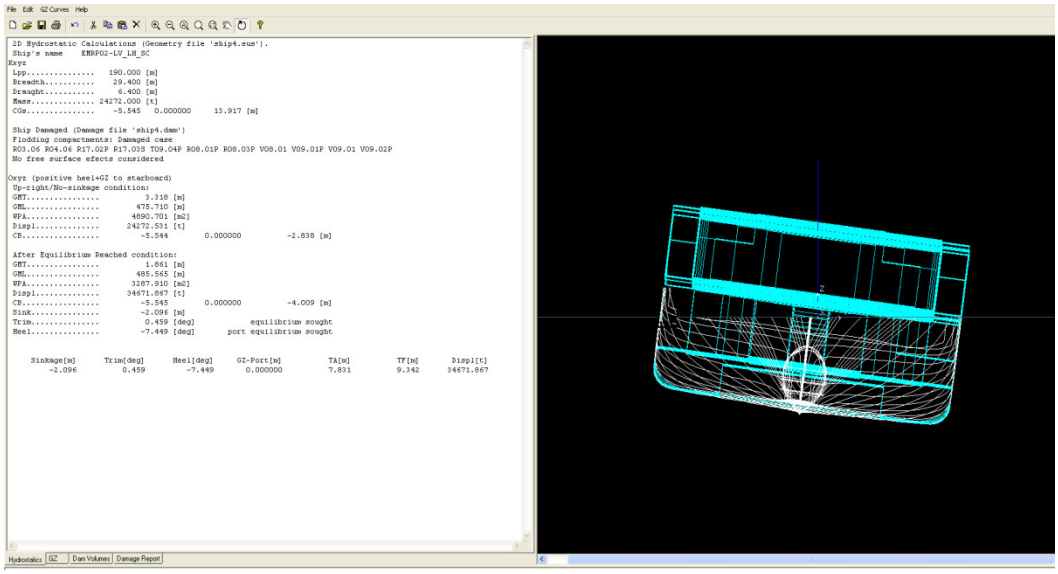

Figure 7.9: Hydrostatics and Stability Information for Single Damage Case

- Environmental conditions: The relevant statistics for wave height recorded during collision were derived in the HARDER project. It disclosed that the sea states (significant wave height H_s) is generally below 4 m at the instance of collision. In this respect, a uniform distribution of H_s for simulation can be assumed by systematically varying H_s from 0 to 5 m with a defined interval of 0.5 m. In addition, it is worth mentioning that H_s is only an averaged measure of the encountered irregular wave. Hence, each considered H_s with different wave realizations (e.g., 10, 20) should be examined repeatedly so as to better reflect its stochastic nature.

7.5.3.2 Casualty-Based Dataset Selection

In case the MC-based simulations addressing enormous damage scenarios are accomplished, the related information of damage inputs and its simulated outputs should be stored in a database for further evaluation of ship survivability when flooding accidents take place. In situations of emergencies, once the exact information of damage is ascertained following collision / grounding, the casualty-based damage cases pertinent to the incident / accident would be selected from the existing database and to be investigated for the subsequent decision support.

7.5.3.2.1 Database Platform

It is appreciated that the system needs to accommodate great amount of simulation data for process. Hence, the identification of an appropriate platform plays an important role for an effective operation of the whole system. In this respect, the following aspects should be closely adhered to: i) the database should be capable of storing gigantic data effectively, ii) query running and the subsequent data retrieval can be implemented promptly and iii) the platform should facilitate further data processing in a flexible way.

Following the evaluation of a list of available platforms for data management, the Microsoft SQL (Structured Query Language) Server platform (MICROSOFT, 2012) has been identified. This is attributed to the following considerations:

- It is a system dedicated for database management, which has been widely accepted as a powerful and popular platform allowing complex data handling operations (i.e. input, storage, retrieval, processing). With the capability of storing and processing billions (or even trillions) of records stored in complex relational tables, the platform is deemed appropriate for this deployment (e.g. hundreds of thousands of numerical records). Figure 7.10 shows an example of the database management interface.

- The SQL is a programming language designed for effectively implementing the aforementioned various data management operations (Davidson et al., 2008). Figure 7.11 illustrate a sample of SQL syntax for query running.

- This platform allows easy communication with other platforms (e.g. Visual Studio) for further development (e.g. web-based applications, stand-alone work package / code). Or it can export the selected data into text file if the raw data is needed.

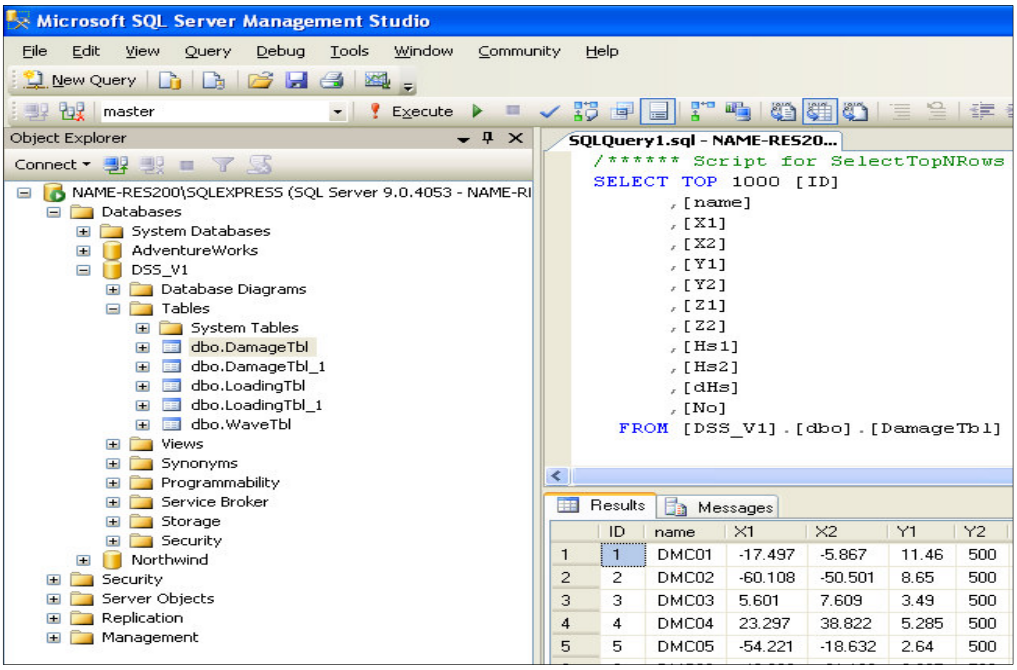

Figure 7.10: A Snapshot of the Microsoft SQL database Interface

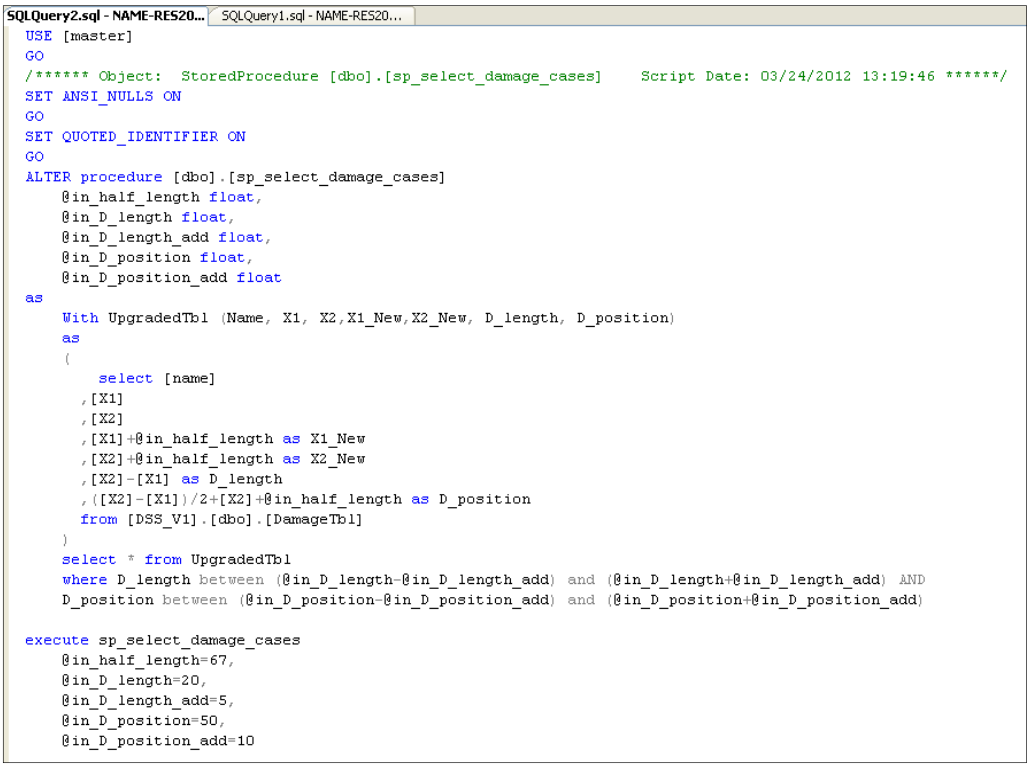

Figure 7.11: A Snapshot of the SQL Syntax to Implement Various Data Management Operations

7.5.3.2.2 Data Selection

As elaborated previously that the generation of the simulation database takes place before a flooding accident actually occur. In this way, the time-consuming computation can be avoided in the event of a casualty. The process of data filtering will be initiated when flooding takes place following collision / grounding accidents. In this case, the instant information collected in the monitoring module will be applied directly.

In the knowledge that it is extremely difficult (or unlikely) for a simulated case in the database to match exactly with the reported actual one, concerning the information collected about damage in operation, the underlying consideration in this section is to select a list of the most relevant scenarios from the pre-generated database. Such casualty-based dataset will be used for model estimation to approximate the correlation between the phenomenon of ship capsizing and the given condition that the damage arises. It is important to note that as the selected simulated data is supposed to be very close to the encountered case, the estimated model can be regarded as a dedicated model for assessing ship survivability.

Deriving from the foregoing, the method for collecting relevant damage scenarios is by considering all the simulated scenarios with the comparable damage characteristics, loading conditions and sea environment. Accordingly, a definition of the criteria for similar case selection is desired, that should be based on the information of key inputs under consideration.

An intuitive way of filtering data is to identify the upper bound and lower bound of each input variable and thereby to ensure the selected values vary within a predefined interval. For instance, if the extent of damage L_d is ascertained as 30 m, the interval can be considered as $\pm 20\%$ of such value, e.g.$[L_d \times 80\%, L_d \times 120\%]$. Meanwhile, with the same concept applied to all considered input variables, one can identify a set of criteria to limit the selected cases within the defined ranges and to reflect the given damaged condition. Table 7.2 illustrates such a process by setting criteria for both damage characteristics and loading conditions. Along with such information, corresponding SQL query can be set up to select the relevant damage scenarios.

During this process, the assignment of interval does not necessary have to be fixed for all studies. A dynamic approach can be implemented by adjusting the interval when it is needed. For instance, one can extend the intervals to allow more records to be considered if it is deemed that selected data set is not enough for the subsequent model estimation (e.g. less than one hundred records). Conversely, the intervals can be reduced accordingly if the selected dataset is too large to be deployed for fast model estimation (e.g. tens of thousands of cases).

Table 7.2: A list of Filter Criteria for Data Selection

Inputs		**Filter criteria**
Damage characteristics	Location	$X_{l\ lower\_bound} \leq X_l \leq X_{l\ upper\_bound}$
	Length	$L_{d\ lower\_bound} \leq L_d \leq L_{d\ upper\_bound}$
Loading conditions	T	$T_{lower\_bound} \leq T \leq T_{upper\_bound}$
	KG	$KG_{lower\_bound} \leq KG \leq KG_{upper\_bound}$

It is also worth mentioning that criteria about sea environment are not taken into account at this stage. This is mainly attributed to a concept of "*capsize band*" adopted to express stability. It considers a range of sea conditions within which the probability of ship capsizing increases from nearly zero to nearly one as the sea states increases, with a standardised normal distribution.

Being aware of this, it would be very desirable for the ensuing estimated model to establish a relationship between the probability of capsizing and a range of sea states within a fixed simulation length. As such a transition phenomenon (capsize band) plays an important role for the ultimate decision making. All considered sea states in the database will be used.

7.5.3.3 Casualty-Based Model Estimation

Following the selection of casualty-based scenarios from the simulated database, the refined data would be processed for the associated model estimation according to the methodologies elaborated in Chapter 6. In particular, recalling the first three tasks of the proposed procedures for uncertainty quantification as detailed in Section 6.3 (i.e.,

data collection, model estimation, sensitivity study), it is understood that the influential levels for the concerned input variables on the model output can vary significantly when different damage scenarios are considered. Hence, an important concept introduced here is that the regression model for the prediction of ship survivability is dynamically updated and refined rather than a fixed expression. This implies that not only the model coefficients but also the input variables constituting the predictive model are adjusted based on the damage scenario encountered.

An iterative procedure, as illustrated in Figure 7.12, is proposed to realise such a concept. In this process, Bayesian inference techniques are adopted initially to approximate the target densities of the model coefficients. As indicated in Chapter 6, each coefficient is deemed as the sensitivity indicator in the model. Therefore, a quick assessment of the significance of each input variable on the ship survivability can be carried out afterwards. If a variable is identified to have less influence on the model outcome than others, the model will be updated through excluding the less influential variable and retrained to strive for model parsimony. As there are a limited number of variables considered in the model, such an iterative process of sensitivity study will generally reach a stable status fast. The model estimation program has been developed in the R package to automate the process. Both of the MCMC algorithms as the Gibbs sampler and the Metropolis sampler are enclosed in the development.

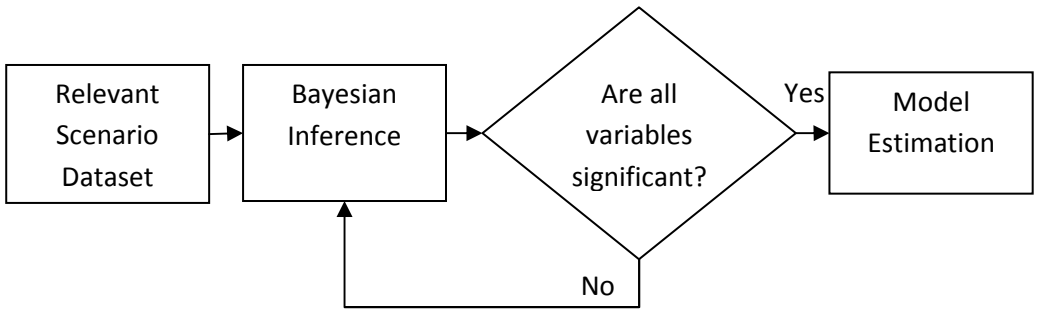

Figure 7.12: A Flowchart of Casualty-Based Model Estimation

In short, the most obvious difference between the above process for model estimation and that elucidated in Section 6.3 is that the data collected is from the numerical simulations rather than from the model experiments. Thus, in line with the

clarification in Section 7.5.3.1.2., large amounts of variations in the damage characteristics can be generated from MC simulation. Moreover, in order to provide a dedicated decision support function in emergency, all the relevant data is generated from the simulation of local damage scenarios rather than a global investigation of experimental observations from various ships (i.e., Table 6.3).

7.5.4 Advice Module

The prediction module elicits a process of estimating casualty-based predictive models. An integrated method addressing the probability of ship capsizing within given period of time, as well as inherent uncertainties associated with the entire assessment process is presented. Accordingly, the advice model attempts to support decisions based upon the available information during the actual crises.

In this respect, initially it is necessary to interpret the model output with the assigned quantitative uncertainty bounds, since the ship's residual stability in the event of an incident is an important consideration for remedial actions to be undertaken. After that, it should prioritise various control options based on relevant evaluation criteria so that the best course of actions could be defined.

The main emphasis in this section is placed on the first part of performing a reliable assessment of ship survivability within a given period. Concerning the process of prioritisation of the control options, it is understood that the deployment of pertinent optimisation techniques is already one step ahead. In particular, the application of case-based reasoning techniques for prioritising the various control options for flooding management in the SSRC has demonstrated its feasibility.

Nevertheless, it is noted the criteria defined for existing optimisation algorithm focus mainly on local time measures (e.g. time to implement a specific ballasting operation), whilst overlooking the improvement of global ship survivability as a whole. Hence, particular attention should be paid on the feasibility of integrating the global survivability measure (i.e. probability of capsizing within given time) into a generic optimisation process.

7.5.4.1 Ship Survivability Prediction

The focus on making predictions based on the estimated model, as mentioned previously, the collected information of the encountered flooding scenario is fed into the model to obtain the preliminary projection of the probability of ship capsizing in relation to the timeline development. Meanwhile, with the deployment of Bayesian inference, 99% uncertainty bounds are estimated to express the degree of inherent uncertainties.

Having the quantitative predictions of ship survivability, it is vital to transform these quantitative measures (e.g. presented in a probabilistic form) into meaningful qualitative message so that appropriate actions can be taken promptly. In this respect, the concept of "criticality index", as illustrated in Figure 7.13, is proposed to facilitate such a process.

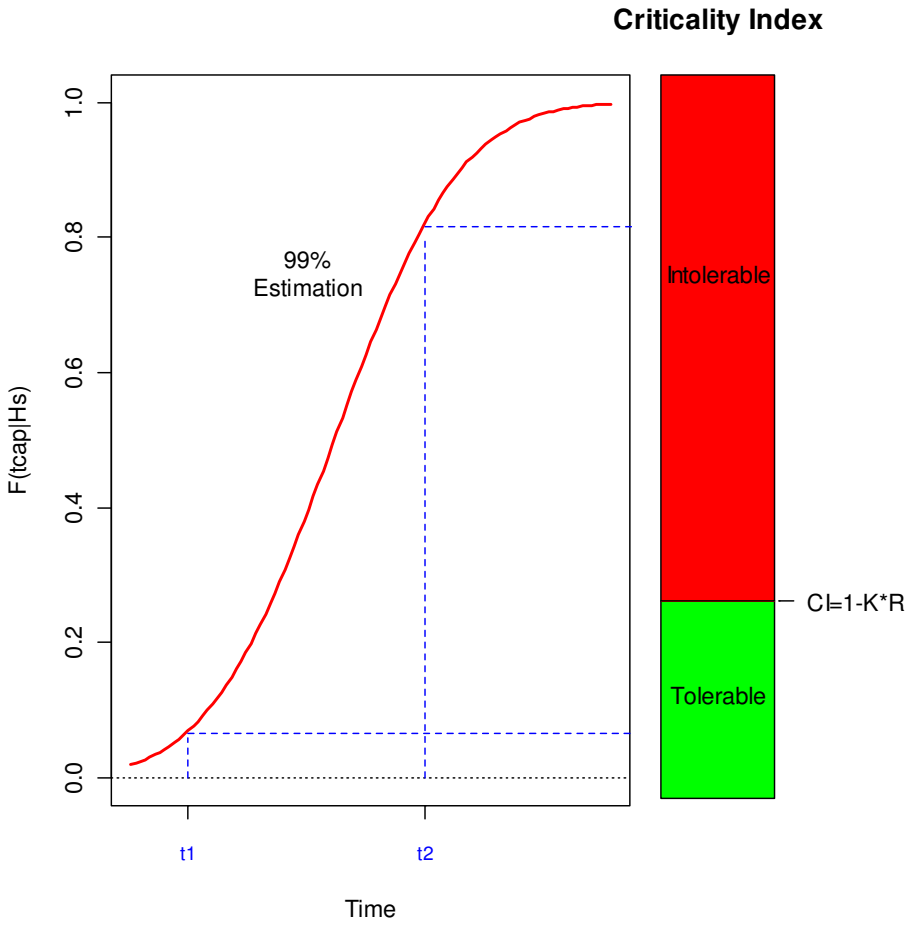

Figure 7.13: A Concept of "Criticality Index"

A decided advantage of making use of the criticality index (CI) is the ability to provide an explicit, transparent, fast and rational means for assisting decision making in emergencies. To achieve this, the following principles need to be adhered to:

1) In the knowledge that it is necessary for ensuring the projected ship survivability is a conservative measure so that confidence can be assured during the decision making process. Therefore, the upper bound of a 99% confidence interval can be adopted. Certainly, the confidence level is flexible to be adjusted according to the actual conditions.

2) The situation of the damaged ship should be determined as either returning to port under its own power or requiring abandonment. The estimated time-related survivability measure $F(t_{cap}|Hs)$ is transformed into a criticality index (varying from 0 to 1) and used as an aid when making decisions.

In Figure 7.13, the CI indices at the different time interval (e.g. t_1, t_2) indicate the two levels of urgency for taking appropriate responses. An implication of each region of the CI is given as below:

- *Tolerable*: In this region, the probability of losing stability is at a low level. The damaged ship still has enough capacity to stay afloat for at least 3 hours (e.g., $t_1 = 3\ hrs$) and should be capable of progressing to a safe haven (e.g. *Sea Diamond*). As a result, immediate abandonment of the ship is not needed. Nevertheless, necessary mitigative measures (concurrent shipboard damage control plan) still should be considered for risk control.

- *Intolerable*: In contrast, this region indicates that there is a very high probability of ship capsizing within 3 hours (e.g., $t_2 = 1\ hr$). Therefore, a mayday must be sent out and such action is to be followed by abandoning the ship immediately.

It is difficult to give an absolute estimation of the boundary to differentiate the two regions. A formalised method should be defined for the sake of consistency. Regarding this, the required subdivision index *R* (SOLAS Regulations II-1/6) can be

deployed as the means to define the boundary of the CI for passenger ships. The proposed approach is to attach a coefficient to R, as shown below.

$$CI = 1 - K \cdot R$$

$$R = 1 - \frac{5000}{L_s + 2.5N + 15{,}225}$$

Where:

N = $N_1 + 2N_2$

N_1 = Number of persons for whom lifeboats are provided

N_2 = Number of persons (including officers and crew) the ship is permitted to carry in excess of N

Associating the definition of CI with the required subdivision index R is attributed to the following concerns:

1) The ship size and the number of passenger are important parameters to consider.

2) The coefficient K is constant which may be assumed as 0.9 in this study. The general idea is that the attained subdivision index (A) has been widely known as an averaged measure of ship overall survivability. Three partial indices (A_s, A_p and A_l) attained for three draughts are not be less than $0.9R$ for passenger ships. In light of this, it can be considered that the damaged ship has sufficient survivability if the vulnerability within given time $F(t_{cap}|Hs)$ is less than $1 - 0.9R$, as the given boundary of CI.

7.5.4.2 Damage Control Options Prioritisation

The decision support approach towards the recommendation of control options is essentially a multi-objective optimisation process (see Appendix 3). Various algorithms have been proposed to determine the most effective one based on a list of evaluation (performance) criteria. Ultimately, the control options can be prioritised by using the overall weighted performance.

This section has no intention to re-elaborate the process of employing optimisation methodology due to their wide applications (e.g. case-based reasoning, Genetic Algorithm). In this respect, the following context aims to suggest a method of

integrating the obtained predictive model into the optimisation process for prioritisation of the relevant control options.

A key observation with current optimisation methodologies is that the performance criteria for evaluating each control option focus mainly on the changes of local stability measures (e.g. trim, damage freeboard), while little attention has been paid on the influence of each control option on the global measures (e.g. time to capsize). Hence, the proposed process is to include the estimated model (for assignment of the probability of ship capsizing within given period of time) as an additional criterion for performance evaluation, as illustrated in Figure 7.14.

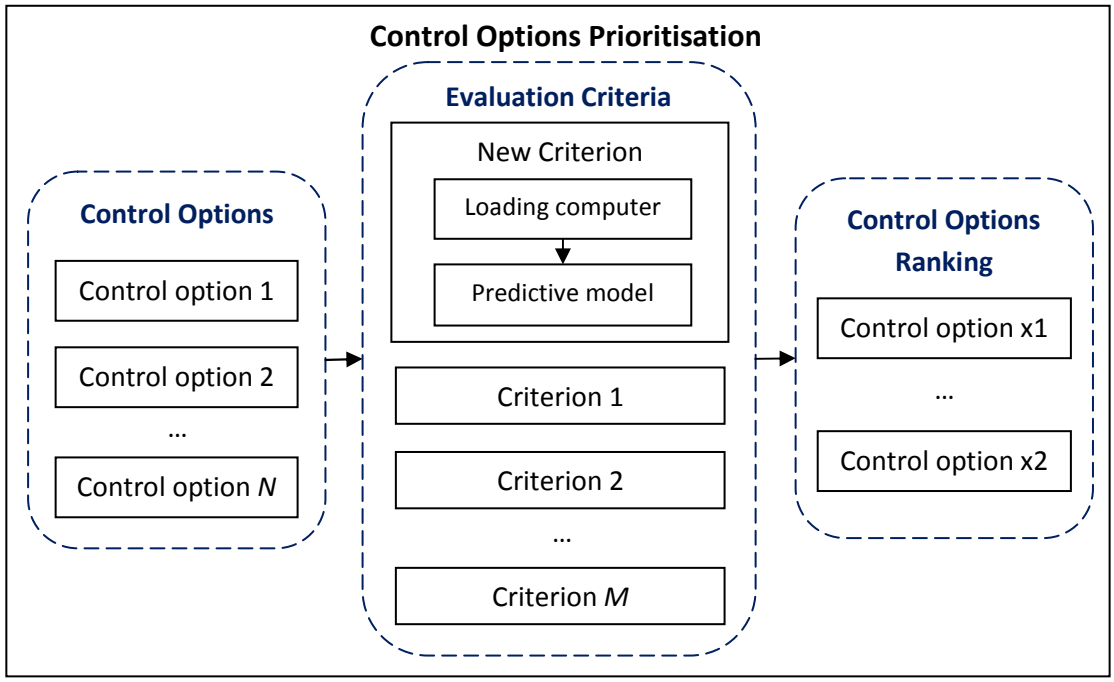

Figure 7.14: A Proposed Prioritisation Process of the Flooding Control Options

Under such a process, the impact of each flooding control option is to be assessed through the hydrostatic computation, whereby the updated loading conditions can be provided for the ensuing appraisal. Then, the casualty-based model is available to make predictions of the capacity of the ship to sustain its floatability within given period of time. Next, making use of the value of CI at a specific time (e.g. 3 hours) as the performance measure of ship losing stability, a transparent and objective method for the evaluation of control options can be achieved.

An example of the evaluation process is given in Figure 7.15, in which each control option is evaluated against the predefined performance evaluation criteria (e.g. Trim, Heel, Damage freeboard). Such a process is able to generate the quantitative sub performance(x_{ji}) for each of the control options (j) with respect to each attribute(i). For instance, the computed CI treated as a sub performance aims to describe the ship vulnerability to flooding within given time, which is deemed as a new attribute under examination.

According to the achieved sub performance, the following two steps are to be performed.

- Calculate the normalized ratings (r_{ji}). This step tries to transform various attribute dimensions into the non-dimensional attribute, which allows comparison across the attributes.

$$r_{ji} = \frac{x_{ji}}{\sqrt{\sum_{j=1}^{N} {x_{ji}}^2}}, \qquad j = 1,2,\cdots,N; i = 1,2,\cdots,K$$

- Calculate the weighted normalized ratings (v_{ji}). A set of attribute weights $\mathbf{w} = \{w_i | i = 1,2,\cdots,K\}$ assessed from the decision maker is assigned to identify the significance level of the ith attribute (i.e. performance criterion).

$$v_{ji} = w_i r_{ji}, \qquad j = 1,2,\cdots,N; i = 1,2,\cdots,K$$

$$\mathbf{w} = (w_1,\cdots,w_K), \qquad \sum_{i=1}^{K} w_K = 1$$

It is worth noting that the new criterion is supplied, under which CI is estimated by considering the influence of implementing each specific control option(j) on ship survivability. Ultimately, through summing up the weighted normalized rating (v_{ji}) pertinent to a set of performance criteria, one can produce the overall ranking with respect to various considered control options.

Concerning the definition of evaluation criteria, the proposed list is inspired by the work presented in (Vassalos et al., 2004), (Olcer and Majumder, 2006) and (Martins and Lobo, 2011):

- Assessment of time needed to implement the proposed control operations (e.g. ballast, de-ballast)
- Assessment of residual structural strength
- Assessment of ship damage stability (criticality index)

By doing so, the proposed method towards criticality index estimation concerning ship damage stability can be integrated into the process for identifying appropriate damage control options. It will offer an overarching and transparent means for relevant decision making.

			Current Evaluation Criteria													
			Criterion 1			Criterion 2			Criterion 3			New Criterion				
No.	Name of tank	Type of tank	Sub performance	Normalized	Weighting Assignment	Performance ratings	Normalized	Weighted normalized	Performance ratings	Normalized	Weighted normalized	Sub performance	Normalized	Weighting Assignment	OTR	Overall Ranking
1	R2115	HT	4.963 290	0.1620	0.0360	0.41 3880	0.0934	0.0415	−1.875 960	−0.2391	−0.0797	0.0733	0.0290	0.0360	0.2833	37
2	R2117	HT	5.456 730	0.1782	0.0396^{NIS}	0.249 040	0.0562	0.0250^{NIS}	−2.429 610	−0.3097	−0.1032^{NIS}	0.1022	0.0000	0.0396	0.0000	38
3	R2205	HT	4.894 500	0.1598	0.0355	0.869 180	0.1961	0.0871	−0.538 140	−0.0686	−0.0229^{PIS}	0.0045	0.1017	0.0355	0.9578	1
4	R2207	HT	5.276 780	0.1723	0.0383	0.872 440	0.1968	0.0875^{PIS}	−0.624 980	−0.0797	−0.0266	0.0081	0.0989	0.0383	0.9240	2
5	R6000	WB	4.278 010	0.1397	0.0310^{PIS}	0.743 030	0.1676	0.0745	−1.028 970	−0.1311	−0.0437	0.0246	0.0779	0.0310	0.7603	9
6	R6001	WB	4.747 170	0.1550	0.0344	0.744 850	0.1680	0.0747	−1.137 420	−0.1450	−0.0483	0.0287	0.0742	0.0344	0.7212	14
7	R6002	WB	4.991 330	0.1630	0.0362	0.729 590	0.1646	0.0731	−1.227 980	−0.1565	−0.0522	0.0330	0.0703	0.0362	0.6803	19
8	R6007	WB	4.929 600	0.1609	0.0358	0.735 690	0.1660	0.0738	−1.194 150	−0.1522	−0.0507	0.0314	0.0718	0.0358	0.6955	17
9	R6008	WB	4.991 570	0.1630	0.0362	0.729 920	0.1647	0.0732	−1.219 580	−0.1554	−0.0518	0.0327	0.0706	0.0362	0.6833	18
10	R6009	WB	5.045 350	0.1647	0.0366	0.724 410	0.1634	0.0726	−1.241 740	−0.1583	−0.0528	0.0338	0.0695	0.0366	0.6725	21
11	R6014	WB	4.876 300	0.1592	0.0354	0.740 720	0.1671	0.0743	−1.174 840	−0.1497	−0.0499	0.0304	0.0727	0.0354	0.7051	16
12	R6113	WB	4.974 590	0.1624	0.0361	0.705 980	0.1593	0.0708	−1.280 310	−0.1632	−0.0544	0.0360	0.0670	0.0361	0.6504	25
13	R6124	WB	4.970 750	0.1623	0.0361	0.632 620	0.1427	0.0634	−1.449 350	−0.1847	−0.0616	Criticality	0.0568	0.0361	0.5533	34
14	R6126	WB	4.984 980	0.1628	0.0362	0.673 790	0.1520	0.0676	−1.354 720	−0.1727	−0.0576	Index	0.0625	0.0362	0.6079	29
15	Control	WB	5.025 420	0.1641	0.0365	0.649 050	0.1464	0.0651	−1.421 900	−0.1812	−0.0604	0.0441	0.0587	0.0365	0.5715	32
16	Options	WB	5.115 640	0.1670	0.0371	0.703 710	0.1587	0.0706	−1.310 190	−0.1670	−0.0557	0.0374	0.0659	0.0371	0.6380	26
17		WB	5.125 870	0.1674	0.0372	0.656 760	0.1482	0.0658	−1.419 110	−0.1809	−0.0603	0.0437	0.0593	0.0372	0.5761	31
18	R6203	WB	4.969 620	0.1623	0.0361	0.756 890	0.1707	0.0759	−1.517 780	−0.1476	−0.0492	0.0292	0.0743	0.0361	0.7180	15
19	R6204	WB	4.947 840	0.1615	0.0359	0.817 050	0.1843	0.0819	−0.973 380	−0.1241	−0.0414	0.0199	0.0842	0.0359	0.8087	5
20	R6206	WB	5.008 360	0.1635	0.0363	0.797 340	0.1799	0.0799	−1.050 500	−0.1339	−0.0446	0.0236	0.0804	0.0363	0.7728	8
21	R6216	WB	4.972 600	0.1623	0.0361	0.783 530	0.1768	0.0786	−1.081 410	−0.1378	−0.0459	0.0252	0.0785	0.0361	0.7567	10
22	R6234	WB	5.114 940	0.1670	0.0371	0.774 200	0.1746	0.0776	−1.139 610	−0.1452	−0.0484	0.0281	0.0760	0.0371	0.7305	13
23	R6244	WB	5.112 890	0.1669	0.0371	0.731 490	0.1650	0.0733	−1.244 800	−0.1587	−0.0529	0.0337	0.0699	0.0371	0.6744	20
24	R6003	SWCO	5.078 860	0.1658	0.0368	0.720 920	0.1626	0.0723	−1.264 970	−0.1612	−0.0537	0.0349	0.0685	0.0368	0.6625	24
25	R6011	SWCO	5.075 300	0.1657	0.0368	0.721 710	0.1628	0.0724	−1.262 240	−0.1609	−0.0536	0.0348	0.0687	0.0368	0.6639	23
26	R6017	SWCO	5.038 850	0.1645	0.0366	0.725 430	0.1636	0.0727	−1.246 260	−0.1588	−0.0529	0.0340	0.0694	0.0366	0.6715	22
27	R5112	PFW	4.900 490	0.1600	0.0356	0.687 680	0.1551	0.0689	−1.303 550	−0.1661	−0.0554	0.0377	0.0651	0.0356	0.6333	27
28	R5115	PFW	4.908 420	0.1603	0.0356	0.540 470	0.1219	0.0542	−1.574 150	−0.2006	−0.0669	0.0554	0.0468	0.0356	0.4581	35
29	R5123	PFW	4.858 700	0.1586	0.0353	0.664 200	0.1498	0.0666	−1.347 440	−0.1717	−0.0572	0.0404	0.0622	0.0353	0.6059	30
30	R5124	PFW	4.918 320	0.1606	0.0357	0.678 380	0.1530	0.0680	−1.325 960	−0.1690	−0.0563	0.0390	0.0638	0.0357	0.6206	28
31	R5133	PFW	4.949 370	0.1616	0.0359	0.637 450	0.1438	0.0639	−1.430 580	−0.1823	−0.0608	0.0449	0.0577	0.0359	0.5624	33
32	R5134	PFW	4.896 840	0.1599	0.0355	0.535 730	0.1209	0.0537	−1.590 270	−0.2027	−0.0676	0.0562	0.0460	0.0355	0.4500	36
33	R5202	PFW	4.892 730	0.1597	0.0355	0.767 040	0.1730	0.0769	−1.111 460	−0.1417	−0.0472	0.0269	0.0765	0.0355	0.7396	12
34	R5203	PFW	4.930 290	0.1610	0.0358	0.800 850	0.1807	0.0803	−1.015 770	−0.1295	−0.0432	0.0220	0.0818	0.0358	0.7877	6
35	R5204	PFW	4.858 420	0.1586	0.0352	0.845 300	0.1907	0.0847	−0.819 750	−0.1045	−0.0348	0.0130	0.0909	0.0352	0.8752	3
36	R5205	PFW	4.867 830	0.1589	0.0353	0.843 450	0.1903	0.0846	−0.840 080	−0.1071	−0.0357	0.0138	0.0902	0.0353	0.8670	4
37	R5213	PFW	4.844 750	0.1582	0.0351	0.785 320	0.1772	0.0787	−1.040 060	−0.1326	−0.0442	0.0234	0.0800	0.0351	0.7736	7
38	R5214	PFW	4.909 190	0.1603	0.0356	0.768 460	0.1734	0.0770	−1.107 850	−0.1412	−0.0471	0.0267	0.0767	0.0356	0.7414	11

Figure 7.15: An Example of the Evaluation of Flooding Control Options

7.6 Closure

This chapter initially develops a discussion around the implementation of the proposed uncertainty modelling in life-cycle safety management. Eventually flooding crisis management is highlighted as a potential field of application due to the attitude of zero tolerance to loss of human life following ship accidents.

In this respect, the state-of-the-art in developments of Decision Support System is reviewed and that leads to a new philosophy of real-time DSS for managing ship stability under damage conditions. The new viewpoint is to shift the intense computation to the pre-casualty phase (i.e. design, operation) so that instant computations can be performed once the detailed information of the actual flooding scenario is ascertained which in the end may help the decisions to be less stressful and thus more rational.

In sequence, a particular elaboration is enclosed on the configuration of the proposed framework of shipboard DSS for flooding damage control, which consists of three essential modules. The emphasis is placed on the prediction module to detail the process of the casualty-based predictive model estimation. It is worth mentioning that an integrated method addressing the probability of ship capsizing within given period of time, as well as inherent uncertainties associated with the entire assessment process is presented. Ultimately, the available information is exported to an Advice module for control options prioritisation when making decisions.

Along with a comprehensive elucidation of the methodology, which devises an integration of the uncertainty modelling into a real-time shipboard DSS for flooding damage control during actual crises, a concrete case study is the main focus of the next chapter.

Chapter 8

A Case Study for Emergency Response

8.1 Preamble

Preparedness is the only viable tool to effectively handle emergencies with severe time constraints today. This will require a creditable and verifiable emergency response system for crisis management, which intends to ensure the most timely and adequate response to tackle various emergencies scenarios, and to remove any threat of serious escalation of the situation.

To meet this requirement, this chapter demonstrates an application of the proposed uncertainty analysis scheme in the context of shipboard emergency management. The output is a fast and reliable assessment of the ship's residual stability in time domain with uncertainties quantified. This will help to assist shipboard personnel in dealing with unexpected emergencies and ensure that the necessary actions can be taken in a prioritised manner.

The case study starts with the description of a flooding damage scenario experienced on a RoPax ship. To show the applicability of the proposed approach for emergency response, a ship-specific simulation database is created, which embraces gigantic data about the performance-based damage stability assessment of tremendous potential flooding scenarios. Following the awareness of an emergency situation, a casualty-based assessment of ship survivability with uncertainty analysis can be performed by adopting the proposed Bayesian approach. The outcomes can be provided to shipboard personnel to assist decision making. As part of the case study, physical model experiments are undertaken to demonstrate the validity of the prediction results.

8.2 Background Description

A background description consists of three aspects: i) the main particulars of a RoPax ship which operates in Northern European waters; ii) the information of a collision damage in ship side shells causing flooding, and iii) a procedure of the response actions could be undertaken onboard for flooding emergency control.

8.2.1 Basic Ship Particulars

The basic information of the RoPax ship at intact loading condition is tabulated in Table 8.1. The general arrangement of the ship is given in Figure 8.1. In particular, the locations of openings on each of the decks under consideration are depicted in the purple colour.

Table 8.1: Ship Particulars

Parameter	**Unit**	**Value**
Length, LOA	[m]	155.4
Length, L_{bp}	[m]	137.4
Moulded Breadth, B	[m]	24.2
Displacement	[m^3]	12,046
Depth, to Main Deck (A Deck)	[m]	7.65
Draught, mean	[m]	5.39
Trim, aft	[m]	0.435
KG	[m]	10.62
GM_T	[m]	1.17
Number of Passengers		2000
Number of Crew		110

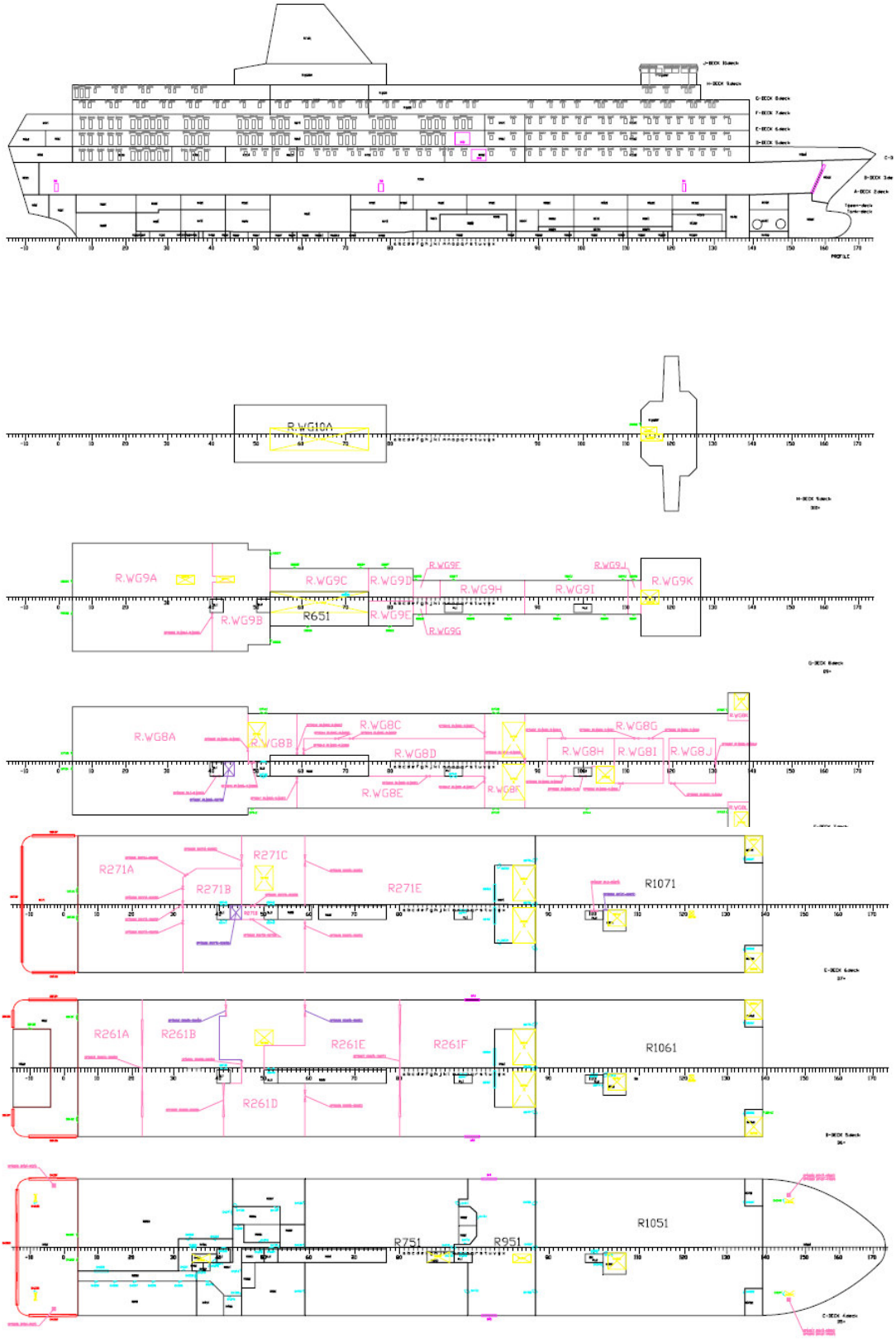
R.WG10A
R.WG9A
R.WG9B
R.WG9C
R.WG9D
R.WG9E
R.WG9F
R.WG9G
R.WG9H
R.WG9I
R.WG9J
R.WG9K
R651
R.WG8A
R.WG8B
R.WG8C
R.WG8D
R.WG8E
R.WG8F
R.WG8G
R.WG8H
R.WG8I
R.WG8J
R.WG8K
R271A
R271B
R271C
R271E
R1071
R261A
R261B
R261D
R261E
R261F
R1061
R751
R951
R1051

(a)

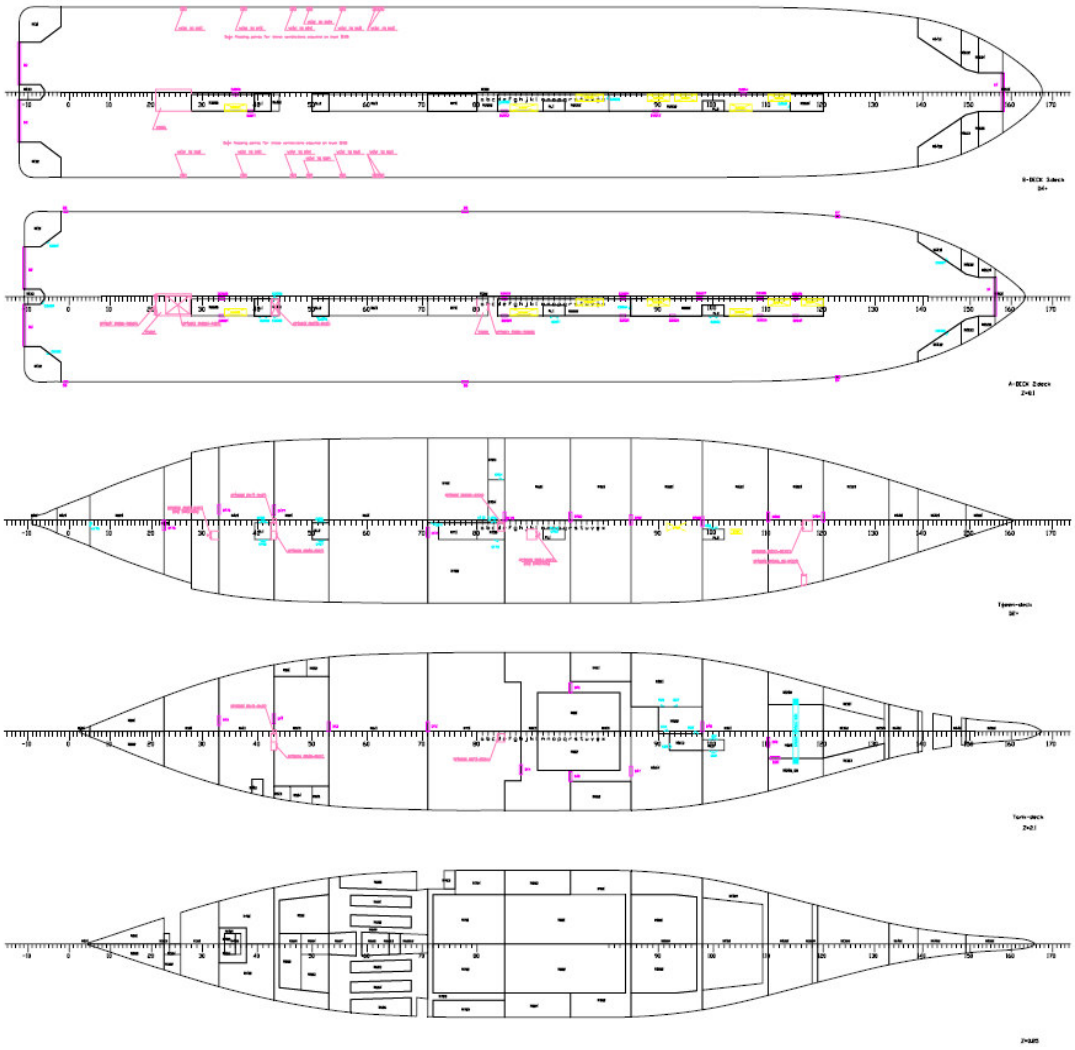

(b)

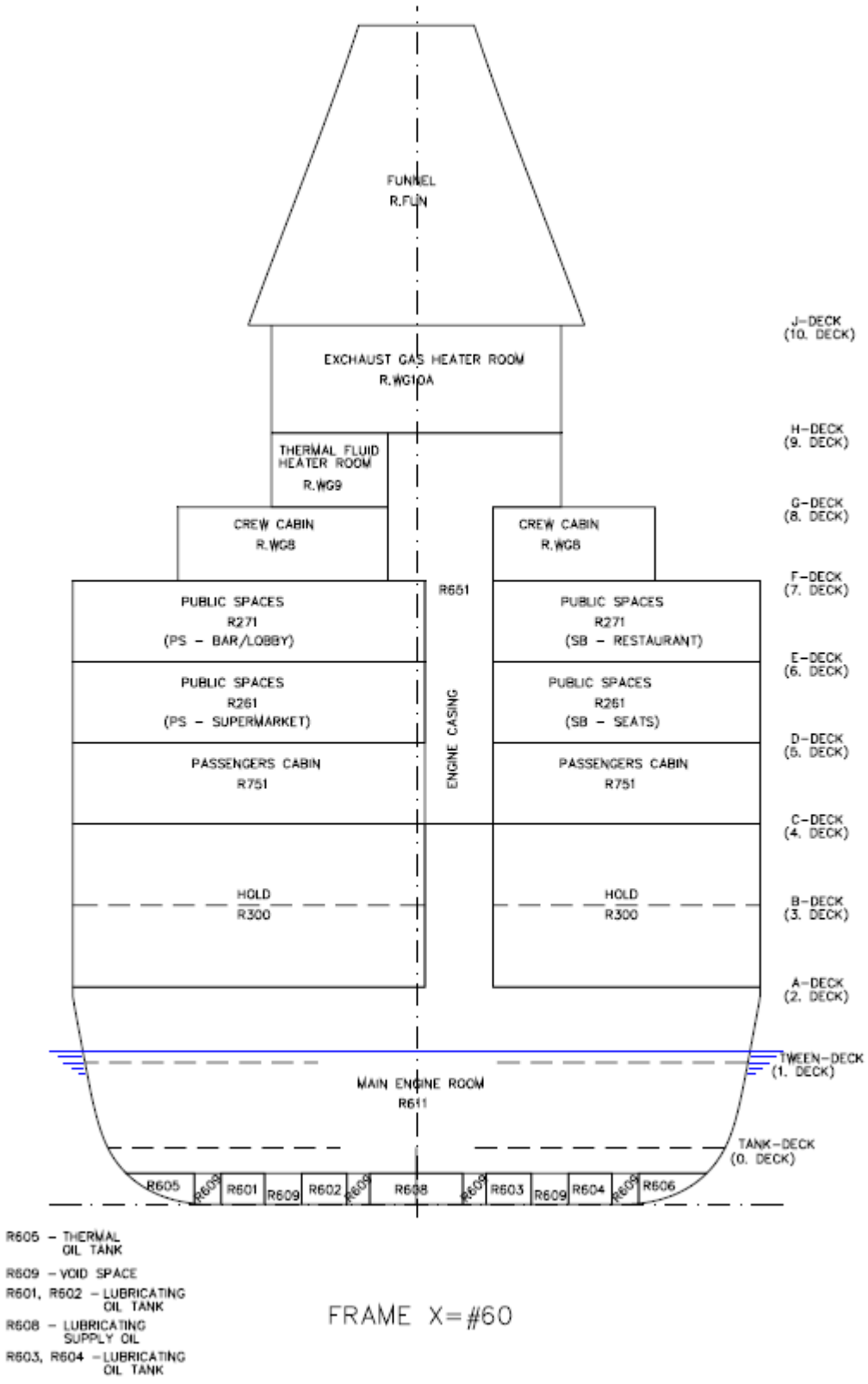

(c)

Figure 8.1: The Simplified Ship's GA

8.2.2 The Hull Damage

A fictitious scenario is that the flooding incident occurred in February 2012 while the RoPax ship was crossing the Baltic Sea, underway from Helsinki in Finland to Stockholm in Sweden. She was struck on port side near amidships by a container ship, sailing from Rotterdam in Netherlands to Kotka in Finland. Strong winds and a significant wave height of 1.5 m to 2.5 m were ascertained during the crisis as shown in Figure 8.2.

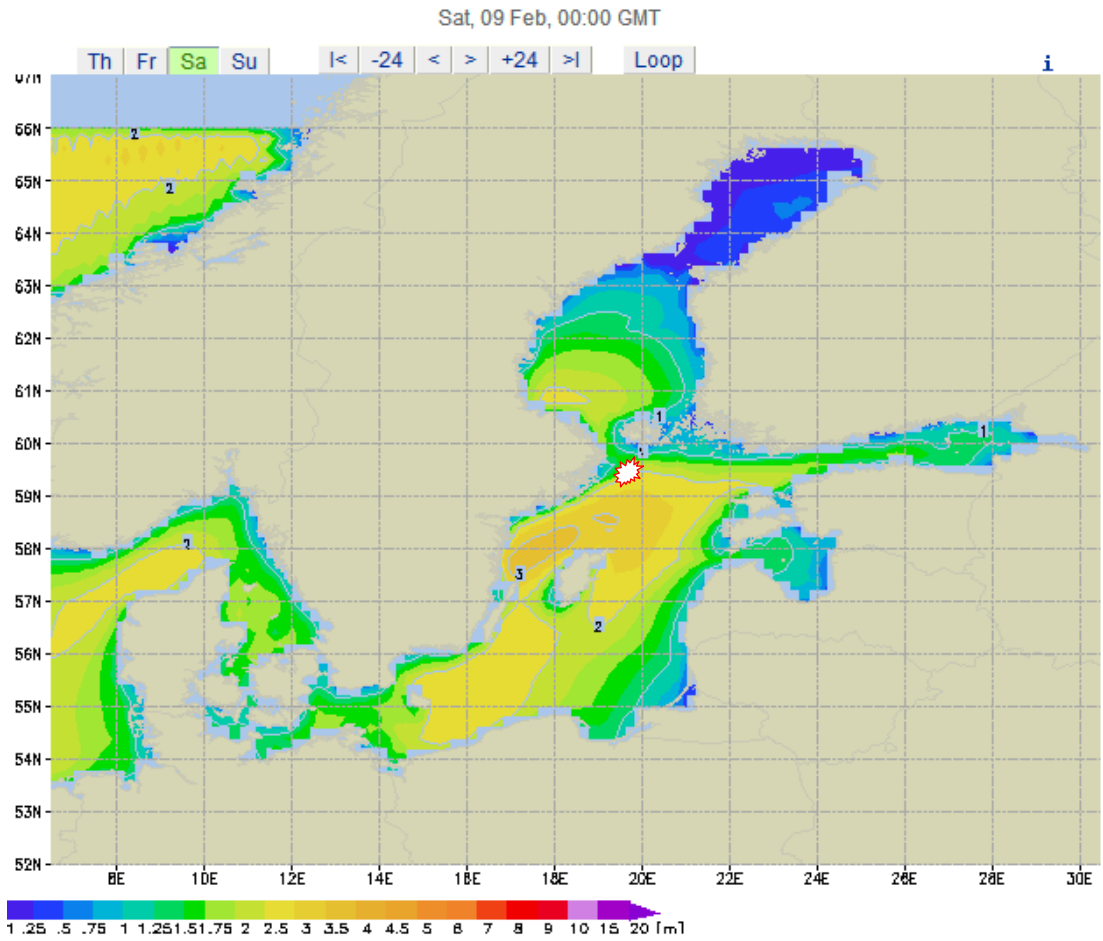

Figure 8.2: Baltic Sea - Wave Heights

Suppose that a quick measure about the emergency situation was taken by the navigational officer of the watch following the collision, while the general alarm was activated by him. Through a fast estimation of the flooding extent, the gathered information disclosed that the hull breach was located on port side towards aft, see

Figure 8.3. The flooded compartments were detected below the car deck as depicted (R511, R512, R519, R521 and R611), leading to the flooding extent within 29.8 m to 52.2 m from the aft. The trim angle of the damaged ship was 0.45 degree towards aft and the heel angle was 1.95 degree towards the port.

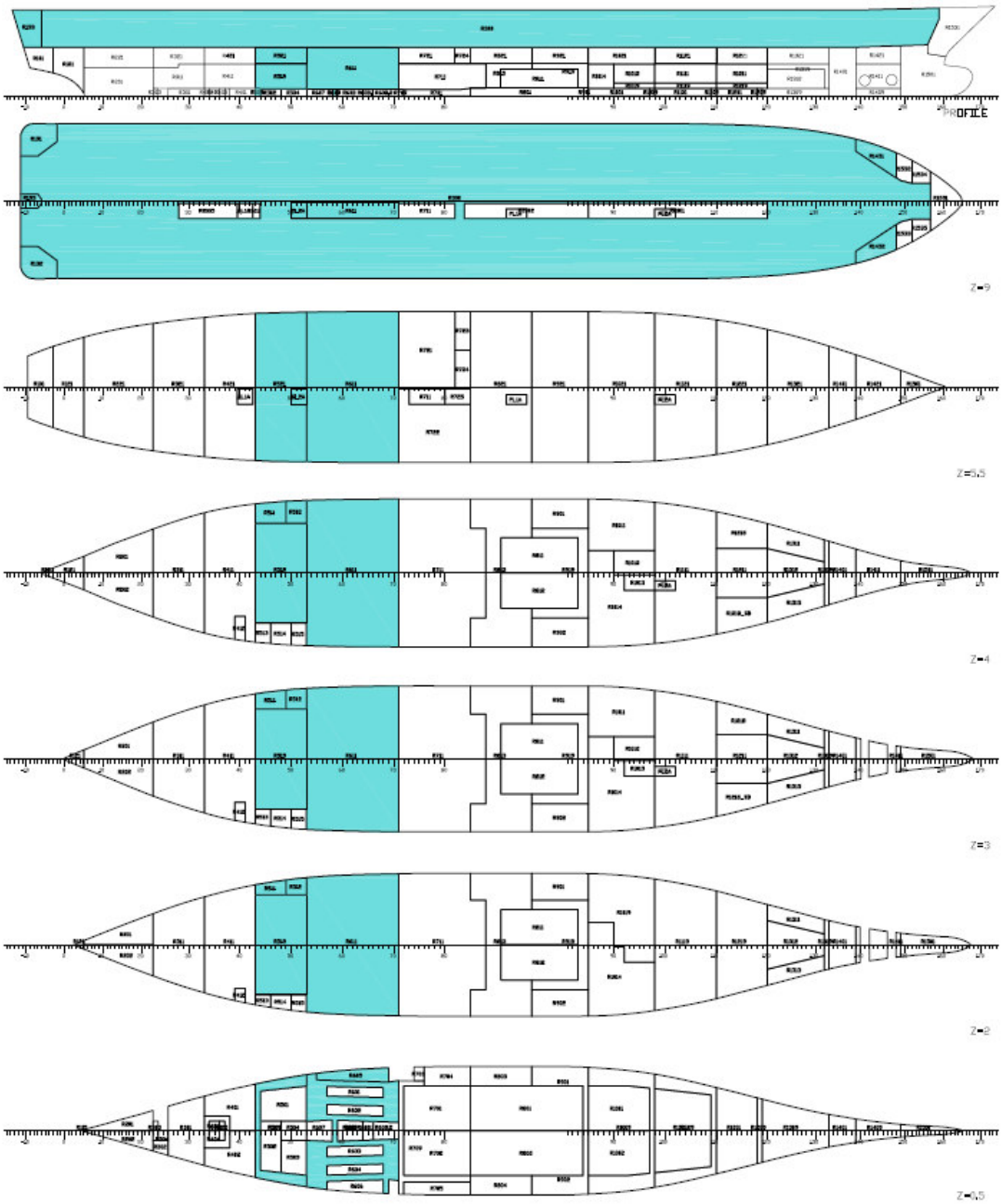

Figure 8.3: Flooded Compartments

8.2.3 Shipboard Emergency Response Actions

In all passenger ships, a required damage decision support system for emergency management has been provided on the navigation bridge in accordance with SOLAS Chapter III/29 since 1 July 1999. The system must include the pre-prepared emergency plans (e.g., printed documents) for handling all foreseeable emergency situations.

With regard to the aforementioned flooding scenario, a procedure of the subsequent response actions as illustrated in Figure 8.4 needs to be implemented onboard promptly. Clearly, the detailed picture of the sequence of priorities links the "initial actions" in an emergency situation with the "subsequent response". Following the initial procedures to quickly ascertain current situation, additional activities should be considered to provide advice and data to assist the shipboard personnel (master) to make their decision. It is worth noting that assessing ship's residual stability is one of the key responses to be followed. Therefore, the proposed uncertainty modelling should support these procedures to evaluate the status of the ship after damage.

8.3 Simulation Database Setting Up

Suppose the RoPax ship has been equipped with a dedicated life-cycle database, which contains ship survivability simulation data. It contains any feasible hull breach deriving from studies of the dynamic behaviour of the damaged ship in realistic environments. This section mainly focuses on a procedure of setting up the MC-based numerical simulation database using PROTEUS3 (P3) in the pre-casualty phase.

In accordance with Section 7.5.3.1, it is necessary to clarify that three operational draughts (d_l, d_p and d_s) have been considered during the simulation to describe a range of loadings (the lightship, the partially and fully loaded conditions). For each of the service draughts, the variation of KG has been investigated. A full description of the simulation matrix is given in Table 8.2.

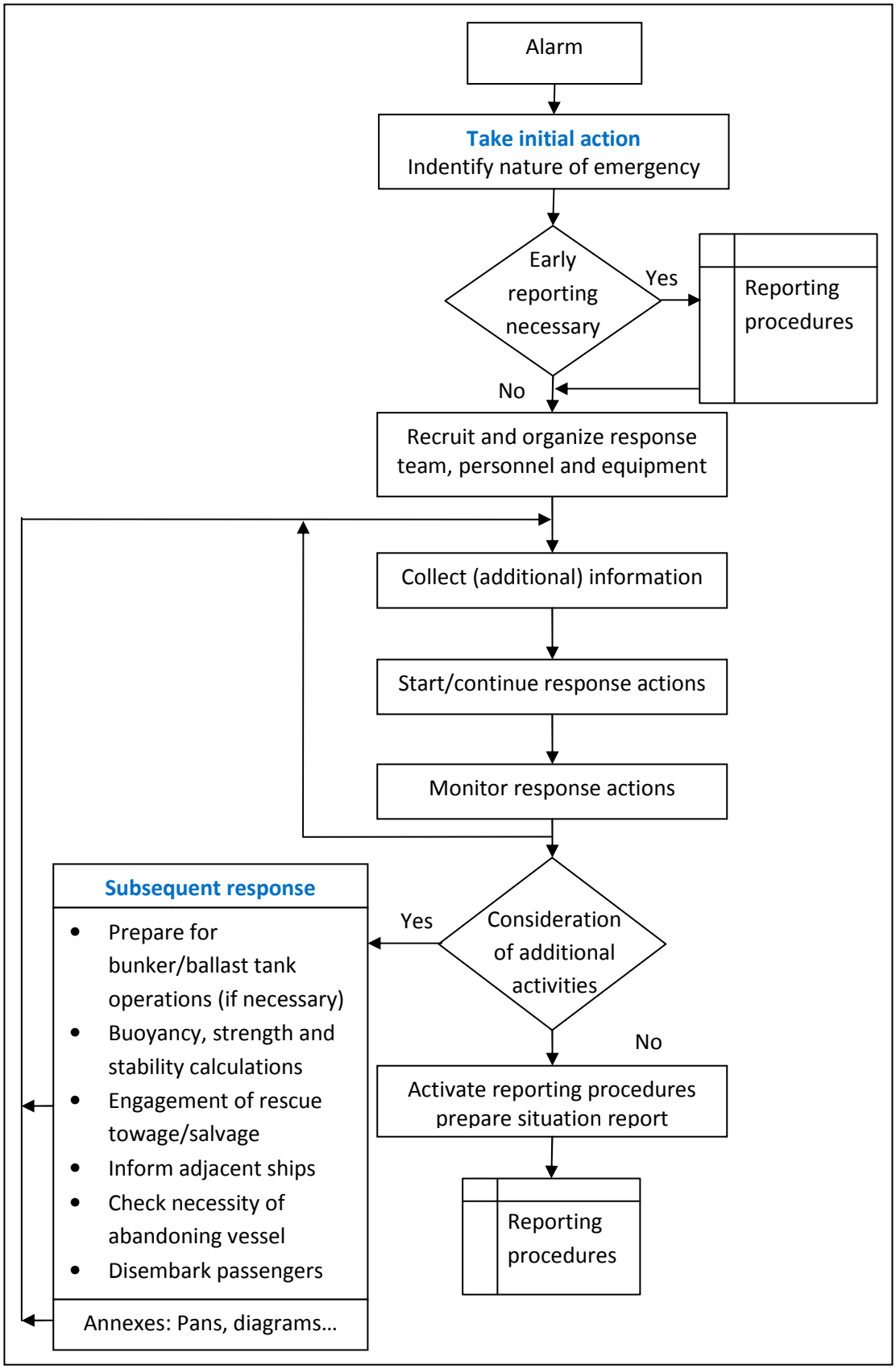

Figure 8.4: Response Actions - Sequence of Priorities Flowchart

Table 8.2: Simulation Matrix

Parameter		No. of Variations	Value
Damage Characteristics	Location (xd)	25000 cases per Loading Condition	Dependent on MC simulations
	Length (Ld)		
	Penetration (Bd)		
	Height (Hd)		
Loading Conditions	Initial draught	3	DL, 5.00 m
			DP, 5.24 m
			DS, 5.40 m
	KG	3	9.557 m
			10.11 m
			10.64 m
Environments (JONSWAP Spectrum)	H_s	8	1.5 m – 5.0 m

As mentioned in the foregoing, all the damage extents that the ship is subjected to are randomly simulated by a MC scheme according to the collision damage statistics. Probability distributions used to derive the damage scenarios are illustrated in Figure 5.2. It is notable that the probability of vertical extent of damage (height) is mainly based on a function of draught, as the formulae are developed for the factor v (SOLAS Chapter II-1/7-2). For instance, $v = 0.8$ (when height = d_l + 7.8 = 12.8 m) represents the probability that the spaces above 12.8 m from the baseline will not be flooded. Therefore, concerning the assumed distribution of the damage height, it is essential to perform MC simulations for sampling the random damage scenarios at each loading condition separately.

There are 25000 damage scenarios related to each operational draught that have been created for the ensuing study on damage ship survivability. A sample of the damages stemming from MC simulation at the lightship condition (DL) is shown in Figure 8.5. Figure 8.6 illustrates the related features of damages, in relation to the distribution of damage location, length and the sustained sea states. In summary, Figure 8.7

indicates the probability distributions for damage characteristics derived from MC sampling are comparable to that drawn from the damage statistics.

DL_mc-damages - Notepad

File Edit Format View Help

Ls= 137.400000
Bs= 24.200000

No	Xd	Ld	Bd	Hd	Hs
1	-15.059541	6.769697	5.793461	8.750719	1.827177
2	34.155287	11.700412	1.831724	9.977838	0.685803
3	16.409981	1.940662	1.670432	12.949227	2.364018
4	56.221302	21.080922	9.306404	5.431488	0.709934
5	21.238878	2.385095	6.711838	9.444321	1.769827
6	31.819842	16.912249	5.382805	9.982896	2.710999
7	23.741877	0.929499	2.320432	15.409812	0.160624
8	18.713574	8.402909	8.977792	8.279094	0.745859
9	45.741007	10.839258	8.584780	5.871870	0.000000
10	44.930050	14.402136	9.696042	10.389952	0.819716
11	29.724490	7.648137	4.910365	9.158965	0.001601
12	-35.080615	14.150496	2.685396	9.213418	1.001858
13	59.916265	10.945054	3.776259	9.529124	0.022782
14	-26.511042	10.091828	3.789223	8.643897	0.000000
15	15.300215	4.011112	7.604206	12.398451	0.486938
16	-26.479835	0.856644	0.205798	13.468392	0.474928
17	-4.798994	0.721469	4.767942	12.610609	0.726019
18	34.867679	17.996828	8.854487	17.261584	1.114716
19	-55.589437	7.111449	8.709624	8.314205	2.701662
20	50.771267	7.078264	0.783661	9.991525	1.597564
21	-44.580274	4.693951	2.033624	7.883642	1.392641
22	46.317393	42.849210	6.073828	6.604451	0.176539
23	-5.788358	32.871418	9.489389	14.609434	0.841083
24	-59.160610	14.573089	4.892795	9.151229	0.000000
25	10.082383	11.520992	11.997896	9.494013	3.328230
26	-43.752409	14.515227	5.958631	7.295078	1.628873
27	-33.030421	2.018449	5.356514	5.734994	0.000000
28	45.227367	8.583874	7.768184	7.060604	0.000000
29	27.476040	5.205976	1.339277	9.196457	0.000000
30	29.413211	9.228886	7.389073	13.531505	0.319982

Figure 8.5: Sample of MC Damages at DL ($d_l = 5.0m$)

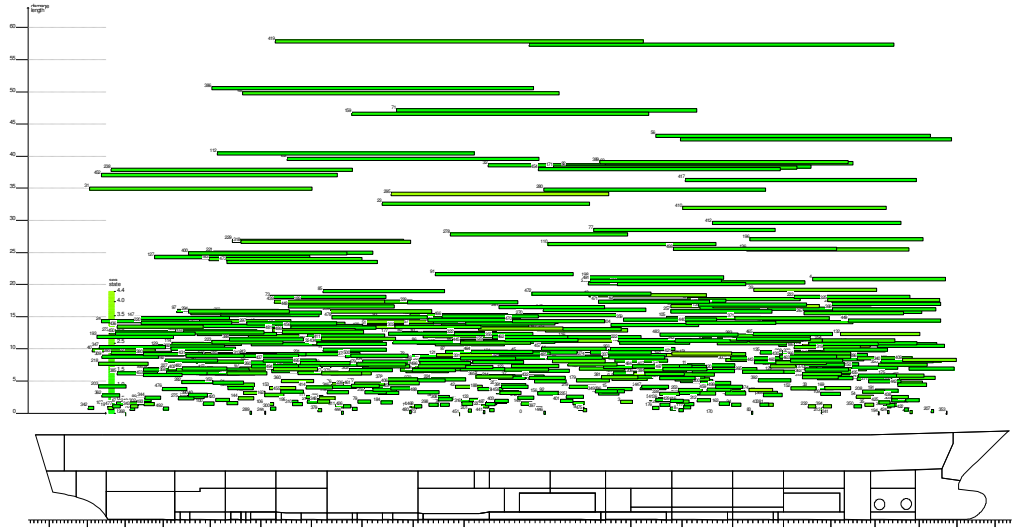

Figure 8.6: Sample of the first 500 out of 25000 MC simulations set-up, distribution of damage location, and length under a constant sea state (L_s=137.4 m, DL)

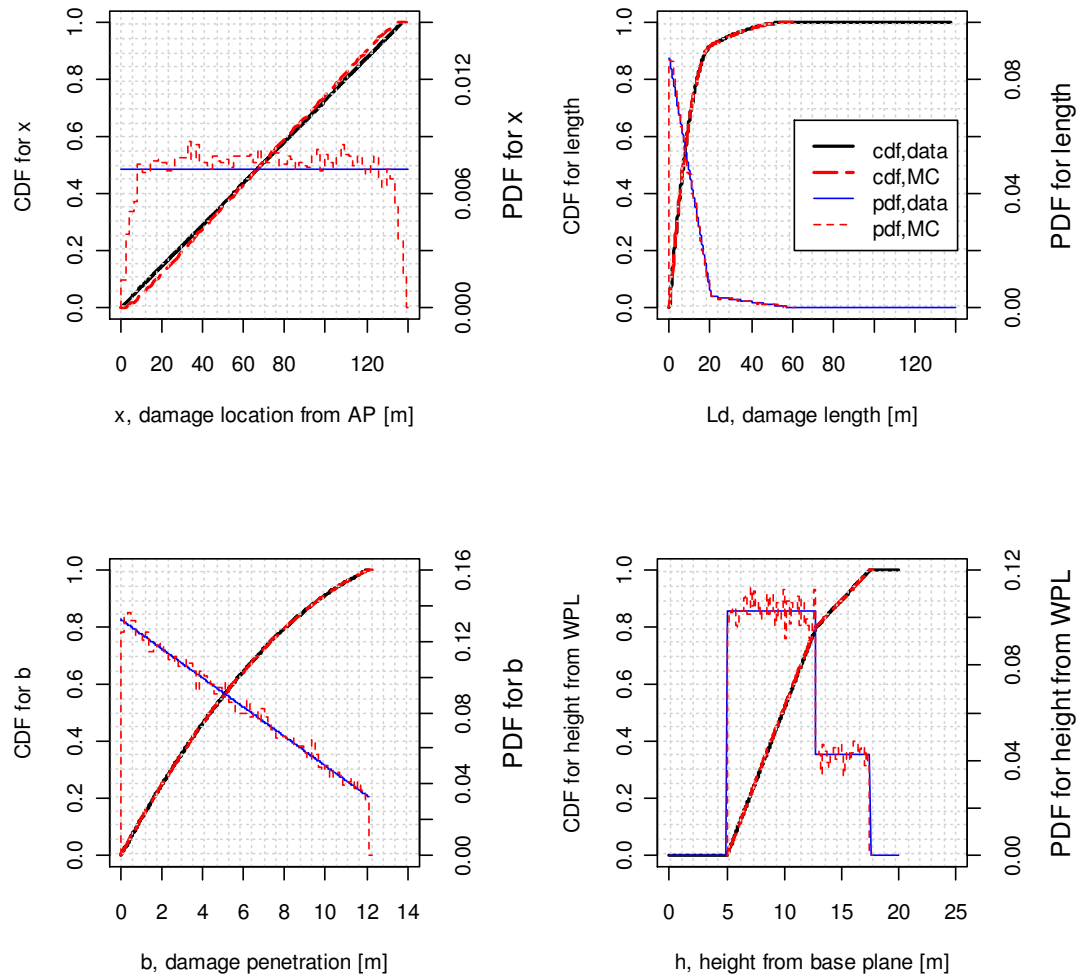

Figure 8.7: Probability Distributions for Damage Characteristics (25000 damages, $d_l = 5.0m$)

For each of the sampled damage cases, eight successive sea states conditions from 1.5 m to 5.0 m, with an interval of 0.5 m have been examined through the time-domain numerical simulations.

8.4 Casualty-Based Dataset Selection

In line with the detected flooding extent caused by the port side collision as shown in Figure 8.3, for the 25,000 damage scenarios of each loading condition, the pertinent damage cases can be filtered to reflect the actual damage condition based on a list of criteria as indicated in Table 7.2. The damage characteristics act the primary filter to limit the location and the length of the damage simultaneously. In this study, the

lower and upper bounds for both parameters are defined as below, where $X_d.ratio = 0.4$ and $L_d.ratio = 0.1$, in order to comply with the range of the measured two-zone damage.

$$X_{d\ lower\_bound} = X_d - L_d/2 \times X_d.ratio,\ \ X_d = -27.7m$$
$$X_{d\ upper\_bound} = X_d + L_d/2 \times X_d.ratio,\ \ L_d = 22.4m$$
$$L_{d\ lower\_bound} = 1$$
$$L_{d\ upper\_bound} = L_d \times (1 + L_d.ratio)$$

As a result, the related damage cases can be selected from the three different loading conditions by applying the same filter criteria. The damage distributions are depicted from Figure 8.8 to Figure 8.10, where 550 MC-based damages at the lightship condition (DL) satisfy the identified bounds. Likewise, 538 and 585 MC-based damages are filtered at the partially loaded (DP) and the fully loaded conditions (DS) separately. The results of numerical simulations are summarized from Table 8.3 to Table 8.5. Accordingly, the input information about the sampled damages and the corresponding output through P3 numerical simulations should be assembled to compose a new casualty-based dataset. In total, there are 40,152 damage cases stored (i.e., $(550 + 538 + 585) \times 3 \times 8$) for the subsequent model estimation.

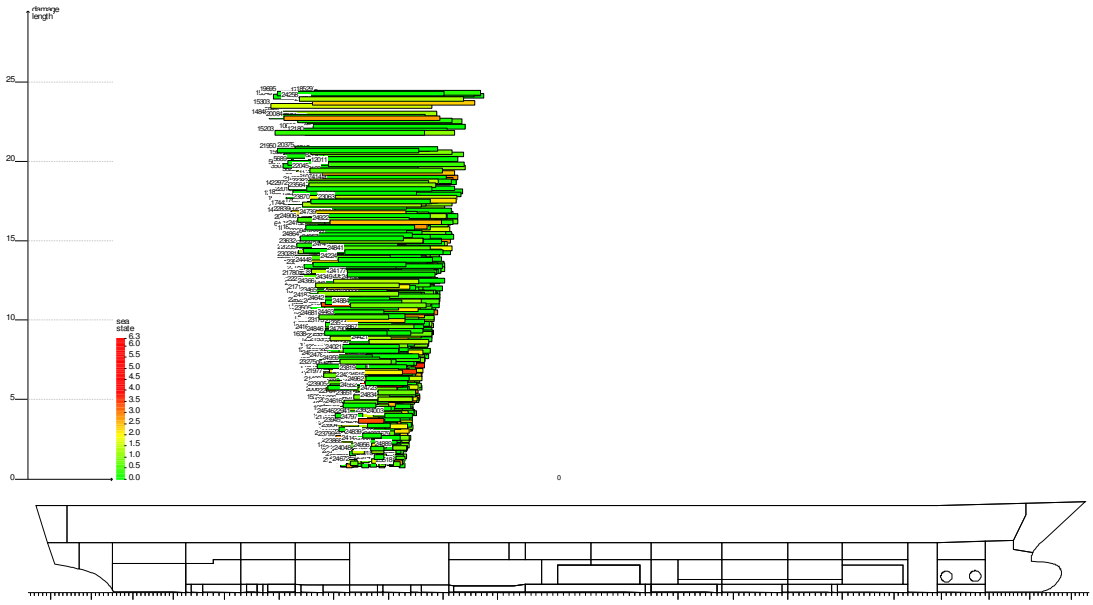

Figure 8.8: The Selected 550 out of 25000 MC Damages at DL

Table 8.3: Summary of Numerical Simulations at DL

Hs [m]	No. of Runs	KG = 9.557 [m]		KG = 10.11 [m]		KG = 10.64 [m]	
		No. of Capsize	Probability of Capsize Pf(t=30min|Hs)	No. of Capsize	Pf (t=30min|Hs)	No. of Capsize	Pf (t=30min|Hs)
1.5	550	0	0	0	0	0	0
2.0	550	0	0	0	0	0	0
2.5	550	11	0.020	54	0.098	118	0.215
3.0	550	178	0.324	226	0.411	294	0.535
3.5	550	181	0.329	227	0.413	319	0.580
4.0	550	177	0.322	238	0.433	325	0.591
4.5	550	197	0.358	239	0.435	330	0.600
5.0	550	208	0.378	244	0.444	328	0.596

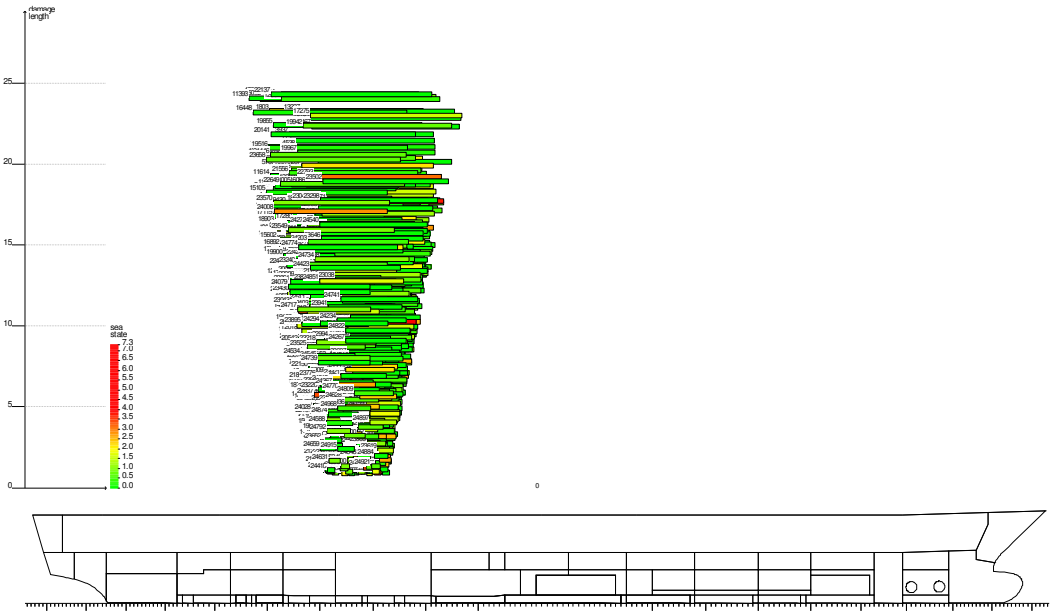

Figure 8.9: The Selected 538 out of 25000 MC Damages at DP

Table 8.4: Summary of Numerical Simulations at DP

Hs [m]	No. of Runs	KG = 9.557 [m]		KG = 10.11 [m]		KG = 10.64 [m]	
		No. of Capsize	Probability of Capsize Pf(t=30min|Hs)	No. of Capsize	Pf (t=30min|Hs)	No. of Capsize	Pf (t=30min|Hs)
1.5	538	0	0	0	0	0	0
2.0	538	0	0	0	0	0	0
2.5	538	48	0.089	118	0.219	157	0.292
3.0	538	235	0.437	282	0.524	363	0.675
3.5	538	234	0.435	293	0.545	397	0.738
4.0	538	229	0.426	286	0.532	400	0.743
4.5	538	243	0.452	299	0.556	412	0.766
5.0	538	251	0.467	290	0.539	397	0.738

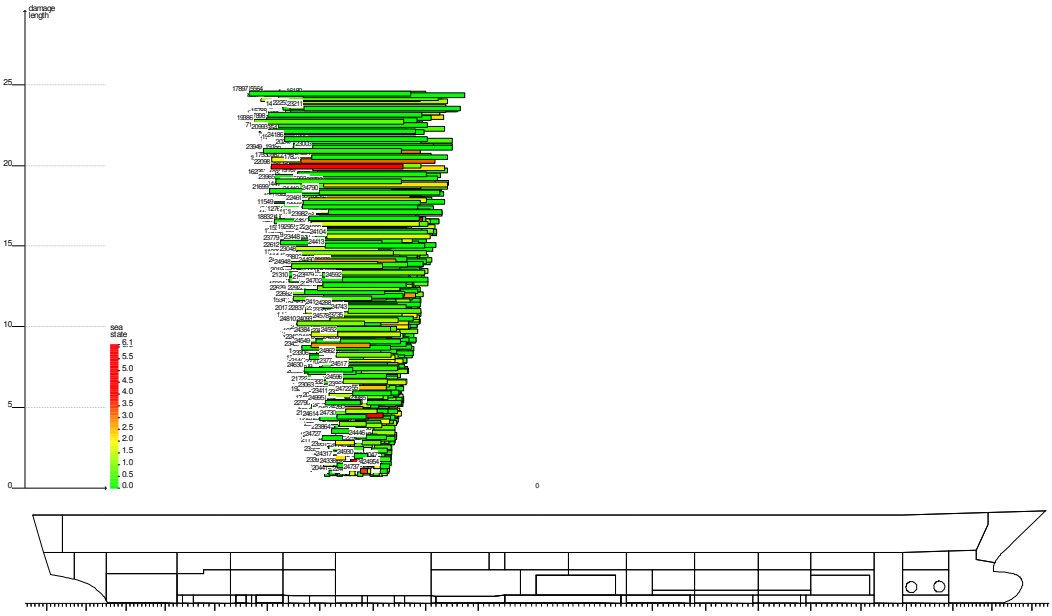

Figure 8.10: The Selected 585 out of 25000 MC Damages at DS

Table 8.5: Summary of Numerical Simulations at DS

Hs [m]	No. of Runs	KG = 9.557 [m]		KG = 10.11 [m]		KG = 10.64 [m]	
		No. of Capsize	Probability of Capsize Pf(t=30min|Hs)	No. of Capsize	Pf (t=30min|Hs)	No. of Capsize	Pf (t=30min|Hs)
1.5	585	0	0	0	0	0	0
2.0	585	0	0	0	0	39	0.067
2.5	585	127	0.217	158	0.270	274	0.468
3.0	585	320	0.547	359	0.614	497	0.850
3.5	585	319	0.545	362	0.619	513	0.877
4.0	585	319	0.545	367	0.627	524	0.896
4.5	585	334	0.571	376	0.643	534	0.913
5.0	585	340	0.581	377	0.644	530	0.906

8.5 Bayesian Computation for Casualty-Based Model Estimation

Similar to the procedures of model estimation based on the experimental data described in Section 6.3, there are three major steps deserving more attention, i) Casualty-based data collection derived from the numerical simulations, which reflects the inputs of the filtered damage cases and their related outputs representing the ship's behaviour (capsize or survive) after the hull breach events, ii) Casualty-

based model estimation founded on the selected simulation dataset and iii) Sensitivity analysis of model inputs to strive for model parsimony.

8.5.1 Casualty-Based Simulation Data Collection

It indicates that the variable L_d/L_s plays the most significant role in estimating the rate of ship stability loss in Section 6.3.3. However, the damage length (L_d) is insufficient to disclose the impact of the extent of flooding on the ship stability after damage entirely. In this way, joint information of the damage location (*xd*), length, penetration (*y*) and height (*z*) charactering the hull breach is applied to represent the extent of flooding. Accordingly, these parameters are considered as the influencing inputs for model training. In fact, the casualty-based predictive model allows examining the sensitivity of the model output $P(t_0, Y = cap|\boldsymbol{\beta}, \boldsymbol{X})$ to a group of rearranged input parameters (on behalf of damage condition) as given in Table 8.6.

The damage characteristics are defined non-dimensional. As illustrated in Figure 8.11, the damage location *xd* denotes the length from the stern to the midpoint of the damage opening in the longitudinal direction. The damage penetration *y* is measured from the centreline of the ship to the side where she suffered damage. The damage height *z* determines the vertical distance from the base line of the ship to the top of the damage, and the parameter *H* indicates the height up to the top of the car deck. In this study the hull is assumed watertight up to Deck 4 (i.e. *H* = 13.40 m above the base line).

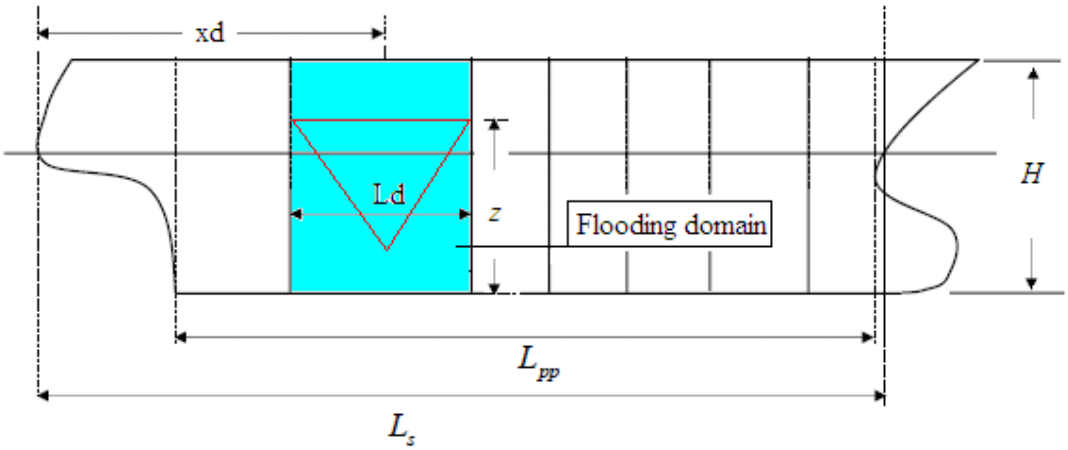

Figure 8.11: The Extent of Flooding as A Result of Damage

Table 8.6: A Summary of the Selected Dataset

Damage Case	No. of Runs	Tested Hs [m]	Intact Condition		Damage Condition				
			KG/KMT	T/D	Heel at EQ	Ld/Ls	xd/Ls	y/0.5B	z/H
DP/10.11	538/ Hs	1.5 ~ 5.0	0.872	0.685	See Figure 8.12				
DP/10.64	538/ Hs	1.5 ~ 5.0	0.917	0.685					
DS/10.11	585/ Hs	1.5 ~ 5.0	0.868	0.706					
DS/10.64	585/ Hs	1.5 ~ 5.0	0.914	0.706					

Based upon the casualty-related damages selected (40,152 cases) in Section 8.4 the secondary level of the case filter concerning the loading conditions (*T*, *KG*) is employed to further reduce the size of the dataset for fast and reliable model estimation. Interpolation is the underlying method of acquiring knowledge of the ship status after the actual hull breach event, which relies on information from the relevant damages stored in the casualty-based dataset. As for the RoPax ship at the intact loading condition, the mean draught is equal to 5.39 m and the *KG* is 10.62 m, in this respect, 4 loading conditions shown in Table 8.6 act as the boundaries for filtering data. So the size of the dataset is reduced to 17,968 cases ($(538 + 585) \times 2 \times 8$) presently.

$$T_{lower\_bound} = DP\ (5.24\ m) \leq T \leq T_{upper_{bound}} = DS\ (5.40\ m)$$

$$KG_{lower\_bound} = 10.11\ m \leq KG \leq KG_{upper\_bound} = 10.64m$$

The information of the selected damage dataset is depicted in Figure 8.12, where the angle of heel at EQ to each of the hull damages is achieved through hydrostatic computations. The non-dimensional damage characteristics stem from the features of MC-based samplings.

Hs	Capsize	KG/KMT	T/D	Heel	Ld/Ls	xd/Ls	y/0.5B	Z/H
1.5	0	0.868184	0.705882	0.374	0.082167	0.326935	0.098061	0.456126
1.5	0	0.868184	0.705882	0.533	0.085489	0.326863	0.966649	0.834265
1.5	0	0.868184	0.705882	0.601	0.081565	0.295008	0.096291	0.856138
1.5	0	0.868184	0.705882	1.459	0.115407	0.316735	0.653236	0.779551
1.5	0	0.868184	0.705882	0.279	0.086645	0.325354	0.301164	1
1.5	0	0.868184	0.705882	2.076	0.116963	0.280622	0.645096	0.818033
1.5	0	0.868184	0.705882	2.416	0.139489	0.335511	0.36856	0.632061
1.5	0	0.868184	0.705882	1.512	0.105823	0.273434	0.195431	0.852896
1.5	0	0.868184	0.705882	0.279	0.082238	0.325184	0.31926	1
1.5	0	0.868184	0.705882	1.459	0.089478	0.299636	0.633516	0.975649
1.5	0	0.868184	0.705882	1.945	0.139088	0.263497	0.189345	0.492632
1.5	0	0.868184	0.705882	1.367	0.089271	0.31321	0.502704	0.762008
1.5	0	0.868184	0.705882	1.764	0.088458	0.258073	0.08241	0.734518
1.5	0	0.868184	0.705882	0.993	0.099151	0.319497	0.125017	0.616339
1.5	0	0.868184	0.705882	1.895	0.085656	0.277421	0.95774	0.814858
1.5	0	0.868184	0.705882	1.99	0.082254	0.290793	0.566646	0.444712
1.5	0	0.868184	0.705882	0.878	0.09111	0.305598	0.14144	0.715998
1.5	0	0.868184	0.705882	0.374	0.086686	0.332386	0.271146	0.863421

Figure 8.12: A Snapshot of the Selected Dataset

8.5.2 Model Estimation based on Simulation Dataset

In the same way as explained in Section 6.3.2, eight input variables including ($H_s, KG/KMT, T/D,$ heel at EQ, $L_d/L_s, xd/L_s, y/0.5B, z/H$) are used to accomplish model estimation. Again, both the Gibbs sampler and the Metropolis sampler are employed to approximate the posterior probability distribution $P(\boldsymbol{\beta}|\boldsymbol{Z}, \boldsymbol{X}, \mathbf{y})$ of the nine model coefficients.

The primary task is to check the chain convergence of the two MCMC samplers. For the outcomes of the Gibbs sampler, after sampling every 100^{th} observation as demonstrated in Figure 8.13, the chain autocorrelation functions (ACF) for the estimations of $\boldsymbol{\beta}$ at lag 10 indicate that the ACF to each coefficient at lag one is under 0.4. On the other hand, for the Metropolis sampler, the acceptance rate is 23.1%. The above findings disclose that the chains have converged. It is available to produce the posterior probability distributions of model coefficients as depicted in Figure 8.14 and meanwhile to summarize the simulated values for each of them as tabulated in Table 8.7.

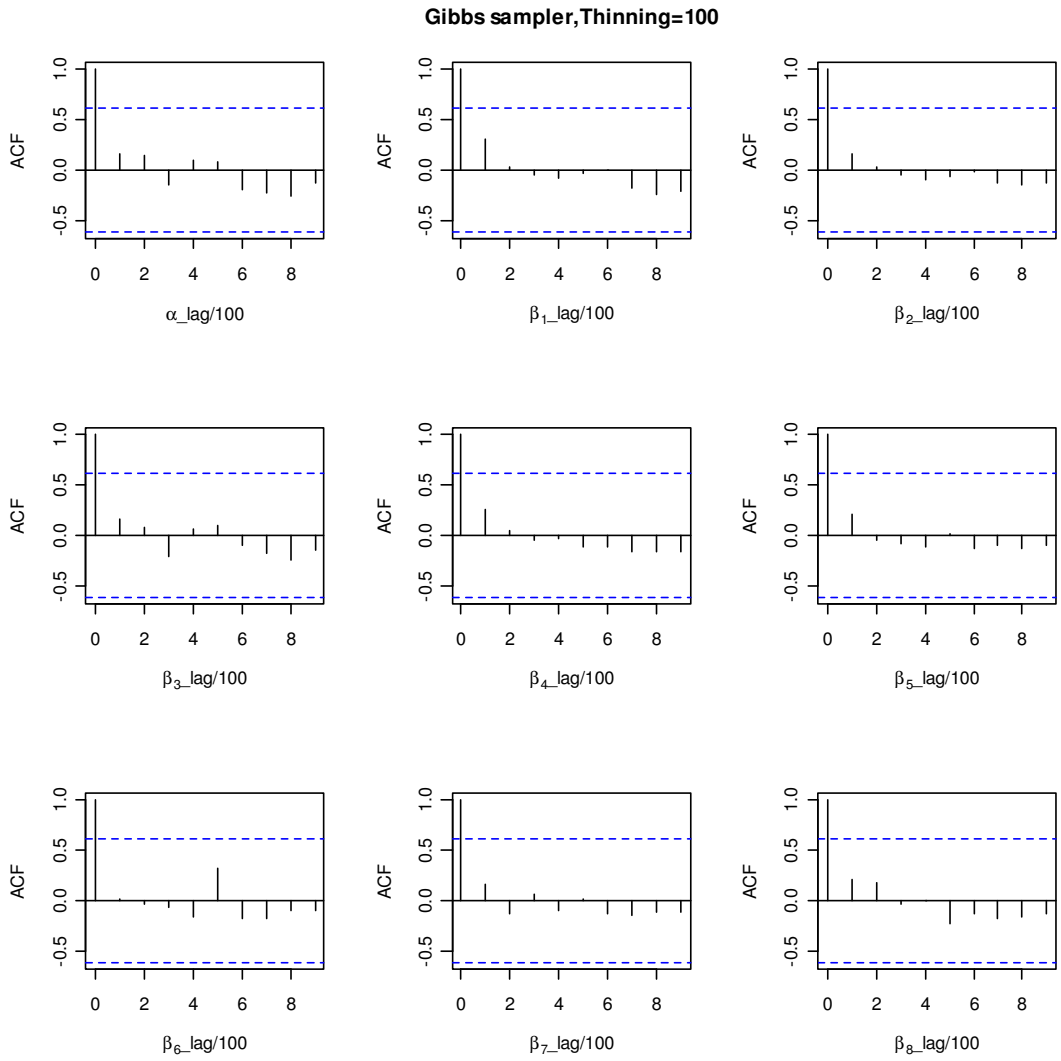

Figure 8.13: Plots of ACF for Model Coefficients_ 9 Variables

Table 8.7: Summary of Markov Chain Samples of Model Coefficients_9 Variables

	Mean		SD		0.5% quantile		99.5% quantile	
Var.	Gibbs	Metro.	Gibbs	Metro.	Gibbs	Metro.	Gibbs	Metro.
α	-35.8233	-36.1398	0.8125	0.6591	-37.946	-38.1504	-32.9812	-34.1466
β_1	0.7898	0.7997	0.0194	0.0121	0.71	0.7647	0.8333	0.8379
β_2	5.7936	5.5345	0.6524	0.3663	4.552	4.2032	9.1269	6.778
β_3	27.0378	27.5105	1.0754	0.6082	21.9641	25.7119	29.2125	29.3075
β_4	1.3977	1.4558	0.1106	0.0243	0.841	1.3883	1.4826	1.5491
β_5	6.8201	6.3405	1.106	0.4836	5.223	4.8536	12.7145	7.7891
β_6	0.2159	0.2913	0.509	0.4748	-1.4647	-1.094	1.7339	1.8196
β_7	-0.0249	-0.0557	0.0853	0.0457	-0.1807	-0.181	0.3866	0.0825
β_8	5.9691	6.0888	0.2221	0.0967	4.9517	5.7785	6.3051	6.3571

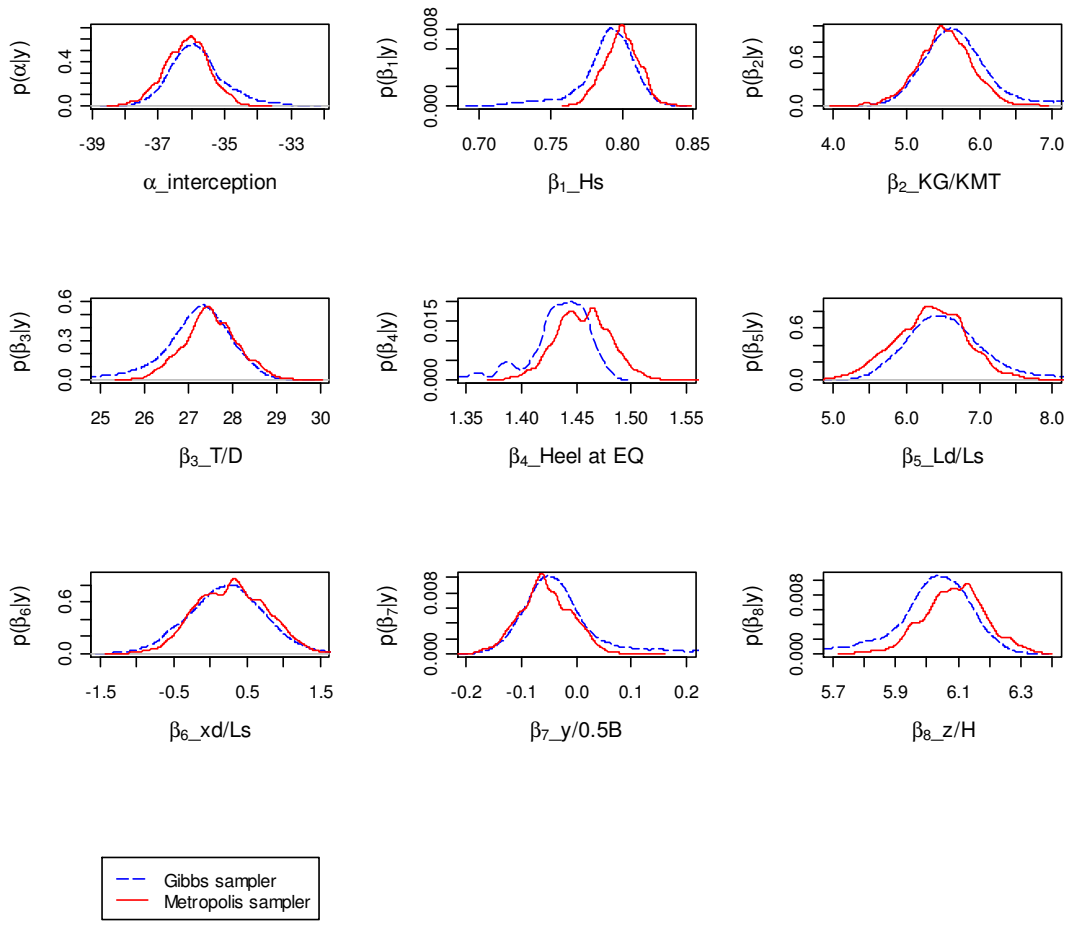

Figure 8.14: MCMC Approximations to Posterior Distributions of Model Coefficients_9 Variables

Deriving from Figure 8.14, it is notable that six input variables (expect β_6 for the damage location and β_7 for the damage penetration) have relatively more influence on damage ship survivability as the 99% quantile-based posterior intervals of $\boldsymbol{\beta}$ are away from zero. The estimated magnitudes of $\boldsymbol{\beta}$ are positive, which shows that the increase in the value of each input parameter will likely increase the rate of ship capsizing within given time after flooding.

In contrast to the above observation, the variations in coefficients β_6 and β_7 include zero. It indicates that the model output is not so sensitive to parameters xd/L_s and $y/0.5B$. Such finding should be attributed to the casualty-based damages selected in the dataset, since the variations of damage location have been defined within a limited range to reflect the actual hull damage. Similarly the parameter of

damage penetration is the other less significant model input at this time. Both of them are to be removed in the model for developing a new relationship.

8.5.3 Sensitivity Analysis of Model Inputs

The simulated model coefficient is perceived as the sensitivity indicator, so a quick assessment of the significance of each input variable on the rate of ship capsizing is available. As mentioned above, because the parameters of damage location and penetration have minor impact on the model outcome than others, it is necessary to update the model by excluding both variables. The major steps for model estimation need to be repeated. Figure 8.15 indicates that the chain converges by applying the Gibbs sampler. Also the Metropolis acceptance rate is 22.48% which meets the requirement.

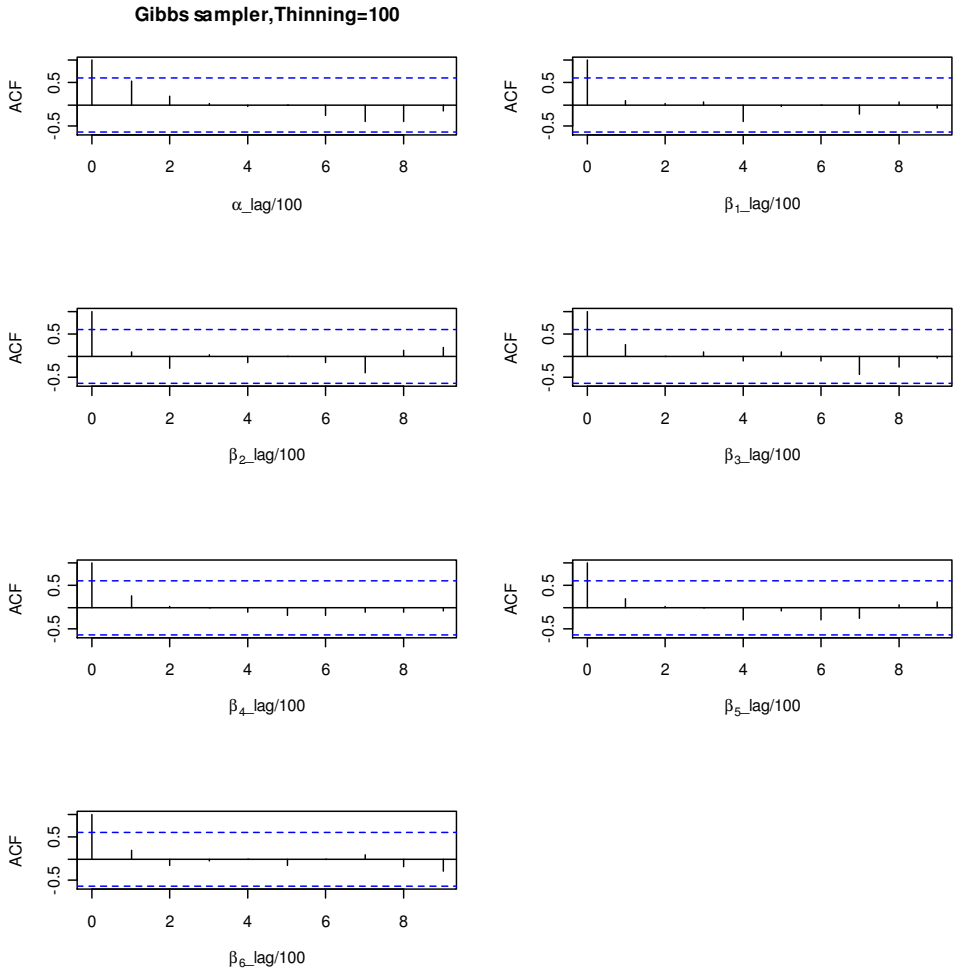

Figure 8.15: Plots of ACF for Model Coefficients_7 Variables

The revised range of variation in each of the remaining coefficients $\boldsymbol{\beta}$ is outlined in Figure 8.16. A parallel summary of the simulated results is tabulated in Table 8.8.

Table 8.8: Summary of Markov Chain Samples of Model Coefficients

	Mean		SD		0.5% quantile		99.5% quantile	
Var.	Gibbs	Metro.	Gibbs	Metro.	Gibbs	Metro.	Gibbs	Metro.
α	-38.0848	-38.2744	1.6594	1.3636	-42.5376	-42.3496	-31.803	-34.0058
β_1	0.8559	0.8591	0.0228	0.0164	0.7677	0.8088	0.9119	0.9085
β_2	11.1441	11.1056	0.8037	0.7316	8.7083	8.8715	13.7076	13.2616
β_3	23.9809	24.1971	1.9387	1.6132	16.6455	19.4252	29.234	29.3722
β_4	1.2741	1.3006	0.0931	0.0301	0.8147	1.1952	1.3712	1.407
β_5	4.159	3.8933	1.0441	0.6615	1.7377	1.9024	8.6251	6.1469
β_6	5.9658	6.0062	0.2349	0.1279	4.9423	5.5903	6.3932	6.3877

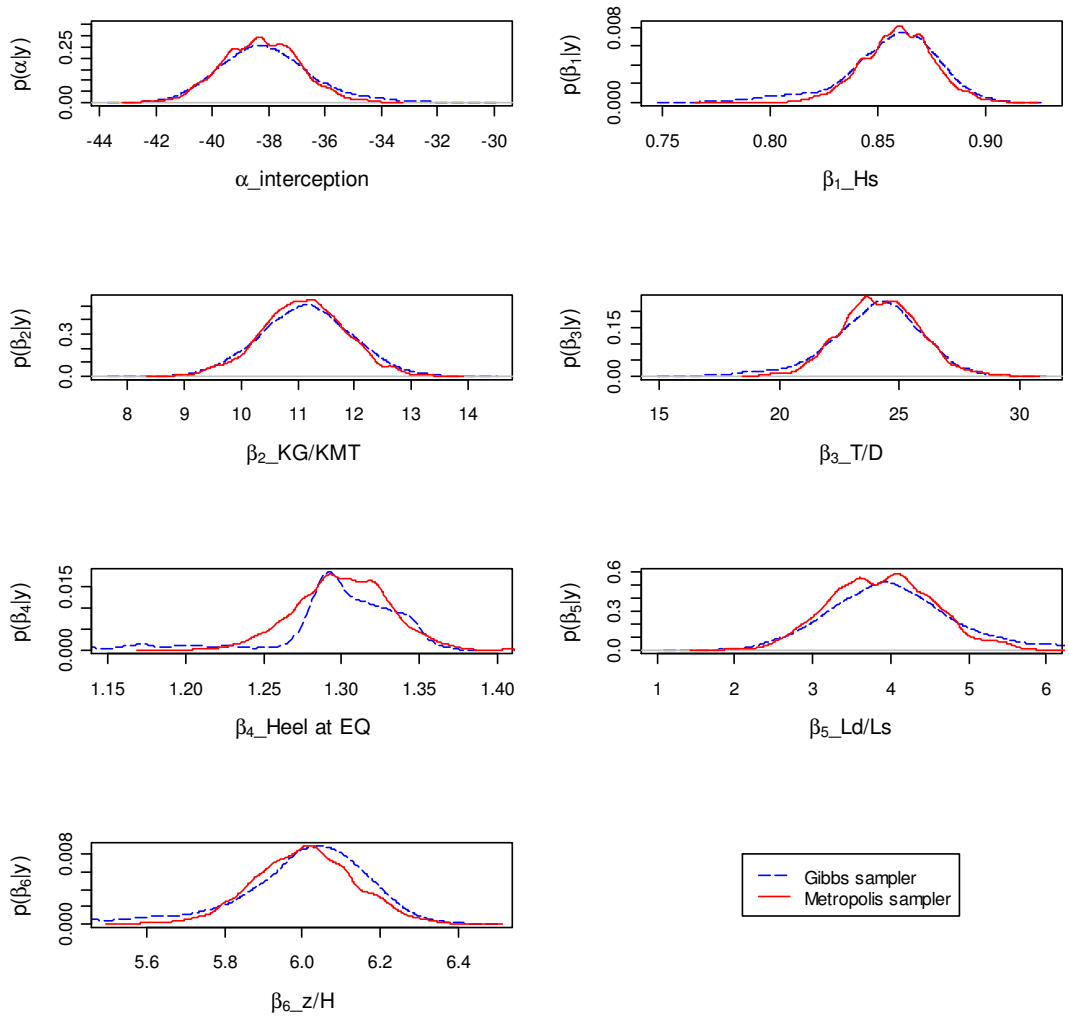

Figure 8.16: MCMC Approximations to Posterior Distributions of Model Coefficients_7 Variables

By comparing the posterior distributions of $\boldsymbol{\beta}$ as illustrated in Figure 8.16 with that in Figure 8.14, it can be concluded that the impact of excluding two variables (damage location, and damage penetration) on the model output is negligible since the features of the remaining $\boldsymbol{\beta}$ are retained. It suggests again that both of the variables should not be considered for model training at present. On the basis of the results shown in Table 8.8, the two Markov chain samplers provide similar approximations to model coefficients. In this case, the casualty-based model estimated through the Metropolis sampler is identified as the one to be further discussed.

$$P(t_0, Y = cap \mid \boldsymbol{\beta}, \boldsymbol{X}) = \Phi(-38.27 + 0.86H_s + 11.11\frac{KG}{KMT} + 24.20\frac{T}{D} + 1.3Heel + 3.89\frac{L_d}{L_s} + 6.01\frac{z}{H}) \quad (37)$$

8.6 Casualty-Based Model Application in Shipboard Decision Support

Evaluation of ship's residual stability is an important response action in the event of an incident. In accordance with the proposed shipboard decision support framework in Figure 7.5, the prediction module is identified as the essential module for casualty-based model estimation. Once it is ready as given in Equation 37, a fast projection of damage ship survivability to an evolving flooding crisis will be anticipated. Meanwhile, a quantitative measure of inherent uncertainties associated with the prediction can be addressed.

Focusing on the specified hull damage caused by a port-side collision, the rate of ship capsizing can be computed after the relevant information of current situation is known. As depicted in Figure 8.17, the ship vulnerability to flooding within 30 minutes as well as the 99% uncertainty bounds is appraised, when the value of input parameters are given $\boldsymbol{X}$ = (H_s, 0.9008, 0.7046, 1.95deg, 0.0518, 1).

In addition, the Equation (34) is used for assigning of probability of capsizing within given period of time t_{cap}, about a specific flooding case. Based on this relationship, a formulation to quantify the time within which the capsizing may be expected to occur with the given probability $F_{t_{cap}}$ can now be derived as Equation (38). In this

way, because the rate of capsizing p_f is worked out from the established model $P(t_0, Y = cap \mid \boldsymbol{\beta}, \boldsymbol{X} = Hs, \frac{KG}{KMT}, \frac{T}{D}, Heel, \frac{L_d}{L_s}, \frac{z}{H})$, the range of variation in time t_{cap} from the level of $F_{t_{cap}} = 0.01$ to $F_{t_{cap}} = 0.99$ can also be estimated at each of the considered sea condition of H_s. As can be seen in Figure 8.17, there is 99% confidence that $t_{cap} > 135$ s when $H_s = 2\ m$, and $t_{cap} < 1689$ s when $H_s = 4\ m$.

$$t_{cap} = t_0 \cdot \frac{\ln\left(1 - F_{t_{cap}}\right)}{\ln\left(1 - p_f\right)} \tag{38}$$

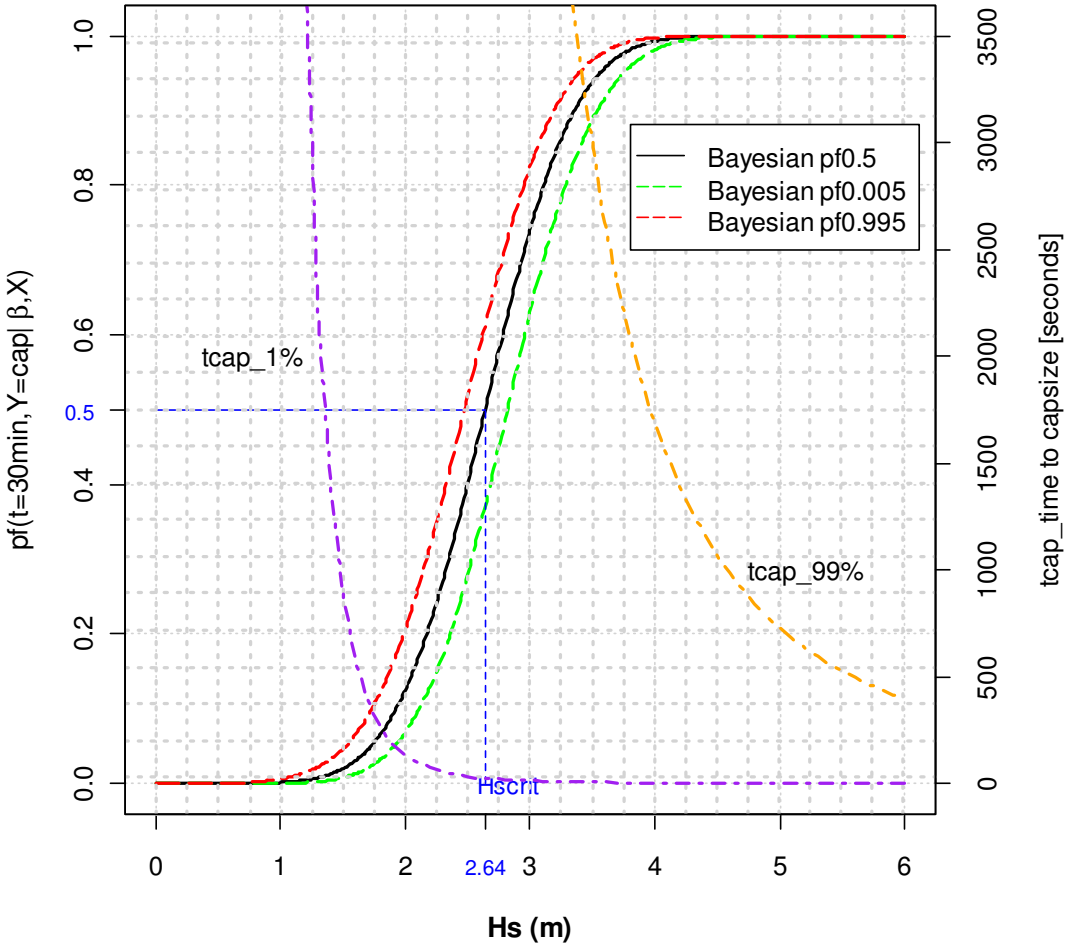

Figure 8.17: 1) The Rate of Ship Capsizing within $t_{cap} = 30\ min$ for the Specified Hull Damage, at the Given Sea Conditions of H_s. 2) The Time to Capsize t_{cap} with the Given Levels of Probability $F_{t_{cap}}$

As elucidated in Section 7.5.4.1, the projected probability of time to capsize $F(t_{cap}|H_s)$ with given sea condition is intended to be transformed into a qualitative measure of criticality index for supporting decision making. According to the 99% estimates of $F_{t_{cap}}$ with a range of H_s (1.5 m, 2 m, 3 m) within 3 hours, the corresponding severity level (either returning to port under its own power or requiring immediate abandonment) is demonstrated in Figure 8.18. In short, for the given flooding case, the decision should be to abandon ship if she is operating in the sea state $H_s \geq 1.59\ m$ (i.e. where CI is not less than the defined boundary).

$$CI = 1 - 0.9 \cdot \left(1 - \frac{5000}{137.4 + 2.5 \times 2110 + 15225}\right) = 0.32$$

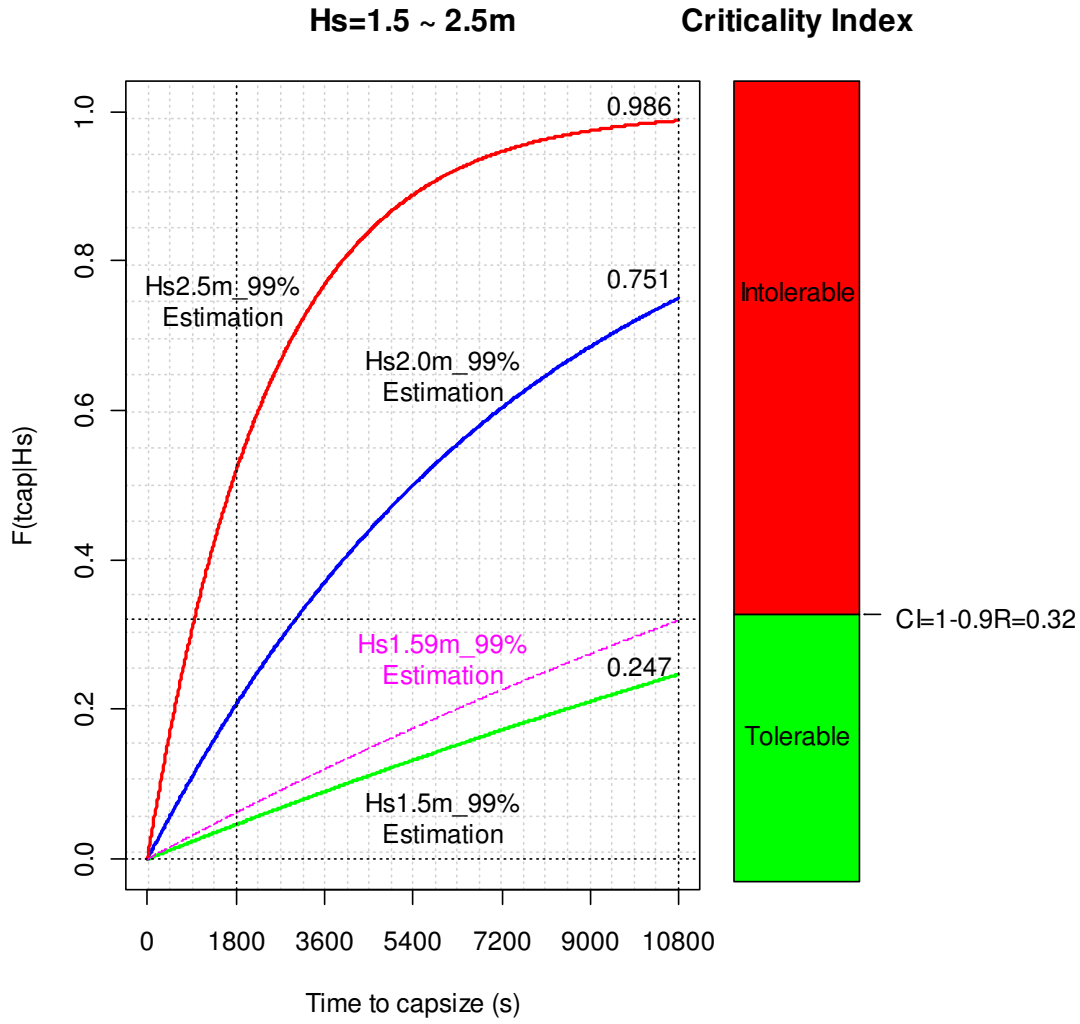

Figure 8.18: The 99% Estimates of $F(t_{cap}|H_s)$ with the Related Criticality Index

8.7 Casualty-Based Model Validation

Validation study on the time to capsize is mainly discussed in this section. Attempting to provide sufficient data for characterising the random nature of the capsize occurrence, a series of different approaches in assessment of damage ship survivability have been undertaken. They are based on of i) casualty-based physical model experiments, ii) casualty-based numerical simulations and iii) Monte Carlo-based numerical simulations.

8.7.1 Physical Model Experiments

A set of physical model experiments aiming at characterising the stochastic process of the time takes a ship to capsize after the specified hull breach event has been carried out at SSPA Sweden AB (http://www.sspa.se/) in the Marine Dynamic Laboratory. A model of the RoPax ship in scale 1:40 was used, and a two compartment damage on the port side was modelled, as shown in Figure 8.19 (Rask, 2010). All the tests were performed in accordance with (EC, 2003), the modelled damage opening fulfilled a set of damage characteristics as specified in (39) to reflect the actual flooding extent.

Damage Location:	$xd = bulkhead\_position$	
Damage Length:	$L_d = 0.03L + 3\,m$	
Damage Penetration:	$y = B/5$	
Damage Height:	$z = \infty$	(39)

The key objective of such dedicated tests is i) to identify the boundary of sea states that specifying the variation of rate of capsizing (p_f) spreads from 0 to 1, as summarised in Table 6.1, ii) to quantify the time to capsize t_{cap} for each test run, further details are available in Appendix 4. Ultimately, the derived benchmark data can be deployed in a validation of the casualty-based model.

The survivability tests were completed in beam sea condition and free drifting of the model was allowed. A range of sea states H_s between 2 m and 3 m were measured. Each of which was represented by 20 different time realizations. A total of 83

experiments were performed. The correlated hydrostatics and stability information is given in Table 8.9.

Figure 8.19: A Hull Breach According to (39), Picture by SSPA

Table 8.9: Hydrostatics and Stability Information

Given Hull Breach	Intact Condition				Damage Stability		
	Permeability	Draught	Trim	KG	GZrange	GZmax	Heel
	0.95	5.39 m	0.435 aft	10.62 m	8.7 deg	0.078 m	2.3 deg to port

8.7.2 Numerical Simulation with Fixed Damage Size

Concerning the very limited information is provided by the physical model tests, a set of further studies on the time to capsize based on numerical simulations have been undertaken. This part puts particular emphasis on the flooding condition with a

fixed damage length including transient phase, for modelling the same situation of the experiments to reflect the specified hull damage, as shown in Figure 8.20 and Figure 8.22. The stability curves for the RoPax ship at the intact and damage conditions are illustrated in Figure 8.21.

The survivability was tested for approximately nine successive sea states, again, each one repeated 20 times, so that a clear distinction between capsize and survival cases could be derived. In total, 180 runs of simulation were performed and Table 8.10 presents the statistical summary of the outcomes. The data of time to capsize is tabulated in Appendix 4.

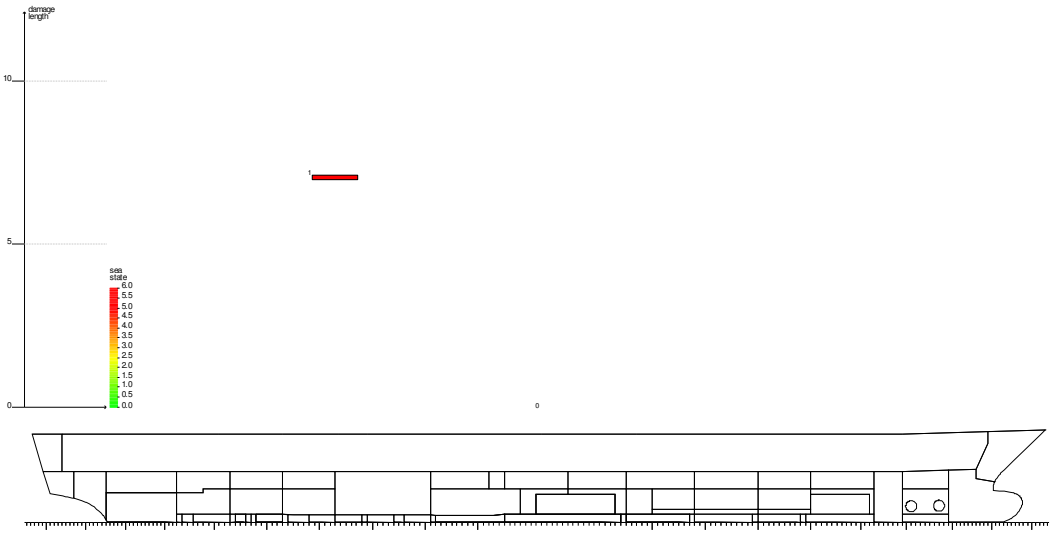

Figure 8.20: A Single Hull Breach Leading to the Same Flooding Extent of the Specified Hull Damage on the RoPax Ship

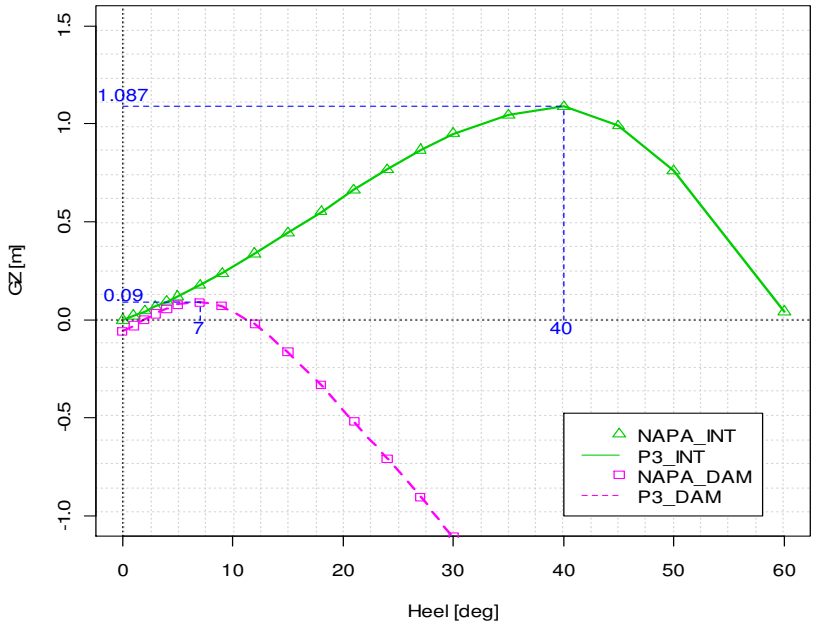

Figure 8.21: Stability Characteristics for Intact Ship and Damaged Conditions

Table 8.10: Summary of PROTEUS3 Simulations with Fixed Damage Size

Hs [m]	No. of Capsize	No. of Runs	Pf=F_{tcap} (t=30min|Hs)
2.0	0	20	0
2.1	1	20	0.05
2.2	5	20	0.25
2.3	7	20	0.35
2.4	9	20	0.45
2.5	17	20	0.85
2.75	20	20	1
3	20	20	1
3.25	20	20	1

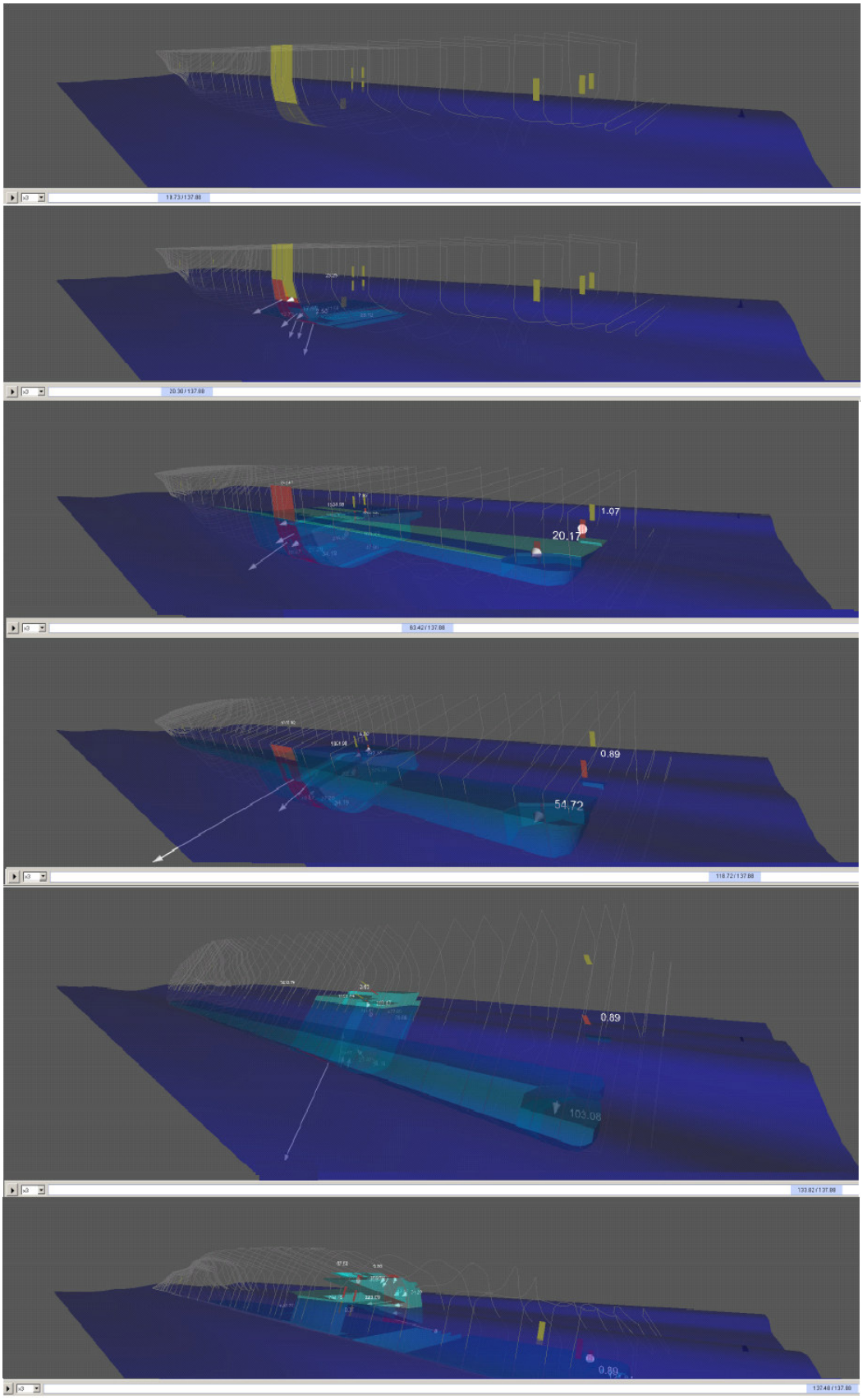

Figure 8.22: Visualization of PROTEUS3 Simulations with a Fixed Damage Size

8.7.3 Numerical Simulation with MC-Based Damages

Other than the condition of fixed damage width, a numerical simulation based on MC sampling as shown in Figure 8.23, has been used to generate a set of 500 random damages to reflect the same flooding extent of the identified hull breach. Transient flooding is considered and Table 8.11 summarises the details of the tested case. The information of time to capsize is outlined in Appendix 4.

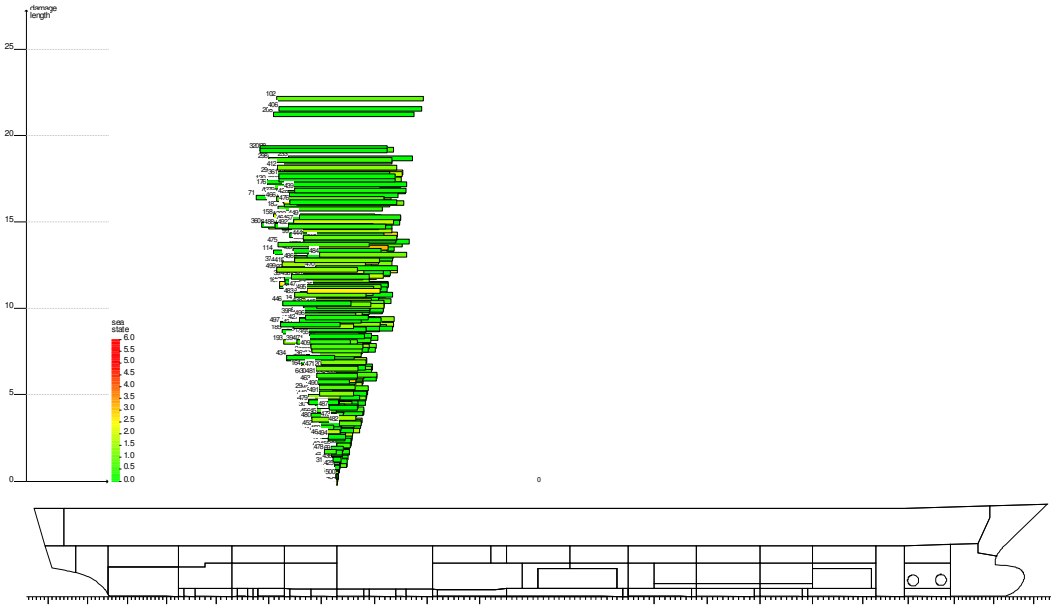

Figure 8.23: A Set of 500 Hull Breaches Leading to the Same Flooding Extent of the Specified Hull Damage on the RoPax Ship

Table 8.11: Summary of PROTEUS3 Simulations with 500 Random Damages

Hs [m]	No. of Capsize	No. of Runs	Pf=F_{tcap} (t=30min|Hs)
1.5	0	500	0
2.0	34	500	0.068
2.5	235	500	0.47
3.0	363	500	0.726
3.5	391	500	0.782
4.0	404	500	0.808
4.5	407	500	0.814
5.0	391	500	0.782
5.5	390	500	0.78
6.0	396	500	0.792

8.7.4 Results Comparison

For the given hull breach, based on the data derived from physical model tests and numerical simulations, the resultant distributions of rate of capsizing (p_f) for a range of sea states are shown in Figure 8.24. Meanwhile, the result from the casualty-based model is also plotted, that is presented by the upper bound of a 99% confidence interval for $P(t = 30min, Y = cap|\boldsymbol{\beta}, \boldsymbol{X})$, with $Hs_{crit} = 2.47\ m$.

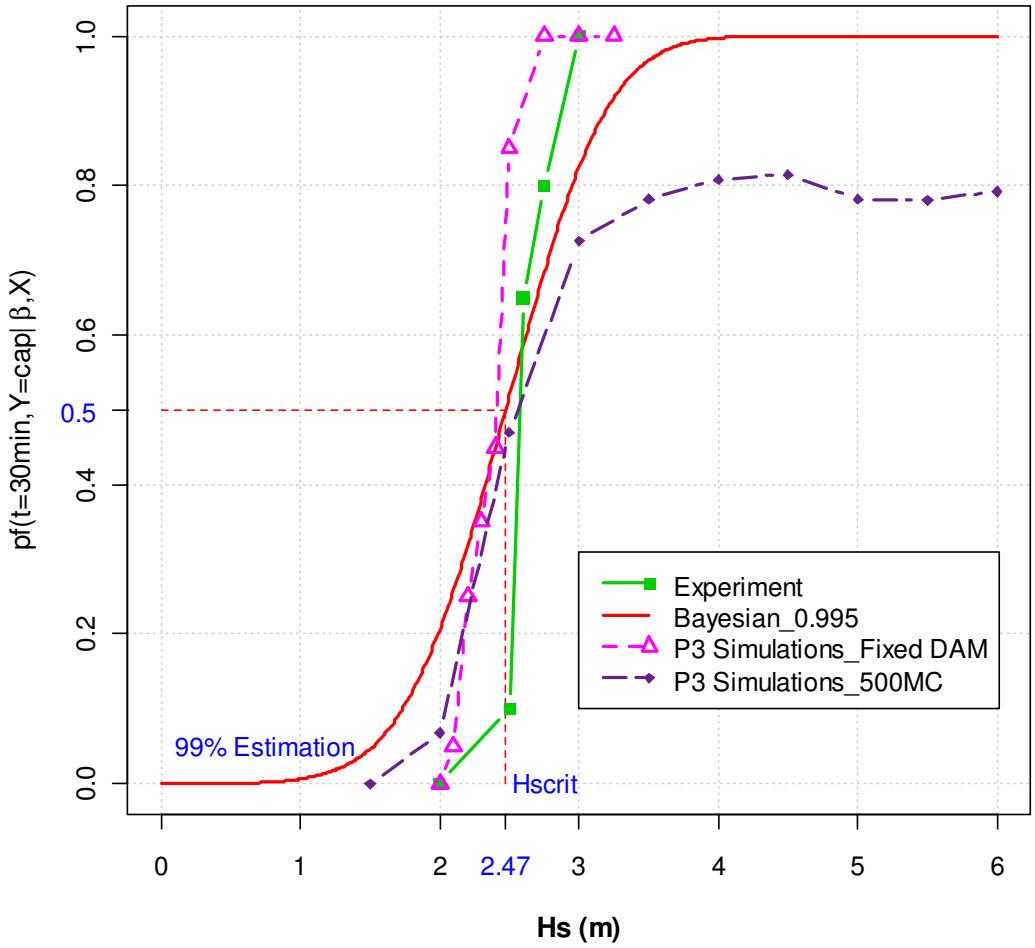

Figure 8.24: Comparison of the Rate of Capsizing within 30 minutes for the Given Flooding Case

Firstly, comparing the data derived from the physical experiments with the numerical simulations, regarding the particular hull breach, it seems that the results from both approaches are comparable, although the numerical estimates are somewhat conservative. The observed difference could be explained as the transient flooding

has not been taken into account during the tank testing. The tests start from an equilibrium stage when the damaged compartments have been flooded. In contrast, the numerical simulations are able to model the ship behaviour from the transient stage in the event of flooding. Even so, the tank testing and the numerical simulation can be used for decision making in case of a known flooding extent even though the exact hull breach leading to this flooding is unclear.

Secondly, comparing the results achieved between the two conditions of numerical simulation, it is obvious that the approximation from the simulations with the fixed damage extent is more conservative than that with random damage extents, as the probability to capsize in 30 minutes reaches 100% for the sea state of $Hs = 2.75\ m$, whereas according to the MC-based numerical estimates, it reaches 81% for the sea state of $Hs = 4.5\ m$, and then it starts decreasing for sea states higher than 4.5 m.

In principle, a set of 500 MC-based hull breaches depicted in Figure 8.23 should lead to the same flooding extent as the one resulted from the fixed damage. However, the observed decreasing trend of p_f may be explained by the resulting ability for water to accumulate for smaller openings. Namely, MC-based numerical estimates can be regarded as an averaged vulnerability for various extents of damage.

Thirdly, comparing the Bayesian estimates with the results from numerical simulations, as can be seen that the ship survivability (or vulnerability) predicted by the casualty-based model is somewhere between the two conditions of numerical estimates. Such phenomenon is rational as the derived model is established according to the simulation database prepared in the pre-casualty phase, which contains numerous data derived from MC-based numerical simulation. The particular feature of the applied dataset for model training is that some criteria have been adopted to filter the damage cases to reflect the actual hull breach.

In addition, based on the data of time to capsize summarised in Appendix 4, the sea state of $Hs = 2.5\ m$ where the Bayesian estimate of $p_f = 0.52$ within 30 minutes has been selected to demonstrate the cumulative probability distributions for time to capsize with the given flooding extent, as shown in Figure 8.25.

(a) Physical Tests_Hs=2.5m

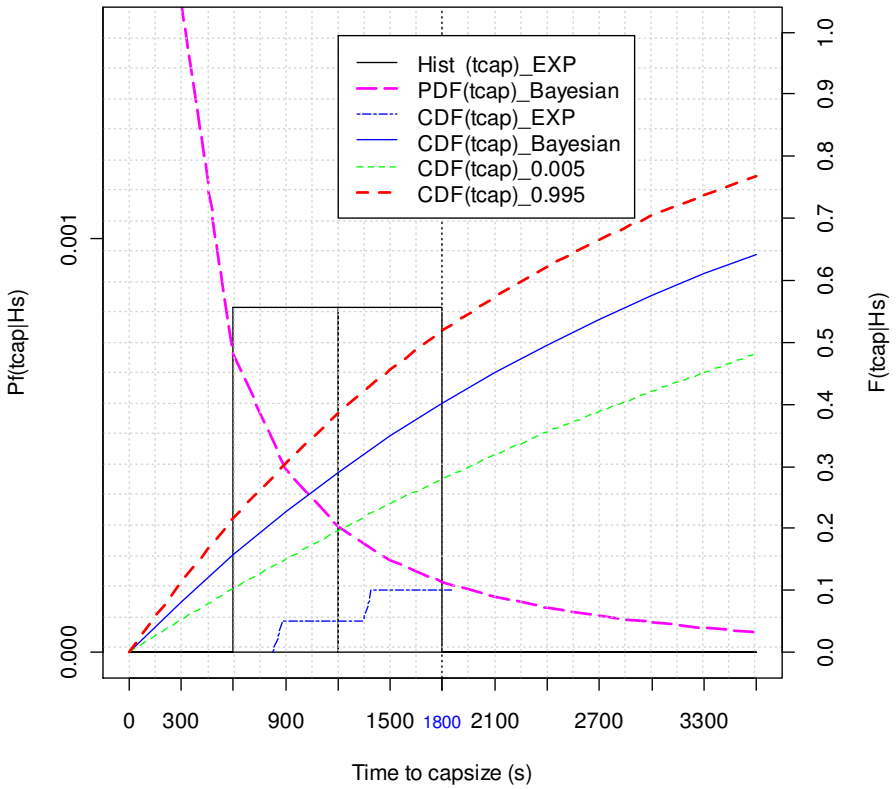

(b) P3 Simulations(Fixed DAM)_Hs=2.5m

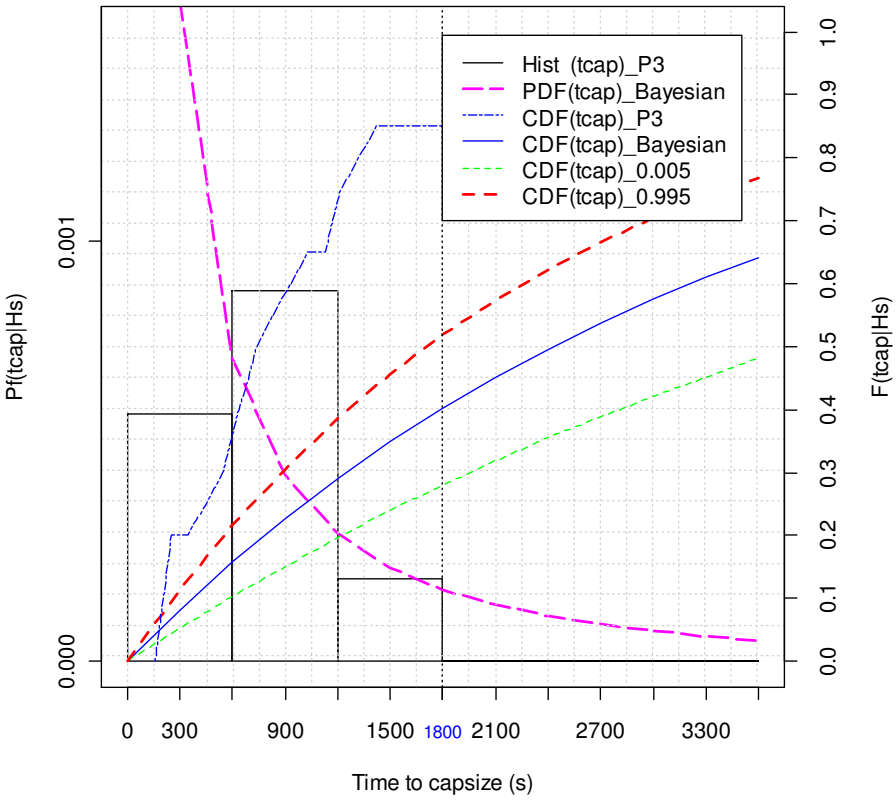

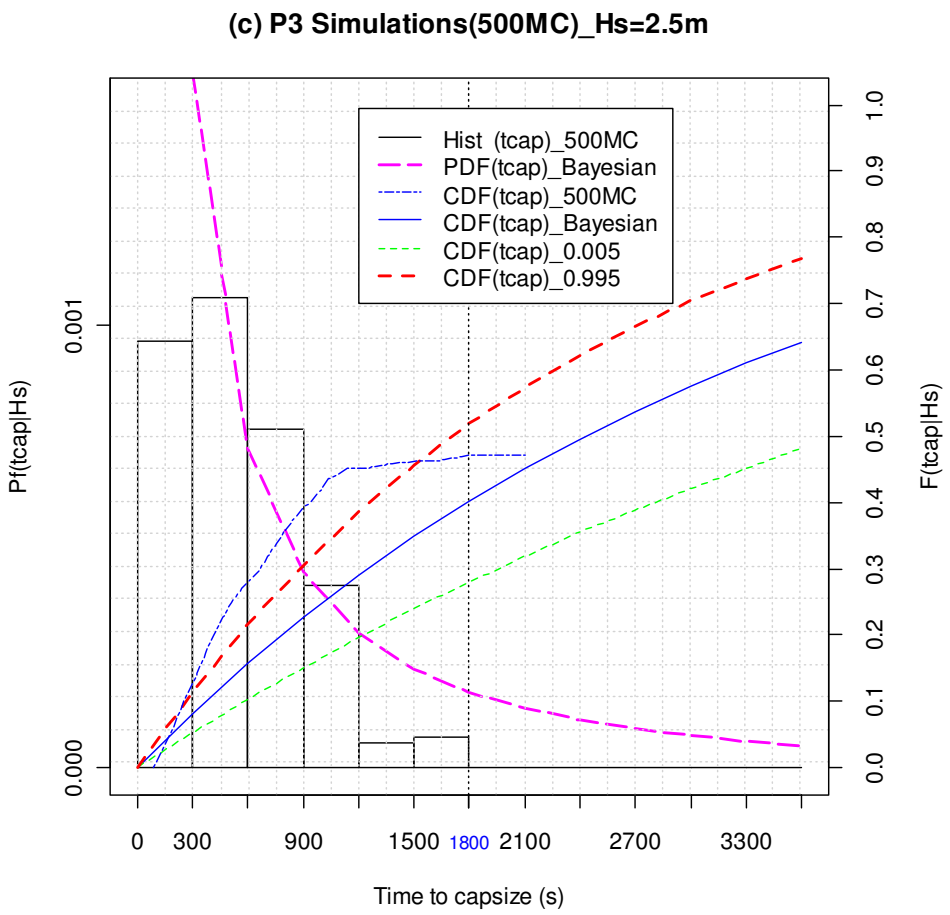

Figure 8.25: Comparison of Cumulative Distribution of Probability for the Time to Capsize Given a Specific Flooding Extent, with $Hs = 2.5\ m$

On the basis of the aforementioned investigations, the estimated casualty-based model, deriving from Bayesian inference together with the MC-based numerical simulation, seems to be well founded in theory and adequate for characterising the process of ship capsizing in waves.

8.8 Closure

This Chapter demonstrates a completed process of implementing the developed methodology for shipboard decision making after a flooding casualty on the RoPax ship. It starts from preparing a dedicated simulation database in the pre-casualty phase to making prediction of damage ship survivability in emergency situations.

According to the validation studies on the time to capsize, it is reasonable to proclaim that the proposed methodology on prediction of the stability deterioration process provides a systematic solution to assist shipboard flooding crisis management.

Chapter 9

Discussion

9.1 Preamble

In this thesis, a tailored methodology for uncertainty quantification in the assessment of ship survivability has been presented. The founding hypothesis of the thesis is that the current practices for performance-based assessment of damage ship survivability are subjected to uncertainty in the whole handling process. Meanwhile, there is a lack of systematic methodology to quantify the inherent uncertainties in such a process. This background calls for the development of a formalised uncertainty analysis scheme for addressing flooding risk analysis. As a result, the emphasis has been put on the various stages constituting the working procedures and methods.

This chapter focuses on a discussion of the major outcomes of the thesis. It starts with a brief summary of the contributions of this research work, which is followed by a general discussion of the difficulties encountered in the development of the various components and methodologies, and how these difficulties have been addressed. Finally, it concludes with recommendations for further research.

9.2 Contribution to the Field

This thesis proposes a novel methodology for uncertainty analysis in the prediction of ship stability deterioration process. This has served the principal aim and objectives. The contribution in the field of performance-based assessment of ship safety is the following:

1) A principle contribution is a framework for ship survivability assessment with uncertainty quantification. It embraces identification of suitable regression models, appropriate model estimation, and uncertainty quantification techniques. The applicability is demonstrated through proposing a shipboard decision support

concept for flooding damage control. The content covered at each stage of the implementation process is believed to be comprehensive and detailed enough for allowing a systematic application.

2) A second contribution of the research undertaken is a rational treatment of modelling the relationship between ship survivability and relevant influencing parameters. The emphasis has been placed on presenting damage ship survivability in a probabilistic manner and in the time domain. This resonates well with the latest industry-wide move to develop performance-based (i.e. probabilistic) measures for addressing various aspects of ship safety. Deriving from this, the presented approach by adopting a Generalised Linear Model with binary outcomes can be easily applied for addressing other accidental phenomenon (e.g. ship collision, shipboard fire occurrence, fire escalation, etc.).

3) A third contribution is the introduction of tailored Bayesian techniques and Markov chain Monte Carlo (MCMC) algorithms to systematically address GLM estimation and uncertainty quantification. Although such techniques are still evolving at a fast pace, the methodology proposed in this thesis still represents the first of its kind application in probabilistic ship safety assessment.

4) A fourth contribution is attributable to the employment of the presented methodology as a tool for evaluating the time-based ship survivability after damage (i.e., time to capsize), so as to provide shipboard decision support for flooding crisis management. Through the proposition of “criticality index”, the obtained quantitative information can be transformed into qualitative implications for decision support. Ultimately, various risk control options can be assessed on a more rational basis so that the most appropriate mitigative actions can be taken.

9.3 Difficulties Encountered

The original aim of this research is to establish a methodology that the uncertainties associated with performance-based ship survivability assessment can be quantified, so that the confidence of relevant estimations based on the state-of-the-art tools can be assured. However, it was soon realised that such an idea requires a comprehensive

understanding of the key characteristics of the current performance-based approach addressing damage ship stability and how uncertainties can be measured within the probabilistic framework.

In this respect, the conventional uncertainty analysis techniques by simply using collected data (i.e., evidence) to establish confidence boundaries is not appropriate since it is applicable mainly to address large sample size problems. While, in the maritime industry, both the physical experimental and actual accident data that can be collected for predicting damage ship survivability are always restricted by the resources allocated (e.g. time, fund).. Hence, a methodology that is suitable for addressing small sample size problems is desired. Deriving from the above, the skeleton of a novel methodology for uncertainty analysis in the assessment of ship survivability within the context of performance-based ship safety framework was shaped and materialised.

In this research, effort has been made to maximise the utilisation of the resources that are available at the Ship Stability Research Centre (SSRC). It is worth mentioning that a series of benchmark tests on survivability assessment of RoPax vessels have been undertaken in the related research projects funded by the European Commission (e.g., HARDER, SAFEDOR, FLOODSTAND), the collected data has been applied for developing the proposed uncertainty analysis scheme and also for validation purpose. The following discussion focuses on specific difficulties encountered during the course of the research at various stages.

The Issue of Modelling Ship Survivability

Ship damaged stability/survivability is one of the important aspects to be examined for assuring passenger ship safety. In this respect, identifying appropriate measures of ship survivability is a key issue in this research. Traditional measures (e.g. GZ curve particulars, A-index) have been formulated in such a manner that time-related factors are not directly included. To address this, “time to capsize” (i.e. cumulative probability of time to capsize for a specific flooding casualty) is deemed as an objective measure to quantify survivability of passenger ships in damaged condition. Under such circumstance, it is necessary to establish a mathematical model for

addressing a time dependent damage ship survivability assessment. Once this model is ready, it can be extended to predict ship survivability at any time interval by considering the stochastic nature of ship capsizing for a given damage in a given time interval follows a Bernoulli trial process. In addition, this model provides a platform for the ensuing uncertainty analysis.

On the other hand, identification of a list of governing input parameters in the model is a challenging task. It is appreciated that the dynamics of a damaged ship in waves is an extremely complex physical phenomenon, which involves the influence of numerous parameters. Nevertheless, it has to be noted that the current mathematical regression model could only handle a handful of parameters. Hence, it is important to ensure the identified parameters are critical to explain the phenomenon of ship capsizing. This issue has been addressed by drawing experience from similar historical studies so that a list of dominant parameters can be identified. This is further verified by performing sensitivity analysis after the predictive regression model is established

The Issue of GLM Model

As the model output variable is to measure whether the ship will capsize for a specific damage in a given time interval, it should be considered as a binary response variable for model estimation. This entails that a more sophisticated regression model is to be pursued so as to best describe the relationship between input variables and the binary outcomes. Following some research, finally GLM has been identified as the platform to be further examined. This is mainly attributed to its transparency and flexibility to establish such a relationship. Further investigations suggest that, within the GLM family, both probit and logit models provide the appropriate link functions to be further explored.

Due to tight schedule within the available time frame, probit model has been selected to put forward to demonstrate the applicability for predicting probabilistically the binary status of ship survivability. If more time is available, Logit model could be examined as well.

The Issue of Bayesian Inference

The Bayesian techniques presented in this thesis are founded on Bayes' Theorem, in which both prior information and evidence exhibited in the collected data sets can be integrated to make inference of the probability distribution of an interested variable. In this respect, it is necessary to stress that the prior information (i.e. shape of distributions) of the unknown parameters is normally not available. Hence, they are generally assumed to be normally distributed. Due to the characteristics of MCMC algorithms, such piece of information will be updated and rectified through the Markov Chain sampling process by using collected evidence

The Issue of Decision Support

Concerning the shipboard decision support methodology proposed for flooding crisis management, it is understood that the most desirable system is to provide binary decision support: i) stay onboard for safe return to port; ii) abandonment. This implies that a clear criterion/boundary needs to be established for translating the obtained probabilistic information into definite qualitative decisions. It is appreciated that more research is needed concerning the definition of criteria. For the time being, the R-index defined in SOLAS 2009 is proposed to be employed so that ship-specific criterion can be established.

Furthermore, regarding the identification of the best flooding control options, emphasis has been placed on integrating the obtained survivability-related information into a transparent and well-informed decision support framework. It is understood that shipboard decision support system for crisis management is still at an early stage and significant research work is still needed to achieve a mature product. Nevertheless, it is believed the methodology presented in Chapter 7 should contribute positively in this direction.

9.4 Recommendations for Further Research

The work presented in this thesis represents a systematic Bayesian approach for uncertainty quantification in flooding risk assessment. The methodologies, tools, techniques, and demonstrative applications are still evolving. The following are some recommendations for further research and development:

- Further investigation of sensitivity of the Bayesian estimates to the choice of link functions. In this research, only the probit regression model is discussed for model estimation.

- Extensive applications of the proposed Bayesian techniques for modelling categorical response data (i.e., multinomial response) rather than binary outcomes, so as to accommodate more types of risk assessment within the probabilistic ship safety framework.

- Further development of first-principles tools towards the prediction of dynamics of damage ships in waves, so that the knowledge-based model uncertainty can be reduced.

- Further study of the critical damage stability parameters of passenger ships, so as to ensure a rational relationship can be modelled to capture the phenomena of losing ship stability in time-domain.

- Further expansion of benchmark data towards time dependent ship survivability in damaged conditions, so that more evidence can be applied for further validation purpose.

- Further investigation of practicability of the proposed methodology, in which uncertainty analysis is integrated into a real-time shipboard decision support system for flooding crisis management.

- Further research on the application of the proposed Bayesian techniques in different phases of ship life-cycle (i.e., design, operation, emergency) to ensure satisfactory safety performance.

Chapter 10

Conclusion

The main conclusion drawn from the research presented in this thesis can be summarised as follows:

- The sources of uncertainty in assessing ship stability in waves have been critically discussed. Emphasis has been placed on the constraints associated with the state-of-the-art performance-based tools or methods used in the flooding-related risk analysis.

- A formalised procedure for the treatment of uncertainties in performance-based assessment of ship survivability has been proposed. By doing so, uncertainty analysis in risk assessment about other critical loss scenarios (e.g. fire, structural failure) can be addressed similarly.

- A mathematical modelling framework has been set up for the assessment of damage ship survivability due to flooding.

- A Bayesian inferential procedure has been presented and elucidated for model estimation and probabilistic uncertainty analysis.

- The applicability of the proposed uncertainty analysis methodology has been demonstrated through a devised framework of shipboard decision support system for flooding damage control.

Reference

Abrahamsson, M. (2002). Uncertainty in quantitative risk analysis : characterisation and methods of treatment. Lund, Sweden, Dept. of Fire Safety Engineering, Lund University.

ABS (2010). American Bureau of Shipping (ABS), Guide for Rapid Response Damage Assessment (RRDA). ABS. New York.

AGCS (2012). Safety and Shipping 1912-2012: From Titanic to Costa Concordia, An insurer's perspective from Allianz Global Corporate & Specialty.

Agresti, A. (2007). An introduction to categorical data analysis. Hoboken, N.J. ; Chichester, Wiley-Interscience.

Albert, J. H. and S. Chib (1993). "Bayesian-Analysis of Binary and Polychotomous Response Data." Journal of the American Statistical Association 88(422): 669-679.

Alefeld, G. and J. Herzberger (1983). Introduction to interval computations. New York, Academic Press.

Allen, P., G. Randall, et al. (2009). European Framework for Safe, Efficient and Environmentally-friendly Ship Operations (FLAGSHIP), D-B2.4 First Test & Evaluation Report BMT.

API. (2012). "A.P.I Marine, API Marine MasterLOAD.", Retrieved 05 March, 2012, from http://www.api-marine.dk/software.aspx.

Autoship (2011). Autoship Systems Corporation, AUTOLOAD Catalogue, Stowage Planning and Onboard Stability Software, Setting the Industry Standard for Integrated Loading Planning Systems.

Bartlett, M. S. (1978). An introduction to stochastic processes with special reference to methods and applications. Cambridge; London; New York, Cambridge University Press.

Bazzurro, P. and N. Luco (2005). Accounting for uncertainty and correlation in earthquake loss estimation. ICOSSAR. Rome, Italy.

Berger, J. O. (1985). Statistical decision theory and Bayesian analysis. New York, Springer-Verlag.

Blendermann, W. (1996). "Wind Loading of Ships-Collected Data from Wind Tunnel Tests in Uniform Flow, Institut fur Schiffbau der Universitat Hamburg, Bericht No 574, pp. 53 ".

Bradley, E. L. (1973). "The Equivalence of Maximum Likelihood and Weighted Least Squares Estimate in the Exponential Family." Journal of the American Statistical Association 68(341): 199-200.

BS (2006). British Standard, BS ISO 16155:2006 Ship and Marine Technology - Computer Applications - Shipboard Loading Instruments. British Standards. BS ISO 16155:2006.

BV (2010). Bureau Veritas (BV), Emergency Response Service (ERS), Rule Note: NR 556 DT R00 E. BV.

Calabrese, F., A. Corallo, et al. (2012). "A knowledge-based decision support system for shipboard damage control." Expert Systems with Applications(0).

Caldeira-Saraiva, F., J. Gyngell, et al. (2004). Simulation of Ship Evacuation and Passenger Circulation. Proceedings of the 2nd International Maritime Conference on Design for Safety, Sakai, Japan.

Chang, B. C. and P. Blume (1998). "Survivability of Damaged Ro-Ro Passenger Vessels." Ship Technology Research Vol. 45: pp. 105-117.

Chen, Q., N. Tsakalakis, et al. (2009). Physical Model Experiments SAFEDOR, D5.6.3.

Cheng, D. (2009). Uncertainty Analysis of Large Risk Assessment Models with Applications to the Railway Safety and Standards Board Safety Risk Model. Doctor of Philosophy, University of Strathclyde.

Chernoff, H. and L. E. Moses (1959). Elementary decision theory. New York, Wiley.

Chib, S. and E. Greenberg (1995). "Understanding the Metropolis-Hastings Algorithm." American Statistician 49(4): 327-335.

Cho, S. K., S. Y. Hong, et al. (2005). Investigation of dynamic characteristics of the flooding water of the damaged compartment of an ITTC RORO Passenger Ship. Proceeding of the 8th Int'l Ship Stability Workshop. Istanbul, Turkey.

Cichowicz, J. (2012). Hydrodynamics of an Unconstrained Cylinder in Forced Roll. PhD Thesis, Department of Ship & Marine Technology, University of Strathclyde.

Cowles, M. K. and B. P. Carlin (1996). "Markov Chain Monte Carlo Convergence Diagnostics: A Comparative Review." Journal of the American Statistical Association Journal of the American Statistical Association 91(434): 883-904.

Cox, D. R. and D. V. Hinkley (1974). Theoretical statistics. London, Chapman and Hall.

Cox, D. R. and E. J. Snell (1989). Analysis of binary data. London; New York, Chapman and Hall.

Davidson, L., K. E. Kline, et al. (2008). "Pro SQL server 2008 relational database design and implementation." from http://dx.doi.org/10.1007/978-1-4302-0867-9.

De Finetti, B. (1974). Theory of probability; a critical introductory treatment. London; New York, Wiley.

de Kat Jan, O. and A. J. Peters (2002). Model Experiments and Simulations of a Damaged Frigate. 10th International Maritime Association of the Mediterranean (IMAM) Congress, Crete, Greece.

De Kat, J. O. (1990). "The Numerical Modelling of Ship Motions and Capsizing in Severe Seas." Journal of Ship Research Vol. 34, pp.289-301.

De Kat, J. O. (2000). Dynamics of a Ship with Partially Flooded Compartment. Contemporary Ideas on Ship Stability, . D. Vassalos, M. Hamamoto, D. Molyneux and A. Papanikolaou. Amsterdam, Elsevier Science Ltd.

De Kat, J. O. and J. R. Paulling (1989). "The Simulation of Ship Motions and Capsizing in Severe Seas." Transactions of Society of Naval Architects and Marine Engineers Vol. 97, pp.139-168.

DeGroot, M. H. (1970). Optimal statistical decisions. New York, McGraw-Hill.

Derrett, D. R. and C. B. Barrass. (2006). "Ship stability for masters and mates." from http://www.engineeringvillage.com/controller/servlet/OpenURL?genre=book&isbn=9780750667845.

DNV (2011). DNV Classification Notes No.20.1 Stability Documentation for Approval, May 2011. DNV. DNV Classification Notes No.20.1

DNV (2012a). DNV Rules for Classification of Ships, Part 6 Chapter 9, Newbuilding Special Equipment and Systems -Additional Class, Loading Computer Systems (LCS) for Stability and Longitudinal Strength, January 2012. DNV. DNV Rules for Classification of Ships, Part 6 Chapter 9.

DNV (2012b). DNV Emergency Response Service (ERS). DNV.

Dobson, A. J. and A. G. Barnett (2009). "An Introduction to Generalized Linear Models, 3rd edition " Biometrics 65(2): 672-673.

EC (2003). "DIRECTIVE 2003/25/EC OF THE EUROPEAN PARLIAMENT AND OF THE COUNCIL on specific stability requirements for ro-ro passenger ships."

Ferson, S. and L. R. Ginzburg (1996). "Different Methods are Needed to Propagate Ignorance and Variability." Reliability engineering & system safety. 54(2/3): 133.

FLAGSHIP (2008). FLAGSHIP, European Framework for Safe, Efficient and Environmentally-Friendly Ship Operations in 6th Framework programme of the European Commission, European Community Shipowners' Associations.

Francescutto, A., A. Serra, et al. (2001). A Critical Analysis of Weather Criterion for Intact Stability of Large Passenger Vessels. Proceedings of the 20th Int'l Conf. on Offshore Mechanics and Artic Engineering (OMAE2001). Rio de Janeiro, Brazil.

Galea, E. R., P. Lawrence, et al. (2004). Integrated Fire and Evacuation in Maritime Environments. Proceedings of the 2nd International Maritime Conference on Design for Safety, Sakai, Japan.

Gao, Q. (2012a). The Effect of Free Surface on Classical Ship Hydrodynamics using RANSE - Resistance, Manoeuvring, Propulsion, Seakeeping and Stability. PhD Thesis, Department of Ship & Marine Technology, University of Strathclyde.

Gao, Z. (2012b). A Hybrid Approach to Flooding and Damaged Ship Dynamics. PhD Thesis, Department of Ship & Marine Technology, University of Strathclyde.

Gao, Z., D. Vassalos, et al. (2009). A Multiphase CFD Method for Predicetion of Floodwater Dynamics. Proc. 10th Int'l Conf. Stability of Ships & Ocean Vehicles, pp. 307-316. St. Petersburg, Russia.

Gelfand, A. E. and A. F. M. Smith (1990). "Sampling-Based Approaches to Calculating Marginal Densities." Journal of the American Statistical Association Journal of the American Statistical Association 85(410): 398-409.

Gelman, A. (2004). Bayesian data analysis. Boca Raton, Fla., Chapman & Hall/CRC.

Geman, S. and D. Geman (1984). "Stochastic relaxation, gibbs distributions, and the bayesian restoration of images." IEEE transactions on pattern analysis and machine intelligence 6(6): 721-741.

GOALDS (2009). GOAL based Damage Stability (GOALDS), Seventh Framework Programme Theme, Annex I - "Description of Work".

Gorski, J. (2002). A Perspective on The Role of RANS Codes for Predicting Large Amplitude Ship Motions. Proceeding of the 6th Int'l Ship Stability Workshop. New York.

Graham, P. (2011). International Union of Marine Insurance (IUMI) Casualty and World Fleet Statistics as at 31.12.2010, IUMI Facts & Figures Committee.

Greene, W. H. (2003). Econometric analysis. Upper Saddle River, N.J., Prentice Hall.

Guarin, L., J. Logan, et al. (2007). Design for Fire Safety. Proceedings of the 3rd International Maritime Conference on Design for Safety, September 26-28, Berkeley, USA.

Ha, T. (2000). A three dimensional prediction of the seakeeping performance of high speed marine vehicles. PhD Thesis, Department of Ship & Marine Technology, University of Strathclyde.

Hacking, I. (1975). The emergence of probability : a philosophical study of early ideas about probability, induction and statistical inference. Cambridge; New York, Cambridge University Press.

Hair, J. F. (2009). Multivariate data analysis. Upper Saddle River, N.J., Pearson Education International ; [Harlow] : Pearson Education Ltd.

HARDER (2003). HARDER - Harmonisation of Rules and Design Rationale, U Contact No. GDRB-CT-1998-00028, Final Technical Report.

Hastings, W. K. (1970). "Monte Carlo sampling methods using Markov chains and their applications." Biometrika Biometrika 57(1): 97-109.

Helton, J. C. (1998). "Uncertainty and Sensitivity Analysis in Performance Assessment for the Waste Isolation Pilot Plant." from http://www.osti.gov/servlets/purl/2438-RQHvvn/webviewable/.

Helton, J. C., D. R. Anderson, et al. (1996). "Uncertainty and Sensitivity Analysis Results Obtained in the 1992 Performance Assessment for the Waste Isolation Pilot Plant." Reliability engineering & system safety. 51(1): 53-100.

Helton, J. C., D. R. Anderson, et al. (2000a). "Conceptual structure of the 1996 performance assessment for the Waste Isolation Pilot Plant." Reliability Engineering and System Safety (Special Journal Issue).

Helton, J. C., J. E. Bean, et al. (1997). "Uncertainty and sensitivity analysis for gas and brine migration at the Waste Isolation Pilot Plant: Permeable shaft with panel seals." Reliability Engineering & System Safety 57(3): 299-316.

Helton, J. C. and F. J. Davis (2002). "Illustration of Sampling-Based Methods for Uncertainty and Sensitivity Analysis." Risk Analysis 22(3): 591-622.

Helton, J. C. and F. J. Davis (2003). "Latin hypercube sampling and the propagation of uncertainty in analyses of complex systems." Reliability Engineering & System Safety 81(1): 23-69.

Helton, J. C., F. J. Davis, et al. (2005). "A comparison of uncertainty and sensitivity analysis results obtained with random and Latin hypercube sampling." Reliability engineering & system safety. 89(3): 305-330.

Helton, J. C., J. D. Johnson, et al. (2004). "An exploration of alternative approaches to the representation of uncertainty in model predictions." Reliability Engineering & System Safety 85(1–3): 39-71.

Helton, J. C., J. D. Johnson, et al. (2006). "Survey of sampling-based methods for uncertainty and sensitivity analysis." Reliability Engineering & System Safety 91(10-11): 1175-1209.

Helton, J. C., M. A. Martell, et al. (2000b). "Characterization of subjective uncertainty in the 1996 performance assessment for the Waste Isolation Pilot Plant." Reliability Engineering & System Safety Reliability Engineering & System Safety 69(1-3): 191-204.

Helton, J. C., U. S. N. R. C. O. o. N. R. R. D. o. S. Technology, et al. (1995a). Uncertainty and sensitivity analysis of chronic exposure results with the MACCS reactor accident consequence model. Washington, DC, Division of Systems Technology, Office of Nuclear Regulatory Research, U.S. Nuclear Regulatory Commission : Supt. of Docs., U.S. G.P.O. [distributor].

Helton, J. C., U. S. N. R. C. O. o. N. R. R. D. o. S. Technology, et al. (1995b). Uncertainty and sensitivity analysis of food pathway results with the MACCS reactor accident consequence model. Washington, DC, Division of Systems Technology, Office of Nuclear Regulatory Research, U.S. Nuclear Regulatory Commission.

Helton, J. C., U. S. N. R. C. O. o. N. R. R. D. o. S. Technology, et al. (1995c). Uncertainty and sensitivity analysis of early exposure results with the MACCS reactor accident consequence model. Washington, DC, Division of Systems Technology, Office of Nuclear Regulatory Research, U.S. Nuclear Regulatory Commission : Supt. of Docs., U.S. G.P.O. [distributor].

Himeno, Y. (1981). Prediction of Ship Roll Damping - State of the Art. Report no 239. University of Michigan, USA.

Hoste, P. (1697). Theorie de la construction des vaisseaux, qui contient plusieurs traitez de mathematique ("Theory of Ship Construction"), Lyon.

Hou, Y., J.-y. Pu, et al. (2009). Intelligent Decision Support System of Ship Unsinkability Design in the First Design Stage. Intelligent Systems, 2009. GCIS '09. WRI Global Congress on.

Hutchinson, B. L. (1995). Water-on-Deck Acumulation Studies by the SNAME ad hoc Ro-Ro Safety Panel. Proceeding of the International Workshop on Numerical and Physical Simulation of Ship Capsize in Heavy Seas. July 24-25, Loch Lomond, Glasgow.

IAEA (1989). Evaluating the reliability of predictions made using environmental transfer models. Vienna, International Atomic Energy Agency.

IEC (1995). International standard Nr 60300-3-9: Dependability management - part 3: Application guide. Section 9: Risk analysis of technological systems. . Geneva, International Electrotechnical Commision.

Ikeda, Y. (2002). Prediction methods of roll damping of ships and their application to determine optinum stabilization devices. Proceeding of the 6th Int'l Ship Stability Workshop. New York.

Iman, R. L., J. M. Davenport, et al. (1980). Latin Hypercube Sampling (a program user's guide), Technical Report SAND79-1473. Sandia National Laboratiories, Albuquerque.

Iman, R. L., M. E. Johnson, et al. (2002). "Assessing hurricane effects. Part 2. Uncertainty analysis." Reliability engineering & system safety. 78(2): 147-155.

IMO (1995). SOLAS'95, Resolution 14, "Regional Agreements on Specific Stability Requirements for Ro-Ro Passenger Ships" - (Annex: Stability Requirements Pertaining to the Agreement; Appendix: Model Test Method), adopted on 29 Novemeber 1995.

IMO (1996). Circular Letter No.1891, "Agreement Concerning Specific Stability Requirements for Ro-Ro Passenger Ships Undertaking Regular Scheduled International Voyages Between or To or From Designated Ports in North West Europe and The Baltic Sea".

IMO (1997a). SOLAS: Consolidated edition 1997 - Annex 5: Resolutions of the 1995 SOLAS Conference. Model test method. IMO, Resolutions of the Conference of Contracting Governments to the International Convention for the Safety of Life at Sea, 1974, adopted on 29 Novemeber 1995.

IMO (1997b). MSC/Circ.836, "Recommendation on Loading Instruments". IMO. MSC/Circ.836.

IMO (1998a). MSC/Circ.854, "Guidelines for Shipboard Loading and Stability Computer Programs". IMO. MSC/Circ.854.

IMO (1998b). MSC/Circ.891, "Guidelines for the On-Board Use and Application of Computers". IMO. MSC/Circ.891.

IMO (1999). MSC/Circ.920, "Model Loading and Stability Manual". IMO. MSC/Circ.920.

IMO (2004). SLF 47/INF.6, "Survivability investigation of large passenger ships - The practical assessment of features that effect the flooding survival of large passenger ships", Submitted by Finland. IMO. London.

IMO (2004a). Sub-Committee on Stability Load Lines and on Fishing Vessel Safety, "Large Passenger Ship Safety" - SLF 47/8, 11 June 2004.

IMO (2004b). Sub-Committee on Stability Load Lines and on Fishing Vessel Safety, "Report to the Maritime Safety Committee" - SLF 47/17, London, 27 Sept 2004.

IMO (2006a). SLF 49/INF.5, Passenger Ship Safety, Time dependent survival probability of damaged passenger ship (HSVA report), Submitted by Germany, 21 April 2006.

IMO (2006b). Implementation of Instruments and Related Matters, In Service Damage Stability Verification for Some Oil, Chemical and Gas Tankers, MSC Res.81/20/3, Submitted by the United Kingdom. IMO. MSC 81/20/3.

IMO (2006c). MSC 82/24/Add.1 Adoption of amendments to the International Convention for the safety of life at sea, 1974, Resolution MSC 216 (82), adopted on 8th December 2006. IMO. MSC 82/24/Add.1.

IMO (2007). MSC.1/Circ.1245, "Guidelines for Damage Control Plans and Information to the Master", 29 October 2007.

IMO (2008). MSC. 85/17/1, "Formal Safety Assessment - Cruise Ships".

IMO (2008c). MSC.1/Circ.1291, "Guidelines for Flooding Detection Systems on Passenger Ships". IMO. MSC.1/Circ.1291.

IMO (2008d). SLF 51/11, "Stability and Seakeeping Characteristics of Damaged Passenger Ships in a Seaway When Returning to Port by Own Power or Under Tow", Report of the Correspondence Group, Submitted by the United Kingdom, 10 April 2008. IMO. SLF 51/11.

Isherwood, M. A. (1973). "Wind Resistance of Merchant Ships." Transactions of Royal Institution of Naval Architects Vol. 115, pp.327-335.

ITTC (2002). The Specialist Committee on Prediction of Extreme Ship Motions and Capsizing - Final Report and Recommendations to the 23rd ITTC. Proc. of the 23rd ITTC, Venice, Italy.

ITTC (2005). The Specialist Committee on Stability in Waves - Final Report and Recommendations to the 24th ITTC. Proc. of the 24th ITTC, Edinburgh, UK.

ITTC (2008). The Specialist Committee on Stability in Waves - Final Report and Recommendations to the 25th ITTC. Proc. of the 25th ITTC, Fukuoka, Japan.

Jasionowski, A. (2001a). An integrated approach to damage ship survivability assessment. PhD Thesis, Department of Ship & Marine Technology, University of Strathclyde.

Jasionowski, A. (2006). Fast and accurate flooding prediction - analytical model. SAFEDOR-D-WP2.1.3-2006-11-30-SSRC-rev-1, submitted on 30 November 2006.

Jasionowski, A. (2011). "Decision support for ship flooding crisis management." Ocean Engineering 38(14-15): 1568-1581.

Jasionowski, A. (2012a). Analytical model of stability deterioration process. FLOODSTAND, FP7-RTD-218532, D4.2, SSRC, rev22.

Jasionowski, A. (2012b). Hybrid model of stability deterioration process. FLOODSTAND, FP7-RTD-218532, D4.4, SSRC, rev7.

Jasionowski, A., K. Dodworth, et al. (1999). "Proposal For Passenger Survival-Based Criteria For Ro-Ro Vessels." International Shipbuilding Progress Vol. 46, No 448.

Jasionowski, A. and D. Vassalos (2001b). Numerical modelling of damage ship stability in waves. Proceeding of the 5th Int'l Ship Stability Workshop. Trieste.

Jasionowski, A., D. Vassalos, et al. (2004). Theoretical Developments On Surivival Time Post-Damage. Proceeding of the 7th Int'l Ship Stability Workshop. Shanghai.

Jasionowski, A., D. Vassalos, et al. (2004). "Theoretical Developments on Survival Time Post-Damage." Proceedings of the 7th International Ship Stability Workshop, Shanghai.

Jasionowski, A., D. Vassalos, et al. (2007). "Ship vulnerability to flooding." 3rd International Maritime Conference on Design for Safety Berkeley California, September 26th - 28th

Jensen, J., C. G. Soares, et al. (2008). Chapter 5: Methods and Tools. Risk-Based Ship Design - Methods, Tools and Application. A. Papanikolaou. Berlin, Springer.

Journee, J., H. Vermeer, et al. (1997). Systematic Model Experiments on Flooding of Two Ro-Ro Vessels. Proc. 6th Int'l Conf. Stability of Ships & Ocean Vehicles (STAB'97). Varna, Bulgaria. Vol. 2: pp. 81-98.

Kalbfleisch, J. G. (1985). Probability and statistical inference, Volume 2: Statistical inference, Second Edition. New York, Springer.

Kaplan, S. and B. J. Garrick (1981). "On the quantitative definition of risk." Risk Analysis 1: 18.

Konovessis, D. (2012). Lecture Notes NM 414 Risk & Reliability. Glasgow, Department of Naval Architecture & Marine Engineering ,Univeristy of Strathclyde.

Lauridsen, K., I. Kozine, et al. (2002). Assessment of Uncertainties in Risk Analysis of Chemical Establishments, The ASSURANCE project, Riso National Laboratory. Roskilde, Denmark.

Lee, C. J., H. K. Yoon, et al. (2006). Wave Force Modelling in Time-Domain Ship Motion. Proc. 9th Int'l Conf. Stability of Ships & Ocean Vehicles. Rio de Janeiro, Brazil.

Lee, P. M. (2004). Bayesian Statistics : An Introduction. London, Hodder Arnold.

Letizia, L. (1996). Damage survivability of passenger ships in a seaway, University of Strathclyde.

Letizia, L. (1997). Damage Survivability of Panssenger Ro-Ro Vessels Subjected to Progressive Flooding in a Random Sea. PhD Thesis, Department of Ship & Marine Technology, University of Strathclyde.

Letizia, L. and D. Vassalos (1995). Formulation of a Non-Linear Mathematical Model for a Damaged Ship with Progressive Flooding. Proceeding of the International Symposium on Ship Safety in a Seaway, Kaliningrad, Russia.

Letizia, L., D. Vassalos, et al. (2003). New Insights into Ship-Floodwater-Sea Dynamics. Proc. 8th Int'l Conf. Stability of Ships & Ocean Vehicles (STAB2003), pp.717-729. Madrid.

Lewis, E. V., A. Society of Naval, et al. (1988). "Principles of naval architecture. Volume I, Stability and strength." from http://www.knovel.com/knovel2/Toc.jsp?BookID=2967.

Li, Y. and B. R. Ellingwood (2006). "Hurricane damage to residential construction in the US: Importance of uncertainty modeling in risk assessment." Engineering Structures 28(7): 1009-1018.

Lindley, D. V. (1965). Introduction to probability and statistics : from a bayesian viewpoint. Cambridge, Cambridge University Press.

LR (2012). Lloyd's Register (LR), Ship Emergency Response Service (SERS). LR.

Lutzen, M. (2002). Damage Distributions. HARDER, EU Project No: GRD-1999-10721, Report No: 2-22-D-2001-01-04.

Lützen, M. (2001). Ship collision damages. PhD, Technical University of Denmark, Department of Mechanical Engineering, Maritime Engineering.

M.Elisabeth, P.-C. (1996). "Uncertainties in risk analysis: Six levels of treatment." Reliability Engineering & System Safety 54(2-3): 95-111.

Martins, P. T. and V. S. Lobo (2011). Real-time decision support system for managing ship stability under damage. OCEANS, 2011 IEEE - Spain.

MCA (2012). The UK Maritime and Coastguard Agency (MCA), Instruction for the Guidance of Surveyors, MSIS 3, Passenger Ship Construction, Classes I, II & II(A), Part 5 Stability and Shipside Marking. MCA. MSIS003/PT 5/REV 1.01.

McKay, M. D., R. J. Beckman, et al. (2000). "A Comparison of Three Methods for Selecting Values of Input Variables in the Analysis of Output from a Computer Code." Technometrics 42(1): 55-61.

Memeris, G. and U. Langbecker (2006). Requirements for Risk-Based Design Support: Identification and Analysis of Risk-Based Simulation Tools. SAFEDOR-D-5.1.5-2006-06-30-GL-RBD_Tools- rev8.

Mermiris, G. and D. Vassalos (2010). Collision Risk Revisited. 4th International Martitime Conference on Design for Safety and 3rd Workshop on Risk-Based approaches in the Marine Industries, Italy.

Mermiris, G. A. (2010). "A risk-based design approach to ship - ship collision [electronic resource]."

Metropolis, N., A. W. Rosenblutn, et al. (1953). Equations of State Calculations by Fast Computing Machines.

MICROSOFT. (2012). "Microsoft SQL Server." Retrieved 22 March, 2012, from http://www.microsoft.com/sqlserver/en/us/default.aspx.

MMA (1993a). M/V KINGS POINTER Damage Control Book. New York, United States, United States Merchant Marine Academy.

Molyneux, D., J. Rousseau, et al. (1997). "Model Experiments to Determine the Survivability Limits of Damaged Ro-Ro Ferries in Waves." Transactions of Society of Naval Architects and Marine Engineers Vol. 105.

Moore, R. E. (1966). Interval analysis. Englewood Cliffs, N.J., Prentice-Hall.

Moore, R. E. and F. Bierbaum (1979). Methods and applications of interval analysis. Philadelphia, Siam.

Morgan, M. G., M. Henrion, et al. (1990). Uncertainty : a guide to dealing with uncertainty in quantitative risk and policy analysis. Cambridge; New York, Cambridge University Press.

Nabavi, Y., S. M. Calisal, et al. (2006). A Computational Investigation of the Three Dimentional Geometric Parameters' Effect on the Discharge Rate of a Ship Opening. Proc. 9th Int'l Conf. Stability of Ships & Ocean Vehicles (STAB'2006), pp. 617-624. Rio de Janeiro, Brazil.

Nelder, J. A. and R. W. M. Wedderburn (1972). "Generalized linear models." Journal of the Royal Statistical Society, Series A 135: 370-384.

Nilsen, T., O. T. Gudmestad, et al. (1998). "Utilisation of principles from structural reliability in quantitative risk analysis: example from an offshore transport problem." Reliability Engineering & System Safety Reliability Engineering & System Safety 61(1-2): 127-137.

Nowacki, H. (2007). Leonard Euler and the theory of ships. Berlin, Max-Planck Institute for the History of Science.

Olcer, A. I. and J. Majumder (2006). "A case-based decision support system for flooding crises onboard ships." Quality and Reliability Engineering International 22(1): 59-78.

OPA (2012). Requirements of USCG Oil Pollution Act (OPA'90) and the Relevant 33 CFR 155.240 Damage Stability Information for Oil Tankers and Offshore Oil Barges, USCG.

Palazzi, L. and J. O. De Kat (2002). Model Experiments and Simulations of a Damaged Ship with Air-Flow Taken into Account. Proceeding of the 6th Int'l Ship Stability Workshop. New York.

Papanikolaou, A. (2001). Benchmark Study on the Capsizing of a Damaged Ro-Ro Passenger Ship in Waves. Final Report to the 22nd ITTC Specialist Committee on the Predicition of Extreme Motions and Capsizing, December.

Papanikolaou, A. (2007). "Review of Damage Stability of Ships - Recent developments and Trends." Proceddings of PRADS, Houston, USA.

Papanikolaou, A. and D. Spanos (2002). On the Modelling of Floodwater Dynamics and Its Effects on Ship Motion. Proceeding of the 6th Int'l Ship Stability Workshop. New York.

Papanikolaou, A. and D. Spanos (2004a). "24th ITTC Benchmark Study on Numerical Predicition of Damage Ship Stability in Waves Preliminary Analysis of Results." Proceedings of the 7th International Ship Stability Workshop, Shanghai, China.

Papanikolaou, A. and D. Spanos (2004b). Benchmark Study on the Numerical Prediction of Damaged Ships in Waves. Final Report. ITTC Sub-Committee on Ship Stability in Waves.

Papanikolaou, A. and D. Spanos (2008). "Validation of Numerical Codes for the Prediction of the Motions and Flooding of Damaged Ships in Waves. SAFEDOR International Benchmark Study." Proceedings of the 10th International Workshop on Ship Stability, Dajeon-Seoul, March.

Papanikolaou, A. and G. Zaraphonitis (1989). Computer Program Newdrift Version 6. Internal Report, National Technical University of Athens.

Papanikolaou, A., G. Zaraphonitis, et al. (2000). Investigation into the Capsizing of Damaged Ro-Ro Passenger Ships in Waves Proceeding of the 7th International Conference on Stability of Ships and Ocean Vehicles STAB2000, Tasmania, Australia.

Pawlowski, M. (2004). Subdivision and damage stability of ships. Gdansk, Fundacja Promocji Przemyslu Okretowego i Gospodarki Morskiej.

Pawlowski, M. (2005). "Probability of Flooding a Compartment (the pi Factor) - A Critique and a Proposal." Proceedings of the Institution of Mechanical Engineers, Part M: Journal of Engineering for the Maritime Environment 219(4): 185-201.

Pawlowski, M. (2008). Closure on Surivival Time. Proc. 10th Int'l Ship Stability Workshop. Daejeon,Korea: pp. 245-252.

Pawlowski, M. (2009). Developing the s factor. Proc. 10th Int'l Conf. Stability of Ships & Ocean Vehicles. St. Petersburg, Russia: pp. 245-252.

Pawlowski, M. (2010). Comparison of s-factors according to SOLAS and SEM for Ro-Pax vessels. Proceeding of the 11th Int'l Ship Stability Workshop. Wageningen, Netherlands: pp. 148-152.

Penttila, P. and P. Ruponen (2010). Use of Level Sensors in Breach Estimation for a Damaged Ship. Proceeding of the 5th International Conference on Collision and Grounding of Ships, Espoo, Finland, Aalto University.

Perez-Rojas, L. P., G. Bulian, et al. (2009). A Combined Experimental and SPH Approach to Sloshing and Ship Roll Motions. Proc. 10th Int'l Conf. Stability of Ships & Ocean Vehicles, pp. 261-270. St. Petersburg, Russia.

Rahola, J. (1939). The judging of the stability of ships and the determination of the minimum amount of stability, especially considering the vessels navigating Finnish waters Doctoral Thesis, The University of Finland.

Raiffa, H. and R. Schlaifer (1961). Applied statistical decision theory. New York, Wiley.

Randall, G. and T. Varelos (2008). European Framework for Safe, Efficient and Environmentally-friendly Ship Operations (FLAGSHIP), D-B2.2 Contingency Manager Specification, BMT.

Rask, I. (2010). Benchmark data on time to capsize for a free drifting model. FLOODSTAND, FP7-RTD-218532, D4.1a, SSPA Report No.: 4007 4581-1 rev2.0.

Runnerstrom, E. (2003). "Human systems integration and shipboard damage control." Naval Engineers Journal 115(4): 71-79.

Ruponen, P. (2006). Model Tests for the Progressive Flooding of a Box-shaped Barge, HUT Ship Laboratory Report. Helsinki, Finland.

Ruponen, P., T. Sundell, et al. (2006). Validation of a Simulation Method for Progressive Flooding Proc. 9th Int'l Conf. Stability of Ships & Ocean Vehicles (STAB'2006). Rio de Janeiro, Brazil.

Ruponen, P., T. Sundell, et al. (2007). "Validation of a simulation method for progressive flooding." International Shipbuilding Progress 54(4): 305-321.

Russell, S. J. and P. Norvig (2010). Artificial intelligence : a modern approach. Boston, [Mass.], Pearson.

Santos, T. A. (2002). "Time domain modelling of the transient asymmetric flooding of Fo-Ro ships." Ocean Engineering 29.

Schreuder, M. (2008). Numerical Simulations of Foundering Scenarios, Research Study of the Sinking Sequence of M/V ESTONIA, Research Report no. 134. Goteborg, Sweden, SSPA.

Shen, L. (2011). Applications of Smoothed Particle Hydrodynamics on 3D Nonlinear Free Surface Flows. PhD Thesis, Department of Ship & Marine Technology, University of Strathclyde.

Shen, L. and D. Vassalos (2009). Applications of 3D Paraller SPH for Sloshing and Flooding Proc. 10th Int'l Conf. Stability of Ships & Ocean Vehicles, pp. 723-732. St. Petersburg, Russia.

Simopoulos, G., D. Konovessis, et al. (2008). "Sensitivity analysis of the probabilistic damage stability regulations for RoPax vessels." J mar Sci Technol 13(2): 164-177.

SMC. (2012). "Ship Motion Control, SMCems - Environmental Monitoring System." Retrieved 17 March, 2012, from http://www.shipmotion.se/smcems.html.

Sobol', I. M. (1974). The Monte Carlo method. Chicago, University of Chicago Press.

Spanos, D. (2002). Numerical Simulation of Flooded Ship Motions in Seaways and Investigation of the Behavior of Passenger/Ro-Ro ferries. Dr. Eng. Thesis, School of Naval Architecture and Marine Engineering, National Technical University of Athens.

Spanos, D. and A. Papanikolaou (2001a). "On the Stability of Fishing Vessels with Trapped Water on Deck." Ship Technology Research Vol. 48: pp. 124-133.

Spanos, D. and A. Papanikolaou (2011b). Numerical simulations for characterizing Time to Capsize. FLOODSTAND, FP7-RTD-218532, D4.3, NTUA-SDL, rev1.0.

Spanos, D., A. Papanikolaou, et al. (1997). On a 6 DOF Mathematical Model for the Simulation of Ship Capsize in Waves. Proc. of the 8th Int'l Congress on Marine Technology (IMAM). Istanbul, Turkey.

Spouge, J. R. (1985). "The Technical Investigation of the Sinking of the Ro-Ro Ferry EUROPEAN GATEWAY." Transactions of Royal Institution of Naval Architects Vol. 127, pp.49-72.

Stein, M. (1987). "Large Sample Properties of Simulations Using Latin Hypercube Sampling." Technometrics 29(2): 143-151.

Strasser, C. (2010). Simulation of Progressive Flooding of Damaged Ship by CFD. PhD Thesis, Department of Ship & Marine Technology, University of Strathclyde.

Strasser, C., A. Jasionowski, et al. (2009). Calculation of the Time-to-Flood of a Box-Shaped Barge using CFD. Proc. 10th Int'l Conf. Stability of Ships & Ocean Vehicles, pp. 733-740. St. Petersburg, Russia.

Tagg, R. and C. Tuzcu (2003). "A Performance-Based Assessment of the Survival of Damaged Ships: Final Outcome of the EU Research Project HARDER." Marine Technology and Sname News 40: 288-295.

Tellkamp, J., H. Gunther, et al. (2008). ADOPT - Advanced Decision Support System for Ship Design, Operation and Training - An Overview. COMPIT 2008, 7th International Conference on Computer Applications and Information Technology in the Marine Industries, Liege.

Tsakalakis, N., J. Cichowicz, et al. (2010). The Capsize Band Concept Revisited. Proceeding of the 11th Int'l Ship Stability Workshop. Wageningen, Netherlands: pp. 262-271.

Turan, O. (1993). Dynamic Stability Assessment of Damaged Passenger Ships Using a Time Simulation Approach. PhD Thesis, Department of Ship & Marine Technology, University of Strathclyde.

Tuzcu, C. and R. Tagg (2001). Model Tests Results - PRR01. HARDER No: GRD1-1999-10721, 2011-06-15, Report No: 3-31-D-2001-01-0.

Umeda, N., T. Kamo, et al. (2004). "Some Remarks on Theoretical Modelling of Damage Stability." Marine Technology: 41 (41), pp45-49.

Umeda, N. and A. Papanikolaou (2000). Revised Guidelines for ITTC Committe on the Prediction of Extreme Ship Motions and Capsizing Benchmark Tests.

Vanem, E. and R. Skjong (2004). "Collision and Grounding of Passenger Ships - Risk Assessment and Emergency Evacuations." Proceedings of 3rd Internatinal Conference on Collision and Grounding of Ships (ICCGS 2004), Japan: pp. 195-202.

Van't Veer, R. and J. O. De Kat (2000). Experimental and Numerical Investigation on Progressive Flooding and Sloshing in Complex Compartment Geometries. Proc. 7th Int'l Conf. Stability of Ships & Ocean Vehicles (STAB'2000). Launceston, Australia.

Van't Veer, R., W. Peters, et al. (2004). Exploring the influence of Different Arrangements of Semi-Watertight Spaces on Survivability of a Damaged Large Passenger Ship. Proceeding of the 7th Int'l Ship Stability Workshop. Shanghai.

Varela, J. M. and C. Guedes Soares (2007). "A virtual environment for decision support in ship damage control." IEEE computer graphics and applications 27(4).

Vassalos, D., Conception, G, Letizia, L (1997a). "Modelling the Accumulation of Water on the Vehicle Deck of a Damaged Vessel." Proceedings of the 3rd Ship Stability Workshop, Greece.

Vassalos, D. (1999). "Shaping Ship Safety: the Face of the Future." Marine Technology 36(2): 61-74.

Vassalos, D. (2008). Chapter 2: Risk-Based Ship Design. Risk-Based Ship Design - Methods, Tools and Application. A. Papanikolaou. Berlin, Springer.

Vassalos, D. (2012a). Damage Stability of Passenger Ships - Notions and Truths. Proceeding of the 11th International Conference on Stability of Ships and Ocean Vehicles STAB2012, Athens, Greece.

Vassalos, D. (2012b). Design for Safety: Risk-Based Design, Life-Cycle Risk Managment. Proceeding of the 11th International Conference on Marine Design, 11-14 June 2012. Glasgow, UK.

Vassalos, D., G. Christiansen, et al. (2002). Evacuability of Passenger Ships at Sea. SASMEX.

Vassalos, D., L. Guarin, et al. (2004a). Effectiveness of Passenger Evacuation Performance For Design, Operation & Training Using First-Principles Simulation Tools. Escape, Evacuation & Recovery. Lloyds Lists Events. London.

Vassalos, D., L. Guarin, et al. (2003). Advanced Evacuation Analysis - Testing the Ground on Ships. Pedestrian and Evacuation Dynamics, Greenwich.

Vassalos, D. and A. Jasionowski (2000). Stockholm Agreement Water on Deck Model Experiments for Passenger/Ro-Ro Vessel, Final Report, PSBG-RE-004-AY., The Ship Stability Research Centre, University of Strathclyde, February 2000.

Vassalos, D. and A. Jasionowski (2002). Damaged Ship Hydrodynamics. Proceeding of the 6th Int'l Ship Stability Workshop. New York.

Vassalos, D. and A. Jasionowski (2006). "Conceptualising Risk." Proc. 9th Int'l Conf. Stability of Ships & Ocean Vehicles.

Vassalos, D., A. Jasionowski, et al. (2004b). "Issues Related to the Weather Criterion." Ocean Engineering Vol. 51, No. 2/3, October, pp. 251-271.

Vassalos, D., H. S. Kim, et al. (2001b). A Mesoscopic Model for Passenger Evacuation in a Virtual Ship-Sea Environment and Performance-Based Evaluation. Pedestrian and Evacuation Dynamics. Duisburg.

Vassalos, D. and L. Letizia (1995). Formulation of a Non-Linear Mathematical Model for a Damaged Ship Subjected to Flooding Proceedings of Sevastianov Symposium. Kaliningrad, Russia.

Vassalos, D., L. Letizia, et al. (2000). Modelling the accumulation of water on the vehicle deck of a damaged Ro-Ro Vessel and proposal of survival criteria. Contemporary Ideas on Ship Stability, . D. Vassalos, M. Hamamoto, D. Molyneux and A. Papanikolaou. Amsterdam, Elsevier Science Ltd.

Vassalos, D., S. C. Shin, et al. (2004c). Decision Support for Flooding Emergencies - An Algorithm for Optimal Ballasting. 2nd International Maritime Conference on Design for Safety, Sakai, Japan.

Vassalos, D. and O. Turan (1994). "A Realistic Approach to Assessing the Damage Survivability of Passenger Ships." Transactions of Society of Naval Architects and Marine Engineers Vol. 102, pp.367-394.

Vermeer, H., A. Vredeveldt, et al. (1994). Mathematical Modelling of Motions and Damaged Stability of Ro-Ro Ships in the Intermediate Stages of Flooding. Proc. 5th Int'l Conf. Stability of Ships & Ocean Structures (STAB'94), pp.717-729. Melbourne, Florida, USA.

Von Mises, R. (1957). Probability, statistics and truth. London; New York, Allen and Unwin; Macmillan.

Vose, D. (2008). Risk analysis : a quantitative guide. Chichester, England; Hoboken, NJ, Wiley.

WEKA. (2012). "WEKA Tank Level Instruments." Retrieved 05 March, 2012, from http://www.weka-ag.ch/frameset.cfm?contentpage=prodgroup%2Ecfm%3Fproduktegruppe_id%3D2&pg=2.

Wendel, K. (1968). Subdivision of Ships. Diamond Jubilee International Meeting, New York.

WINEL. (2012). "WINEL Safety at Sea Level, Watertight Sliding Doors, Watertight Doors." Retrieved 05 March, 2012, from http://www.winel.nl/watertight-sliding-doors-watertight-doors.html.

Winkler, R. L. (1972). An introduction to Bayesian inference and decision. New York, Holt, Rinehart and Winston.

Winkler, R. L. (1996). "Uncertainty in probabilistic risk assessment." Reliability Engineering & System Safety 54(2–3): 127-132.

Woodburn, P., P. Gallagher, et al. (2002). "Fundamentals of Damaged Ship Survivability." Transactions of Royal Institution of Naval Architects pp. 143-163.

WYLER. (2012). "Projects with WYLER products, WYLER AG CH - 8405 WINTERTHUR / SWITZERLAND." Retrieved 17 March, 2012, from http://www.wylerag.com/pages_eng/e9_3.html.

Yuen, K.-V. (2010). Bayesian methods for structural dynamics and civil engineering. Oxford, Wiley-Blackwell.

Zadeh, L. A. (1965). "Fuzzy sets." Information and Control Theory 8: 338-353.

Zaraphonitis, G., A. Papanikolaou, et al. (1997). On a 3-D Mathematical Model of the Damage Stability of Ships in Waves. Proc. 6th Int'l Conf. Stability of Ships & Ocean Vehicles (STAB'97). Varna, Bulgaria: pp. 233-244.

Zhang, S. (1999). The mechanics of ship collision. PhD, Technical University of Denmark.

Appendix 1

Ship Stability Standards Development

A1: A Review of Ship Stability Standards Development

The Merchant Shipping Act of 1854 is the first known legal requirement addressing ship safety at sea and concerning watertight subdivisions. It led to the adoption of the first internationally agreed system of subdivision in SOLAS 1929 after the Titanic catastrophe in April 1912. Then, the first damage stability requirements were introduced following the 1948 SOLAS convention, in which a positive residual metacentric height (GM) was required by a damaged ship. The first specific criterion on residual stability standards was introduced at the 1960 SOLAS convention with the requirement for a minimum residual GM of 0.05m. This represented an attempt to introduce a margin to compensate for the upsetting environmental forces.

Afterwards, the first probabilistic damage stability rules for passenger ships deriving from the work of Kurt Wendel on "Subdivision of Ships", (Wendel, 1968) were introduced in the late sixties as an alternative to the deterministic requirements of SOLAS 1960. Subsequently the 1974 SOLAS convention adopted Rahola's proposals (Rahola, 1939) of using the properties of the righting lever (GZ) curve to measure stability. Simultaneously IMO published Resolution A.265 (VIII), to address subdivision and damage stability on a probabilistic basis as equivalent to SOLAS deterministic rules. The next major step change in stability standards took place in 1992 with the introduction of SOLAS part B-1 (Chapter II-1), containing a probabilistic standard for cargo vessels, using the same principles embodied in the 1974 regulations.

Following the Estonia accident with the loss of 852 lives and a public outcry, "Stockholm Agreement" was reached by the North West European Nations in December 1994. In the 1995 SOLAS Diplomatic Conference, SOLAS 1990 was adopted as a global safety standard of damage stability. Based on proposals put forward by the Panel of Experts on the safety of roll on-roll off passenger ships, which was established following the sinking of the Estonia, the conference adopted a series of amendments to SOLAS 1974 (in force from 1st July 1997) related to the stability of Ro-Ro passenger ships in Chapter II-1: i) A new regulation 8-2 was accepted, containing special requirements for Ro-Ro passenger ships carrying 400 passengers or more. This was intended to pass out ships built to a "one-compartment

standard" and ensure that they could survive without capsizing with two main compartments flooded following damage; ii) Resolution 14 – "Regional agreements on specific stability requirements for Ro-Ro passenger ships" was adopted, which permitted regional agreements to be made on special safety requirements for Ro-Ro passenger ships if it was considered that prevailing sea conditions and other local conditions required specific stability requirements in a designated area. This agreement has subsequently been adopted across all EC States by the Directive 2003/25/EC (EC, 2003).

In 2006, a revised SOLAS 1974 Chapter II-1 was adopted with entry into force set for 1st January 2009 (IMO, 2006c-b). This revision has taken into account the results of the HARDER research project and was intended to harmonize the provisions on subdivision and damage stability for passenger and cargo ships. The amendments were based on the "Probabilistic" method of determining damage stability, on the basis of the detailed study of data collected by IMO relating to collisions. The probabilistic concept is believed to be far more realistic to addressing damage stability than the previously used "deterministic" method.

Appendix 2

ITTC Benchmark Testing

A2.1: The 23rd ITTC Benchmark Study

The selected ship for this investigation was a Ro-Ro Passenger ship (i.e. Length = 170 m). The model tests have been carried out at the SSRC (Universities of Glasgow and Strathclyde) according to the Model Test Method of IMO SOLAS'95, Resolution 14 (Vassalos and Jasionowski, 2000). In this study, a midship damage condition was defined as described in SOLAS 1997 (IMO, 1997). Wave conditions were set in the benchmark guidelines (Umeda and Papanikolaou, 2000). In turn, the range of tests was conducted in both regular and irregular beam seas.

The first international benchmark study was completed on December 2001 reported by (Papanikolaou, 2001) with the participation of the following five organizations:

1) Flenburger Schiffbau Gesellschaft (FSG)
2) Maritime Research Institute Netherlands (MARIN)
3) National Technical University of Athens (NTUA)
4) Osaka University
5) Ship Stability Research Centre, Universities of Glasgow and Strathclyde (SSRC).

All the numerical models employed are non-linear time domain potential flow codes, based on strip theory or 3D panel methods with different damping models. The floodwater is generally considered as variable masses moving within the flooded compartments and interacting with the ship. The floodwater free surface condition is modelled as either plane and horizontal or plane and free movable. Water ingress/egress through the damage opening is estimated based on Bernouilli's dynamic pressure head equation.

The results presented by all the participants suggest the need of further research in roll damping models, hydrodynamic coefficients of damaged ships, floodwater dynamics and its coupling with ship motion.

A2.2: The 24th ITTC Benchmark Study

Based on the deficiencies identified in the predictions in the first benchmark study, further development of this work was agreed and initiated. The basic objective of the second benchmark study was to provide insight into the basic properties of the numerical methods employed for the prediction of motions and capsizing of damaged ships in waves.

The 2nd benchmark study was completed on December 2004. Some detailed results can be found in (Papanikolaou and Spanos, 2004a) (Papanikolaou and Spanos, 2004b). The participants are listed below:

1) Instituto Superior Tecnico de Lisboa (IST)
2) Korea Research Institue of Ships and Ocean Engineering (KRISO)
3) Maritime Research Institute Netherlands (MARIN)
4) National Technical University of Athens, Ship Design Laboratory (NTUA-SDL)
5) Ship Stability Research Centre, Universities of Glasgow and Strathclyde (SSRC).

This benchmark study was divided into two phases. In the 1st phase, the ship models were numerically tested in calm water conditions. In the 2nd phase, the effects of wave induced forces were considered. However, the published results referred to the 1st phase only. A range of benchmark tests regarding the free roll motion of ship models in calm water has been defined as below:

- The Ro-Ro passenger ship (PRR01[1]) that has been tested in the first benchmark study was used to perform a new test in damaged condition. The test started with the damage compartment fully flooded and the damage opening remained open during the test. The main interest of this test was placed on the flooding process and the floodwater dynamics.
- The model of a tanker (length = 310.2 m) was tested in partially flooded conditions. The model had one rectangular compartment amidships. There was

[1] The ship model has been tested in systematic model experiments within the E.U. funded research project NEREUS (2000), HARDER (2000-2003).

no damage opening and subsequent flooding process. The test focused on the floodwater dynamics and its effect on ship motions.

- A second Ro-Ro passenger ship (PRR02[2]) (length = 174.8 m) was tested in transient flooding. The test started with the intact equilibrium condition. Following this, a standard SOLAS damaged opening was released and the water ingress was initiated. The flooding process was of dominant significance in this study. No experimental results have been published for further comparison.

The basic attributes of all the participating numerical methods in this study are summarized in Table A2.1 in (Papanikolaou and Spanos, 2004b).

Table A2.1: Basic attributes of the applied numerical methods in the benchmark study

Attribute	**Numerical Method**				
	P1	**P2**	**P3**	**P4**	**P5**
Ship's degrees of freedom	6	6	6	4	6
Strip theory	*	*		*	*
3D panel method			*		
Hydrostatic forces by direct integration	*	*	*	*	*
Incident wave forces by direct integration	*	*	*	*	*
Memory effects	*	*	*	*	*
Semi-empirical roll viscous	*		*	*	*
Roll viscous analysis in components		*			
Floodwater with horizontal free surface		*		*	*
Floodwater with moving free surface	*		*		
Internal motion by shallow water equations				*	
Flooding by simple hydraulic model	*	*	*	*	*

Some remarks were concluded based on the results of 1st phase:

- Regarding the test of Ro-Ro passenger ship in damaged condition, it was observed that the prediction of roll damping effects appeared unsatisfactory. Special attention should be given to the employed semi-empirical roll damping models.

[2] The ship model has been tested in systematic model experiments within the E.U. funded research project HARDER (2000-2003).

- Concerning the tested tanker case, numerical methods that consider the floodwater having its free surface being continuously horizontal could not properly capture the floodwater dynamics.

- The results of the transient flooding tests showed that the semi-empirical flow coefficients for openings (discharge coefficients) affect the simulated results significantly.

A2.3: The 25th ITTC Benchmark Study

The first part of the 25th ITTC benchmark study was carried out in conjunction with the European research project SAFEDOR (2005-2008). As a continuation of the two earlier benchmark studies, this work persisted in reviewing the developments in numerical models in a comparative way: i) concerning the prediction of survival wave heights of a damaged Ro-Ro passenger in waves, ii) concerning the sensitivity of the numerical predictions on basic simulation parameters (e.g. the ship loading condition, the spectral sea wave period, the roll viscous damping and the discharge coefficients). Four institutes participated in the 1st sub phase study:

1) National Technical University of Athens, Ship Design Laboratory (NTUA-SDL)
2) Ship Stability Research Centre, Universities of Glasgow and Strathclyde (SSRC)
3) Maritime Research Institute Netherlands (MARIN)
4) Instituto Superior Tecnico de Lisboa (IST).

Moreover, in order to contribute to the IMO's work programme titled "time-dependent survivability criteria of passenger ships", this benchmark study also assessed the length of time to sink or capsize (time-to-flood) for damaged passenger ships by using existing tools. Five participants were involved in this study:

1) Ship Stability Research Centre, Universities of Glasgow and Strathclyde (SSRC)
2) Helsinki University of Technology (TKK)
3) Maritime Research Institute Netherlands (MARIN)
4) Maritime and Ocean Engineering Research Institute (MOERI)
5) National Technical University of Athens, Ship Design Laboratory (NTUA-SDL)

On the one hand within the SAFEDOR project, as reported in (Papanikolaou and Spanos, 2008), the Ro-Ro passenger ship (PRR02) with the midship damage scenario that has been used in the 24th ITTC benchmark study was selected for investigating the numerical prediction of damage stability in waves. Key findings could be drawn from the delivered simulation results:

- It appeared that the survival boundaries predicted through the two codes (P1 and P4) matched well with the experimental results, as shown in Table A2.2.

- The numerical estimates on survivability of the benchmarked ship were found to be most sensitive to the ship loading condition (e.g. KG) and the periods of waves, while less sensitive to the discharge coefficients.

- The effect of viscous roll damping was small, but it appeared to challenge the conclusions from the 24th benchmark test results.

Table A2.2: Survival Boundary in (m) for the Basic Test Case

Participant	H_s, surv	Mean	Diff. from mean	Exp.
P1	3.23	3.00	+0.23	≤3.00
P2	1.75		-1.25	
P3	4.00		+1.00	
P4	3.00		+0.00	

On the other hand, looking into the benchmark testing on numerical methods for the prediction of time-to-flood of damaged ships in waves, two sub phases of studies were conducted as defined below:

1. A benchmark study based on a barge for which detailed model experimental data (tested at the Helsinki University of Technology, TKK) was available, as presented in (Ruponen, 2006) ;

2. A benchmark study was based on a realistic passenger ship (designed by SSRC) with complex internal geometry. No model test data was available.

Based on the delivered results of the 1st sub phase study, it was concluded that: i) the prediction of flooding rates, especially for unventilated or partially ventilated compartments showed large variations; ii) most of the tools/codes could provide a reasonable prediction of the equilibrium position after flooding and iii) rational time-to-sink predictions appeared feasible by most tools/codes, at least for ships having a relatively simple internal configurations and interconnections between flooded compartments under calm water conditions.

Alternatively, regarding the 2nd sub phase testing of the time-to-flood for a large passenger ship with complex interior layout, there was no experimental data available to conduct a true benchmark study. Due to the complexity of the simulation, only two participants (i.e. SSRC, MARIN) completed this study. The results indicated that: i) for the most severe flooding and sea conditions there were considerable differences in the predictions from the two numerical codes for the time-to-flood and ii) the true performance of the current codes could be evaluated when accurate experimental model benchmark data was available for comparison.

Appendix 3

Decision Support System for Crisis Management

In the event of a ship sustaining damage due to an accident / incident, applicable information (e.g. damage stability, fire safety) is crucial for the officers (the master) on the bridge (the master) to make a decision on the best course of action with severe time constraints to mitigate the risk to life, environment and property.

In this respect, there are a number of instruments that can be used by the master to evaluate the state of the vessel after damage. Relative reviews are outlined in the following context.

A3.1: Documented Damage Stability Information

As far as a flooding-related damage is considered, relevant requirements are already in place necessitating a list of minimum level of information concerning damage controls to be provided to the ship's officers, i.e. SOLAS regulation II-1/19 (IMO, 2006b-a), and guidelines in (IMO, 2007) (DNV, 2011) (MCA, 2012). The primary damage stability information to be provided to the master consists of two sets of printed documents: damage control plan and damage control booklet, which intent to provide clear information on the ship's watertight subdivisions and equipments related to maintaining the boundaries and effectiveness of the subdivisions. Therefore, in the event of hull breach with flooding, proper precautions can be taken to prevent progressive flooding through openings and effective actions can be initiated quickly to mitigate and recover the ship's loss of stability.

The damage control plan is a set of scaled graphic presentations, which indicate the locations and arrangements of important flooding-control instruments (e.g. watertight boundaries, cross-flooding systems, watertight closing appliances, doors in the shell of the ship, weathertight closing appliances, all bilge and ballast pumps and associated valves), as illustrated in Figure A3.1. On the other hand, the damage control booklet is a reference containing the following information:

1) Repeated information listed in the damage control plan;
2) General instructions for controlling the effects of damage (e.g. immediately closing watertight and weathertight closing appliances, establishing the locations and safety of persons on board to ascertain the extent of damage);

3) Additional details to the information shown on the damage control plan (e.g. location of flooding detection systems, sounding devices, pump capacities, piping diagrams);
4) Locations of non-watertight openings and guidance for the conditions of unsymmetrical flooding ;
5) The results of the subdivision and damage stability analyses based on the assumed flooding scenarios;
6) The criteria which the damage stability analyses are based on (e.g. the initial conditions of the ship's loading, locations of damage, permeability).

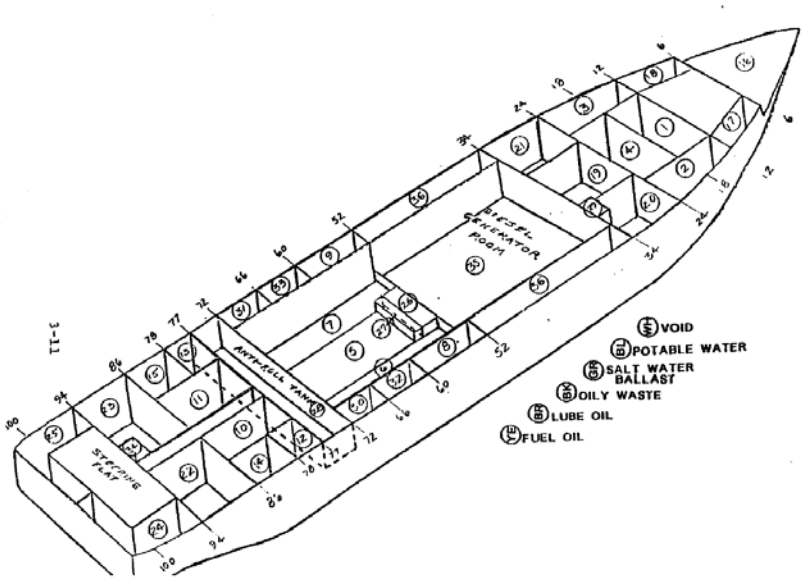

Figure A3.1: An Example of a Damage Control Plan (MMA, 1993a)

Obviously, the documented ship stability information aims to provide the master with assistance on how to ascertain the immediate conditions of the ship and, if satisfactory, what actions may be taken to mitigate the operational risk level. The main benefits and limitations of this instrument are pointed out as below:

Merits:

- The damage control documents represent a fast and clear source of information for approximating ship damage stability. Based on the pre-prepared graphical plan and descriptive guidance, a list of survivable damage

conditions are laid out in a concise manner so that the master can make decisions accordingly.

- The information is presented in a printed and documented form, which can be more reliable than the electricity-powered systems in emergency situations.

Limitations:

- To comply with the minimum requirement of the damage stability information for use on passenger ships (as specified in the new SOLAS regulation II-1/19), a broad range of drawings, diagrams and plans will be generated. In this case, the more damage scenarios postulated the more complex that the book is to be carried on board. As a result, its applicability would greatly abate when the user is under pressure.
- The presented damage stability calculations are based on the assumed initial conditions including ship's loading, extents of flooding, permeability, etc. Hence, they can only be used as a rough guidance to assist the master onboard in estimating the ship's relative survivability. For instance, investigations have revealed that ship actual loadings often deviate from the ones used for generating stability information booklet at the design stage (IMO, 2006b-b).
- Due to the large number of variables characterising each damaged scenario, it becomes practically difficult to exhaustively consider all possibilities and compile a comprehensive damage stability book. Hence, the support information should be used with extreme caution due to the discrepancy between the actual casualty case and the one assumed in the book.

A3.2: Loading Computers Rules, and Regulations

The deployment of loading computer systems on the bridge provides a means of obtaining real-time information on stability and structural strength. Although such a system in its current form is regarded only as supplementary to the loading manual and the stability booklet (DNV, 2012a), more installations are observed onboard passenger ships in relation to the add-on requirements in SOLAS Regulation II-1/20 (IMO, 2006b-a).

With the introduction of a series of standards and guidelines (BS, 2006) (DNV, 2012a) (IMO, 1997b) (IMO, 1998a) (IMO, 1998b) (IMO, 1999), it can be seen that an increasing number of software systems have been tailored to be installed on the bridge (Autoship, 2011), as shown in Figure A3.2. Their applications are not restricted only to checking ship stability prior to departure, but also the appraisal of residual stability and strength from flooding following damage. Both strength and weaknesses of using loading computers are studied next.

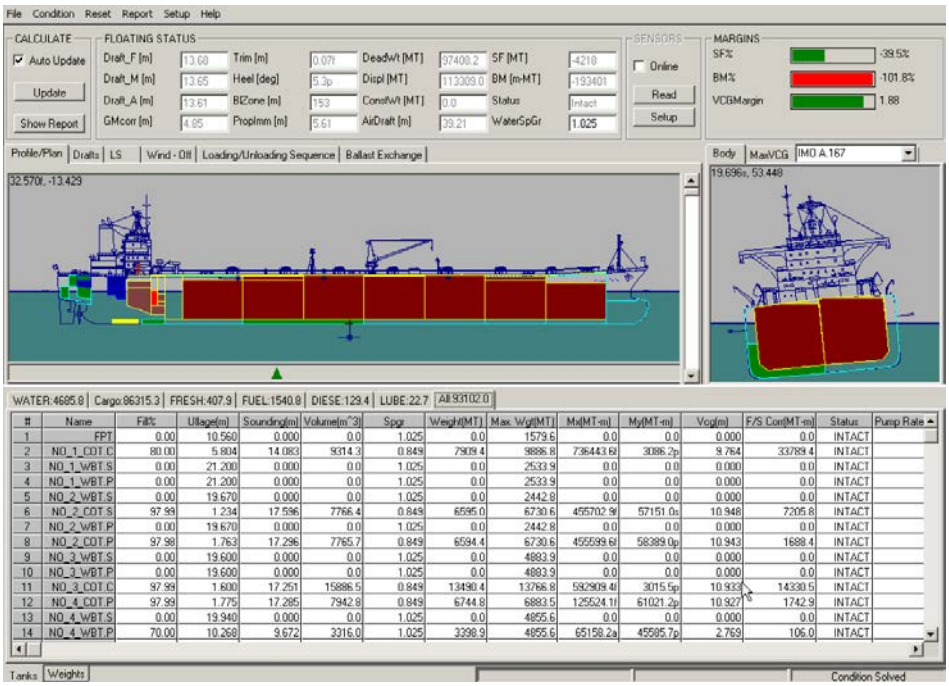

Figure A3.2: A Snapshot of Autoship's AutoLoad Loading Computer Interface

Merits:

- These systems are capable of providing real-time information to the master (e.g. with actual ship loading conditions). In particular, if the input loading data is obtained directly from remote sensors (e.g. automatic draught gauge system), the efficiency and accuracy in the assessment of damage stability can be improved considerably.
- Due to the interactive nature, the system can be used to run “What-if” analysis to check remedial actions or further flooding scenarios.

Limitations:

- It can be expected that the system (especially for damage stability calculation functions) will be used rarely, prompt and proficient operations of the system can be difficult to achieve.
- It requires special training programs to be conducted for the personnel to work on the computer programs.
- The essential concept of the formulations for damage stability calculations is derived from a hydrostatic point of view, the lack of consideration of the time factor and environmental impact in the current appraisal can penalise the quality of predictions.
- Given “what if” analysis is performed to identify appropriate remedial actions and considering the amount of possible alternatives, it can be a time-consuming process to identify the most suitable one(s).

A3.3: Emergency Response Service (ERS)

The requirement of shore-based emergency response service, in its current form, is made mandatory only for oil tankers according to Annex I of MARPOL 73/78 (IMO, 2006c-a) and the Oil Pollution Act (OPA) 90 requirements in USA following the disaster of "*Exxon Valdez*" accident (OPA, 2012). Nevertheless, due to the additional safeguard provided by the service, it can be an attractive option for other ship types (in particular passenger ships) to assist the decision making process in emergencies.

The ERS can be provided by the owners' shore-based system or a third party (e.g. classification societies). The major players include DNV Emergency Response Service (ERS) (DNV, 2012b), Ship Emergency Response Service (SERS) from Lloyd's Register (LR, 2012), Rapid Response Damage Assessment (RRDA) from ABS (ABS, 2010), and BV's Emergency Response Service (BVERS) (BV, 2010).

One of the core services with ERS is the remote calculation of ship damage stability, residual strength, and grounding force so as to provide timely assistance to the master on the bridge. Advantages and challenges offered by shore-based ERS are elaborated as follows:

Merits:

- With the subscription of this service, there is no need to deploy dedicated personnel on board to learn the software (functions) concerning the assessments of damage stability and residual strength.
- As shore-based teams generally employ experienced naval architects and specialists to provide technical support when crew are in a very stressful situation, the chance of making elementary errors by using on-board loading software can be avoided.
- Detailed "what if" scenarios can be carried out by using various software platforms with service providers, so that appropriate remedial actions can be identified.

Limitations:

- The service can be costly, particularly with those operators having a large number of ships in the fleet. Considering the already very tight profit margin and intensity of competition among ship owners/operators, it could be an extra burden imposed by such persistent investment.
- The current practice with remote ship survivability assessment still requires a significant amount of information to be exchanged between the officers on the bridge and the shore, which may cause significant delay due to relaying of information.
- The quality of remote assessment relies heavily on the accuracy of the information transferred between the vessel and the response team, which can be very difficult to assure in emergency situations, such as the exact loading condition, damage characteristics and sea conditions measured on board and the response actions advised from shore-based naval architects.
- In the process of decision making, it is very important for the involved personnel in the response team to have very good knowledge of the vessel and well understanding of her status, so that the most appropriate actions can be taken in time. Nevertheless, this may not be an easy task as the ERS service providers generally hold a large number of subscribers worldwide.
- Upon receiving relevant information from the damaged ship, the effort needed to establish the models for the reported case and the subsequent evaluation can take a significant time to implement. In particular, if first-principles tools are deployed for damage stability assessment, the response time will be seriously prolonged, which is not acceptable.

A3.4: Automated Decision Support Systems (DSS)

The need for decision support systems dedicated for assisting shipboard damage control is due to the acknowledgement of the criticality of taking prompt actions to address onboard accidents, which could potentially lead to disastrous consequences. In this respect, the demand is even more critical for flooding-related accidents as they generally lead to significant damages to the property, not mentioning the large number of fatalities a single flooding case can claim.

Historical experience suggests that one of the critical factors contributing towards the heavy losses in flooding accidents is the fact that the officers on the bridge have very limited time to effectively and confidently implement the three key aspects, which are the essential functions to be addressed by a DSS:

1) Synthesising key real-time information on ship status and damage details;
2) Predicting ship behaviour using the collected information on a scientific background;
3) Providing recommendations on actions to be taken through evaluations of the appropriateness of a list of promising control measures.

As a result, growing endeavours are observed in the maritime industry in recent years aiming to develop intelligent decision support systems so as to provide the master with real-time assistance. During this process, it is worth noting that naval vessels pioneered the research work in developing pertinent DSSs, as damage control operations are more essential to be considered within their life-cycle (Runnerstrom, 2003) (Calabrese et al., 2012) (Martins and Lobo, 2011).

Allowing for the three key functions to be included in a DSS, there is a number of pioneering research focusing on these elements.

a) Information Collection and Synthesis

For information synthesis, the rapid advancement in information technology and pertinent applications in electronic products has enabled the installation of various types of shipboard sensors at negligible costs. These include generic tank level gauge systems installed for loading assessment (API, 2012) (WEKA, 2012), status of watertight doors and fire doors (WINEL, 2012), and flooding detection systems to be installed onboard passenger ships (IMO, 2008c).

Furthermore, a 3D virtual environment was developed in (Varela and Soares, 2007), which integrates real-time information from shipboard sensors and simulates it in a dynamically updated platform, as illustrated in Figure A3.3. By doing so, the officers on the bridge can monitor the ship's systems and conditions simultaneously in various compartments in the event of damage.

Figure A3.3: A snapshot of the 3D Virtual Environment (Varela and Soares, 2007)

b) Prediction of Ship Behaviour

Although the GZ curve is a standard mechanism to be equipped by majority of shipboard loading software systems to evaluate residual stability. Nevertheless, it is widely acknowledged that the current approach for survivability assessment pays little attention on the actual damage details, the instantaneous environmental conditions, and the time factor. Hence, there is a growing effort to predict the dynamic behaviour of a ship after damage by developing first-principles tools.

In fact, technological advancement in computing power over the last fifteen years has facilitated the solution of many computationally challenging problems in the engineering sector in ever decreasing amount of time. Moreover, the progress in understanding the universe through modelling based on the fundamental physical laws has been significant as well. In the case of approximating the dynamic behaviour of a damaged ship in the seaway, there is a growing number of published works attempting to achieve advanced prognosis. The prediction of ship response to flooding progression can be simulated through: i) direct solution to conservation of momentum laws (Letizia and Vassalos, 1995) (Letizia, 1996) (Jasionowski, 2001a) (Papanikolaou et al., 2000) (Schreuder, 2008) (de Kat Jan and Peters, 2002), ii) or quasi-static iterative approximations (Ruponen et al., 2007) (Varela and Soares, 2007).

In this process, it is worth noting the predictive function proposed in (Jasionowski, 2011), which is one of the very few pioneering research focusing on real-time subdivision management for crisis management. The Vulnerability Log (VLog) module, as illustrated in Figure A3.4, is designed to inform the crew at all times on the instantaneous vulnerability to flooding of the vessel, considering its actual loading conditions, the environmental conditions and the actual watertight integrity architecture. The vulnerability is proposed to be measured in terms of the probability that a vessel might capsize within given time when subject to any feasible flooding scenario.

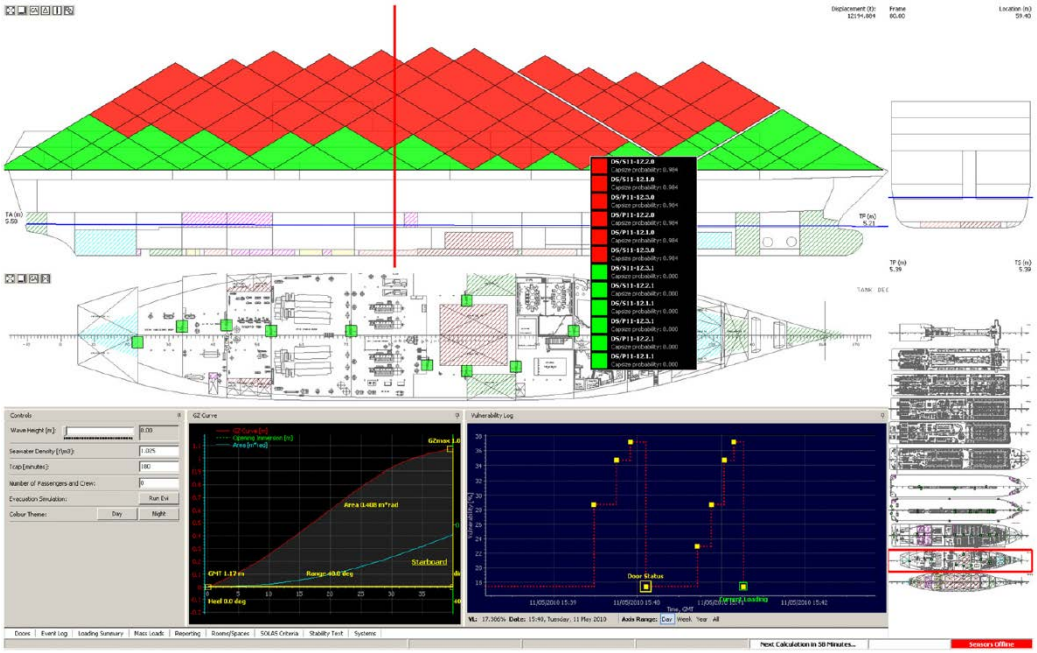

Figure A3.4: A Snapshot of the VLog Interface for Vulnerability Prediction

These progresses represent a significant step forward for predicting ship dynamic behaviour in damaged conditions. However, the following difficulties still requires further work:

- Time consuming feature: Due to the computational complexity to perform time-domain calculations, it is still a challenging task for the first-principles tools to provide timely predictions, even with today's supercomputers. There is a time lag of several hours, which is obviously unacceptable. Although it is expected that the computing power will increase rapidly, it would still be very difficult to bring the computation time from the magnitude of "hours" to the magnitude of "seconds"
- Uncertainty of the input information: It has to be appreciated that the quality of the input information for detailed simulation can play an important role on the outcome. Nevertheless, accurate estimations of the damage characteristics and the environmental conditions are difficult to obtain in emergency situations. Hence, the effect of uncertainties associated with the input information can easily propagate and undermine the subsequent consequence analysis.

- Uncertainty of the model: the first-principle techniques are generally recognised as a simplified way to approximate the physics governing the interested phenomenon. Hence, the inherent uncertainties resulted from the underlying assumptions and simplifications will inevitably affect the computation quality.

Consequently, the question as how to make an effective (fast) prediction of ship behaviours after damage allowing for inherent uncertainties in modelling, remains as a key challenge before the true deployment of such predictive instrument on the bridge for crisis management.

c) Advice Module

With the assessed ship damage stability in time-domain, it is necessary for the DSS to recommend a list of best course of actions to be taken in order to mitigate the potential risk. Such an advice module entails a two-stage process: i) identification of a list of possible actions, ii) prioritisation of the action list to identify the most adequate damage control operations.

In this respect, two separate treatments are needed. The former requires the setup of a knowledge bank of remedial operations. The latter needs appropriate optimisation algorithms to be implemented so that the list of remedial operations can be prioritised on the basis of pre-defined evaluation criteria.

A knowledge-based decision support system was developed for naval vessels in (Calabrese et al., 2012), which is capable of centralising real-time readings from all related sensors and visualizing actions from a pre-defined procedural checklist when handling emergency situations. A similar work is proposed in the FLAGSHIP project (FLAGSHIP, 2008), in which a DSS is elicited to provide the crew with the action checking lists for damage control, as illustrated in Figure A3.5 (Randall and Varelos, 2008) (Allen et al., 2009). Nevertheless, it is worth emphasising that these platforms make use of pre-documented action lists without much prioritisation process. As a result, they are more suitable to provide generic guidelines and checklists for the officers to appraise.

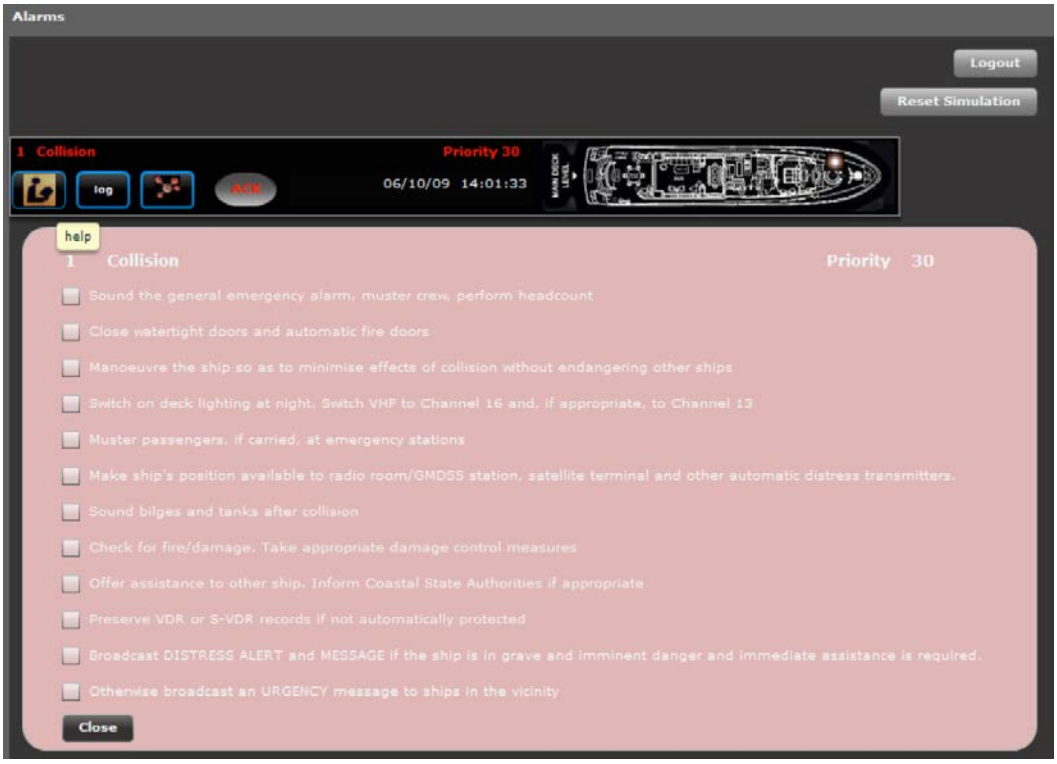

Figure A3.5: A Snapshot of the New Decision Support System in the FLAGSHIP Project (Allen et al., 2009)

On the other hand, considering the virtually multi-criteria optimisation process, relevant Artificial Intelligent (AI) techniques have been applied in this area (Russell and Norvig, 2010). For instance, the Genetic Algorithm (GA) is employed in (Martins and Lobo, 2011) and (Hou et al., 2009) to optimise the searching process to evaluate the appropriateness of available control options. Moreover, the Case-based Reasoning (CBR) technique is deployed in (Vassalos et al., 2004c) (Olcer and Majumder, 2006) to prioritise the damage control options.

With the rapid evolvement in computer science, it is expected more intelligent learning techniques will emerge. Nevertheless, in acknowledging the inherent multi-criteria optimisation characteristics, great emphasis should be placed on the definition of evaluation criteria. In the respect, the limitations can be outlined for the current practice:

- Although it is recognised that the decision making process for crisis management is time critical, a time-based damage stability criterion has yet to be defined. This is attributed to the stochastic nature of time to capsize. As a result, the current criteria concentrate mainly on employing the fragmented time-related elements as the evaluators, such as the time needed to set off the drainage of the flooded compartments, and the time needed to implement the ballast operations.

- Regarding the requirements on damage stability applied at the ship design stage, the residual stability is mainly evaluated through the properties of the GZ curve. Therefore, the difference between GZ particulars in the damaged condition and that as required in the regulations can be included as an indicator of ship survivability. Nevertheless, the hydrostatic stability calculations provide little information on time-related information. Furthermore, the current rules are often considered as a set of the minimum requirements on damage stability to be complied in the design process. Thus the identified criteria of the minimum residual GZ reflect only the minimum level of ship safety status, which suggest limited information on how safe the damaged ship is.

- Uncertainties associated with the process of predicting ship behaviour could potentially challenge the quality of the outcome (i.e. ship vulnerability to flooding in time domain). Hence, how to effectively quantify the underlying uncertainty in assessment of ship survivability is vital to be addressed properly for the decision support process of flooding crisis management.

Appendix 4

Validation Studies on Time to Capsize

Table A4.1: Summary of Experimental Studies on Time to Capsize

No. of Runs	Hs [m]				
	2	2.5	2.6	2.75	3
1	1800	1800	1800	921	543
2	1800	1358	1024	1116	570
3	1800	1800	1800	847	591
4		1800	1800	708	554
5		1800	766	674	653
6		1800	916	1129	453
7		1800	1800	1034	785
8		1800	1446	1800	886
9		1800	1781	894	848
10		1800	1297	886	725
11		1800	1249	705	878
12		1800	764	1136	587
13		1800	911	1800	525
14		1800	1297	1138	767
15		1800	1800	1046	565
16		828	1800	1228	579
17		1800	1023	1800	615
18		1800	978	1800	600
19		1800	1800	1779	548
20		1800	959	1787	565

Table A4.2: Summary of PROTEUS3 Simulations with Fixed Damage Size, Time to Capsize [s] for A Range of Sea States

No. of Runs	Hs [m]								
	2	2.1	2.2	2.3	2.4	2.5	2.75	3	3.25
1	2000	2000	2000	2000	2000	2000	757.69	251.61	174.99
2	2000	2000	2000	2000	2000	614.76	450.16	343.3	522.83
3	2000	2000	343.69	2000	174.69	684.68	589.36	316.37	281.65
4	2000	2000	2000	2000	2000	228.54	446.68	510.79	255.04
5	2000	2000	2000	2000	919.14	1320.7	787.61	553.59	219.67
6	2000	2000	2000	2000	2000	478.64	384.17	337.2	488.94
7	2000	2000	2000	2000	412.9	1312.89	233.28	180.71	552.09
8	2000	997.27	2000	285.67	2000	2000	556.6	385.97	272.65
9	2000	2000	231.92	315.89	2000	155.5	246.68	650.33	643.34
10	2000	2000	312.47	1174.33	2000	188.85	866.15	378.95	211.14
11	2000	2000	2000	2000	202.05	966.79	373.19	167.07	287.85
12	2000	2000	445.82	1929.78	2000	395.44	680.58	475.83	248.86
13	2000	2000	2000	2000	2000	888.33	172.97	184.66	192.18
14	2000	2000	2000	2000	722.54	1182.43	405.08	245.43	165.01
15	2000	2000	2000	2000	2000	1139.69	714	395.41	184.39
16	2000	2000	2000	2000	1129.07	192.58	478.4	222.7	270.06
17	2000	2000	2000	153.23	586.45	713.5	743.84	271.07	705.06
18	2000	2000	2000	307.04	2000	2000	194.58	477.83	416.61
19	2000	2000	792.64	2000	726.79	822.9	354.14	277.94	255.35
20	2000	2000	2000	1573.34	1312.61	640.02	381.25	272.23	126.71

Table 3: Summary of PROTEUS3 Simulations. 500 Damages based on MC Sampling. Time to Capsize [s] for A Range of Sea States

No. of Runs	Hs [m]									
	1.5	**2**	**2.5**	**3**	**3.5**	**4**	**4.5**	**5**	**5.5**	**6**
1	2000	2000	899.192	202.347	322.511	292.092	189.332	218.294	178.727	1665.029
2	2000	2000	2000	2000	2000	2000	2000.042	2000.043	140.797	2000
3	2000	2000	2000.016	2000	2000	185.011	2000.05	2000	2000	2000
4	2000	803.885	2000	120.389	243.508	219.727	139.886	77.339	127.164	73.119
5	2000	2000	812.416	319.509	205.602	224.242	213.556	103.681	169.349	734.705
6	2000	2000	151.881	537.637	159.467	228.191	273.595	162.924	205.98	153.151
7	2000	2000	1238.39	455.026	353.345	159.455	232.586	347.916	321.598	940.258
8	2000	2000	455.457	449.121	60.579	565.948	68.178	248.431	57.494	55.847
9	2000	2000	283.364	344.746	175.145	219.868	291.762	210.783	137.985	165.528
10	2000	2000	2000	2000.001	2000	2000	2000	2000	2000	2000
11	2000	2000	357.281	233.986	75.019	110.041	107.884	157.145	83.835	332.705
12	2000	2000.008	298.437	153.695	227.688	230.23	279.405	380.054	157.124	1849.907
13	2000	2000	801.699	86.953	815.114	445.658	59.906	93.178	1405.879	456.823
14	2000	2000	1350.816	450.684	194.039	286.713	188.61	593.286	605.142	855.588
15	2000	2000	2000	270.452	616.256	228.199	311.373	230.286	233.841	1394.19
16	2000	2000	703.082	340.782	375.463	205.124	202.39	70.985	165.137	136.81
17	2000	2000	249.77	234.583	227.77	187.935	302.881	182.175	1645.233	102.595
18	2000	2000	2000	2000	1057.244	2000.038	1228.02	2000	2000	867.095
19	2000	2000	2000	734.603	490.103	433.191	131.849	292.4	466.536	76.255
20	2000	2000	503.753	337.759	338.535	852.351	195.186	1433.115	677.853	74.635
21	2000	2000	2000	234.642	440.464	185.315	258.707	349.232	369.888	160.553
22	2000	2000	2000	2000	2000	2000	2000	2000	2000	2000
23	2000	2000	2000	265.731	305.051	163.312	175.426	208.084	269.48	310.878
24	2000	2000	459.027	367.27	326.577	91.886	64.869	145.36	62.229	58.181
25	2000	2000	216.124	147.623	138.271	165.594	54.937	148.196	53.252	218.983
26	2000	2000	2000	381.765	162.944	270.346	347.465	170.848	617.011	149.133
27	2000	2000	2000	237.526	185.99	383.903	292.177	239.627	272.932	271.338
28	2000	2000	2000	2000	2000	2000	2000.033	2000	2000	2000
29	2000	2000	827.903	473.457	183.61	157.287	273.97	268.501	244.064	791.91
30	2000	2000	661.194	78.182	232.07	403.297	96.821	80.249	75.656	101.829
31	2000	2000	2000	2000	981.892	2000	2000	2000	2000	86.799
32	2000	2000	2000	2000	2000	2000	2000	2000	2000	2000
33	2000	792.26	407.656	126.137	155.139	147.693	188.783	122.717	118.778	242.817
34	2000	2000	2000	2000	2000	2000	1092.343	2000	967.363	101.237
35	2000	2000	2000	325.592	261.032	350.506	157.68	201.06	229.081	536.009
36	2000	2000	692.758	269.894	503.81	228.472	236.14	419.684	430.665	308.747
37	2000	2000	316.84	221.755	102.764	111.429	81.847	78.98	67.126	88.741

38	2000	2000	2000	222.5	210.902	145.948	165.343	160.25	208.715	824.9
39	2000	2000	2000	415.304	584.268	211.232	174.341	423.167	562.892	343.147
40	2000	2000	2000	1977.097	556.693	81.968	329.408	63.678	734.557	70.77
41	2000	2000	2000	307.016	455.557	249.908	293.334	172.993	326.362	2000
42	2000	284.142	279.128	257.881	77.999	127.402	107.197	116.549	65.076	102.16
43	2000	2000	660.212	196.15	484.033	111.816	125.236	140.812	77.446	72.362
44	2000	2000	958.322	325.657	230.058	273.11	275.853	197.771	123.434	1185.57
45	2000	2000	2000	469.85	161.697	154.891	457.941	375.342	1552.889	2000
46	2000	2000	2000	2000	2000	1808.536	611.661	2000	2000	2000
47	2000	2000	867.656	2000	643.645	218.786	119.13	161.587	2000	201.335
48	2000	2000	2000	220.117	540.542	2000	1497.488	55.286	859.828	2000.014
49	2000	2000	2000	2000	2000	600.3	313.698	482.28	2000	988.19
50	2000	2000	2000	445.937	141.139	199.635	431.707	191.892	194.811	738.764
51	2000	2000	2000	327.323	270.988	373.209	141.605	315.602	214.917	222.804
52	2000	2000	160.726	279.756	109.748	180.54	229.396	126.794	92.306	83.222
53	2000	2000	885.757	195.916	506.969	437.138	74.488	66.359	77.585	93.087
54	2000	2000	2000	2000	2000	2000	2000	2000	834.986	1701.653
55	2000	2000	2000	2000	2000	2000	156.47	2000.007	2000	829.62
56	2000	2000	406.764	336.991	247.359	176.779	241.995	193.614	955.377	231.275
57	2000	2000	828.188	469.602	258.575	354.864	119.391	476.296	55.089	101.118
58	2000	1146.402	160.613	143.882	157.952	121.408	120.624	117.186	82.509	68.827
59	2000	2000	2000	1736.476	2000	702.857	1259.441	2000.001	635.183	2000
60	2000	2000	131.207	137.209	262.704	94.009	76.546	121.207	130.214	303.882
61	2000	2000	2000	2000	2000	1711.567	840.828	2000	2000	54.051
62	2000	2000	2000	2000	1480.21	2000.008	2000	2000	2000.02	2000.033
63	2000	2000	309.013	150.085	203.274	348.23	153.86	93.715	155.698	118.324
64	2000	2000	2000	242.969	242.685	218.134	242.685	228.584	382.94	427.314
65	2000	2000	849.539	427.262	306.193	313.352	311.643	260.412	325.484	369.352
66	2000	2000	545.816	560.6	230.626	217.929	295.511	187.174	212.982	537.497
67	2000	2000	2000	2000	2000	407.249	2000	2000	160.858	2000
68	2000	2000	2000	2000	2000	796.865	992.364	2000.034	474.138	915.787
69	2000	2000	2000	2000	1579.51	109.735	246.141	165.024	684.274	1369.274
70	2000	2000	2000	183.496	509.338	2000	775.557	55.818	2000	220.202
71	2000	2000	2000	787.686	139.37	249.998	65.232	142.847	127.912	56.637
72	2000	2000	2000	283.501	591.709	190.464	243.367	248.975	445.638	225.942
73	2000	2000	2000	2000	2000	2000	2000	2000	2000	2000
74	2000	640.102	85.508	111.021	86.256	111.015	103.249	190.323	182.593	82.023
75	2000	2000	690.16	378.133	230.747	308.343	142.271	527.544	710.796	688.034
76	2000	2000	589.357	2000	383.29	1362.147	535.549	829.781	266.664	822.78
77	2000	2000	2000	872.602	275.575	218.641	79.102	79.847	1866.832	633.714
78	2000	2000	240.066	444.422	354.373	343.209	143.727	257.706	217.77	211.693
79	2000	2000	2000	2000	2000	2000	1184.51	2000	2000	1029.005
80	2000	2000	2000	2000	2000	2000	2000.003	2000	2000	2000

81	2000	2000	2000	2000	1060.252	2000	2000	2000	2000	2000
82	2000	2000	2000	2000	2000	2000.028	2000	2000	2000.021	2000
83	2000	2000	221.578	290.889	147.291	200.391	114.725	203.851	629.972	371.025
84	2000	2000	2000	810.546	212.655	192.341	221.083	287.495	550.054	378.542
85	2000	505.067	120.713	122.451	172.098	248.325	220.697	80.67	96.275	84.107
86	2000	2000	2000	2000	164.576	278.27	385.403	475.589	777.086	1766.872
87	2000	2000	1800.608	247.513	245.35	303.918	207.275	258.835	204.146	371.443
88	2000	2000	2000	2000	338.045	525.613	1338.243	99.752	1984.84	1118.151
89	2000	2000	2000	210.339	361.485	215.997	212.52	519.787	1335.696	754.973
90	2000	2000	2000	547.202	132.202	48.215	57.241	53.839	91.179	53.8
91	2000	2000	2000	209.384	141.69	316.706	197.337	177.407	91.692	721.692
92	2000	2000	519.983	136.042	235.002	120.46	114.522	155.174	76.546	96.78
93	2000	2000	2000	2000	2000	2000	2000	2000	2000	594.465
94	2000	2000	2000	812.803	231.682	301.49	315.262	259.971	188.321	544.539
95	2000	2000	363.32	680.159	71.026	117.827	163.733	66.614	55.877	114.239
96	2000	2000	2000	317.279	660.412	200.056	293.78	290.28	183.151	804.929
97	2000	2000	2000	2000	810.296	479.968	396.82	734.549	755.63	942.795
98	2000	808.635	380.633	65.622	87.477	56.159	84.834	62.352	62.351	114.355
99	2000	903.736	526.25	127.414	87.51	168.773	2000	107.217	80.329	133.337
100	2000	2000	2000	394.536	611.768	306.721	235.042	347.697	461.903	1458.853
101	2000	2000	2000	2000.002	2000	2000	2000	944.691	2000	2000
102	2000	2000	1731.707	249.569	181.059	351.409	162.514	201.331	467.748	128.316
103	2000	2000	997.638	585.557	276.727	97.747	492.713	282.521	198.29	178.477
104	2000	2000	255.947	137.079	292.553	255.091	178.787	162.235	509.958	293.605
105	2000	2000	2000	846.468	176.03	221.874	240.903	137.059	517.989	489.159
106	2000	2000	2000	466.841	318.156	253.977	119.321	79.113	234.73	71.85
107	2000	2000	864.504	167.387	157.862	172.02	143.048	112.266	125.15	99.938
108	2000	2000	2000	886.239	2000	793.892	724.074	2000	2000.01	2000
109	2000	2000	180.956	182.656	168.349	140.396	118.545	177.351	187.023	109.459
110	2000	2000	2000	2000	2000	1834.433	2000	2000	1321.478	2000.017
111	2000	2000	2000	2000	1761.842	847.752	107.012	190.62	131.923	891.638
112	2000	2000	2000	430.555	499.086	279.131	185.767	121.465	267.561	794.55
113	2000	2000	2000	2000	2000	2000	2000	2000	2000.018	2000
114	2000	2000	2000	486.782	2000	2000	2000	1490.447	1572.198	557.837
115	2000	2000	2000	2000	2000.05	2000	2000	2000	1970.549	817.94
116	2000	2000	420.288	347.956	59.836	191.377	128.061	497.384	179.378	99.952
117	2000	2000	2000	2000	163.803	108.919	860.28	146.248	178.337	207.704
118	2000	2000	483.405	243.063	289.413	90.303	114.816	54.53	134.946	85.232
119	2000	2000	967.51	346.392	96.518	123.783	132	134.438	96.131	78.209
120	2000	716.824	158.231	114.772	143.209	68.524	95.661	96.046	56.075	77.715
121	2000	2000	692.03	2000	670.405	177.405	225.599	540.416	192.089	2000
122	2000	2000	2000	2000	2000	2000	709.944	2000	2000	78.181
123	2000	2000	2000	869.152	265.828	276.652	96.735	238.396	116.497	78.786

124	2000	2000	2000	2000	2000	2000	2000	2000	2000	2000.029
125	2000	2000	410.413	130.511	132.822	112.191	175.855	81.061	118	95.473
126	2000	2000	446.086	380.904	186.704	370.995	160.396	318.492	122.941	481.749
127	2000	2000	780.053	91.07	253.519	205.104	61.649	53.055	72.31	66.759
128	2000	2000	2000	2000	2000	2000	2000.013	2000	2000	2000
129	2000	2000	2000	2000	2000	2000	2000	2000	2000	2000
130	2000	2000	160.54	327.689	97.156	107.368	81.948	113.945	73.923	42.024
131	2000	2000	2000	2000	2000	2000	2000	2000	2000	1105.158
132	2000	2000	2000	2000	2000	2000	2000.037	2000	2000.031	2000
133	2000	2000	456.418	452.968	261.108	212.023	226.13	213.149	204.323	1083.872
134	2000	2000	2000	2000	2000	1232.756	97.794	2000	2000.008	2000
135	2000	2000	95.849	950.711	442.886	131.948	97.483	224.625	118.938	51.797
136	2000	2000	2000	2000	486.552	2000	2000	2000	2000	2000
137	2000	1099.637	416.093	118.332	136.461	87.455	159.958	116.247	129.35	201.513
138	2000	2000	795.769	927.892	215.008	166.667	144.784	49.449	63.341	100.292
139	2000	2000	2000	865.836	202.867	215.013	237.965	267.75	286.165	222.423
140	2000	2000	603.665	563.472	200.6	76.847	109.552	124.269	70.081	80.474
141	2000	649.588	685.272	171.907	257.593	130.631	115.586	74.032	329.981	71.719
142	2000	2000	2000	347.576	427.653	297.033	60.728	114.27	1503.234	141.057
143	2000	2000	130.577	157.419	101.96	148.347	125.006	87.944	173.458	56.694
144	2000	2000	2000	2000	931.227	255.833	525.905	1084.18	1364.604	421.735
145	2000	2000	2000	2000	766.189	2000	2000	145.735	2000	2000
146	2000	2000	208.315	208.259	423.856	223.09	258.306	55.499	71.762	90.213
147	2000	230.455	212.742	93.462	121.944	280.744	203.355	89.19	135.413	63.561
148	2000	2000	2000	2000	1969.03	782.785	2000.001	2000	2000	2000
149	2000	2000	2000	236.248	390.198	140.577	273.345	141.396	248.422	237.594
150	2000	2000	759.625	197.05	257.088	231.676	293.406	191.471	480.953	661.917
151	2000	2000	184.127	156.378	127.752	101.092	96.806	108.065	140.925	100.686
152	2000	2000	658.823	243.438	401.576	224.09	238.65	362.776	286.189	612.369
153	2000	2000	2000	570.841	368.844	223.74	199.949	339.463	221.559	159.256
154	2000	2000	2000	508.016	135.557	138.006	105.228	217.093	386.049	2000
155	2000	2000	2000	2000	2000	2000	2000	2000	729.623	2000
156	2000	2000	2000	350.256	116.604	221.855	282.156	257.43	72.893	275.884
157	2000	2000	2000	2000	2000	2000	2000	2000	64.911	2000
158	2000	2000	2000	2000	1182.613	767.973	878.714	2000	137.165	1385.178
159	2000	2000	609.906	643.271	723.797	216.88	143.581	320.187	704.616	224.564
160	2000	2000	2000	2000	2000	700.173	528.844	2000	2000.019	2000
161	2000	1326.557	2000	195.655	263.795	302.531	88.732	107.738	259.257	60.015
162	2000	2000.009	989.246	290.735	192.548	394.066	228.833	189.55	430.967	154.422
163	2000	2000	215.582	280.511	171.275	100.009	165.48	111.595	287.045	89.552
164	2000	2000	294.899	211.604	178.769	144.132	175.688	202.235	245.48	96.835
165	2000	2000	496.598	534.818	797.757	105.542	379.291	358.125	506.046	107.666
166	2000	2000	348.154	286.367	213.284	216.962	254.987	477.698	164.031	318.718

167	2000	2000	294.945	232.555	83.038	73.219	111.546	98.333	96.594	101.943
168	2000	2000	719.92	118.801	335.232	164.215	196.27	250.71	253.323	270.151
169	2000	2000	2000	275.256	1651.732	501.653	327.147	620.43	1290.777	702.474
170	2000	2000	2000	2000	2000	386.151	106.193	125.665	1610.435	2000
171	2000	2000	2000	339.595	245.41	142.139	288.274	409.936	1120.685	860.332
172	2000	2000	2000.01	2000	538.313	727	2000	2000	851.616	1238.992
173	2000	2000	2000	2000	2000	2000	1116.739	121.321	769.811	2000
174	2000	2000	2000	2000	247.328	2000	2000	2000	2000	2000
175	2000	2000	420.701	278.487	209.341	369.115	291.764	210.689	475.766	789.32
176	2000	2000	2000	265.502	129.475	228.424	128.056	149.399	185.751	230.054
177	2000	279.041	201.221	100.503	119.863	195.016	97.521	92.929	80.236	81.36
178	2000	2000	2000	329.104	174.488	210.15	285.57	310.884	283.417	1149.669
179	2000	2000	2000	2000	2000	2000	2000	893.556	2000	2000.006
180	2000	2000	1510.244	590.935	448.508	207.309	174.215	357.146	666.959	164.843
181	2000	2000	343.686	124.133	157.595	131.206	181.784	106.956	169.873	568.686
182	2000	2000	2000	380.945	1757.154	88.766	124.59	428.29	68.182	508.739
183	2000	2000	1723.071	1207.029	291.552	371.948	550.136	744.103	424.094	295.605
184	2000	2000	152.755	87.539	196.769	143.566	68.719	85.405	100.188	87.059
185	2000	2000	763.071	768.346	277.383	337.633	156.599	160.008	350.06	177.005
186	2000	2000	564.552	375.786	212.98	211.691	271.052	156.566	326.007	197.818
187	2000	2000	2000	2000	980.955	224.019	130.157	129.415	509.713	71.419
188	2000	2000	2000	151.918	211.154	265.113	339.924	128.344	734.035	101.007
189	2000	372.726	764.168	223.144	133.639	85.31	78.448	96.444	58.232	86.185
190	2000	2000	190.859	245.049	84.557	574.56	1714.801	2000	2000.044	100.155
191	2000	2000	2000	952.811	654.59	531.434	139.07	66.09	112.342	85.179
192	2000	2000	2000	2000	2000	2000	2000	2000	2000	2000
193	2000	2000	258.545	84.199	578.818	241.835	124.01	335.688	61.977	558.706
194	2000	2000	214.599	501.551	462.399	382.579	321.364	160.68	237.39	328.318
195	2000	2000	999.687	741.012	365.977	376.514	245.768	421.125	183.392	1115.891
196	2000	2000	2000	2000	2000	2000	2000	398.637	2000	2000
197	2000	2000	2000	1127.03	2000.038	336.723	348.51	944.879	2000	2000
198	2000	2000	555.069	233.298	115.392	128.643	107.966	87.847	151.886	136.751
199	2000	2000	279.758	195.99	62.201	64.463	140.364	216.976	145.917	43.994
200	2000	2000	708.59	421.229	381.791	210.75	174.116	147.048	127.525	632.423
201	2000	933.939	108.415	105.103	132.059	297.776	182.797	133.093	384.256	125.816
202	2000	2000	1122.781	765.247	207.744	252.35	297.634	203.415	205.629	395.383
203	2000	2000	2000	365.602	564.181	665.994	655.262	2000	2000.025	2000
204	2000	2000	271.348	402.665	370.554	78.57	125.719	301.305	221.29	64.69
205	2000	2000	2000	319.469	404.842	223.075	317.398	708.434	215.68	499.77
206	2000	2000	272.621	340.903	195.655	304.525	315.874	100.525	485.487	1417.662
207	2000	2000	2000	848.685	212.101	520.29	568.413	460.689	90.749	149.057
208	2000	2000	2000	640.67	495.578	202.893	269.747	53.794	190.216	1430.058
209	2000	2000	143.149	154.542	72.523	119.457	88.509	75.475	118.408	82.314

210	2000	2000	2000	267.653	141.797	266.766	145.592	269.261	405.563	685.24
211	2000	2000	2000	2000	2000	2000	2000	353.47	2000.005	2000
212	2000	2000	219.697	475.695	159.955	167.386	160.725	154.598	116.364	64.709
213	2000	2000	223.315	389.637	225.621	119.105	109.996	69.564	161.265	77.805
214	2000	2000	261.07	92.457	117.201	114	106.633	109.071	150.768	334.808
215	2000	2000	1103.167	2000	116.37	368.052	108.799	215.921	469.876	84.022
216	2000	177.598	696.251	129.045	60.979	51.646	98.295	77.035	48.88	120.544
217	2000	2000	917.521	313.876	244.264	198.431	268.535	233.208	277.472	447.718
218	2000	2000	2000	1877.15	683.451	253.485	465.495	2000	204.629	2000
219	2000	2000	358.235	232.249	148.316	116.98	383.051	152.054	379.064	222.757
220	2000	2000	2000	402.858	259.832	757.362	170.179	598.713	342.423	2000
221	2000	2000	2000	2000	2000	1268.625	2000	816.457	2000	2000.039
222	2000	2000	2000	1037.401	2000	2000	2000	2000	2000	964.214
223	2000	2000	499.171	213.065	56.213	76.981	67.31	281.287	116.007	134.367
224	2000	2000	685.469	343.274	137.291	206.083	122.138	108.355	104.024	159.725
225	2000	2000	2000	420.547	579.402	879.555	477.088	93.033	552.887	80.813
226	2000	2000	2000	2000	1257.029	2000	69.359	1860.591	1573.674	1284.998
227	2000	2000	589.625	396.891	299.574	142.361	182.929	86.646	153.791	110.152
228	2000	175.941	2000	95.439	384.281	79.904	162.728	211.514	89.457	239.758
229	2000	2000	2000	686.66	295.429	152.431	194.197	301.648	183.993	269.618
230	2000	2000	2000	2000	2000	2000	2000	2000	1243.527	1114.001
231	2000	2000	361.833	636.427	278.147	272.806	226.347	224.085	236.283	411.794
232	2000	442.408	327.883	479.623	226.596	296.689	101.312	121.979	67.329	224.039
233	2000	2000	2000	2000	2000	2000	321.348	112.952	77.099	91.147
234	2000	2000	2000	1125.908	369.586	482.867	91.618	138.259	1266.759	1862.177
235	2000	2000	156.838	264.848	106.192	145.378	110.88	119.987	365.171	270.986
236	2000	2000	954.1	316.852	216.162	398.222	382.979	182.657	568.19	2000.01
237	2000	2000	159.181	121.558	254.487	124.239	87.512	74.086	58.999	134.299
238	2000	2000	2000	2000	536.709	167.771	2000	134.314	337.121	2000
239	2000	2000	828.054	809.684	191.196	310.242	235.642	162.324	153.628	834.512
240	2000	2000	562.829	394.456	136.831	241.17	122.784	67.139	523.767	646.595
241	2000	2000	2000	2000	2000	2000	667.598	576.96	367.519	89.031
242	2000	267.122	243.123	367.897	299.962	317.175	172.553	145.787	123.291	187.553
243	2000	2000	2000	564.262	2000	678.547	2000	57.035	2000	2000
244	2000	2000	2000	2000	2000	804.815	619.906	2000	2000	2000
245	2000	2000	2000	865.236	394.189	90.966	75.414	145.638	1156.213	2000
246	2000	2000	522.511	327.588	108.709	157.388	46.691	76.178	132.65	270.127
247	2000	2000	2000	253.223	151.187	202.98	146.294	125.325	293.528	151.835
248	2000	2000	642.632	203.851	213.648	67.176	83.848	130.748	128.314	457.568
249	2000	2000	2000	2000	2000	2000	2000.048	2000	219.991	776.257
250	2000	2000	2000	145.633	2000	1828.309	595.811	635.704	87.195	486.116
251	2000	2000	278.863	600.539	321.517	188.881	265.348	267.218	472.955	360.441
252	2000	2000	2000	2000	2000	2000	2000	2000	2000	2000

253	2000	2000	978.546	235.839	274.962	203.128	126.01	447.272	226.825	188.744
254	2000	2000	2000	828.779	2000	560.655	118.395	824.95	2000	78.841
255	2000	2000	818.779	180.128	371.463	258.497	347.78	234.022	788.139	525.291
256	2000	2000	2000	218.132	450.962	214.19	473.213	427.098	974.177	161.262
257	2000	2000	2000	414.609	170.044	575.674	408.415	294.385	215.248	1812.085
258	2000	186.277	236.438	193.759	124.154	162.58	89.789	61.819	138.777	120.469
259	2000	2000	2000	1860.386	946.651	2000	2000	2000	2000.029	2000
260	2000	2000	104.352	1526.221	2000	434.998	55.644	627.588	879.296	160.138
261	2000	2000	290.062	659.111	302.568	237.174	144.976	142.515	327.249	2000.027
262	2000	2000	1059.35	326.479	570.498	102.61	227.403	139.196	2000	51.271
263	2000	2000	2000	208.556	54.748	229.886	157.745	272.27	72.963	243.219
264	2000	2000	566.959	173.479	126.12	199.032	148.203	128.924	120.314	404.008
265	2000	2000	2000	575.771	2000	393.204	752.848	1466.606	90.652	2000
266	2000	2000	2000	2000.041	2000	2000	2000	2000	92.159	2000
267	2000	2000	2000	2000	2000	2000	2000	2000	2000	69.89
268	2000	883.541	388.645	244.512	129.046	246.586	192.391	150.248	149.973	109.726
269	2000	2000	2000	2000	2000	2000	2000	2000.007	2000	2000
270	2000	2000	2000	704.221	307.444	360.072	162.526	167.075	296.181	676.757
271	2000	2000	2000	2000	2000	2000	2000	2000	2000.018	2000
272	2000	2000	141.111	96.497	368.381	123.546	114.548	120.057	255.641	122.676
273	2000	2000	997.84	315.895	608.618	197.14	247.362	277.997	908.955	385.806
274	2000	2000	416.625	283.323	472.717	129.914	230.226	205.43	240.689	863.594
275	2000	2000	986.402	233.508	238.023	258.958	124.843	516.333	188.134	129.37
276	2000	2000	2000	2000	2000	2000	1138.926	2000	2000	2000
277	2000	2000	2000	2000	2000.005	2000	2000	2000	2000	2000
278	2000	2000	2000	1011.92	2000	2000	2000	2000	2000	905.034
279	2000	2000	2000	505.091	766.923	325.503	496.902	96.045	901.395	69.654
280	2000	2000	558.623	111.373	197.315	256.462	133.187	263.899	115.688	378.461
281	2000	2000	434.53	110.649	154.817	111.042	120.704	82.161	131.52	152.894
282	2000	2000	2000	2000	2000.045	2000	2000	2000	2000	2000
283	2000	2000	2000	2000	2000	2000	2000	2000	2000	2000
284	2000	2000	2000	424.19	96.487	63.214	69.903	116.209	69.466	140.307
285	2000	2000	2000	471.376	359.672	2000	125.144	2000.015	2000	2000
286	2000	2000	2000	172.72	396.773	2000	2000.03	2000	2000	2000
287	2000	2000	167.325	157.831	195.821	206.864	49.275	89.163	79.179	73.448
288	2000	2000	2000	1432.748	629.222	114.712	700.583	752.817	121.486	52.183
289	2000	2000	958.386	390.88	282.744	317.011	171.244	247.289	212.396	221.359
290	2000	2000	764.444	874.661	173.783	240.738	159.073	186.167	600.959	781.88
291	2000	2000	2000	89.033	73.348	744.022	1696.73	60.753	2000	440.503
292	2000	2000	443.795	555.863	465.145	563.273	69.256	144.887	68.934	119.854
293	2000	2000	284.166	233.766	349.82	317.44	221.315	144.508	280.007	136.133
294	2000	2000	2000	2000	2000	1644.339	2000	2000	70.183	1046.871
295	2000	2000	2000	2000	460.541	221.154	2000	213.905	127.644	202.561

296	2000	2000	2000	277.882	241.504	152.779	211.609	314.7	172.743	205.741
297	2000	548.135	2000	825.119	217.093	294.98	184.319	354.094	519.115	494.321
298	2000	2000	2000	2000	2000	416.175	2000	2000	2000	2000
299	2000	2000	2000	1092.823	194.068	304.987	2000	2000	339.367	83.048
300	2000	2000	1095.625	794.27	769.298	365.229	205.341	486.037	2000	422.095
301	2000	2000	1072.886	537.861	381.444	150.638	416.272	329.718	597.079	178.254
302	2000	205.097	833.676	485.432	321.705	270.983	230.676	113.155	330.954	74.553
303	2000	2000	1296.303	681.068	327.649	299.68	143.892	83.925	52.47	52.689
304	2000	2000	563.466	535.089	261.297	306.186	305.461	283.163	167.7	609.271
305	2000	2000	2000	2000	2000	2000	2000	2000	2000	2000.044
306	2000	2000	2000	542.803	540.746	421.239	294.795	195.281	707.389	264.206
307	2000	2000	2000	511.7	828.428	1846.675	2000	2000	2000.021	2000
308	2000	2000	206.235	104.175	88.718	165.664	88.959	126.5	79.643	118.375
309	2000	2000	667.663	526.255	236.905	195.497	240.797	292.339	111.25	225.233
310	2000	2000	2000	2000	2000	2000	2000	2000	2000	365.341
311	2000	2000	2000	971.339	2000	2000	2000	2000	2000	134.579
312	2000	2000	2000	309.769	203.289	167.334	302.028	311.283	666.372	1014.723
313	2000	2000	1053.028	979.43	170.05	240.504	217.701	303.943	557.076	2000
314	2000	2000	2000	242.24	2000	171.955	2000	2000	2000	2000
315	2000	2000	2000	262.371	167.873	125.018	215.006	143.625	300.909	352.099
316	2000	2000	232.358	431.576	323.284	88.223	119.206	85.416	72.726	115.651
317	2000	2000	2000	442.091	545.882	315.95	240.755	297.612	344.804	569.241
318	2000	2000	2000	257.292	322.738	286.97	201.793	276.039	318.486	490.831
319	2000	2000	1001.267	722.11	502.66	328.976	279.256	172.823	347.124	578.856
320	2000	2000	200.736	175.761	57.275	78.4	70.833	66.627	85.247	110.041
321	2000	2000	407.225	162.914	384.953	170.242	175.99	91.22	98.953	472.386
322	2000	617.775	857.664	725.504	135.111	140.794	167.444	262.104	199.174	204.655
323	2000	2000	2000	599.046	122.291	230.338	203.881	126.605	199.829	431.679
324	2000	2000	845.038	383.352	500.509	176.327	322.153	336.661	413.035	549.796
325	2000	2000	700.235	147.392	392.879	309	111.305	223.348	201.226	155.528
326	2000	2000	2000	2000	101.506	2000	275.971	2000	1513.145	66.093
327	2000	2000	1060.66	616.123	357.882	239.315	222.686	138.323	297.189	147.537
328	2000	2000	1339.074	155.27	1079.688	209.459	826.255	436.86	80.156	2000
329	2000	2000	710.562	361.584	156.782	261.865	316.164	685.847	160.154	222.018
330	2000	2000	243.702	74.062	321.153	93.821	105.592	42.828	76.531	737.881
331	2000	2000	2000	234.393	254.65	143.728	131.325	125.432	170.677	72.347
332	2000	2000	1037.113	614.874	225.195	179.363	193.146	641.236	233.265	395.169
333	2000	2000	566.016	357.338	229.478	291.674	255.765	229.41	185.664	284.367
334	2000	2000	387.139	2000	151.874	74.363	1204.172	614.097	253.778	98.878
335	2000	2000	2000	376.986	323.792	155.387	228.955	205.793	532.722	266.78
336	2000	2000	2000	561.104	273.47	556.837	731.095	324.618	75.419	1004.245
337	2000	1072.363	930.611	305.487	229.177	147.445	389.661	353.816	110.053	182.111
338	2000	2000	171.519	274.379	80.85	79.655	92.47	94.003	61.005	96.841

339	2000	2000	2000	321.432	129.715	633.54	407.594	726.855	853.571	70.725
340	2000	2000	2000	2000	2000	2000	542.544	82.693	2000	2000
341	2000	2000	2000	2000	2000.026	462.37	969.662	2000	2000.021	2000
342	2000	2000	2000	149.963	364.08	477.524	184.438	108.673	184.366	71.038
343	2000	1008.988	142.416	203.412	130.368	168.244	131.768	182.869	98.507	128.208
344	2000	2000	2000	985.892	115.624	189.865	111.427	635.035	135.859	2000.02
345	2000	2000	726.994	296.851	194.029	222.169	93.188	115.965	414.826	93.627
346	2000	2000	2000	326.676	533.801	357.476	347.611	154.648	110.052	41.808
347	2000	2000	2000	118.23	289.453	106.556	720.418	91.29	282.352	115.042
348	2000	2000	2000	2000	106.587	352.168	2000	1615.439	60.927	2000
349	2000	2000	750.892	385.135	130.566	220.344	95.138	120.075	100.314	208.676
350	2000	2000	2000	2000	172.65	143.989	306.621	142.944	800.066	1051.886
351	2000	2000	2000	2000	2000	1780.186	2000	340.1	918.114	66.311
352	2000	2000	2000	622.64	154.87	184.601	196.084	260.745	615.769	2000.037
353	2000	2000	407.539	2000	647.359	174.117	710.652	567.602	1210.382	942.733
354	2000	2000	2000	642.777	1847.143	274.512	610.755	114.433	60.866	556.038
355	2000	2000.003	136.366	824.064	2000	151.587	568.795	1510.186	1195.285	188.823
356	2000	2000	411.791	229.338	307.208	104.631	203.015	192.31	152.117	155.252
357	2000	2000	2000	589.007	200.316	223.051	434.38	170.769	164.641	315.76
358	2000	2000	2000	213.823	249.136	98.823	92.281	175.93	314.963	125.514
359	2000	2000	511.496	183.814	92.381	92.373	128.436	110.003	83.649	183.22
360	2000	2000	120.335	184.572	119.531	196.548	71.742	74.261	86.107	91.322
361	2000	2000	802.361	59.482	374.216	234.489	95.872	116.026	148.952	372.145
362	2000	2000	2000	2000	2000	2000	2000	2000	132.417	1644.82
363	2000	2000	2000	166.226	401.24	207.228	259.68	105.28	711.781	108.199
364	2000	2000	2000	2000	2000	2000	1184.328	2000	1272.952	1264.959
365	2000	2000	2000	97.747	594.976	311.324	107.148	99.103	151.88	60.035
366	2000	2000	441.445	405.426	225.534	88.424	175.204	170.214	84.963	193.944
367	2000	2000	247.95	224.312	498.304	67.431	312.913	65.71	636.228	88.085
368	2000	2000	644.725	678.518	157.321	207.479	97.189	319.89	238.898	72.237
369	2000	2000	348.108	527.032	78.968	318.304	123.881	81.549	151.497	283.211
370	2000	2000	2000	567.697	114.59	85.896	235.856	277.131	63.313	70.061
371	2000	2000	2000	2000	180.162	496.186	229.396	527.139	2000	2000.031
372	2000	2000	2000	401.349	67.818	167.458	141.005	126.376	587.18	53.584
373	2000	2000	2000	2000	875.99	2000	2000	2000	2000	50.82
374	2000	138.652	297.429	168.088	93.978	119.779	77.218	112.468	85.58	91.312
375	2000	2000	240.574	118.171	117.782	145.758	114.705	195.509	155.065	220.202
376	2000	2000	285.758	439.345	289.547	111.811	327.634	369.81	195.869	252.805
377	2000	1870.19	392.945	412.445	245.748	127.062	200.245	175.312	427.933	506.889
378	2000	2000	2000	2000	2000	717.802	631.772	61.931	1154.356	74.709
379	2000	2000	2000	2000	2000	1291.679	247.891	571.034	888.011	243.595
380	2000	2000	527.529	238.477	399.548	113.449	64.207	379.058	767.37	119.569
381	2000	2000	1012.442	159.651	223.773	333.587	291.758	322.677	214.007	950.611

382	2000	2000	2000	2000	2000	147.599	2000	2000	174.467	344.444
383	2000	2000	369.484	282.053	134.798	213.448	286.019	227.012	279.799	222.942
384	2000	248.743	529.13	348.512	163.092	105.205	123.11	93.63	144.029	128.554
385	2000	2000	2000	2000.001	2000	2000	2000	2000	2000	1103.396
386	2000	2000	409.624	298.107	118.673	109.148	218.301	76.642	205.759	292.968
387	2000	2000	2000	566.586	1664.311	2000	2000	1568.683	2000.001	2000
388	2000	2000	218.758	294.791	281.305	215.979	358.948	302.202	238.934	853.905
389	2000	2000	2000	2000	2000	2000	2000	2000	2000.021	642.602
390	2000	2000	556.724	506.632	394.931	278.436	132.218	373.229	486.356	211.295
391	2000	2000	242.522	218.073	267.764	427.052	131.706	371.696	436.837	1626.273
392	2000	2000	2000	2000	2000	2000	1927.615	2000	110.958	2000
393	2000	2000	2000	2000	351.711	2000	1654.05	2000	110.833	68.178
394	2000	2000	424.898	900.316	79.294	666.991	822.205	93.22	172.711	159.334
395	2000	2000	265.523	121.445	170.003	135.134	170.485	199.51	166.709	142.823
396	2000	2000	514.233	997.082	310.991	208.234	317.497	740.882	499.418	196.977
397	2000	1188.108	161.427	517.865	83.464	287.287	90.214	77.807	309.229	77.508
398	2000	2000	2000	2000	2000	2000	2000	2000	2000.035	2000
399	2000	2000	2000	465.189	959.969	710.556	2000	2000	2000	581.508
400	2000	2000	335.823	203.68	126.916	115.771	101.408	112.851	146.863	191.822
401	2000	2000	2000	481.837	377.456	369.396	384.374	411.083	1197.616	311.315
402	2000	2000	594.937	518.9	259.67	263.398	231.322	230.283	971.014	658.215
403	2000	2000	1050.534	485.786	269.371	391.154	241.25	213.208	167.658	2000
404	2000	2000	344.255	269.948	146.771	96.668	171.46	129.111	725.729	98.487
405	2000	2000	1922.178	2000	221.681	387.484	259.979	2000	402.987	2000
406	2000	703	529.883	216.513	137.288	66.514	41.378	47.15	65.804	43.183
407	2000	2000	2000	290.973	2000	271.507	707.004	104.995	1862.765	128.94
408	2000	2000	2000	2000	2000	2000	2000.027	2000	2000	2000
409	2000	2000	803.228	102.751	273.164	286.656	369.244	78.348	72.486	548.688
410	2000	2000	2000	2000	2000	2000	2000	2000	2000	1543.28
411	2000	2000	2000	337.032	324.783	235.677	607.369	118.262	263.87	79.545
412	2000	2000	140.973	119.714	174.317	126.479	120.085	58.852	94.242	56.424
413	2000	2000	896.467	108.318	213.062	82.679	117.496	338.311	123.335	57.736
414	2000	2000	1620.471	772.437	345.575	160.406	64.875	152.512	152.059	265.246
415	2000	1878.019	335.798	227.119	79.686	243.89	211.895	164.934	86.443	91.551
416	2000	2000	392.83	656.282	195.309	231.212	173.333	246.686	129.502	407.825
417	2000	2000	320.454	155.419	145.298	190.121	87.992	82.382	63.908	215.554
418	2000	2000	885.424	545.559	172.532	413.606	130.732	249.003	273.353	543.545
419	2000	2000	2000	2000	756.365	2000	983.034	2000.024	2000	2000
420	2000	2000	488.483	346.89	157.439	352.246	238.096	309.064	421.921	619.325
421	2000	2000	995.381	445.003	168.975	242.153	378.552	212.859	341.362	180.997
422	2000	2000	2000	2000	1078.238	2000	1756.388	2000	2000.044	2000.031
423	2000	2000	2000	2000	315.549	603.227	779.076	2000	2000	2000
424	2000	2000	2000	2000	2000	2000	2000	2000	2000	2000

425	2000	2000	2000	2000	2000	2000	2000	2000	2000	83.56
426	2000	2000	2000	835.807	124.392	205.695	219.388	49.646	63.075	170.173
427	2000	2000.01	2000	853.449	318.866	267.726	326.787	170.729	125.835	1155.267
428	2000	2000	396.28	2000	329.432	449.168	429.688	2000	2000	1068.373
429	2000	2000	2000	600.01	183.132	374.64	161.533	167.163	294.028	305.911
430	2000	2000	972.507	172.879	192.628	198.707	177.608	263.199	1278.834	315.712
431	2000	243.524	258.924	796.782	386.394	94.094	115.833	181.424	317.162	92.257
432	2000	2000	352.269	493.958	248.083	371.117	318.786	572.413	172.365	630.543
433	2000	2000	856.112	746.872	754.575	650.641	1301.392	62.974	159.68	86.92
434	2000	2000	2000	1109.866	678.438	655.345	210.289	91.004	132.336	698.007
435	2000	2000	749.627	866.573	318.11	645.289	1853.866	115.218	2000	2000
436	2000	903.567	2000	595.658	131.592	518.925	88.266	320.26	654.531	482.356
437	2000	2000	2000	291.086	349.319	246.99	255.95	277.89	319.364	572.115
438	2000	2000	2000	1530.974	985.471	523.789	650.483	146.619	1316.961	209.311
439	2000	2000	2000	178.08	282.427	161.695	85.59	264.273	64.7	244.566
440	2000	2000	2000	2000	2000	897.864	2000	2000	2000	2000
441	2000	2000	2000	394.41	200.728	374.899	211.101	188.64	425.175	713.297
442	2000	2000	2000	452.253	254.602	167.898	265.592	188.388	149.806	492.286
443	2000	2000	2000	848.691	2000	2000	157.647	723.965	283.359	2000.027
444	2000	2000	920.083	234.662	91.565	625.817	107.665	54.718	162.411	91.116
445	2000	2000	1677.987	2000	734.968	252.461	299.772	275.117	2000	1490.639
446	2000	2000	2000	2000	2000	2000	1604.04	2000	2000	2000
447	2000	2000	2000	2000	2000	126.694	213.027	2000	2000.043	2000
448	2000	2000	938.26	611.688	169.539	247.348	224.571	206.437	620.544	325.232
449	2000	2000	2000	2000	2000	331.437	2000	2000	184.094	907.241
450	2000	2000	2000	2000	2000	2000	2000	2000	2000	2000
451	2000	2000	2000	2000	1054.753	1085.51	302.515	124.08	2000	474.598
452	2000	2000	2000	2000	2000	2000	2000	2000	2000	2000
453	2000	2000	2000	2000	2000	2000	2000.006	2000	2000	360.156
454	2000	2000	421.919	308.025	196.555	158.935	197.678	319.213	146.892	1624.197
455	2000	2000	2000	2000	2000	412.246	2000	76.649	2000.013	2000.026
456	2000	2000	2000	238.503	220.187	225.653	209.49	243.941	901.238	228.443
457	2000	2000	777.144	295.127	287.321	122.717	119.68	106.783	62.53	211.043
458	2000	2000	2000	315.79	134.816	123.999	63.223	109.188	381.422	120.171
459	2000	2000	575.025	234.543	325.972	329.67	130.911	197.273	134.191	1555.674
460	2000	2000	524.059	244.704	136.938	160.791	160.676	101.295	158.192	125.854
461	2000	2000	674.25	296.103	68.043	56.308	64.657	124.876	46.431	267.114
462	2000	2000	2000	561.489	484.721	2000	458.826	2000	157.141	460.698
463	2000	2000	722.934	677.763	169.861	69.448	109.58	219.272	840.694	674.418
464	2000	2000	2000	2000	2000	2000	2000	2000	2000	2000
465	2000	2000	310.49	349.233	78.763	97.012	85.119	140.777	113.976	99.441
466	2000	2000	2000	2000	602.964	154.521	766.961	99.387	2000	886.297
467	2000	2000	2000	870.573	232.715	1388.336	388.951	126.368	83.909	75.061

468	2000	2000	305.497	670.511	197.552	111.465	215.46	244.269	285.58	1017.715
469	2000	2000	2000	804.531	908.705	1272.7	2000	2000	2000	2000
470	2000	2000	778.214	463.644	348.843	145.08	112.725	288.403	109.373	128.561
471	2000	2000	2000	2000	95.712	354.341	1338.129	64.879	267.466	104.61
472	2000	2000	454.69	102.584	148.676	118.805	129.579	70.524	83.071	257.196
473	2000	2000	2000	450.572	105.209	501.854	90.167	184.78	86.751	2000
474	2000	2000	862.582	443.607	195.483	210.569	229.692	139.398	784.281	1515.355
475	2000	2000	2000	2000	758.625	2000	1014.095	229.697	121.338	215.123
476	2000	2000	119.882	267.898	110.751	116.626	75.437	64.057	56.861	139.572
477	2000	2000	619.124	256.045	167.217	78.971	77.152	178.436	87.851	65.976
478	2000	2000	2000	836.926	2000	233.504	528.13	2000	274.114	75.674
479	2000	2000	2000	1252.568	2000	2000	1689.394	2000	2000	119.311
480	2000	2000	2000	2000	1081.742	161.69	100.263	143.299	123.03	142.339
481	2000	2000	588.004	795.186	174.135	73.855	80.866	546.866	105.363	98.978
482	2000	2000	2000	2000	2000.022	346.699	2000	2000	2000	2000.042
483	2000	2000	2000	747.458	332.999	226.141	138.323	250.338	151.372	281.355
484	2000	2000	2000	302.781	56.646	172.818	602.145	251.525	80.521	93.576
485	2000	827.418	993.485	486.542	167.287	180.608	278.874	93.476	233.979	312.045
486	2000	2000	401.595	358.135	464.879	228.088	397.35	47.634	248.467	169.884
487	2000	2000	2000	2000	620.178	2000.014	2000	2000.022	2000	2000
488	2000	2000	2000.012	509.604	333.598	154.818	200.689	89.614	213.193	221.827
489	2000	2000	2000	713.632	2000	2000.012	1071.727	1722.55	1973.787	142.845
490	2000	2000	2000	2000	2000	78.268	96.82	284.76	97.298	626.473
491	2000	2000	2000	2000	2000	2000	2000	2000	2000	69.001
492	2000	2000	194.952	124.857	71.561	91.35	77.057	77.831	52.678	67.932
493	2000	2000	930.494	533.969	248.357	258.907	159.799	264.848	450.911	224.889
494	2000	2000	2000	2000	331.1	2000	2000	1306	2000	2000
495	2000	2000	2000	288.974	323.372	200.82	254.861	258.826	274.405	454.72
496	2000	2000	2000	2000	2000	748.266	2000.049	396.988	2000	2000
497	2000	2000	2000	92.925	95.869	65.013	395.913	528.805	794.609	67.838
498	2000	2000	2000	2000	2000	2000	2000	2000	2000	971.475
499	2000	2000	670.867	384.991	288.356	187.837	326.415	346.158	266.869	418.119
500	2000	2000	531.794	606.468	306.458	209.898	340.658	513.166	231.273	437.929